Interactions of Pyrethroids with the Voltage-Gated Sodium Channel

By Susan Atkinson, BA.

Thesis submitted to The University of Nottingham
for the degree of Doctor of Philosophy, October 2002

Chapter 1. Introduction

Chapter 2. Materials and Methods

Chapter 4. Sensitivity of the *para* T929V and T929M voltage gated sodium channel mutant to deltamethrin.

Chapter 5. Sensitivity of rat IIA brain voltage-gated sodium channel mutants to deltamethrin

Chapter 8. Final Discussion

APPENDICES AND REFERENCES

Abstract

Pyrethroid insecticides act on the voltage-gated sodium channel and mutations of the channel can confer resistance in many insect species. For example, the kdr (L1014F) mutation found in domain IIS6 and the super-kdr (M918T) mutation found in the IIS4-S5 linker of the insect *Drosophila melanogaster para* sodium channel reduces the sensitivity of the channel to pyrethroids.

Two mutations found in different pyrethroid-resistant strains of *Bemisia tabaci* were incorporated individually into the *para* wild type sodium channel of *Drosophila* and expressed in *Xenopus laevis* oocytes to investigate their effect on pyrethroid sensitivity. Voltage clamp assays showed that the M918V mutation conferred a 16-fold and a 800-fold reduction in *para* sensitivity to deltamethrin and permethrin respectively. The T929V mutation, caused a 2600-fold reduction in *para* channel sensitivity to deltamethrin. A T929M mutation, which at the equivalent residue position in the human skeletal muscle sodium channel causes Hyperkalemic Periodic Paralysis in humans, gave similar deltamethrin insensitivity. All three mutations reduced the sensitivity of *para* channel populations by reducing the number of channels in the open state, to which deltamethrin and permethrin bind preferentially, and by reducing the affinity of the pyrethroid for the channel.

The rat IIA voltage-gated sodium channel, which is approximately 4500-fold less sensitive to pyrethroids than the insect *para* sodium channel, has an isoleucine at the equivalent super-kdr residue. Replacement of this with either methionine or cysteine, increased the sensitivity of the channel to deltamethrin >80-fold and to permethrin by 150-fold.

These mutations highlight possible locations of pyrethroid binding sites and give insights into the mechanisms by which pyrethroids modify sodium channel behaviour.

Kdr and super-kdr mutations are found in the housefly and a DNA diagnostic was used to show that the genotypes present in field populations reflected the selection pressure imposed by different insecticide regimes.

Abbreviations

A	amp(s)
ATP	adenosine triphosphate
ATX-II	anemonia sulcata toxin
BSA	bovine serum albumen
bp	base pairs
CTP	cytidine triphosphate
cDNA	complementary DNA
dATP	deoxyadenosine 5' triphosphate
dCTP	deoxycytidine 5' triphosphate
DEPC	diethylpyrocarbonate
dGTP	deoxyguanosine 5' triphosphate
DNA	deoxyribonucleic acid
dNTP	deoxynucleotide 5' triphosphate
DTW	DEPC-treated water
E.Coli	*Escherichia coli*
EDTA	ethylenediaminetetraacetic acid
EtOH	ethanol
g	gram(s)
gDNA	genomic DNA
GABA	gamma-amino butyric acid
GDP	guanosine diphosphate
GPT	gentamicin, thephylline, Na-pyruvate
GTP	guanosine triphosphate
HEPES	N-2-hydroxyethylpiperazine-N'-2-ethanesulfonic acid
Hz	hertz
hrs	hour(s)
Kd	dissociation constant
kdr	knockdown resistance
kDa	kilodalton
l	litre(s)
M	molar
mA	milliamp(s)
mg	milligram(s)
min	minute(s)
ml	millilitres
mm	millimeter(s)
mM	millimolar
mRNA	messenger RNA
mV	millivolt(s)
MΩ	megaohm
ng	nanogram(s)
nA	nanoamp(s)
nm	nanometer(s)
PCR	Polymerase Chain Reaction

pg	picogram(s)
REN	restriction endonuclease
RNA	ribonucleic acid
rpm	revolutions per minute
S	Siemens
SSCP	Single Stranded Conformational Polymorphism
s	second(s)
TAE	tris-acetate-EDTA
TEMED	tetramethylethylene diamine
TBE	tris-borate-EDTA
UTP	uradine 5' triphosphate
UV	ultraviolet radiation
V	volt(s)
µA	microamp(s)
µg	microgram(s)
µl	microlitre(s)
^{o}C	degrees centigrade
τ	time constant

For my brother, Karl.

Acknowledgments

I would like to thank my supervisors, both past and present, Prof. Alan Devonshire, Prof. Peter Usherwood and Dr. Lin Field, for all their support and guidance.

I am really grateful to Martin Williamson and Horia Vais for all their brilliant advice, friendship and apparently limitless patience.

I would also like to thank other members of the BCH department at Rothamsted and the EPU department at Nottingham, including Dr. Graham Moores, Dr. Ian Mellor, Dr. Alastair Boyes and Dr. Bupindar Khambay.

Thanks to all my lab colleagues and friends at Rothamsted and Nottingham, especially Susannah, Amanda and Rach, Mat and Kev, Fit Tim, Kate C, Sue and Ollie, Emma and Sarah D.

All my friends from Uni have been really great, but I'd like to pick out Chen and Robbie, Mike W, Raj, Amaryllis and Laura, Rob and Shelley for being so encouraging and helping me to keep everything in perspective.

Lastly to my family, Mum, Dad and Karl, without whom I couldn't have done this.

CHAPTER 1

INTRODUCTION

Introduction

1.1 The continuing need for insecticides

The world population in the year 2025 is predicted to be over 8 billion people. They will require 3 billion tons of cereal with each hectare of farmland having to produce an average global yield of 4 tons. This is over three times that reached by the partially organic agricultural practices of 1960 (Dyson, 1999). An additional 850 million hectares of similar quality land would have been needed to even meet today's global cereal output had the average global cereal yield remained at the1960 level (Borlaug, 2000). Such land is not available. Future wholesale organic farming is not a realistic, worldwide option.

Approximately 35% of crops sown are lost to herbivory by insects (McEwen, 1978) and so pest control measures are vital. Whilst genetic modification does offer solutions through the engineering of more durable, pest- resistant plant species, it is a technology in its infancy and is yet to be accepted by a sceptical public, at least in the developed world. Other control strategies such as semiochemicals are also still at the developmental stage and so modern farming will continue to use insecticides to protect crops and enable us to meet the nutritional demands of a growing global population.

1.2 Pyrethroid insecticides

Pyrethroids are a major class of neurotoxic insecticides, making up around 23% of the world market (Casida and Quistad, 1998). They are synthetic analogues of the pyrethrins, six naturally occurring insecticidal compounds found in species of

Chrysanthemum. The first written account of the insecticidal use of powdered chrysanthemum flowers was produced in 1697, although the plants' toxic properties had been recognised many centuries earlier (Ruigt, 1985). Full-scale commercial production of pyrethrins began in the mid 19th century (McLaughlin, 1973), however their general use in agriculture was limited by their low stability in air and light. Subsequent structural modification of pyrethrins during the 1960s and 70s produced the first synthetic pyrethroids; photostable compounds with high insecticidal activity and low mammalian toxicity, valuable characteristics that account for their commercial success.

1.3 Pyrethroid structure and development

Pyrethrins are esters of cyclopropanecarboxylic acid and a cyclopentenolone alcohol. Synthetic pyrethroids were developed by the sequential replacement of structural elements of these two pyrethrin groups, with moieties that conserved the shape and physical properties of the template structure (Figure 1.1).

Pyrethrin I is the most insecticidally active constituent of pyrethrum extract and was used as the prototype for the development of photostable pyrethroids. Constituent photosensitive groups were identified and substituted with moieties less vulnerable to photodegradation. One of the first photostable pyrethroids, permethrin, was produced by replacing the isobutenyl side chain of chrysanthemates, which is vulnerable to oxidative attack, with a dihalovinyl group (Elliott *et al.*, 1973). Although degradation of permethrin does eventually occur, rapid photo-oxidative routes cannot take place and therefore the compound persists for longer.

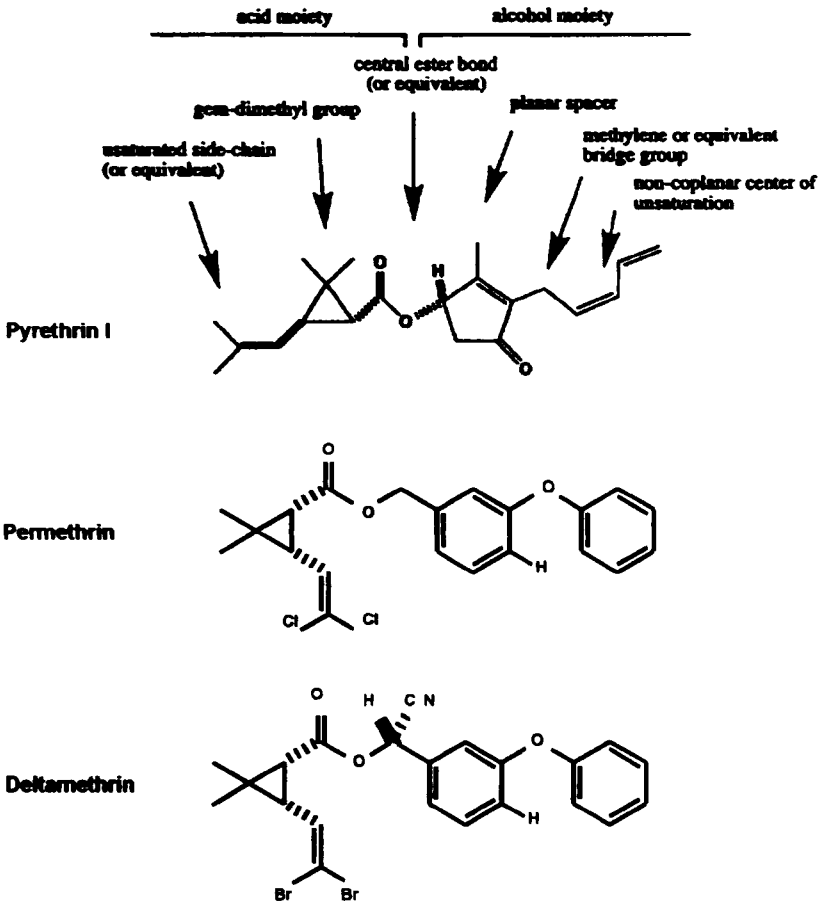

Figure 1.1. Essential features of pyrethroid structure-activity relationships illustrated by pyrethrin I and two synthetic pyrethroids. (Adapted from Soderlund *et al.*, 2002, *Toxicology*, 171; 3-59).

Many of the modifications made to pyrethrin I and its pyrethroid analogues reduced its insecticidal activity (Ruigt, 1985). One important exception was the addition of a cyano group to the alpha carbon of 3-phenoxybenzyl-alcohol ester, which approximately trebled insecticidal activity. Addition of the cyano group at the α-benzylic position to dihalovinyl pyrethroids such as permethrin, culminated in the isolation of deltamethrin (Elliott *et al.*, 1974), a compound that remains one of the most powerful commercial insecticides against a wide range of insect pests.

Pyrethroid toxicity is dependent on a combination of target site sensitivity and the ease with which the compounds are detoxified. Studies with an isolated enzyme system indicate that the rate of pyrethroid cleavage is dependent on the accessibility of the ester linkage. Conjugation of pyrethroid metabolites with glycine, glucuronic acid and sulphate increase their water solubilities and so accelerate their rate of excretion.

Studies on the toxicity of different pyrethroid compounds have been described extensively in the rat. They can be divided into two groups according to the symptoms they induce and in most cases, these correlate with the presence or absence of the α-cyano group (Verschoyle and Aldridge, 1980). Type I pyrethroids without the α-cyano group, such as permethrin, cause whole body tremors in mammals termed T syndrome, while Type II pyrethroids with the α-cyano group, exemplified by deltamethrin, cause abnormal locomotion and sinuous writhing termed CS syndrome (Staatz *et al.*, 1982).

These symptoms strongly suggest that the nervous system is the primary target of pyrethroid action.

Early studies of invertebrate nerve preparations treated with the pyrethroid allethrin, showed heightened levels of nerve firing before conductance was blocked and no further activity could be initiated (Narahashi, 1962a)b)). Subsequent voltage clamp experiments, to clarify the effect of pyrethroids on the nerve membrane, were done without separating the sodium and potassium currents, both of which are involved in generating nerve action potentials. Although both conductances were altered, reduction of the transient peak sodium current was most significant (Narahashi and Anderson, 1967). Later studies showed that in the absence of the potassium current and in the presence of allethrin, the inward sodium current was prolonged (Wang *et al.*, 1972, Murayama *et al.*, 1972). This led to the proposal that the voltage-gated sodium channel is the target site of pyrethroids. Direct evidence to support this has now come from a radioactive-labelled pyrethroid derivative, which revealed high-affinity specific binding to the α-subunit of the sodium channel protein (Trainer *et al.*, 1997).

1.4 The voltage-gated sodium channel is fundamental to neurotransmission in animals.

The voltage-gated sodium channel plays a critical role in controlling the electrical excitability of animal cells. It is responsible for the regulated influx of sodium ions into the nerve axon and the resulting generation and propagation of an action potential.

Action potentials are the electrical messages of the central nervous system, peripheral nervous system, heart and skeletal muscles as well as a number of other muscle groups. They move rapidly along axons, initiating the secretion of neurotransmitters at the nerve terminal or signalling the contraction of muscles.

The negative membrane potential of an unstimulated axon, the resting membrane potential, is established by the different external and internal concentrations of sodium and potassium ions. When the membrane potential is depolarised beyond a critical threshold value in response to a stimulus, the membrane permeability to sodium ions rapidly increases. This causes another localised depolarisation in the negative electro-chemical field and a rapid increase in sodium ion permeability further along the membrane and so a depolarising wave propagates along the nerve axon. This rapid, ion-specific, mono-directional wave is achieved by the gating conformations that the voltage-gated sodium channel adopts in response to small but significant changes in membrane potential i.e. the open, inactive and deactivated states (Stühmer *et al.*, 1989).

1.5 Sodium channel structure

Most of the functional and pharmacological properties of the voltage-gated sodium channel are conferred by the α-subunit, a large ~260kD protein that forms the ion-

conducting pore in the membrane (Messner and Catterall, 1985). It was initially identified using specific neurotoxic compound labels, which modified the generation of action potentials (Beneski and Catterall, 1980, Agnew *et al.*, 1980). The cDNAs encoding the sodium channel protein were subsequent identified, cloned and sequenced. The primary amino acid sequence revealed a large protein with four internally homologous domains (Noda *et al.*, 1984). Hydrophobicity plots of the amino acid sequence suggested an assembly of six or more hydrophobic transmembrane segments within each domain (Noda *et al.*, 1984). Subsequent molecular modelling of the sodium channel also predicted six α-helical transmembrane segments (S1-S6) in each of the four homologous domains (DI-DIV) and a reentrant loop that enters the transmembrane region between transmembrane segments S5 and S6 and forms the outer pore of the channel. Large intracellular loops were predicted to connect the four homologous domains while smaller intracellular and extracellular loops connected each of transmembrane segments (Guy and Seetharamulu, 1986) (Figure 1.2).

Comparisons of the primary structure of the principle subunit of potassium channels suggest that it is based on the same motif as that of the sodium channel; four homologous domains composed of transmembrane segments. Structure and functional models of potassium channels can therefore be used to predict the arrangement of the voltage-gated sodium channel.

X-ray crystallography of the smaller bacterial potassium channel KcsA, an inward rectifier from *Streptomyces lividans*, revealed a tetramer similar to the proposed

Figure 1.2. A two-dimensional molecular map of the α-subunit of the voltage-gated sodium channel, showing how it folds and transverses the plasma membrane. The α-subunit is composed of four homologous domains each of which contains six transmembrane segments. Cylinders represent the α-helical transmembrane segments. Red cylinders indicate the S4 transmembrane segments, which act as voltage sensors. Green cylinders indicate the S6 transmembrane segments, which together with SS1/SS2 segments (P loops) form the walls of the sodium-ion-conducting pore. The position of important charges essential for ion conductance and selectivity are indicated in white circles. Charges important for channel activation are shown on the S4 transmembrane segments. (h) indicated the position of the IFM motif which is thought to block the conducting pore during inactivation. Reprinted by permission from Nature (Catterall, 409; 988-990) copyright (2001).

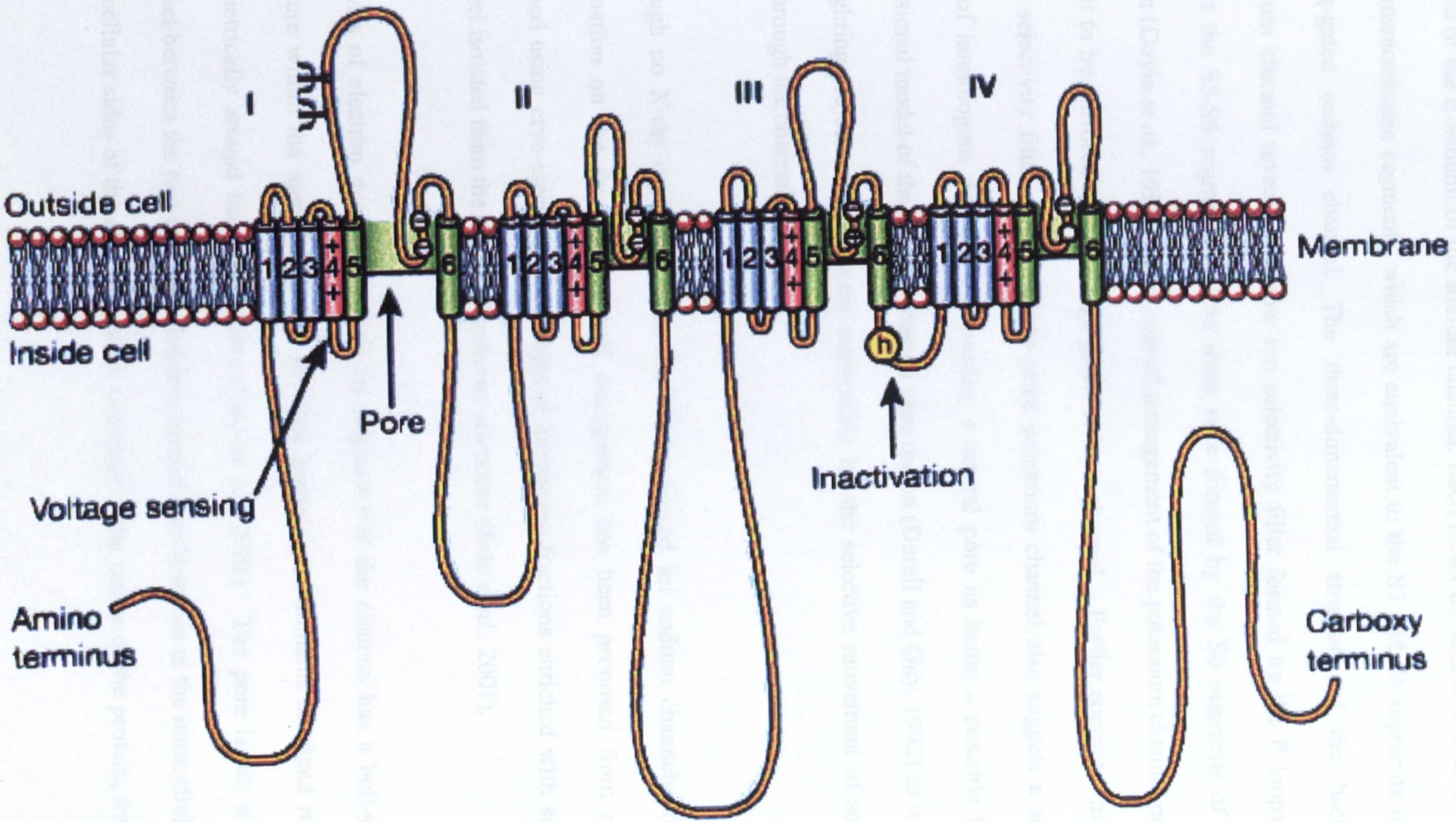
I
II
III
IV
Outside cell
Inside cell
Membrane
1 2 3 4 5 6
Pore
Voltage sensing
Inactivation
h
Amino terminus
Carboxy terminus

structure of the α-subunit of the sodium channel. Each KcsA domain comprises of only two transmembrane segments, which are equivalent to the S5 and S6 segments of the voltage-gated sodium channel. The three-dimensional structure of the bacterial potassium channel reveals a narrow ion selectivity filter formed by the P loops that connect the S5-S6 segments and an inner pore formed by the S6 segments of each domain (Doyle *et al.*, 1998). This conical arrangement of the potassium channel pore is thought to be mirrored in the voltage-gated sodium channel. Earlier computer models of the selectivity filter of the voltage-gated potassium channel also suggest a square array of homologous domains surrounding a central pore as being a possible three-dimensional model of the sodium channel pore region (Durell and Guy, 1992) as well as highlighting regions of the protein responsible for the selective movement of sodium ions through the channel.

Although no X-ray crystal structure has been achieved for sodium channels, further information on the three-dimensional arrangement has been proposed from results obtained using cryo-electron microscopy of membrane fractions enriched with sodium channel isolated from the eel *Electrophorus electricus* (Sato *et al.*, 2001).

Analysis of electron microscopy sections suggests that the channel has a bell-shaped structure within the membrane, with the four homologous domains arranged roughly symmetrically around the central pore (Sato *et al.*, 2001). The pore is not a direct channel between the two bathing solutions, instead four branches at the intracellular and extracellular sides of the channel, which converge at the centre of the protein, transport

sodium ions from the cell exterior to the axoplasm (Sato *et al.*, 2001). Four peripherally located transmembrane pores are also located in each domain and these are thought to hold the voltage sensors of the protein, which detect any change in the surrounding membrane potential (Catterall, 2001) (Figure 1.3).

1.6. Additional subunits associated with voltage-gated sodium channel

The α-subunit of the sodium channel can be expressed to form a functional, autonomous channel (Goldin *et al.*, 1986). However, some sodium channel isoforms expressed in conjunction with smaller subsidiary units have altered kinetic behaviour and different levels of expression in the membrane. β1, a 36kD protein associated with mammalian brain and skeletal sodium channels, modulates channel gating, increasing both the speed of channel opening and inactivation, as well as increasing peak current. β2, a smaller 33kD subunit also accelerates channel inactivation in addition to increasing the functional expression of the protein. Studies of the primary structure of both subsidiary units (Isom *et al.*, 1992, 1995) have highlighted a close structural relationship with a group of cell adhesion molecules that mediate cell-cell interactions in the nervous system and other tissues (Vaughn and Bjorkman, 1996). These auxiliary units influence neuronal migration and mediate interactions with substrates and other cells. β-subunits may perform a similar role, and direct the formation of specialised areas of high sodium channel density such as at the nodes of Ranvier (Xiao *et al.*, 1999).

In insects, auxiliary units include the Tip E protein (Feng *et al.*, 1995), which alters the gating properties of the sodium channel (Hodges *et al.*, 2002), as well as influencing

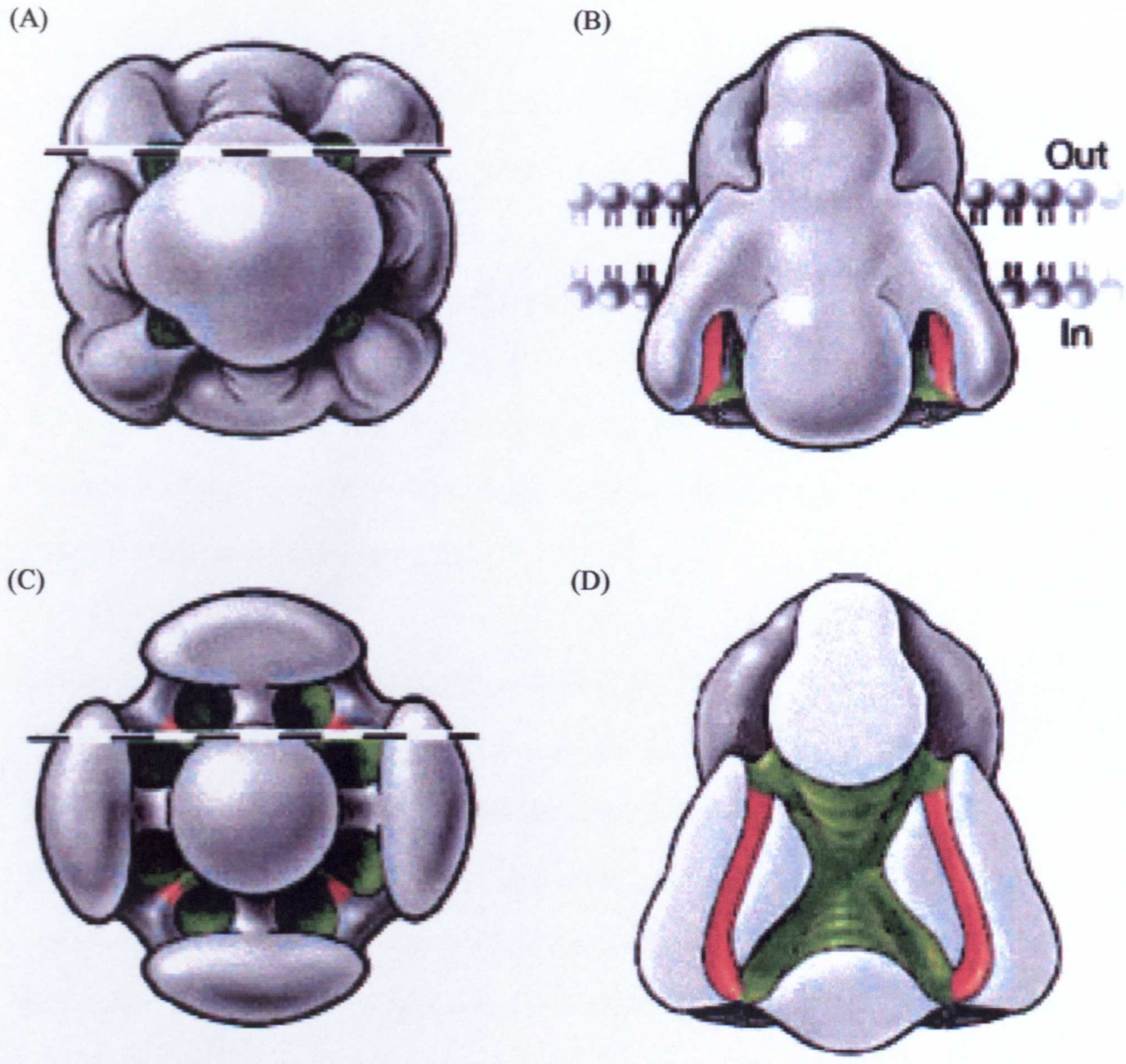

Figure 1.3. Three-dimensional representation of the voltage gated sodium channel. (A) top view (B) side view (C) bottom view (D) cross section. Red shows the position of the gating channels, which contain the S4 voltage sensors. Green indicates the ion-conducting pore. The dashed lines show the position at which the cross-section was taken. Reprinted by permission from Nature (Catterall, 409; 988-990) copyright (2001).

channel expression by acting as a chaperone and aiding the movement of the α-subunit to the membrane surface (Moore *et al.*, 2001).

1.7 Sodium channel activation; the detection of voltage change and channel opening

For sodium ions to flow through to the axoplasm, the sodium channel must be activated or open, a process that involves the recognition of a voltage change and a resulting conformational alteration of the protein.

Membrane depolarisation is detected by voltage sensors within the channel, thought to be the S4 segments of each domain. These transmembrane segments contain repeats of positively charged arginine or lysine residues followed by two hydrophobic residues (Guy *et al.*, 1989). This is a highly conserved motif, found in all voltage-gated potassium and sodium channels and implies a fundamental role in the functioning of the protein. The positive S4 charges are paired with three fixed negatively charged residues, also highly conserved, found in the S1, S2 and S3 regions that surround the transmembrane segment (Keynes, 1994). A depolarisation of the membrane increases the outward force acting on these positive charges and induces the S4 segments to operate as screw helices (Catterall, 1986) with each positively charged residue rotating through 60° and moving 0.45nm towards the exterior of the channel to pair up with the next fixed negative charge (Keynes and Elinder, 1999). The outward gating current created by the movement has been directly measured. 12 electronic charges are transferred (Hirschberg *et al.*, 1995) when each S4 segment twists three times in

succession through 60°. This suggests an equal transfer of three positive charges by each S4 helix.

The outward, rotational movement of the S4 transmembrane segment of domain IV (D4S4) helix has been detected directly (Yang *et al.*, 1996). Charged residues of the voltage sensors were replaced with cysteine residues and the rate at which the cysteine reacted with the charged sulfhydryl reagent MTSET was measured. The reaction rate plotted as a function of membrane potential, showed that the substituted cysteine residues in D4S4 became progressively more available for modification by the extracellular MTSET reagent as the membrane depolarised. This movement coincided with three positively charged amino acid residues in the S4 segment of domain IV becoming accessible outside the cell during channel gating (Yang *et al.*, 1996). Such a transfer of charge would require a substantial outward movement of the S4 segments, their screw helical movement projecting the outermost positively charged arginines as far as 1.45nm into the external aqueous phase (Keynes, 2001). The discovery that a large proportion of the D4S4 transmembrane segment was surrounded by hydrophilic crevices led to the proposal of a narrow-waisted hydrophobic gating pore which would allow a relatively small physical movement to rapidly translocate several of the charged residues across the electrical field (Yang *et al.*, 1996, 1997, Mitrovic *et al.*, 2000) (Figure 1.4). This model agrees with the structural information gained from cryo-electron microscopy, which identified peripherally located pores in each of the four domains (Sato *et al.*, 2001). The screw helical movement of the S4 segments within these pores is however complicated by their non-linear shape

Figure 1.4. Helical screw mechanism of the movement of S4 voltage sensors. On depolarisation, the solid S4 helices move outward and their positive charges (yellow) are neutralised by negatively charged residues (white) found in segments S2 and S3. The narrow hydrophobic waist allows small physical movements to rapidly translocated several charged residues across the electrical field. (From Catterall, 2001. *Neuron*, 26; 13-25. Reprinted with permission from Cell Press.)

Figure 1.5. Hinged-lid mechanism of fast inactivation of the voltage gated sodium channel. The linker between domains III and IV contains the critical IFM (isoleucine, phenylalanine, methionine) motif. During fast inactivation, phenlyalanine blokes the channel pore preventing ion conduction, while methionine maintains the rigid alpha helix or lid. (From Catterall, 2001. *Neuron*, 26; 13-25. Reprinted with permission from Cell Press.)

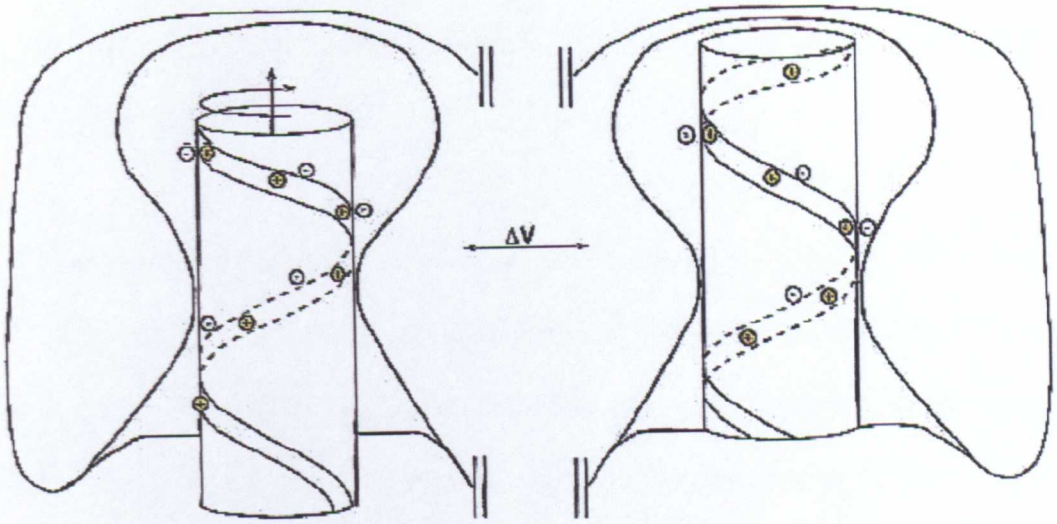

Figure 1.4

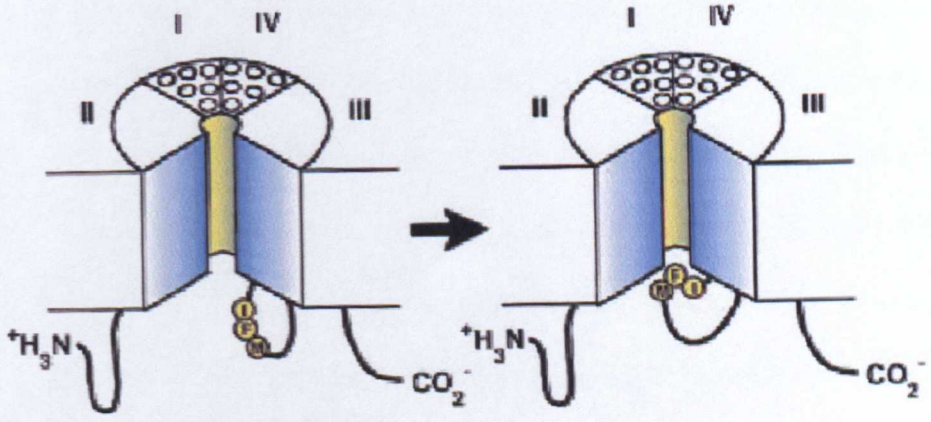

Figure 1.5

and a further gating process to straighten the tunnel in response to a depolarisation has been suggested (Catterall, 2001).

Although all four S4 segments are involved in activation gating, their contribution to the process is not equal. Significant positive shifts in the voltage dependence of activation of channels containing mutated sensors in domains I and II suggest their constituent S4 helices underlie the process of activation. Mutations of the analogous charged residues in D3S4 and D4S4 have only minor effects on the kinetics of activation (Kontis *et al.*, 1997).

Detection of membrane depolarisation and the resulting realignment of the S4 helices are thought to precede the opening of the pore (Yellen, 1998). However, although the two processes are energetically coupled, it is not known how the numerous kinetic steps involved in the movement of gating charge initiate the opening of the channel or in what form the opening occurs. One suggestion is that the outward twists of the S4 segments force the opening of an activation gate, which is located near the cytoplasmic end of the channel's four S6 segments, at the end of the permeation pathway. Evidence for this has come from studies with K^+ channel pore blockers and state dependent cysteine modification of the channel (Armstrong, 1971; Shapiro, 1977; Yeh and Narahashi, 1977; Liu *et al.*, 1997).

Many blockers that act on the intracellular side of K^+ channels initiate blockage of the open state; they can only obstruct the channel and prevent the movement of K^+ ions once the activation gates have opened. In the presence of a tetraethylammonium (TEA)

derivative blocker, channels still activate, indicating that they are not already blocked prior to the voltage step, however K^+ current declines exponentially as the TEA derivative binds and obstructs the now open channels (Armstrong, 1971). These TEA-blocked channels can only close once the molecule has dissociated from the protein, an effect termed 'foot in the door' (Yeh and Armstrong, 1978). This not only highlighted a binding site for channel blockers but also indicated the intracellular mouth of the potassium channel as being a possible location for an activation gate (Yellen, 1998). Similar results were found with positively charged intracellular blockers of sodium channels, which competed with the activation gate to prevent ions passing through the channel (Shapiro, 1977, Yeh and Narahashi, 1977).

The location of the potassium channel gate was further pinpointed when site-directed cysteine substitution of the middle of the S6 transmembrane segments showed large state-dependent changes in the reactivity of the replacement amino acid and its reagent. Cysteines substituted into the intracellular S6 region of the potassium channel were 100,000-fold less accessible to charged sulfhydryl reagents when the protein was closed than when it was open (Liu *et al.*, 1997). A model based on these studies proposes a conical arrangement of the four S6 helices, with the activation gate located at the apex. Following the detection of a membrane depolarisation and movement of the S4 voltage sensors, study of spin labelled cysteines within the S6 helices suggest that these transmembrane segments move apart consistent with a widening of the pore (Perozo *et al.*, 1998). The conserved structural arrangement of the potassium and sodium channels implies a similar activation gate occurs within the sodium channel.

1.8 Sodium channel selectivity

Once sodium channels open, only sodium ions flow through to the axoplasm at approximately 10^6 ions per second. This is specific for sodium ions and this specificity is thought to be the consequence of a "selectivity filter" located in the channel's outer pore. This position was originally identified by voltage clamp studies, as a binding site for the pore blockers tetrodotoxin and saxotoxin (Hille, 1984).

Site-directed mutagenesis has identified the location of a significant component of the filter. Substitution of the rat brain IIA channel Glutamate residue 387 with other residues in the extracellular membrane re-entrant loop of Domain I, conferred a significant reduction in tetrodotoxin and saxotoxin binding (Noda *et al.*, 1989). The finding of other negatively charged residues in analogous positions within the remaining three domains (Terlau *et al.*, 1991) led to the hypothesis that these amino acids form an inner ring that acts as a receptor for the two pore blockers and as the selectivity filter in the outer pore of the sodium channel. Support for this view came from sodium channel mutants that could be made selective for calcium ions by replacing the four sodium ion selective DEKA (aspartate, glutamate, lysine, alanine) residues, found in the inner ring of domains I-IV, with the four EEEE (glutamate) residues thought to confer the ionic selectivity of the calcium channel (Heinemann *et al.*, 1992). Mutations of the DEKA ring also have a great effect on the selectivity for organic and inorganic monovalent cations (Sun *et al.*, 1997). However it is not thought to be the only element which mediates conductance and selectivity. Mutations within a second outer ring composed of four residues EEDD (glutamate, aspartate) also significantly affect ion conductanceand selectivity (Tsushima *et al.*, 1997a; Chiamnvimonvat *et al.*, 1996a,b).

The two selectivity filter rings are part of the "P" or pore-lining loops that are contributed by each domain and lie deep within the external vestibule of the channel protein. They are asymmetrically arranged (Benitah *et al.*, 1997), with the domain IV loop the most internal and the domain II loop lying closest to the channel extracellular surface (Chiamnvimonvat *et al.*, 1996a). Cysteines that substituted selectivity filter residues, demonstrated the region to be highly mobile, with disulphide bridges being formed between the side chains of distantly apposed replacement residues (Pérez-García *et al.*, 1996). Cross-linking was further enhanced following activation and indeed studies have indicated that some of the selectivity filter residues are involved in channel gating (Benitah *et al.*, 1999; Hilber *et al.*, 2001).

Mutation of an alanine in the inner selective filter to a positively charged residue, aspartate, resulted in little change in ion selectivity but greatly interfered with rearrangement of the P-loops during channel opening (Hilber *et al.*, 2001). Mutation of lysine, again a constituent residue of the inner selective filter, also resulted in alteration of channel gating as well as in a substantial loss of ion selectivity (Heinemann *et al.*, 1992). Channel regions are therefore not mutually exclusive in the functions they perform.

1.9 Sodium channel fast inactivation

Within a few milliseconds of opening, sodium channels inactivate, halting sodium ion conductance, a process known as fast inactivation. Fast inactivation is structurally and energetically distinct from channel closure.

Fast inactivation is mediated by an inactivation gate, which blocks the intracellular pore of the channel and terminates the flow of sodium ions. Following abolition of the inactivation process by selective removal of an inactivation particle by protease treatment of the interior of a squid axon, a 'ball and chain' mechanism was proposed (Armstrong, 1977). This suggested a mobile inactivation component extending away from the protein and hence the idea of an intracellular flexible 'chain' tethering a 'ball' that blocked the pore after the activation gates opened. Possible regions that could act as the inactivation ball and chain include the intracellular loops found between each domain. Their extension into the cytoplasm means that they could act as a mobile component and they would be accessible for protease degradation. Inactivation was also prevented when the short, highly conserved intracellular loop between domains III and IV was treated with anti-peptide antibodies. Similar treatment with antibodies specific to other interdomain loops had no effect on channel inactivation (Vassilev *et al.*, 1989).

Subsequent mutagenesis of this III-IV interdomain loop revealed a hydrophobic triad of isoleucine, phenylalanine and methionine (IFM) residues that are critical for fast inactivation. Removal of any one of the three residues impairs inactivation (West *et al.*, 1992), while their inclusion in single peptide units can restore inactivation to channels where the IFM region has been mutated (Eaholtz *et al.* 1994). A cysteine replacement of the central phenylalanine residue of the triad becomes inaccessible to MTS reagents as the inactivation gate closes (Kellenberger *et al.*, 1996). Substitution of the same central amino acid with progressively more hydrophilic residues impairs inactivation suggesting a hydrophobic interaction between the inactivation particle and its receptor

(Kellenberger *et al.*, 1997b). Glycine and proline residues that border the IFM motif may act as molecular hinges allowing the inactivation "lid" to close across the channel pore (Kellenberger *et al.*, 1997a) (Figure 1.5).

Multidimensional NMR techniques on the central portion of the loop, expressed as a separate peptide, revealed a rigid α-helix followed by two turns, the second of which contains the IFM motif (Rohl *et al.*1999). The IFM motif's position within the three dimensional protein has also been identified as being a small indentation on one side of the intracellular mass (Catterall, 2001). The structure is maintained by a strong interaction between two tyrosine residues within the alpha helix and the methionine of the IFM motif. As a consequence, a phenylalanine is thrust into the surrounding solvent, despite its hydrophobic nature and this allows it to interact with the inactivation dock, which scanning mutagenesis has revealed as being a number of residues within the intracellular end of segments S6 of domain IV (McPhee *et al.*, 1994) and the intracellular loops between segments S4 and S5 of domains III (Smith *et al.*, 1997) and IV (McPhee *et al.*, 1998).

Channel inactivation derives most of its voltage dependence from the outward movement of S4 sensors (Armstrong, 1981), especially the D4S4 segment (Cha *et al.*, 1999) whose realignment is thought to signal the closure of the intracellular fast inactivation gate. The activation and inactivation processes can be separated using α-scorpion toxins. These bind to the extracellular end of the D4S4 voltage sensor segment

and trap it in an inward, partially activated position, which continues to allow activation but prevents fast inactivation (Sheets *et al.*, 1999).

Further evidence that the D4S4 segment is coupled to the process of inactivation comes from fluorescent probes incorporated into the transmembrane helices, which reveal that the S4 segments of domains III and IV are immobilized in the outward position by fast inactivation, while S4 in domains I and II remain unaffected (Cha *et al.*, 1999).
Similar trapping experiments of the S4 segments using cysteine accessibility scanning, also showed a slow down in the rate of inactivation, however the immobilisation of one segment does not effect the kinetics of another, implying that S4 segments act independently from each other. In addition, cysteine reagents added intracellularly prevented activation while the same reagent added extracellularly prevented inactivation, suggesting that D4S4 makes two sequential movements in response to a depolarisation; the first is coupled to the activation gate and the second coupled to the inactivation gate (Horn, 2000, 2001).

1.10 Sodium channel slow inactivation

Two further forms of inactivation, slow and ultra-slow, are thought to regulate the availability of sodium channels in the resting state from which channels can again be activated (Ruff, 1997). The processes are structurally and kinetically distinct from fast inactivation, and are initiated if a depolarisation exceeds ~20ms with the rate of decay of ultra-slow inactivation is of the order of 100ms, in contrast to the 2-3 ms for fast inactivation.

The two processes are thought to be coupled. The onset of fast inactivation and the stabilization of the channel through the binding of the inactivation particle, inhibits the initiation of ultra-slow inactivation, by preventing a molecular rearrangement that may involve both the extracellular and intracellular pore (Hilber *et al.*, 2002). Other studies have suggested that slow and fast inactivation are distinct and that mutations in the S5 and S6 segments, the S4-S5 linkers and the central arginine and neutral residues in the S4 segment of domain IV contribute towards the voltage dependence of slow inactivation (Cummins and Sigworth, 1996; Wang and Wang, 1997; Takahashi and Cannon, 1999; Bendahhou *et al.*, 1999; Mitrovic *et al.*, 2000). Mutations that affect the probability of the onset of ultra-slow inactivation have also been implicated in acting as part of the mobile ion selectivity filter. This has led to the proposal that slow inactivation involves a substantial rearrangement of the channel pore (Hilber *et al.*, 2001).

1.11 Sodium channel deactivation

Fast-inactivated sodium channels must become deactivated before they can activate again i.e. they cannot pass directly to the activated state (Kuo *et al.*, 1994). The rate of inactivated-state deactivation is regulated by the D3S4 sensor and the outer and central charged residues of the D4S4 sensor. Immobilization of the gating charge with fast inactivation slows the rate of deactivation. Neutralisation of these central gating charges has the reverse effect and accelerates the rate of recovery from inactivation (Kühn and Greef, 1999).

Following brief depolarisation, open sodium channels deactivate directly in response to hyperpolarization, without passing through the inactivated confirmation, a transition

termed open-state deactivation. The decay in current of this transition is best described by a single exponential function suggesting a one step process. This is thought to be the translocation of one voltage sensor to its hyperpolarized favoured position. Neutralisation mutagenesis, where each of the charge residues is mutated singly to a neutral residue, has clarified that the movement is regulated by each of the eight charged residues within D4S4 (Groome *et al.*, 2002).

1.12 The sodium channel gating pathway

For simplicity, the cycle of sodium channel configurations is often described as activation (or opening), followed by inactivation and then deactivation (or channel closure) before activation again. In reality, the configurative pathway is neither this rigid nor simple. Channels may bypass activation and go straight from the deactivated state to the inactivated state, known as closed-state inactivation (Patlak, 1991). Equally, single channel studies have revealed that during a depolarising pulse, a channel may reopen without first inactivating (Correa *et al.*, 1994). This supports the notion that there are more than three channel conformations which result from different arrangements of the voltage sensors in varying kinetic states and the gates which open and close in response to the voltage sensor movement (Taddese and Bean, 2002).

A recent allosteric model describes the relationship between the channel states. A channel is thought to move through a series of successively activated states, which increase the probability of the channel inactivating. As the successive voltage sensors transfer charge through the gating pore and the activation gate opens, so the affinity for interaction with the inactivation particle increases (Taddese and Bean, 2002).

1.13 Voltage clamp as a method of studying channel function and behaviour

Most "models" predicting the function of regions of the voltage-gated sodium channel are based on interpretations of electrophysiological data collected from either single channel studies using the patch clamp method, or channel populations using voltage clamp.

The conformational state of a sodium channel population is revealed by the voltage-dependent current it conducts. The presence of a current in response to a change in potential means channels are open and are allowing sodium ions to pass from the cell exterior to the interior. A decrease in current following a change in potential, suggests channels are either inactivating or closing.

Under normal *in vivo* conditions, changes in the transmembrane current change cell membrane potential, which feeds back and further changes the conductance. It is therefore difficult to determine the behaviour of membrane currents unambiguously in response to specified voltage change. To measure current, the voltage must be kept constant. The voltage clamp method achieves this by continually checking the membrane potential and injecting current to counter any deviation from the specified potential (Cole and Moore, 1960). The amount of current needed to maintain the voltage, is taken as a measure of channel population conductance, which in turn gives an indication of their conformational state.

The voltage and speed at which the current occurs, its size and the rate at which it decays, are all parameters which can be used to deduce the configurative sodium channel response to an internal alteration such as a mutation within the protein or to an external stimulus, such as an insecticide.

1.14 Pyrethroid modification of the voltage-gated sodium channel

Early voltage-clamp studies of the effect of pyrethroids on sodium currents were done on the squid giant axon. The pyrethroid allethrin prolonged the period of sodium ion conductance and shifted the voltage dependence of inactivation in the hyperpolarizing direction (Wang *et al.*, 1972). Later studies found that the sodium current of tetramethrin-treated axons decayed more slowly than in control untreated axons. The treated axons also showed a large residual current which increased the depolarising after-potential to the threshold membrane potential for the generation of repetitive discharges (Vijverberg and van den Bergen, 1982) Following repolarisation, currents of axons under normal conditions rapidly decayed. In contrast, tetramethrin-treated axon currents displayed large tail currents that decayed slowly (Lund and Narahashi, 1981). Similarly pronounced tail currents were reported in cockroach giant axons that had been treated with the pyrethroid allethrin (Pelhate *et al.*, 1980). Nerve axons treated with type II pyrethroids such as deltamethrin and cyphenothrin displayed tail currents with smaller amplitudes than Type I tail currents, although the rate of decay was significantly slower (Lund and Narahashi, 1983). This is consistent with the different action potential patterns seen following neuronal exposure of neurons to Type I and Type II pyrethroids. For Type I pyrethroids, the induction of long trains of action potentials following a single stimulus is consistent with only transient prolongation of sodium

channel inactivation and deactivation seen in the moderately slow decay of tail currents. Exposure to Type II pyrethroids results in the total block of an action potential upon repeated nerve stimulation, which is in accord with the persistent prolongation of sodium channel inactivation and deactivation seen in the very slow decay of tail currents (Vijverberg *et al.*, 1983, Soderlund *et al.*, 2002).

Patch clamp studies on the action of pyrethroids on single sodium channels gives direct support to the above findings. In the absence of pyrethroid, channels open briefly in response to a depolarising pulse. Tetramethrin, a Type I pyrethroid, increases the mean open time of individual sodium channels approximately 10-fold which corresponds with only a moderate delay of inactivation and deactivation (Yamamoto *et al.*, 1983). In contrast, deltamethrin and fenvalerate, both Type II pyrethroids, increase the mean open time of single sodium channels by up to 200-fold, a consequence of the substantial delay in channel closure (Chinn and Narahashi, 1986; Holloway *et al.*, 1989). Deltamethrin also delays channel opening in response to a voltage pulse. Single modified channels were found to continue opening even after the termination of the depolarising pulse (Chin *et al.*, 1986), which accounts for the appearance of prominent tail currents. A number of channel states are therefore stabilized through a pyrethroid interaction, and this shifts their voltage dependence of activation and inactivation in the hyperpolarizing direction (Salgado *et al.*, 1989, Tatebayashi and Narahashi, 1994), slowing their transition to different conformations in response to voltage change.

Voltage and patch clamp studies have also been used to analyse the contrasting effects of the two pyrethroid types on sodium channel behaviour. Voltage clamp records

showed that the initial slowly decaying tail currents, characteristic of deltamethrin (Tabarean and Narahashi, 1998) and fenvalerate (Song *et al.*, 1996), are replaced by rapidly decaying tail currents following the application of tetramethrin. This displacement of the deltamethrin by tetramethrin has been confirmed by patch clamping of single channels, which showed that the extensive channel opening caused by the Type II pyrethroid is replaced by the shorter channel opening characteristic of modification by a Type I pyrethroid (Motomura and Narahashi, 2001). The differing effects of pyrethroid action are therefore antagonistic and subtractive rather than cooperative and additive. This could be explained by either the molecules competing for a common binding site or by an allosteric coupling so that binding to one site prevents the occupancy of another.

Pyrethroids do not modify all of the individual sodium channels within a population of insecticide-treated channels. The distribution of channel open times following tetramethrin exposure can be fitted by two exponentials. One exponential is similar to that recorded in the absence of the pyrethroid and the other is significantly slower. These two functions are thought to represent modified and unmodified fractions of the channel population. In contrast, the distribution of channel open times in untreated conditions can be fitted with a single exponential (Motomura and Narahashi, 2001). To initiate the repetitive firing of tetramethrin modification, only a small percentage of the channel population must have their opening prolonged to increase the depolarising after-potential to the threshold level for repetitive nerve excitation. A minimum effective concentration of 100nM tetramethrin modifies 0.62% of channels in Purkinje neurons, which is sufficient to initiate the discharges causing hyperexcitation in animals (Song and Narahashi, 1996b). This fraction can be increased if channels are kept open for an

extended period. Tail currents following multiple depolarisations that continually activate channels, have larger peak currents than those following a single depolarisation of equal duration. This has lead to the proposal that pyrethroids bind preferentially to the channel open state (Vais *et al.*, 2000).

Binding studies have provided further information on the interaction of pyrethroids with the sodium channel and the effect they have on the functioning of the protein. Studies on the effects of pyrethroids in conjunction with other neurotoxins on sodium channels suggested a pyrethroid-specific binding site, designated Site 6 (Lombet *et al.*, 1988). Although pyrethroids alone have no effect on radio-labelled sodium ion uptake into mammalian brain synaptosomes, they do enhance uptake in the presence of the alkaloid neurotoxins veratridine and batrachotoxin. Pyrethroids are also thought to enhance the binding of an analogue of batrachotoxin, BTX-B, to the sodium channel. This suggests that the pyrethroids have a distinct binding site separate from other ligand binding sites but that there is allosteric coupling between the two sites. A potent pyrethroid radioligand has now been used to directly labelled site 6 and this has confirmed both the high affinity binding to the brain sodium channel and the allosteric coupling to other binding domains predicted by the BTX-B studies (Trainer *et al.*, 1997).

Despite the extensive studies reviewed above, the number of pyrethroid binding sites in the sodium channel remains unclear. Deltamethrin dose response relationships from the *para* wild type insect channel of *Drosophila melanogaster*, suggest that there are two binding sites, one of which is lost through the introduction of resistance mutations in the S6 segment and the S4-S5 linker of domain II (Vais *et al.*, 2000). This is supported by

similar resistance mutation studies where a number of residue changes in distant regions of the intracellular side of the protein affect pyrethroid potency and could therefore be part of potential binding sites (e.g. Liu *et al.*, 2002). Other electrophysiological studies with dorsal root ganglion neurons and biochemical studies using mammalian brain sodium channels suggest the presence of only one pyrethroid binding site per channel protein (Soderlund *et al.*, 2002).

1.15 The pyrethroid sensitivity of different types of sodium channel

The low toxicity of pyrethroids to mammals is thought to be, in part, a consequence of the insensitivity of their sodium channel proteins. A number of highly homologous but distinct sodium channel genes have been isolated from mammals (Goldin, 1999) and heterogeneity is introduced by alternative mRNA splicing (Gustafson *et al.*, 1993). These different isoforms, found in specific tissues, show varying degrees of sensitivity to the insecticide. Drosophila melanogaster, in contrast, appear to have only two single sodium channel α-subunit genes, *DSC1* (Salkoff *et al.*, 1987) and *para* (Loughney and Ganetzky, 1989) although only the *para* gene product has a known physiological role (Wu and Ganetzky., 1980).

Sodium channels that are differentially sensitive to the toxin tetrodotoxin TTX also show differential sensitivity to pyrethroids. TTX-resistant channels are far more sensitive to the pyrethroids allethrin, tetramethrin and deltamethrin than TTX-sensitive channels (Ginsburg and Narahashi, 1993; Song and Narahashi 1996a; Tabarean and Narahashi, 1998).

Further electrophysiological studies have found the rat brain IIA channel is comparatively insensitive compared to the insect *para* sodium channel to several Type I pyrethroids (Smith and Soderlund, 1998). Tetramethrin did not initiate or propagate the T syndrome characteristic of Type I pyrethroid poisoning despite direct injection into the rat brain (Gray and Soderlund, 1985). This suggests that whole body mammalian sensitivity is conferred by different sodium channels to those found in abundance within the adult brain.

Other sodium channel isoforms which have been tested in the oocyte expression system for their pyrethroid sensitivity include the rat SNS/PN3 channel which is preferentially expressed in the peripheral nervous system and is highly resistant to TTX (Akopian *et al.,* 1996; Sangameswaren *et al.,* 1996). In contrast to rat brain IIA sodium channels, rat SNS/PN3 channels are highly sensitive to both Type I and Type II pyrethroids, with the SNS/PN3 threshold concentration of cypermethrin-dependent modification being over 60-fold lower than the concentration needed to modify rat IIA channels (Smith and Soderlund, 2001).

In vitro, the sensitivity of the rat IIA channel to pyrethroids varies depending on whether it is expressed singly, or in conjunction with the β1 subunit. The α-subunit alone is sensitive to modification by cypermethrin and this identifies it as being the primary pyrethroid binding site. However, sensitivity is increased over 20-fold if the larger α-

subunit is co expressed with β1, suggesting an allosteric effect on pyrethroid binding sites when the channel complex consists of both subunits (Smith and Soderlund, 1998).

1.16 The effect of temperature on sodium channel sensitivity to pyrethroids

Temperature has a significant effect on the activity of DDT and pyrethroids on nerve preparations with sensitivity to these insecticides being increased at lower temperatures (Stakus and Narahashi, 1978). Analysis of tetramethrin-induced tail currents indicates that the percentage of channels modified by the insecticide is slightly increased when the temperature is lowered from 35°C to 25°C. The rate of tail current decay is slowed and the peak current is increased as the temperature lowers (Song and Narahashi, 1996b).

It has been suggested that the increase in pyrethroid potency at lower temperatures is the result of reduced degradation and this may be the basis for its selective toxicity, as the rate of enzymatic degradation of the insecticide within endothermic mammals will be greater than in poikiothermic insects. Although enzymatic detoxification of pyrethroids certainly contributes to the reduced sensitivity of mammals, for the 10°C temperature difference the rate of enzymatic detoxification is estimated to be only three times faster than in invertebrates (Bradbury and Coats, 1989).

1.17 Pyrethroid target sites other than the voltage-gated sodium channel.

Pyrethroids have been shown to act at three other target sites that may contribute to intoxication *in vivo*. Some isoforms of the mouse voltage-gated calcium channel are blocked by Type I pyrethroids (Yoshii *et al.*, 1985) and in housefly thoracic neurons, L

and T type calcium channels react differently to treatment with the Type II pyrethroid, deltamethrin (Duce *et al.*, 1999). In a response to deltamethrin similar to the TTX-sensitive sodium current, the voltage dependence of activation of T-type calcium current is shifted in the hyperpolarizing direction. Additionally, deltamethrin causes an increase in the frequency of spontaneous oscillations of internal Ca^{2+}, and enhances the amplitude of the depolarisation-induced increase in Ca^{2+} (Duce *et al.*, 1999). The external flux of voltage-sensitive calcium channels located in the presynaptic nerve terminal is responsible for the highly organised release of neurotransmitters (Llinas, 1982). Modification of the calcium current by pyrethroid insecticides may in turn result in the enhanced release of neurotransmitters associated with pyrethroid intoxication (Doherty *et al.*, 1986).

Blockage of voltage-gated chloride channels by some pyrethroids is associated with the profuse salivation characteristic of Type I pyrethroid poisoning i.e. the CS intoxication syndrome (Ray *et al.*, 1999). Furthermore, the enhanced convulsions caused by the action of the insecticide at these voltage-gated ion channels may be enhanced by the concurrent effect of pyrethroids on peripheral-type benzodiazepine receptors located in non-neuronal tissues (Devaud and Murray, 1988). Other putative sites identified *in vitro* as targets for pyrethroid action, do not appear to contribute significantly to whole animal pyrethroid intoxication. The aminobutyric acid receptor (GABA receptor) –chloride ionophore complex, an important mediator of inhibitory neurotransmission in the mammalian nervous system, and the nicotinic acetylcholine receptors, mediators of fast excitatory transmission, have both been highlighted as possible pyrethroid target sites (Lawrence and Casida, 1983; Abbassy *et al.*, 1982). However, modification of these

complexes has not been observed at the low concentrations known to significantly disrupt sodium channel function (Soderlund *et al.*, 2002)

1.18 The use of pyrethroids and occurrence of resistance

Widespread, intensive use of pyrethroid insecticides since the early 1970s has led to numerous instances of genetic resistance in target insects. This now poses significant risks and challenges for the control of vectors of infectious disease and agricultural pests (Georghiou, 1990).

Resistance is an evolutionary process, arising through the selection of low-frequency mutations that confer a survival advantage. These may reduce the penetration of the toxicant, increase its rate of metabolic detoxification or reduce the sensitivity of the target site. All three mechanisms are illustrated in some pyrethroid-resistant strains of the housefly *Musca domestica*, which have reduced cuticular penetration, enhanced oxidative metabolism and reduced neuronal sensitivity. These flies are approximately 6000-fold more resistant to permethrin than their wild type counterparts (Scott and Georghiou, 1986).

Reduction in neuronal sensitivity to pyrethroids was first identified in houseflies and was termed 'knockdown resistance' or kdr because it resulted in the ability to resist or delay the rapid 'knockdown' paralysis usually observed after pyrethroid or DDT exposure (Busvine 1951). Subsequent work showed kdr to be conferred by a single gene on autosome 3 (Farnham, 1977; Farnham, 1987), and identified other putative allelic variants including the more potent super-kdr factor (Sawicki 1978). Kdr confers

moderate levels of resistance (10-30 fold) to Type I pyrethroids and Type II pyrethroids (Farnham *et al.*, 1987a)b), while super-kdr confers up to 500-fold resistance to Type II pyrethroids (Farnham and Khambay, 1995) and slightly enhanced resistance (50-fold) to Type I pyrethroids. Restriction fragment length polymorphisms of the Msc sodium channel gene in houseflies, which has close homology to the *para* gene of *Drosophila melanogaster*, were identified in kdr, super-kdr and susceptible strains and shown to co-segregate with resistance in controlled crosses involving these strains, indicating that the genetic basis of resistance was located at this gene locus (Williamson *et al.*, 1993).

1.19 Mapping and identification of the kdr and super-kdr mutations.

Subsequent cloning and sequencing of the sodium channel gene from different housefly strains containing the kdr and the more potent super-kdr variation, revealed two amino acid substitutions that correlated with the resistant phenotypes. A leucine to phenylalanine replacement (L1014F) in the hydrophobic D2S6 transmembrane segment was found in two independent kdr strains and six super-kdr strains of diverse geographical origin, while an additional methionine to threonine replacement (M918T) within the intracellular D2S4-S5 loop was found only in super-kdr strains (Williamson *et al.*, 1996).

The same kdr leucine to phenylalanine mutation has since been identified in a range of other insect species including pyrethroid resistant strains of the peach potato aphid *Myzus persicae* (Martinez-Torres *et al.*, 1999), the German cockroach *Blattella germanica* (Miyazaki *et al.*, 1996; Dong *et al.*, 1997), the malaria transmitting mosquito *Anopheles gambiae* (Martinez-Torres *et al.*, 1998), the tobacco budworm *Heliothis*

virescens (Park *et al.*, 1997) the diamondback moth *Plutella xylostella* (Schuler *et al.*, 1998), and the horn fly *Haematobia irritans* (Guerrero *et al.*, 1997). The super-kdr mutation has been found in conjunction with the kdr in housefly (Williamson *et al.*, 1996) and horn fly (Guerrero *et al.*, 1997) (Figure 1.6). This suggests a common mechanism for this type of resistance between species.

Both the kdr and super-kdr mutations map to the intracellular mouth region of the channel pore, a site consistent with the known role of pyrethroids in modifying channel gating. Other resistance mutations have been found in the same region. A T929I mutation has been found in conjunction with the kdr mutation in a pyrethroid resistant strain of *Plutella xylostella* (Schuler *et al.*, 1998) and in conjunction with an L932F mutation in headlice, *Pediculus capititus* (Lee *et al.*, 2000). Resistance mutations have also been located in other regions of the channel, indicating that kdr, super-kdr and other domain II mutations are not the only amino acids affecting binding or pyrethroid action.

Resistance mutations found in field populations have been located in the D3S6 transmembrane segment of the cattle tick *Boophilus microplus* (He *et al.*, 1999) and the D1-D2 linker in *Blattella germanica* (Liu *et al.*, 2002). In addition certain *para* mutant strains of *Drosophila melanogaster* have amino acid changes located within the S5 and S6 transmembrane segments of domains I and III and the S4-S5 and S5-S6 intracellular loops that connect them (Pittendrigh *et al.*, 1997) (Figure 1.6). One interpretation of these data is that the kdr and super-kdr sites do not form the pyrethroid binding site in isolation but act in conjunction with other amino acids highlighted by resistance mutations located in the three remaining domains. However, detection of these resistance mutations in Domain I and III in wild pest populations is probably rare

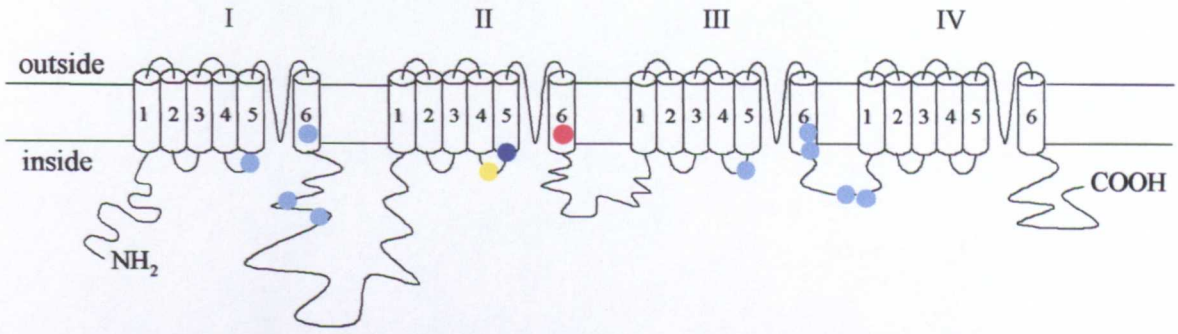

Insect	Strain	Super-kdr 918 mutation ●	Super-kdr 929 mutation ●	Kdr 1014 mutation ●	Mutations outside domain II ●	Location	Ref.
M. domestica	Kdr			L1014F		IIS6	19
M. domestica	Super-kdr	M918T				IIS4-S5	19
B. germanica	VT ectoban-R			L1014F		IIS6	11
H. irritans	Kdr			L1014F		IIS6	2
H. irritans	Super-kdr	M918T		L1014F		IIS4-S5	2
H. virscens	Field			L1014H		IIS6	13
A gambiae	Field			L1014F		IIS6	8
A gambiae	Field			L1014F L1014S		IIS6	16
P. xylostella	FEN		T929I	L1014F		IIS4-S5	17
L. decemlineata	PE-R			L1014F		IIS6	5
M. persicae	E4-types			L1014F		IIS6	10
C. pipiens	PERM			L1014F		IIS6	9
C. pipiens	CHANG			L1014S		IIS6	9
P capititis	Bristol		T929I			IIS4-S5	6
B. tabaci	GRB	M918V				IIS4-S5	12
B. tabaci	AZ-R		L925I			IIS4-S5	12
B. tabaci	LNFU		T929V			IIS4-S5	21
A. gossypii	Adana	M918L				IIS4-S5	20
H.virescens	Field				V410M	IS6	14
D. melanogaster	Para-ts1				I265N	IS4-S5	15
D. melanogaster	Para-DN7				A1414V	IIIS4-S5	15
D. melanogaster	Para-74				M1528I	IIIS6	15
H. amigera	JSFX				D1561V E1565G	III-IV linker	4
H.virescens	NIR				D1561V E1565G	III-IV linker	4
B. microplus	MP				F1541I	IIIS6	3
B. germanica					E434K C764R	I-II linker	7 18

Figure 1.6. Location of pyrethroid resistance mutations found in field and laboratory insect strains.

1. Dong, K. (1997) A single amino acid change in the *para* sodium channel protein is associated with knockdown resistance (kdr) to pyrethroid insecticides in German cockroach. *Insect Biochemistry and Molecular Biology* **27**:93-100

2. Guerrero, F.D., Jamroz, R.C., Kammlah, D. and Kunz, S.E (1997) Toxicological and molecular charaterization of pyrethroid-resistant, *Haematobia irritans*: Identification of kdr and super-kdr point mutations. *Insect Biochemistry and Molecular Biology* **27**:745-755.

3. He, H.Q., Chen, A.C., Davey, R.B., Ivie, G.W. and George, J.E. (1999) Identification of a point mutation in the *para*-type sodium channel gene from a pyrethroid-resistant cattle tick. *Biochemical and Biophysical Research Communication* **261**:558-561.

4. Head, D.J., McCaffery, A.R., and Callaghan, A. (1998) Novel mutation in the *para*-homolgous sdoium channel gene associated with phenotypic expression of nerve insensitivity resistance to pyrethroids in *Heliothine lepidoptera Insect Molecular Biology* **7**:191-196.

5. Lee, S.H., Dunn, J.B., Clark, J.M. and Soderlund, D.M. (1999) Molecular analysis of kdr-like resistance in a permethrin resistant strain of Colorado potato beetle. *Pesticide Biochemistry and Physiology* **63**:63-75.

6. Lee, S.H., Yoon, K.S., Willimson, M.S., Goodson, S.J. Takano, M, Edman, J.D., Devonshire, A.L., and Clark, J.M. (2000) Molecular analysis of kdr-like resistance in permethrin-resistant strains of head like, *Pediculus capitis*. *Pesticide Biochemistry and Physiology* **66**:130-143.

7. Liu, Z.Q., Valles, S.M. and Dong, K. (2000). Novel point mutations in the German cockroach *para* sodium channel gene are associated with knockdown resistance (kdr) to pyrethroid insecticides. *Insect Biochemistry and Molecular Biology* **30**:991-997.

8. Martinez-Torres, D., Chandre, F., Williamson, M.S., Darriet, F., Berge, J.B., Devonshire, A.L., Guillet, P., Pasteur, N. and Pauron, D. (1998) Molecular characterization of pyrethroid knockdown resistance (kdr) in the major malaria vector *Anopheles gambiae* S.S. *Insect Molecular Biology* **7**:179-184.

9. Martinez-Torres, D., Chevillon, C., BrunBarlae, A., Berge, J.B., Pasteur, N. and Pauron, D. (1999a) Voltage-dependent Na^+ channels in pyrethroid-resistant *Culex pipiens L* mosquitoes. *Pesticide Science* **55**:1012-1020.

10. Martinez-Torres, D., Foster, S.P., Field, L.M., Devonshire, A.L. and Williamson, M.S. (1999b) A sodium channel point mutation is associated with resistance to DDT and pyrethroid insecticides in the

peach-potato aphid, *Myzus persicae* (Sulzer) (Hemiptera: *Aphididae*). *Insect Molecular Biology* **8**:339-346.

11. Miyazaki, M., Ohyama, K., Dunlap, D.Y. and Matsumara, F. (1996) Cloning and sequencing of the *para*-type sodium channel gene from susceptible and kdr-resistant German cockroaches (*Blattella germanica*) and housefly (*Musca domestica). Molecular & General Genetics* **252**:61-68.

12. Morin, S., Williamson, M.S., Goodson, S.J., Brown, J.K., Tabashinik, B.E. and Dennehy, T.J. (2002). Mutations in the *Bemisia tabaci* sodium channel gene associated with resistance to pyrethroid plus organophosphate mixture. *Insect Biochem. Mol. Biol.* In Press.

13. Park, Y. and Taylor, M.J.F. (1997) A novel mutation L1029H in sodium channel gene hscp associated with pyrethroid resistance for *Heliothis virescens* (Lepidoptera:Nocituidae). *Insect Biochemistry and Molecular Biology* **27**:9-13.

14. Park, Y. and Taylor, M.J.F. and Feyereisen, R. (1997) A valine 421 to methionine mutation in IS6 of the hscp voltage-gated sodium channel associated with pyrethroid resistance in *Heliothis virescens* F. *Biochemical and Biophysical Research Communications* **239**:688-691.

15. Pittendrigh, B., Reenan, R., ffrench-Constant, R.H. and Ganetzky, B (1997) Point mutations in the *Drosophila* sodium channel gene *para* associated with resistance to DDT and pyrethroid insecticides. *Molecular and General Genetics* **256**:602-610.

16. Ransom, H., Jensen, B., Vulule, J.M. Wang, X., Hemingway, J. and Collins, F.H. (2000). Identification of a point mutation in the voltage-gated sodium channel gene of Kenyan *Anopheles gambiae* associated with resistance to DDT and pyrethroids. *Insect Molecular Biology* **9**:491-497

17. Schuler, T.H., Martinez-Torres, D., Thompson, A.J., Denholm, I., Devonshire, A.L. Duce, I.R. and Williamson, M.S. (1998) Toxicological, electrophysiological and molecular characterization of knockdown resistance to pyrethroid insecticides in the diamondback moth, *Plutella xylostella* (L.). *Pesticide Biochemistry and Physiology* **59**:169-182.

18. Tan, J., Liu, Z., Tsai, T.D., Valles., S.M., Goldin, A.L., and Dong, K. (2002). Novel sodium channel gene mutations in *Blatella germanica* reduce the sensitivity of expressed channels to deltamethrin. *Insect Biochemistry and Molecular Biology* **32**: 445-454.

19. Williamson, M.S., Martinez-Torres, D., Hick, C.A. and Devonshire, A.L. (1996). Identification of mutations in the housefly *para*-type sodium channel gene associated with knockdown resistance (kdr) to pyrethroid insecticides. *Molecular & General Genetics* **252**:51-60.

20. Yang, X., Denholm, I. And Williamson, M.S. (2002). A novel mutation in the *para*-type sodium channel of *Aphis gossypii* that confers resistance to pyrethroids but not DDT. Manuscript in preparation.

because they have a fitness cost. All aspects of electrical signalling in the nervous system are mediated by sodium channel function, hence mutations that even slightly impair the normal activity of these channels are likely to have adverse effects and would therefore not be maintained unless the disadvantages are outweighed by the selective advantages conferred by resistance.

Equally, changes in the usual kinetic behaviour of the channel may be the mechanism by which resistance to pyrethroids and DDT is conferred, rather than by a direct alteration of the binding site (Pittendrigh *et al.*, 1997). The pharmacological effect of these insecticides is to cause persistent activation of the sodium channel by delaying the normal voltage-dependent inactivation and deactivation (Soderlund and Bloomquist, 1990). Mutations may therefore confer resistance by altering the kinetic behaviour of the channel and thereby countering the gating modifications induced by pyrethroid action (Pittendrigh *et al.*, 1997). Mutations within the S5 segment of domain II, the S4-S5 loop of domain III and the S6 segment of domain IV, have previously been shown to affect sodium channel inactivation and cause the skeletal muscle disorder hyperkalemic periodic paralysis (Ptacek *et al* 1991; McClatchey *et al.*, 1992; Rojas *et al.*, 1991). Analogous mutations in insect channels may confer similar kinetic changes, but rather than cause the debilitating effect of momentary paralysis, they may reduce or override the neurotoxic effects of the insecticide by offsetting the gating changes it generates.

Until recently, all strains of pyrethroid-resistant insects with the super-kdr methionine to threonine mutation have also had the kdr leucine to phenylalanine mutation (Williamson *et al.*, 1996, Guerrero *et al.*, 1997). A further super-kdr like mutation, T929I, detected in

the diamond back moth *Plutella xylostella* and human head lice *Pediculus humanus capitis* is also found in conjunction with kdr mutations (L1014F and L932F respectively) (Schuler *et al.*, 1998; Lee *et al.*, 2000). Furthermore, mutations found in the D1-D2 linker of *Blattella germanica* only confer high levels of deltamethrin resistance if they similarly, are co expressed with the domain II kdr leucine to phenylalanine mutation (Tan *et al.*, 2002). However, super-kdr mutations have now been found in the absence of the kdr. Substitution of the wild type methionine at the super-kdr position with valine or leucine is thought to confer pyrethroid resistance in *Bemisia tabaci* and *Aphis gossypii* respectively (Morin *et al.*, 2002, Yang *et al.*, personal communication).

1.20 Electrophysiological studies of the kdr and super-kdr mutation

Voltage clamp experiments on oocytes expressing mutated and wild type voltage-gated sodium channels have clarified the kinetic changes that the resistance mutations confer. Initial studies of rat channels expressing the kdr mutation, detected a sizable shift of the steady-state activation towards a more positive membrane potential, which would counter the relatively small negative shift induced by permethrin (Vais *et al.*, 1997). Subsequent studies of the L1014F kdr mutation in *Drosophila melanogaster para* sodium channels showed that the voltage dependence of activation and inactivation shifted by ~5mV towards more positive potentials. Channels are therefore less likely to activate following a depolarising potential and this may manifest itself in the sluggish response of the phenotype. However, in combination with the super-kdr, no change in the voltage dependence of activation was recorded (Vais *et al.*, 2000). This is found in

other resistance mutations where the gating kinetics of one mutation are neutralised by the co-expression of another (Tan *et al.*, 2002).

Where resistance mutations have been electrophysiologically characterised, they show a reduction in the peak tail current and acceleration in the rate of tail current decay, reflecting the reduced effect of the pyrethroid (Smith *et al.*, 1997; Vais *et al.*, 2000; Zhao *et al.*, 2000). The basis of this reduction is the consequence of a reduction in the number of channels entering the open state to which pyrethroids preferentially bind, and a reduction in the affinity between the protein and insecticide (Vais *et al.*, 2000).
Further exploration of the structural nature of this reduction in affinity will be fundamental to the design of future pyrethroid insecticides effective against increasingly resistant insect pests.

1.21. Aims and objectives of the project

(1) Using voltage clamp to determine whether a super-kdr mutation (M918V) found alone in a pyrethroid resistance strain of *Bemisia tabaci* can confer pyrethroid insensitivity to the *Drosophila para* sodium channel, and if so, by what mechanisms. (Chapter 3)

(2) Using voltage clamp to compare the pyrethroid sensitivity conferred on the *para* sodium channel by a super-kdr mutation (T929V), found in a pyrethroid resistant strain of *Bemisia tabaci*, and a T929M mutation, which when expressed at the

equivalent residue site in human skeletal muscle sodium channels causes the condition hyperkalemic periodic paralysis (Chapter 4).

(3) Using voltage clamp and pyrethroid chemistry to investigate the basis of the relative insensitivity to pyrethroids of the mammalian rat brain IIA sodium channel when compared with the relative sensitivity of the insect *para* sodium channel. (Chapters 5 and 6)

(4) To develop a rapid screening technique for detection of the kdr (L1014F) and super-kdr (M918T) mutations and other possible resistance mutations in different *Musca domestica* field populations. (Chapter 7)

CHAPTER 2

MATERIALS AND METHODS

2.1 Materials

2.1.1 Chemicals

Cis Deltamethrin [(S)-α-cyano-3-phenoxybenzyl (1R, 3R)-3-(2,2-dibromovinyl)-2,2-dimethylcyclopropanecarboxylate], 1R-cis Permethrin [3-phenoxybenzyl (1RS, 3RS; 1RS, 3SR)-3-(2,2-dichlorovinyl)-2,2-dimethylcyclopropanecarboxylate], Etofenprox [2-(4-ethoxyphenyl) -2-methylpropyl 3-phenoxybenzyl ether] and 10042, were purchased either from the Crescent Corporation. (U.S. distributor for Riedel-de Haen) or had been synthesised in house at Rothamsted. Stock solutions between 1μM and 10mM were made with absolute ethanol and dilutions were made with ND96 bath solution (see below).

The isoleucine isoform of toxin II from *Anemonia sulcata* (ATX-II) was obtained from Calbiochem Corporation.

2.1.2 Houseflies

Housefly *Musca domestica* strains Cooper (susceptible), 579 (kdr) and 530 (super-kdr) were standard strains, which had been selected at Rothamsted.

Cooper is a reference insecticide-susceptible strain. It lacks visible markers and is homozygous for the wild type allele at both kdr & super-kdr loci. Strains 579 and 530 are homozygous for the expression of kdr and super-kdr resistance phenotypes. They were obtained by transferring alleles conferring these phenotypes from multimarked strains into a common genetic background by repeated backcrossing to Cooper flies, followed by re-selection for pyrethroid resistance (Farnham *et al.*, 1987). Molecular analyses have shown that 579 contains a single mutation

(L1014F) in domain IIS6 of the para-type sodium channel. 530 also contains this mutation together with an additional M918T mutation in the IIS4-IIS5 linker region of the channel protein (Williamson *et al.*, 1996).

Houseflies were maintained at 28°C with a 12 hour photoperiod. Adults were held in rearing cages and fed on water, sugar and fresh milk. The life-cycle lasted for two weeks. Strains were checked regularly for resistance status by members of the Insecticide Resistance Group. (Rearing undertaken by Mr. M. Collins, and Mr. M Hedges, Rothamsted).

Other housefly strains More, Pax, New and Rail were established from samples collected from pig houses of four different farms. All flies were dosed with a diagnostic dose of 0.016% pyrethrin and 0.1% piperonyl butoxide and scored as either dead (i.e. KD = knocked down) or alive (Survivors) (Collection and bioassays undertaken at MAFF-Central Science Laboratory, York). These were then frozen individually in plastic tubes using liquid nitrogen, transported to Rothamsted on dry ice and stored at -80°C.

2.1.3 Cloned DNA sequences

The cDNA clone pGH19-13-5, containing the full coding sequence of the *Drosophila para* sodium channel gene was provided by Dr J. Warmke, Merck Research Laboratories. The TipE construct was generated previously at Rothamsted by PCR amplification of the tipE gene coding sequence from *Drosophila melanogaster* cDNA cloned into the pGH19 T7 transcription vector (as described in Vais *et al.*, 2000).

The rat brain sodium channel gene construct (pVA2580) and the rat β1 gene construct were provided by Dr. C. Labarca, California Institute of Technology, and Dr T. Tanada, University of Washington, respectively.

2.1.4 Oligonucleotide Primers

Oligonucleotide primers for site directed mutagenesis and sequencing were bought commercially from MWG-Biotechnology Ltd.

2.2 Molecular Biology

2.2.1 Site Directed Mutagenesis

Site directed mutagenesis of sodium channel gene constructs was carried out using the Quikchange Site Directed Mutagenesis kit (Stratagene). All procedures were carried out according to the manufacturer's instructions (Figure 2.1 for overview). Briefly, 50ng of the chosen sodium channel construct was added to 125ng each of the forward and reverse primer (Appendix 1) with 5μl of 10x reaction buffer (100mM KCl, 100mM (NH_4) 2SO4, 200mM Tris-HCl (pH 8.8), 20mM $MgSO_4$, 1% Triton X-100, mg/ml nuclease-free BSA), 1μl 10mM dNTP mix and 0.2U/μl PfuTurbo DNA polymerase in a reaction volume of 50μl. The PfuTurbo polymerase incorporates the mutagenic primers into nicked circular strands, which were amplified by thermal cycling. Each cycle consisted of 95°C for 30sec (denaturation) 55°C for 60secs (primer annealing), 68°C for 12mins (extension) and was repeated 16 times. The non-mutated parental DNA template was then destroyed by digestion for 2 hours at

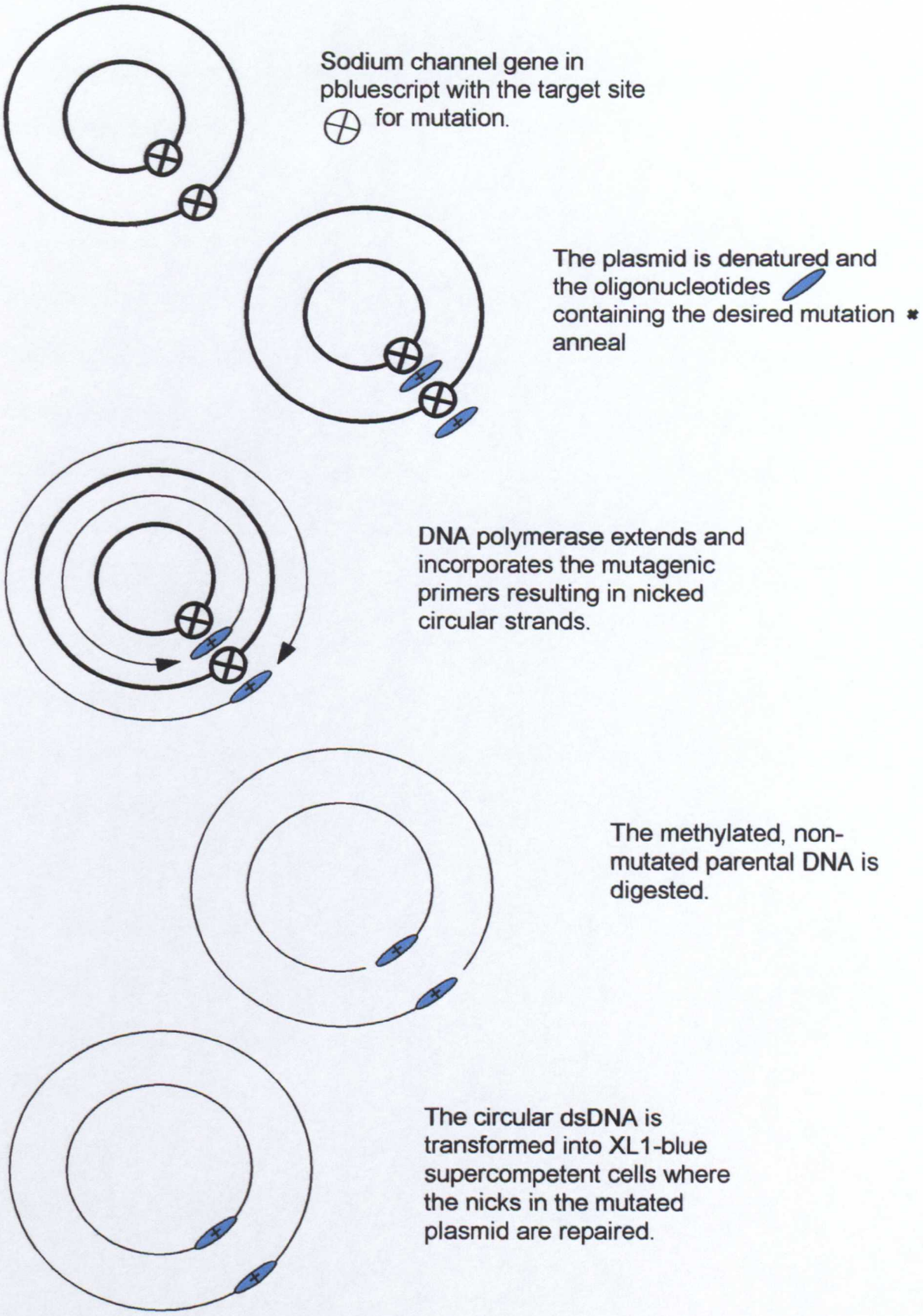

Figure 2.1 Overview of site directed mutagenesis applied to the sodium channel gene

(adapted from Stratagene Quikchange mutagenesis manual)

37°C using Dpn 1 and the remaining mutated dsDNA transformed into XL1- Blue supercompetent cells

2.2.2 Transformation.

Plasmid DNA (either 10pg of supercoiled plasmid or 1µl Dpn-1 digested SDM reaction mix) was used to transform 50µl aliquots of XL1-Blue supercompetent cells (Stratagene) according to the manufacture's instructions. Cells and plasmids were incubated on ice of 30 min, heat-shocked for 45sec at 42°C and then returned to ice for a further 2min. 0.5ml of NYZ+ broth (10g of NZ amine (caesein hydrolysate); 5g of yeast extract; 5g NaCl; 125mM $MgCl_2$; 125mM $MgSO_4$; 200mM glucose made up to 1L with distilled H_20) heated to 42°C was added to the transformation reaction and incubated at 30°C for 2h with shaking at 225-250rpm. The relatively low incubation temperature reduces both the probability of rearrangement and expulsion of these large recombinant plasmids from the bacterial host cells. Cells transformed with *Drosophila* TipE or rat β1 constructs were incubated at 37°C for 1h. Transformed cells were then recovered by plating 100µl aliquots onto agar plates containing the antibiotic Ampicillin at a concentration of 50mg/l as a selective antibiotic. Plates were incubated at 30°C for 24hrs to allow small, distinct colonies to develop.

2.2.3 Cell culture

Single colonies were subcultured into 2ml of 2xYT broth (16g tryptone, 10g yeast extract, 5g NaCl and 50mg ampicillin made up to 1litre distilled H_2O) in 10ml sterile test tubes. They were incubated at 30°C for 24hrs with vigorous shaking (225-250 rpm). Cultures were either used for small-scale plasmid extraction (minipreps) or

0.5ml was used to inoculate 50ml cultures that were incubated for a further 16 hrs (midiprep).

2.2.4 Plasmid extractions

Plasmid DNAs were extracted from either 2ml or 50ml cultures using Qiagen Miniprep or Midiprep kits respectively. The procedure was carried out following the manufacture's instructions. Briefly, pelleted cells were resuspended in P1 buffer, lysed using P2 lysis buffer for 1min only (longer lysis releases bacterial DNA) and neutralised with buffer N3. The mixture was then spun for 10min at 10 000 rpm to pellet cell debris. The supernatant was passed through a column that captured plasmid DNA, which was then released with warmed elution buffer.

2.2.5 Linearisation and purification of plasmid DNA.

Wild type and mutated plasmids were linearised using the appropriate restriction endonucleases (10U µg-1 DNA) in 1x buffer (Appendix 2) at 37°C for 1-2hrs. The restriction endonucleases were then degraded using Proteinase K (in 0.5% SDS) at 65°C for 30mins. Plasmid DNA was recovered by extraction with an equal volume of phenol/chloroform mix and then precipitated with 0.1 volume 3M sodium acetate (pH 5.5) and 2 volumes absolute ethanol at -20°C for 2hrs followed by a centrifugation at 14 000rpm at 4°C for 20mins. The resulting pellet was washed with 70% ethanol, air dried for 1hr at room temperature and resuspended in DEPC treated water.

2.2.6 *Transcription of sodium channel templates*

Transcripts were synthesised from the T7 promoter using the mMessage mMachine kit (Ambion). A 20μl reaction containing 1ug linear template DNA, 2μl 10x reaction buffer (salts, buffer, dithiothreitol, and other ingredients), 10μl 2x NTP/Cap (15mM ATP, 15mM CTP, 15mM UTP, 3mM GTP, 12mM cap analogue), 1μl supplementary GTP (30mM) and 2μl enzyme mix (RNA polymerase) was incubated for 2 hrs at 37°C. Following transcription, the DNA template was digested for 15mins at 37°C using DNase 1and RNA extracted with an equal volume of phenol/chloroform (1:1) and then re-extracted with an equal volume of chloroform. RNA was precipitated by addition of isopropanol and incubating at -20°C for 1hr. RNA was pelleted by centrifugation at 14000rpm at 4°C for 20 mins. The pellet was washed in 70% ethanol, air dried for 10mins and resuspended in 10μl DEPC treated water to be stored at -80°C until ready for use. The integrity and yield were checked by running 0.5μl of the sample on a denaturing agarose gel.

2.2.7 *Genomic DNA extraction from houseflies*

Genomic DNA was extracted from adult houseflies using the Nucleon Phytopure DNA extraction kit (Scotlab Bioscience) following the manufacturer's instructions.
A quicker and cheaper method was to freeze individual fly heads in liquid nitrogen, then boil each one singly in 10μl single colony lysis buffer (20Mm Tris pH 8.5; 2mM EDTA; 1% Triton X-100) for 10mins and then spin at 12 000rpm for 5minutes at room temperature. This released sufficient gDNA for PCR amplification from 2μl aliquots of the supernatant.

2.2.8 PCR amplification with Genomic DNA templates

Primary PCR amplifications were done in 50µl reactions containing 25-100ng of gDNA, 1x DyNAzyme reaction buffer (10mM Tris-HCl pH 8.8; 1.5mM $MgCl_2$; 50mM KCl and 0.1% Triton X-100), dNTPs (0.2mM of each), sense and antisense primers (200ng of each) (Appendix 3) and DyNAzyme II DNA Polymerase (2U) (Flowgen, UK) using a thermal cycler with heated lid (Eppendorf Mastercycler Gradient, Techne Progene or Hybaid Omnigene). A 'hot start' of 94°C for 2mins was incorporated at the beginning of the cycling program. DyNAzyme II DNA polymerase was subsequently added at a holding temperature of 80°C to reduce the probability of non-specific template/primer annealing and to ensure that the DNA was fully denatured. Each cycle consisted of 95°C for 40sec (denaturation) 52-60°C for 40secs (primer annealing), 72°C for 40sec (extension) and there were 35 cycles before ending with a final extension of 72°C for 10mins.

1µl of the primary PCR product was taken into a 50µl secondary reaction. The reaction mix was identical to that of primary mix except nested primers (Appendix 3) were used to increase the specificity of the amplification. The cycle parameters were the same as those of the primary reaction and were repeated 25 times, again starting with a hot start and ending in a 10min extension at 72°C.

The PCR products were electrophoresed in 1.5-2% agarose gel and stained with ethidium bromide alongside standards, to estimate the size and quantity of product (Section 2.2.13). Samples were stored at -20°C.

2.2.9 Single Stranded Conformational Polymorphism Analysis

SSCP (Single Stranded Conformational Polymorphism) detects differences in the base sequence of single stranded DNA fragments of equal size and charge when they are electrophoresed on a high percentage polyacrylamide or agarose gel. Base differences alter the secondary conformation that single stranded DNA adopts and this in turn affects the speed at which the fragments migrate through a gel. Fragments amplified from the super-kdr region of wild type flies and super-kdr flies only differ by one base. Wild type flies have thymine at the super-kdr locus while super-kdr flies have cytosine at the super-kdr locus and this difference can be detected using SSCP (Figure 2.2 for general overview).

50-100ng of secondary PCR product amplified from the super-kdr region of genomic housefly DNA was mixed with an equal volume of loading buffer (95% formamide, 20mM EDTA, 0.05% bromophenol blue, 50mM NaOH). Samples were denatured by boiling for 15mins and then snap chilled on ice. Denatured samples were separated on 10% polyacrylamide gels (5g glycerol; 7.5ml 10x TBE; 20ml 2% Bis acrylamide; 36.5ml 40% acrylamide; 25% APS, 50ul TEMED to 100ml with distilled water) run at 100V for 15 hours in 1x TBE buffer (40mM Tris acetate pH 8.0; 1.0mM EDTA) maintained at 6°C. The gel was then silver stained.

2.2.10 Silver staining of SSCP gels

The gels were fixed in 10% acetic acid for 10mins and washed 3 times for two minutes in distilled water and then stained for 10 mins in 0.5g silver nitrate/litre. They were then rinsed in distilled water and developed in 0.37mM NaOH, 4ml/litre formaldehyde with 100mg/litre sodium borohydride. The developing solution was

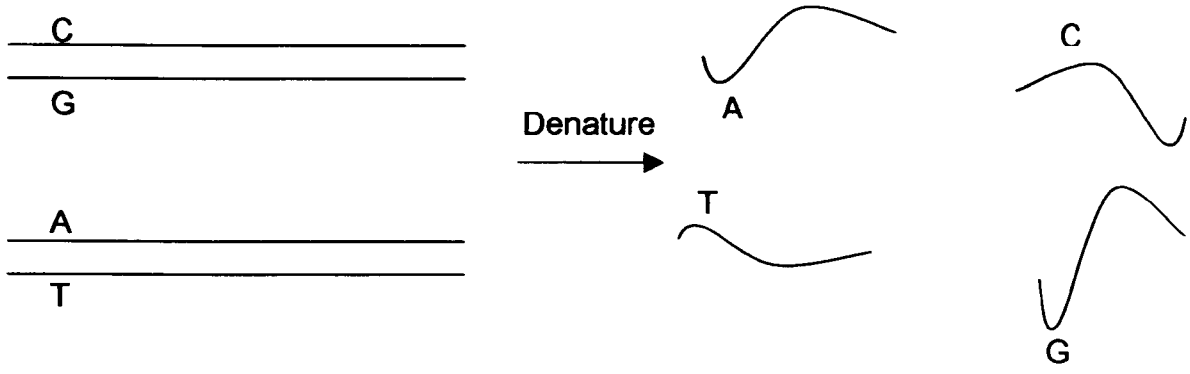

Sequences identical except for single base change.

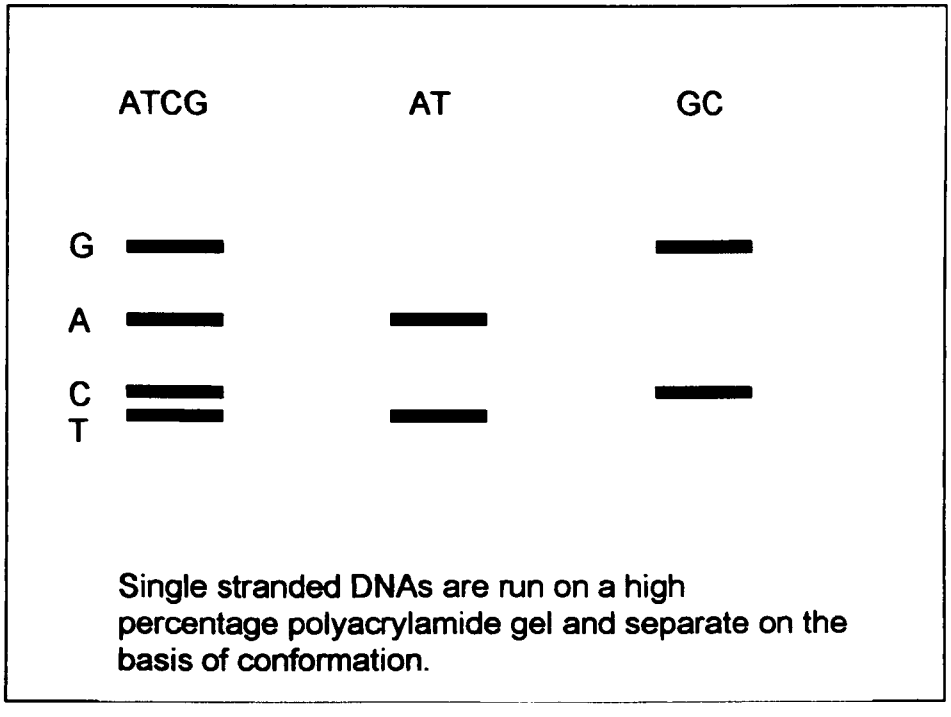

Figure 2.2. A general description of Single Stranded Conformational Polymorphism. Denatured single stranded DNA of equal size and charge adopts different conformations depending on the base change. These separate on high percentage polyacrylamide gel.

added in three aliquots; the first to remove excess silver, the second to develop slightly the background and the third to develop the DNA bands. When a clear brown banding pattern could be seen the developing solution was removed and a 10% acetic acid solution was added to stop the reaction. The gel was photographed using Ultra-violet Products Ltd, Cambridge package.

2.2.11 Diagnostic endonuclease digestion

The sequences of wild type and kdr flies differ such that the kdr mutation introduces a restriction site recognised by the endonuclease Tsp 509 I (Flowgen, UK). 50-100ng of secondary PCR product amplified from the kdr region of genomic housefly DNA was digested in a 20µl reaction mix with Tsp 501 (1U) and 1x Tsp 501 reaction buffer at 37°C for 2 hours. Digests were separated by agarose gel electrophoresis and the fragments visualised by ethidium bromide staining under UV light (Section 2.2.13)

2.2.12 Sequencing Reactions

Plasmid constructs and PCR products were sequenced using the Applied Biosystems BigDyeTM Terminator Cycle Sequencing Ready Reaction Kit, following the Supplier's protocol. A 20µl reaction containing template DNA (0.5µg plasmid DNA, or 30-90ng PCR product) were mixed with 30ng of the appropriate sequencing primer (Appendix 3), 8µl Terminator Ready Reaction Mix (A-Dye terminator; T-Dye terminator, C-Dye Terminator, G-Dye Terminator, dATP; dTTP; dCTP; dGTP; Tris-HCl ; pH 9.0; magnesium chloride, pyrophosphatase, AmpliTaqR DNA polymerase, FS) diluted with an equal volume of dilution buffer (final concentration 200mM Tris-HCl pH9.0; 5mM magnesium chloride). Each cycle consisted of 94°C

for 30secs, 50°C for 30secs, 60°C for 4mins and 25 cycles were used. Products were precipitated with 0.1 volumes of sodium acetate and 2 volumes of absolute ethanol at room temperature for 10mins (longer incubation at lower temperatures precipitates unincorporated dye terminators). Products were centrifuged for 15min at 14 000rpm at room temperature, wash in 70% ethanol and dried in a vacuum centrifuge for 10 mins. Samples were analysed using an ABI 310 Sequencer on site at Rothamsted. Sequence data files were analysed using the Staden and Wisconsin GCG software packages running on a UNIX server at Rothamsted, and accessed on PCs using Xwindows.

2.2.13 Agarose Gel Electrophoresis

The concentration, size and quality of DNA and RNA samples were established by agarose gel electrophoresis. 1µl of each RNA sample was mixed with 4µl distilled water and 5µl of 1 x loading buffer (95% Formamide, 0.025% xylene cyanol; 0.025% bromophenol blue; 18mM EDTA; 0.025% SDS) and heated for 4mins at 80-90°C. 1µl of each DNA sample was mixed with 4µl distilled water and 5µl of 1x loading buffer (60% glycerol; 0.025% xylene cyanol 0.025% bromophenol blue 0.1 mM EDTA) and separated on gels ranging between 0.8% and 2% agarose (Flowgen). Large fragments were separated on low percentage gels while smaller fragments were resolved on high percentage gels. Gels were run in 1 x TAE (40mM Tris-acetate, 1mM EDTA) at voltages between 20-100V (lower voltage for low percentage agarose gels). Samples were run with DNA markers, 100bp ladder, Lambda/HindIII marker (1µg each, MBI Fermentas). Following 20min gel staining in ethidium bromide (0.5µg/ml) and 20min destaining in distilled water, RNA and DNA fragments were visualised using an UV transilluminator. Gels were

photographed and images stored using Ultra-violet Products Ltd, Cambridge package.

2.3 Electrophysiology using *Xenopus laevis* Oocytes

2.3.1 Xenopus laevis ooctyes.

Oocytes for the expression of the voltage gated sodium channels were obtained from the South African clawed frog, *Xenopus laevis*. Frogs were purchased from Blades Biological Ltd, UK and housed in temperature-controlled tanks at 20°C with a light-dark cycle of 12 hr each (maintained by Mr T. Smith, School of Life and Environmental Sciences, University of Nottingham).

2.3.2 Anaesthesia and surgery on Xenopus laevis

Each frog was anaesthetised in 500ml water supplemented with 2g/l of 3-aminobenzoic acid ethyl ester (Sigma, A5040) for 45mins. Before ovarian surgery, the spinal chord was cut and a lethal injection of 1M KCl given into the heart. The frog was laid on its back and a small incision made on the right side of the lower abdomen. Both the skin and the underlying fascia were peeled back to expose the ovary. Ovarian lobes containing the oocytes were removed carefully with forceps and placed in petri dishes containing calcium free OR2 (85mM NaCl; 2.5 mM KCl; 1mM $MgCl_2$; 1mM Na_2HPO_4 5mM HEPESpH7.8

2.3.3 Preparation of the oocytes for mRNA injection

The follicle cell layer that surrounds the oocyte was removed with collagenase treatment. Lobes were teased apart before being submerged in calcium free OR2 supplemented with 2mg/ml collagenase (Sigma, C-9891) for 90 min. Oocytes were treated in horizontal capped test tubes gently shaken in an incubator held at 19°C.

Following collagenase treatment, the eggs were washed five to six times in calcium free OR2 and the healthiest stage IV and V eggs transferred to GPT-ND96 solution (96mM NaCl, 2mM KCl, 1.8mM $CaCl_2$, 1mM $MgCl_2$, 5mM HEPES, pH 7.5 with NaCl supplemented with 50mg/l gentamicin, 0.5mM theophylline, 2.5mM Na-pyruvate).

2.3.4 Injection of mRNA into ooctyes

Needles to inject mRNA into oocytes were made from 3.5nl glass bores (World Precision Instruments, Florida) using a vertical pipette puller (Knopf, Germany). The tips were broken with fine forceps to give a slanted point 1-2μm in diameter. The needles were then filled with paraffin oil and fastened to a microinjector (World Precision Instruments, Florida).

mRNA was briefly centrifuged before 1μl of *para* or rat mRNA (concentration1μg/μl) was gently pipette-mixed with 1μl of the appropriate subunit mRNA, TipE or Rat β1 (concentration1μg/μl) respectively, and 3μl DEPC treated water, the final mixture having 1:1:3 ratio by volume. Solutions were then slowly sucked up through the tip of the injection needle avoiding the accumulation of air bubbles.

Oocytes were lined up in a ridged petri dish to prevent them moving during injection. The membrane was gently pierced and 10nl of Rat brain IIA/β1 or 50nl *Para*/Tip E injected into each egg. Injected eggs were flushed into fresh ND96 solution and incubated at 19°C for 12-15hrs. Healthy oocytes were transferred to fresh solution every day.

2.3.5 Electrophysiology on Oocytes

Whole cell electrophysiology was carried out on ooctyes between two and ten days after injection. The oocyte is a standard heterologous expression system for plasma membrane proteins, including ion channels, carriers and receptors (Sumikawa *et al.*, 1981). Foreign mRNA is successfully translated and the protein products are often correctly post-translationally modified before being directed to the correct cellular location (Barnard *et al.*, 1982, Goldin, 1991).

Sodium currents were measured using the two-electrode voltage clamp technique (figure 2.3). An intracellular electrode injected current into the oocyte to maintain the desired potential difference between the intracellular voltage electrode and the agar bridges in the surrounding bath. The current needed to maintain a given potential was measured.

Electrodes were pulled from 225pcs filamented borosilicate glass capillaries (Harvard Apparatus, GC150TF – 10) using an electrode puller (Flaning Brown Sutter Instruments). Heat and pull durations were set to give electrodes with resistances of between 0.5-1MΩ. The current electrode was filled with a solution of 0.7M potassium chloride plus 1.7M potassium citrate while the voltage electrode contained a solution of 1M potassium chloride. Electrodes were lowered into the bath filled with ND96 and any offset was adjusted. The resistance of each was checked with a z test, which passes a 10nA current between the electrode and the ground and records the resulting potential difference.

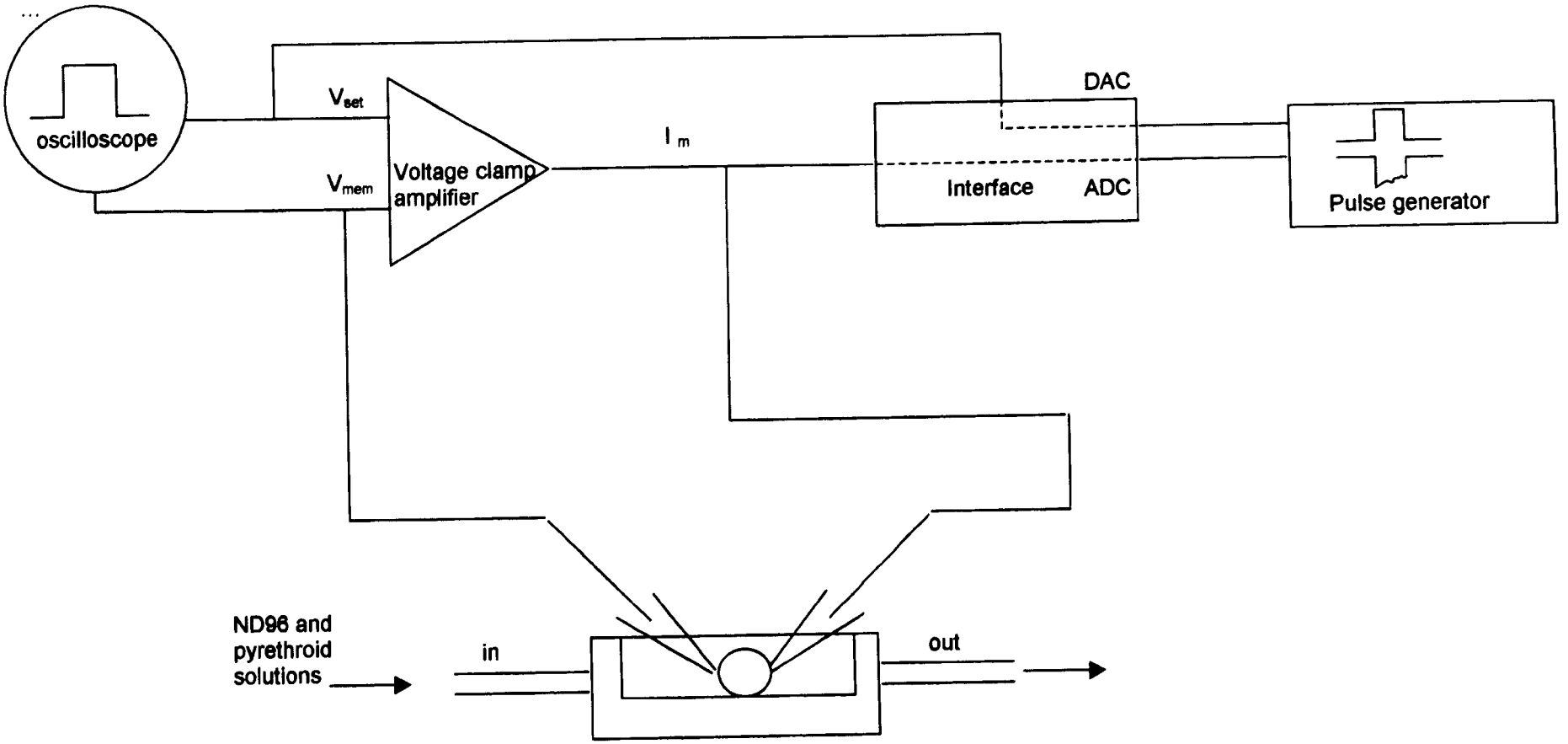

Figure 2.3. Schematic diagram of the experimental set up of two-electrode voltage clamp.

The oocyte was placed in a bath supplied with 1x ND96 solution. The animal pole of the oocyte was impaled with each electrode and the unclamped membrane potential measured. This value should be equal for both electrodes; any difference was usually due to the tip of one of the electrodes being blocked. Eggs with a membrane potential more positive than –15mV were considered too current leaky and were discarded.

Oocytes were initially clamped to –70mV (Dagan, CA-1B Clampator One). Test pulses to -10mV were given and the current response observed on an oscilloscope. To increase the speed of the clamp, the gain was turned to maximum. Series resistance and voltage electrode capacitance were compensated for.

Test pulses were generated by PULSE software (Heka Elektronic, Germany) and recorded on a PC where they could later be analysed using PULSEfit (Heka Elektronic, Germany) Excel and Prism software.

2.3.6 Voltage protocols and analysis of channel kinetics

The kinetics of the voltage gated sodium channel were obtained and analysed using PULSE and PULSEFit software (Heka Electronik, Germany). The pulse protocols are described briefly here and Table 2.1. The voltage dependence of activation was estimated by stepping the oocyte membrane in 5mV increments from a holding potential of –70mV by depolarising test potentials (32ms) in the range of –60 to +20mV. Peak currents were plotted as a function of test potential and fitted to a current/voltage relationship from which the voltage dependence of activation could be estimated.

The voltage dependence of inactivation was analysed by stepping the oocyte membrane holding potential from –70mV using a series of 200ms inactivating pre-pulses in the range of –90- -20mV, followed by a –10mV test potential. Peak current were plotted as a function of the inactivating pre-pulse potential and fitted with a Boltzmann relationship from which the voltage dependence of inactivation could be estimated.

Onset of inactivation was obtained by measuring the current evoked by a –10mV test pulse following a conditioning pre-pulse of increasing duration applied to membranes clamped at a holding potential of –70mV. The conditioning pre-pulse ranged from –50mV to –30mV and progressively increased in duration by a factor of 2 starting at 0.5ms and reaching 256ms. Each peak current was plotted as a function of pre-pulse duration and fitted by a single exponential function.

Recovery from inactivation was obtained by measuring the current evoked by a –10mV test pulse applied to an oocyte that had first undergone a –10mV activating pulse followed by a conditioning pulse between –110mV and –50mV of increasing duration. The conditioning pulse increased in duration by a factor of 2 starting at 0.5ms and reaching 256ms. Each peak current was plotted as a function of conditioning pulse duration and fitted by a single exponential function.

2.3.7 ATX-II treatment of sodium channels.

Oocytes were treated with 500nM of the toxin ATX-II from the sea anemone *Anemonia sulcata* (ATX-II, Calbiochem Corp, USA), which almosts eliminates *para* sodium channel fast inactivation and increases maximum sodium channel conductance (Warmke

et al., 1997). The toxin was added directly into the oocyte bath and test pulses of -10mV amplitude and 32ms duration from a holding potential of –100mV were then continually applied until inactivation during the test pulse stopped and the peak current remained constant.

2.3.8 Pyrethroid treatment of sodium channels.

Pyrethroid solutions, of concentration between 1nM and 10μM, were introduced into the 5ml oocyte bath using a gravity driven perfusion system. Solutions were gently sucked out through a separate bath section, keeping the solution level constant and avoiding disturbance of the oocyte. Oocytes were exposed to 10ml of the pyrethroid solution before test pulses were administered and current recordings taken.

In the presence of ATX-II and a pyrethroid, oocytes were stepped from a holding potential of –100mV to a 320ms test potential of –10mV before repolarisation to –110mV. Time constants (τ) were calculated from one or more exponential fits of tail current decays. These were fitted iteratively using the equation;

$$I(t) = a_0 + a_1\exp(-t/\tau_1) + a_2\exp(-t/\tau_2) + a_3\exp(-t/\tau_3)$$

Where a_0 is the offset and a_1, a_2 and a_3 are the coefficients of the exponential terms. t is time and τ_1, τ_2 , and τ_3 are the time constants of the decay.

In the absence of ATX-II and in the presence of a pyrethroid, oocytes were subjected to a train of depolarisations of varying pulse number and duration. Oocytes were step depolarised between 10 and 400 times at 66Hz (5ms duration) from a holding potential of −100mV to 0mV amplitude and with a 10ms interval between each pulse. Time constants (τ) were calculated from one or more exponentials fitted iteratively to the tail current decays.

A fresh oocyte expressing a channel mutant was used in each experiment. Experiments were repeated at least three times for each sodium channel mutant and pyrethroid compound. The peak tail current and rates of tail current decay were pooled for each concentration of the pyrethroid and the average taken as measure of channel sensitivity.

Activation

Voltage mV	V-membrane	-60	-70
Duration ms	20	32	5
Voltage increase		5	

Inactivation

Voltage mV	-90	-90	-10	-60
Duration ms	198	2	32	5
Voltage increase	5	5		

Onset of inactivation

Voltage mV	-70	-40	-40	-10	-70
Duration ms	10	0.5	0.5	16	5
Time factor		2			
Time increase ms		0.5			

Recovery from inactivation

Voltage mV	-70	-10	-50	-10	-70
Duration ms	2	8	0.5	10	5
Time factor			2		
Time increase ms			0.5		

Table 2.1 Pulse protocols applied to oocyte membranes to determine the voltage dependence of activation and inactivation and rates of onset of, and recovery from inactivation.

CHAPTER 3

SENSITIVITY OF THE PARA M918V VOLTAGE-GATED SODIUM CHANNEL MUTANT TO DELTAMETHRIN AND PERMETHRIN

3.0 Introduction

The super-kdr mutation confers resistance against the knockdown effects of pyrethroid insecticides in a number of insect species. Until recently, the classic super-kdr mutation, (M918T), has only been found in conjunction with the kdr mutation (Williamson *et al.*, 1996). There are now reports of single super-kdr mutations at the 918 locus in the white fly *Bemisia tabaci* and the aphid *Aphis gossypii* (Morin *et al.*, 2002; Xieowen, personal communication) although surveys of a number of pest species continue to report their co-expression with kdr (Guerrero *et al.*, 1997, Williamson *et al.*, 1996).

Why is the super-kdr as the sole resistance mutation apparently so rare? The principles of natural selection dictate that if the fitness costs outweigh the benefits conferred by a phenotypic change then that characteristic is lost from the population. It could be that the "benefits" of the single 918 mutation only narrowly exceed its costs. Here, the electrophysiological basis of a super-kdr resistance mutation alone is investigated for M918V, which is found in the Grb strain of *Bemisia tabaci*.

3.1 A comparison of the *para* wild type sodium channel and a channel with the super-kdr M918V mutation.

3.1.1 The voltage dependence of activation

The mutant channel M918V and the *para* wild type channel were expressed in *Xenopus laevis* oocytes. The oocytes were clamped at a holding potential of -70mV and repetitively depolarised to a test potential for 32ms. The interval between each test potential was 25ms. Test potentials ranged between –60mV and +20mV. The peak

sodium current for each test pulse was recorded and plotted as a function of the test potential. The data points were then fitted with a current voltage relationship.

$$Y = \frac{G_{\max}(V - V_{rev})}{1 + \exp[(V - V_{1/2})/k]}$$

(Equation 3.1)

Where Y is the current, V is the test potential, G_{max} is the total sodium conductance, V_{rev} is the reversal potential of the Na^+ current, $V_{1/2}$ is the midpoint potential of activation and k is the slope function in mV (Vais *et al.*, 2000).

The mid-point potentials for activation, $V_{1/2}$, for the two channel types (M918V $V_{1/2}$ = 13.9mV$\pm$ 1.2, *para* wild type $V_{1/2}$= 16.9mV$\pm$ 1.4) were not significantly different ($p>0.01$) (Table 3.1). The voltage dependence of activation is therefore not affected by the M918V mutation.

3.1.2 Voltage dependence of inactivation

To obtain information on the voltage dependence of sodium channel inactivation, oocytes were clamped at a holding potential of –70mV before the application of a single 200ms inactivating pre-pulse. This was followed by a –10mV test pulse of 32ms duration. The inactivating pre-pulse ranged between –90mV and –20mV. As the inactivating pre-pulse was made more positive, more sodium channels inactivated and the peak sodium current elicited by the test potential decreased. The peak amplitudes of sodium currents elicited by the –10mV test potentials were plotted against the amplitudes of the inactivating pre-pulse. Data points were fitted by a Boltzmann

		Para wt	M918V
Activation			
	$V_{1/2}$ (mV)	-16.9±1.4	-13.9±1.2
	k	5.43±0.40	7.59±0.29
Inactivation			
	$V_{1/2}$ (mV)	-43.7±0.7	-54.7±0.7
	k	4.52±0.14	5.9±0.12
	τ onset (ms) (-40)	13.9±1.6	3.7±0.47
	τ recov (ms) (-50)	11.4±1.1	5.26±0.43
ATX-II			
	$V_{1/2}$ (mV)	-5.6±4.2	-15.8±3.3
	G_{max} Fold increase	2.2±0.4	5.9±1.47

Table 3.1. Kinetics of activation and inactivation and the onset of, and recovery from, inactivation of M918V and *para* wild type channels. τ is the time constant for the onset or recovery of M918V channels and *para* wild type channels from inactivation.

relationship (Equation 3.2), from which the mid-point potentials of inactivation were estimated (Figure 3.1).

$$Y/Y_{max} = \frac{1}{1+\exp[(V - V_{1/2})/k]}$$

(Equation 3.2)

where Y is the peak current for a single test pulse and Y_{max} is the maximum current for the series of test pulses, $V_{1/2}$ is the midpoint potential of inactivation and k is the slope factor in mV. $V_{1/2}$ for M918V channels was significantly ($p<0.01$; two-tailed t-test) more negative than $V_{1/2}$ for the wild type channel (M918V, $V_{1/2}$=-54.7mV±0.72, *para* wild type, $V_{1/2}$=-43.7mV ± 0.70). M918V channels inactivated more at negative potentials than wild type channels.

3.1.3 Onset and recovery from inactivation

To measure the speed of onset of inactivation, a single pre-pulse to –40mV was applied to oocytes clamped at a holding potential of –70mV. This was followed by a 32ms test pulse to –10mV. The pre-pulse duration was progressively increased by a factor of 2, starting at 0.5ms and reaching a maximum of 256ms. The peak amplitude of the sodium current elicited by the –10mV test pulse was plotted against the pre-pulse duration. Data points were best fitted with a single exponential function from which the time constant for the onset of activation was determined. The amplitudes of the pre-pulse potentials were then varied from –50mV to –30mV and the time constant of inactivation for each membrane potential was calculated.

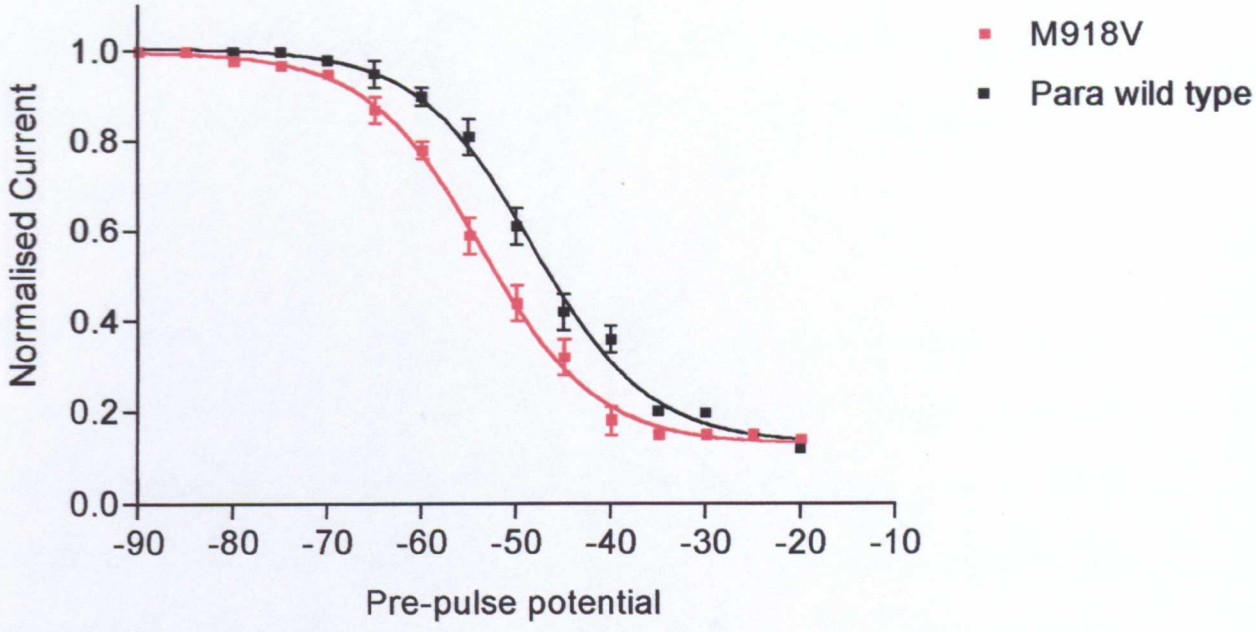

Figure 3.1. Voltage dependence of inactivation of M918V and *para* wild type channels. Channels were pulsed to the inactivating pre-pulse followed by a 10mV depolarising pulse. The resulting peak current was normalised, plotted as function of the pre-pulse potential and fitted with a Boltzmann relationship (Equation 3.2). M918V channels inactivate at significantly more negative potentials than *para* wild type channels (M918V, $V_{1/2}$ = -54.7±0.72mV; para wild type, $V_{1/2}$ = -43.7±0.7mV). (Points show the mean ± SEM, n = 6)

M918V channels inactivated significantly faster than wild type channels at all pre-pulse potentials. (E.g. for the test pulse of -40mV, the onset time constant for M918V was 3.7ms $\pm$ 0.47, whereas that for the wild type was 13.9ms $\pm$1.6; P=0.0009, two-tailed t-test) (Figure 3.2).

Rates of recovery from inactivation were also determined using a multi-pulse protocol. A single 8ms activating pulse to –10mV was applied to oocytes clamped at –70mV. This was followed by a -50mV conditioning pulse and then a test pulse of –10mV amplitude and of 10ms duration. The duration of the conditioning pre-pulse was progressively increased by a factor of 2, starting at 0.5ms and reaching a maximum of 256ms. The peak amplitude of the sodium current elicited by the –10mV test pulse was plotted against the duration of conditioning pulse. The data points were best fitted with a single exponential function from which the time constant for the recovery from inactivation was determined. As the conditioning pulse duration increased, more channels recovered from inactivation. Recovery from inactivation was also determined for other conditioning pulse amplitudes. -50mV was the conditioning pulse amplitude at which recovery was at its slowest. At -50mV, recovery from inactivation was significantly faster for M918V channels than for wild type channels (M918V, τ=5.26 ms $\pm$ 0.43; wild type, τ=11.4ms $\pm$1.1; P=0.002, two-tail t-test). This was not the case at all negative conditioning pulse potentials, where no difference (P>0.01, two-tailed t-test) could be detected between the two channel types (Figure 3.3).

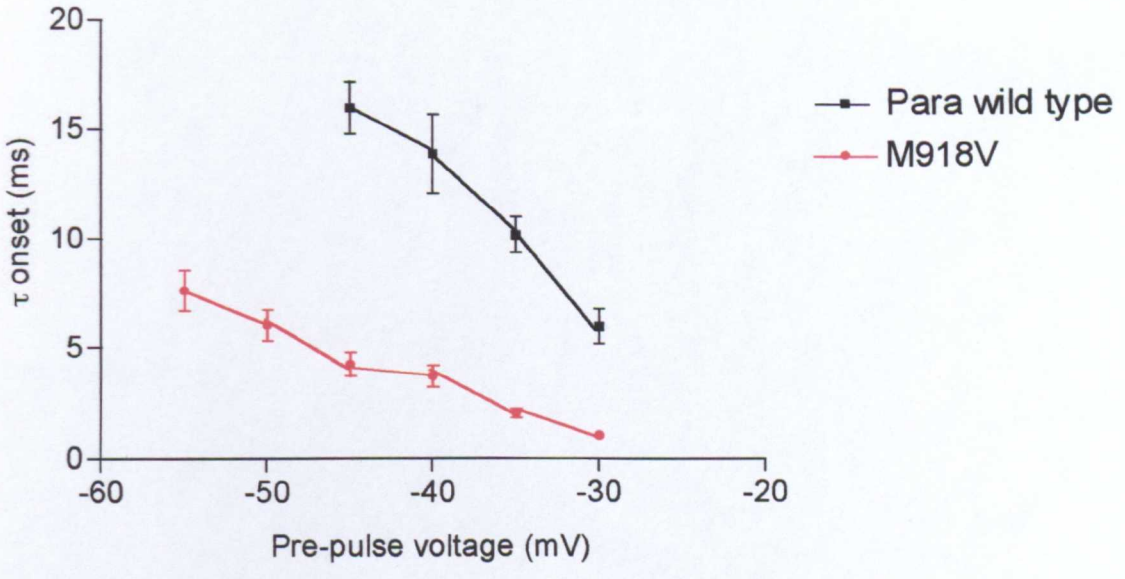

Figure 3.2 The onset of inactivation for M918V channels and *para* wild type channels. Channels were pre-pulsed to the inactivating test potential for a duration of between 0.5ms and 256ms before a –10mV depolarising pulse. The resulting peak currents, as a function of the inactivating test pulse duration were described by an exponential relationship, from which the time constant (τ) for the onset of inactivation was determined. The time constant (τ) is plotted as a function of the inactivating test potential. M918V channels inactivate significantly faster (for test pulse of –40mV, $p=0.0009$; two-tailed t-test) than *para* wild type channels. (Points show the mean $\pm$ SEM, $n = 4$).

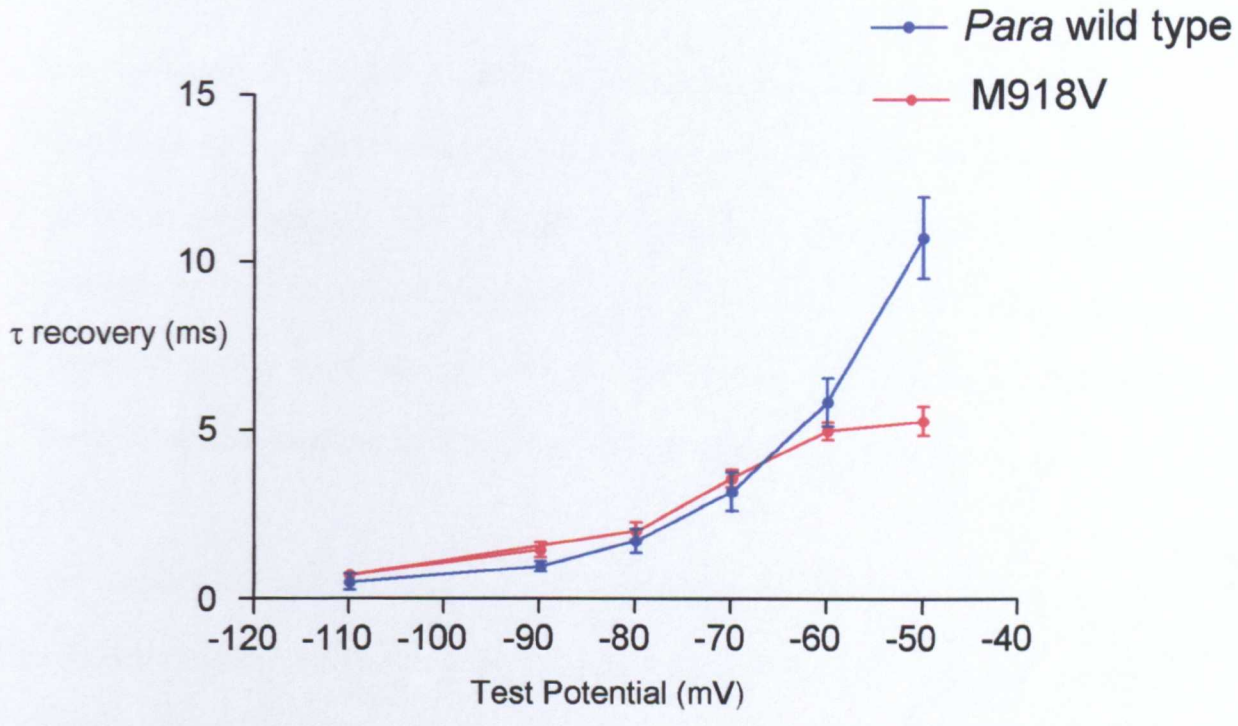

Figure 3.3 Recovery from inactivation of M918V and *para* wild type channels. Channels were activated with a single -10mV test pulse and then pre-pulsed to the test potential for durations between 0.5ms and 256ms before a final –10mV depolarising pulse. The resulting peak currents, as a function of the test pulse duration were described by an exponential relationship, from which the time constant (τ) for the recovery from inactivation was determined. The time constant (τ) is plotted as a function of the test potential. M918V channels recovered from inactivation significantly faster for a test pulse of –50mV, ($p=0.002$; two-tailed t-test) than *para* wild type channels. (Points show the mean $\pm$ SEM, $n = 4$).

3.2 The effect of the M918V mutation on sensitivity to deltamethrin

3.2.1 Analysis of the effects of deltamethrin insecticide on channel gating

Pyrethroids slow channel activation, inactivation and deactivation giving rise to tail currents in voltage clamp studies following repolarisation from a test depolarisation. Although the effects of the insecticide can already be detected during a test depolarisation, the amplitude and rate of decay of the tail current seen following repolarisation provided a better measure of channel sensitivity (Figure 3.4).

3.2.2 Binding of deltamethrin to the M918V channel.

Sodium tail current amplitudes, in the presence of deltamethrin, were larger following a train of a hundred 5ms depolarisations to 0 mV at 66Hz from a holding potential of –100mV, than following a single pulse to 0mV of equal duration (Vais *et al.*, 2000). For the M918V mutation, tail current following a train of 100 5ms pulses, separated by 10ms intervals to allow channels to recover from open state inactivation, were approximately six times the amplitude of those induced by a single depolarisation (Figure 3.5). Increases in the number of 5ms pulses within a train increased the amplitude of the tail current in the presence of deltamethrin (Figure 3.6). This pulse protocol encourages continual channel activation and thus it can be concluded that deltamethrin binds preferentially to the M918V open state. The percentage of channels modified by deltamethrin (section 3.2.4) increased in an exponential fashion as the number of pulses was increased (Figure 3.14). Following 400 pulses the percentage of channels modified by deltamethrin remained constant and could not be increased with further pulsing (data not shown). This was not the case with *para* wild type channels where the percentage of

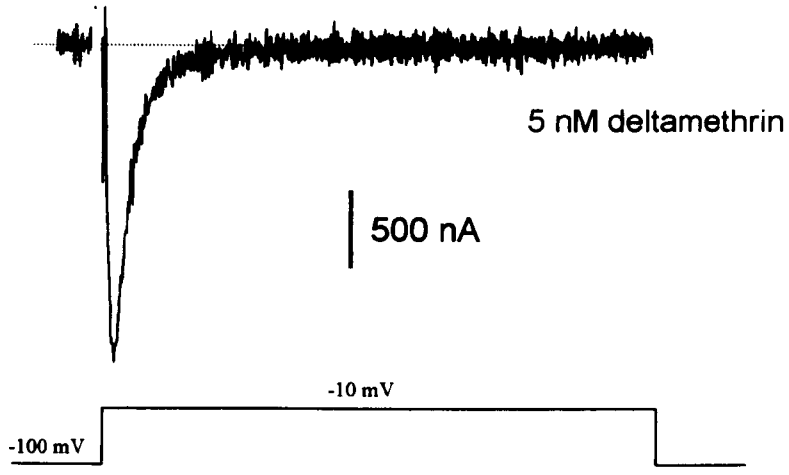

(B)

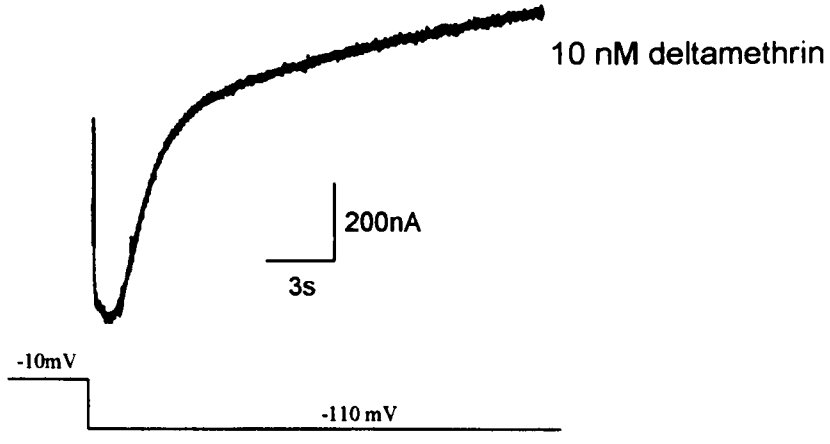

Figure 3.4 Effects of deltamethrin on para wild type current. (A) *Para* wild type current during a depolarising pulse to -10mV from a holding potential of –100mV in the presence of 5nM deltamethrin. (B) *Para* wild type tail current in the presence of 10nM deltamethrin, following a depolarising pulse to 0mV from a holding potential of –100mV. The peak tail current is significantly increased and the rate of tail current decay greatly slowed. (From Vais *et al.*, 1998)

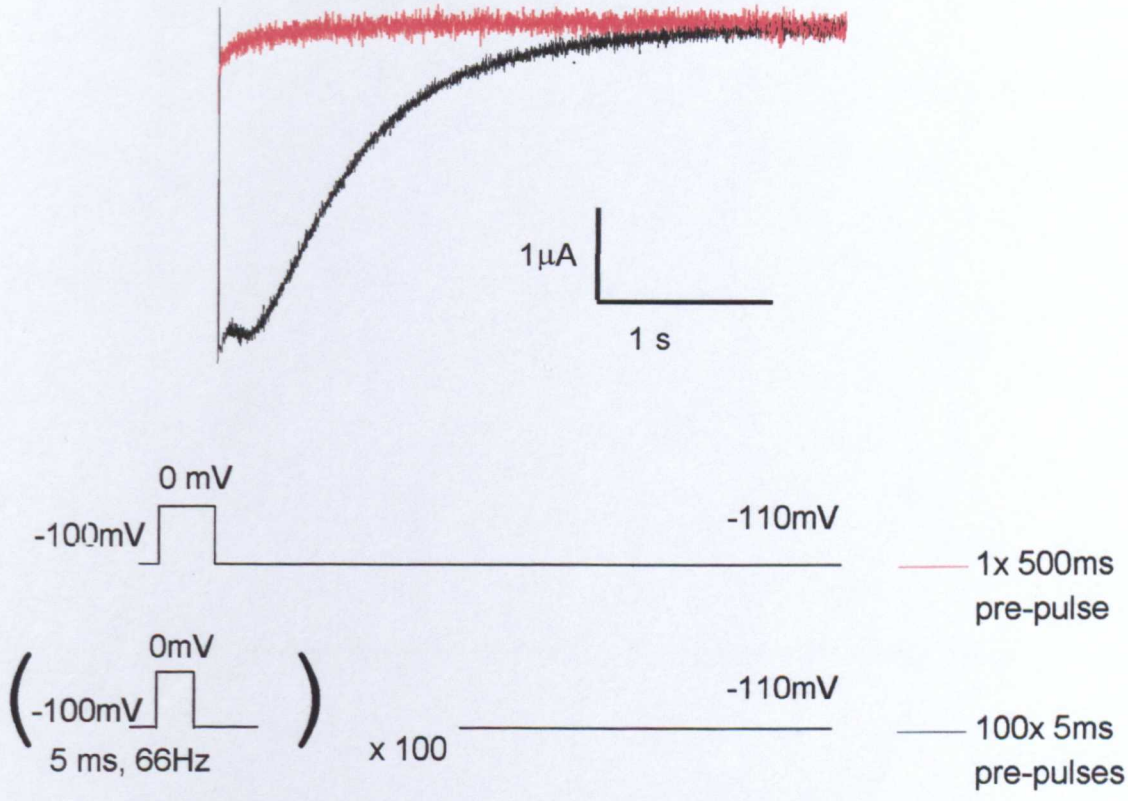

Figure 3.5. M918V tail currents elicited following either a single 500ms depolarising pulse to 0mV from a holding potential of –100mV, or 100 depolarising pulses of 5ms duration at 66Hz to 0mV from a holding potential of –100mV, in the presence of 1μM deltamethrin. The tail current following a train of pulses is larger in amplitude than the tail current following a single pulse.

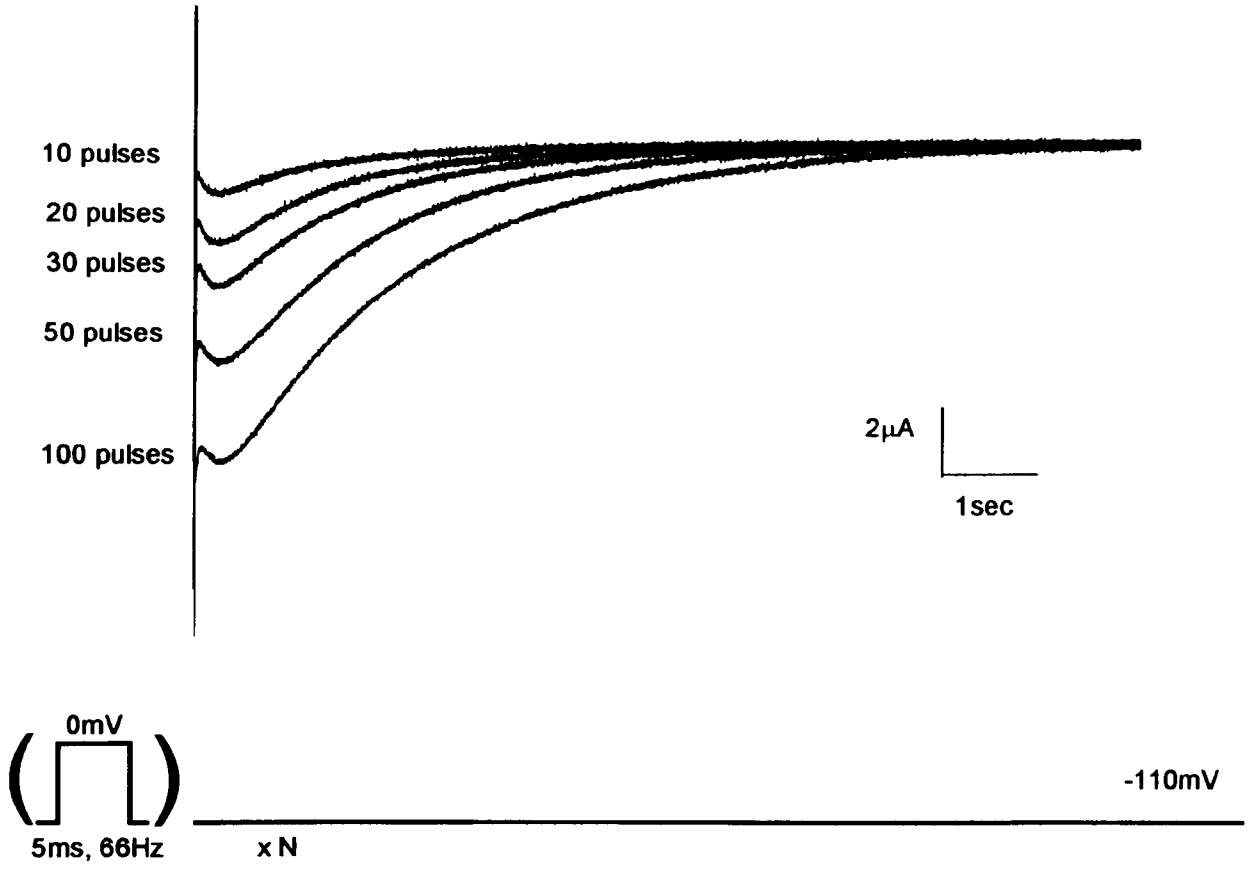

Figure 3.6 Changes in the tail current amplitude are induced by varying the number of depolarizing pulses in a train in the presence of 10μM deltamethrin. Tail currents were measured following 5ms depolarisations to 0mV at 66Hz from a holding potential of −100mV. N represents the number of pulses in a train and is shown to the left of each tail current.

modified channels continued to rise following a 1600 pulse series (See figure 3.15) (Vais *et al.*, 2000).

3.2.3 The effect of M918V mutation on closed state inactivation

There are many drugs that bind preferentially to the sodium channel open state. Compounds which reduce sodium channel activation and opening, reduce the potency of [H3]-batrachotoxinin-20-alpha-benzoate, which specifically binds and stabilises the open state of the channel (Postma and Catterall, 1984). This reduction in channel opening is also thought to underlie kdr and super-kdr effects on the channel (Vais *et al.*, 2000). They too inhibit sodium channel activation by increasing the number of channels that inactivate from the closed state, rather than open following a strong depolarization. This is termed closed-state inactivation (Patlak, 1991). Does M918V alone confer the same shift in the state equilibrium, and if so, to what extent?

ATX-II, an anemone toxin, inhibits closed-state and open-state fast inactivation. Previous studies have shown that the number of *para* wild type channels that conduct sodium ions following a single depolarization is doubled in the presence of ATX-II (Warmke et al., 1997). For the kdr mutation the increase is approximately four-fold and in the case of the kdr and the super-kdr double mutation it is about five-fold (Vais *et al.*, 2000). This indicates that the peak sodium current elicited by a test depolarization is increased by eliminating closed state inactivation. By comparing the maximal sodium conductance, $G_{Max,ATX\text{-}II}$, in the presence of ATX-II with the maximal sodium conductance in the absence of the toxin, $G_{Max\text{-}ATX\text{-}II}$, the proportion of channels that conduct sodium ions following a single depolarisation can be estimated.

$$\% \text{ channels conducting} = \frac{G_{max-ATX-II}}{G_{max+ATX-II}} \times 100$$

(Equation 3.3)

Oocytes were subjected to the same pulse protocol used to study the voltage dependence of activation (See section 3.1.1). $G_{Max\text{-}ATX\text{-}II}$ was determined from the IV relationship fitted to the plot of voltage dependence of activation data collected in the absence of ATX-II. $G_{max+ATX\text{-}II}$ was determined from the IV relationship fitted to the plot of voltage dependence of activation data collected in the presence of 500nM ATX-II (Figure 3.7). At this concentration of ATX-II, the oocyte sodium channel population is saturated with the toxin (Warmke *et al.*, 1997).

The effect of ATX-II on the maximum conductance of the M918V mutation is shown in Figure 3.8. ATX-II increased M918V maximum conductance approximately six-(5.9±1.47) fold. In the absence of the toxin only 16% of the available M918V channels opened during a single 320ms depolarization to 0mV. This is not however, 16% of the entire channel population. The use of ATX-II eradicates inactivation; it does not increase the probability of channel opening.

3.2.4 The effect of M918V on the number of channels modified by deltamethrin.

To estimate and to compare the proportions of channels that bind the insecticide, differences in the proportion of channels that open during a test pulse must be removed. To this end, all concentration-response experiments were carried out in the presence of ATX-II because this toxin removes the influence of closed-state inactivation.

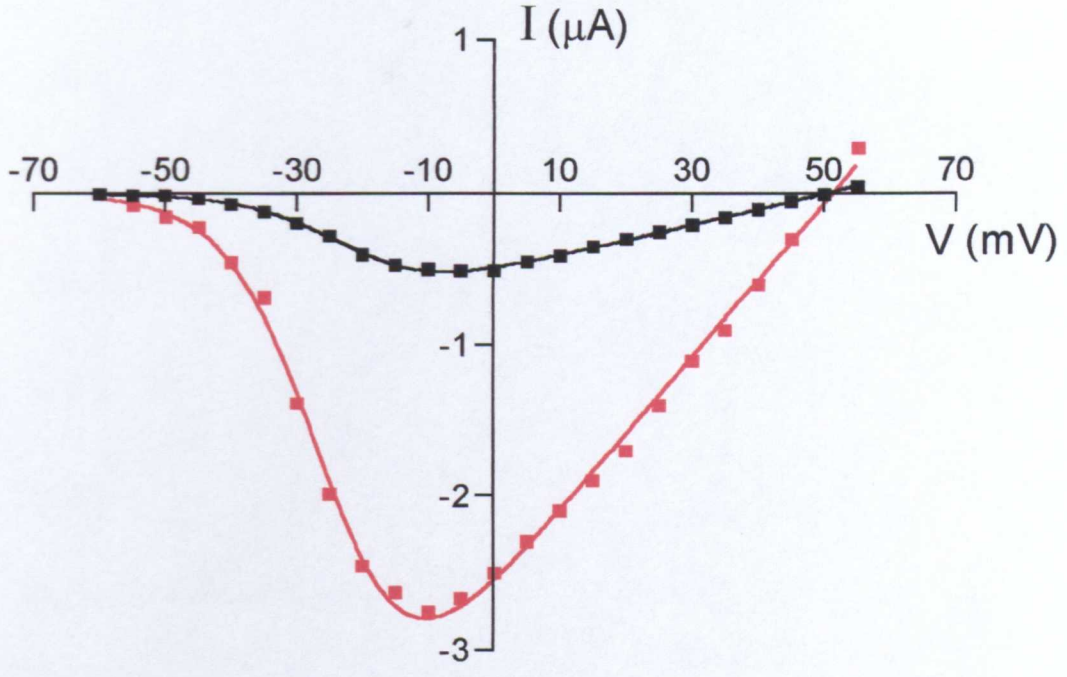

Figure 3.7. M918V peak sodium current plotted as a function of depolarizing voltage (Section 3.1.1) in the presence and absence of 500nM ATX-II and fitted with the IV relationship described by Equation 3.1. ■ –ATX-II, G_{max}= 10μS, V_{rev}= 49mV, $V_{1/2,}$ =-21mV, k= 7mV. ■ +ATX-II G_{max}= 50μS, V_{rev}= 51, $V_{1/2}$ -24, k= 6.

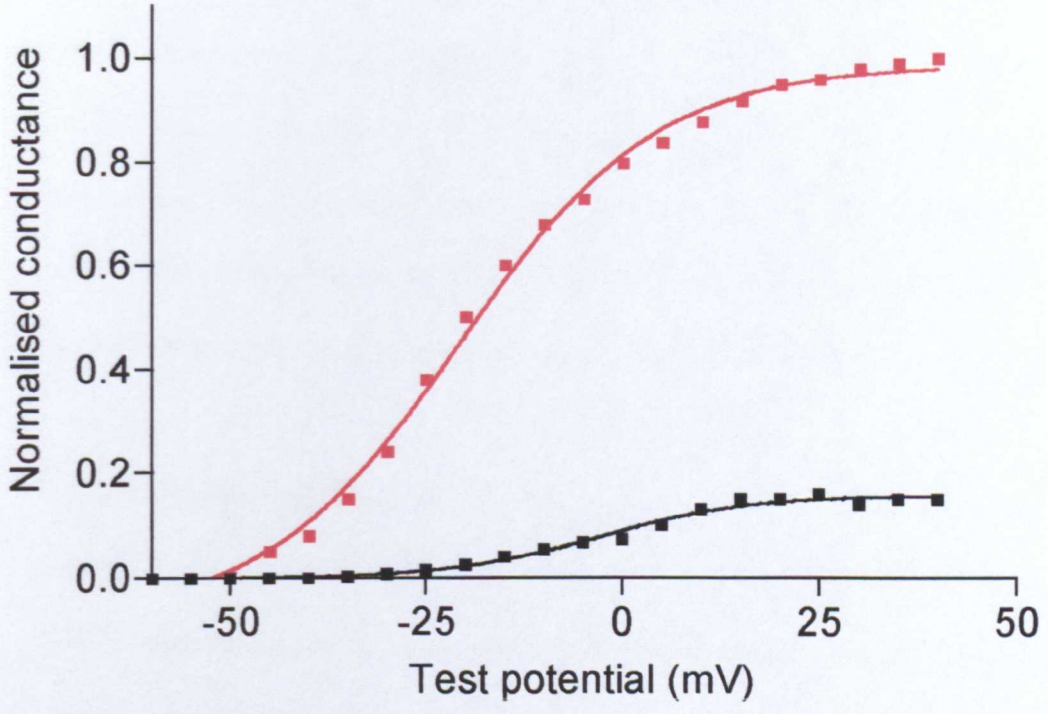

Figure 3.8 Single experiment showing the relative conductance as a function of test voltage of M918V channels in the presence (▪) and absence (▪) of 500nM ATX-II. Conductance of channels in the presence and absence of ATX-II at each test potential was calculated using Equation 3.5 and the resulting curve is fitted with a Boltzmann relationship. ATX-II increased M918V maximum conductance 5.9±1.47-fold.

The peak tail currents induced by a single 320ms step depolarisation to 0mV of oocytes clamped at -100mV in the presence of 500nM ATX-II were much smaller for the M918V mutant channels than for the wild type channels at all concentrations of deltamethrin. Wild type channel tail currents did not recover following exposure to 10nM deltamethrin (Vais *et al.*, 2000) whereas M918V channel tail currents decayed to zero following exposure to 10μM deltamethrin (Figures 3.9 and 3.10).

To quantify this reduction in sensitivity to deltamethrin, the fraction of channels modified by the insecticide (Tatebayashi and Narahashi, 1994) in the presence of 500nM ATX-II was estimated for a range of insecticide concentrations. The fraction of channels modified is equal to the conductance of deltamethrin modified channels, $G_{Na,Delt}$, (calculated using the amplitude of the peak tail current following a single 320ms depolarization to 0mV) divided by the total maximal sodium conductance in the absence of the drug, $G_{Na,\ Max}$ (calculated from the IV curve of the voltage dependence of activation in the presence of 500nM ATX-II), (section 3.1.1).

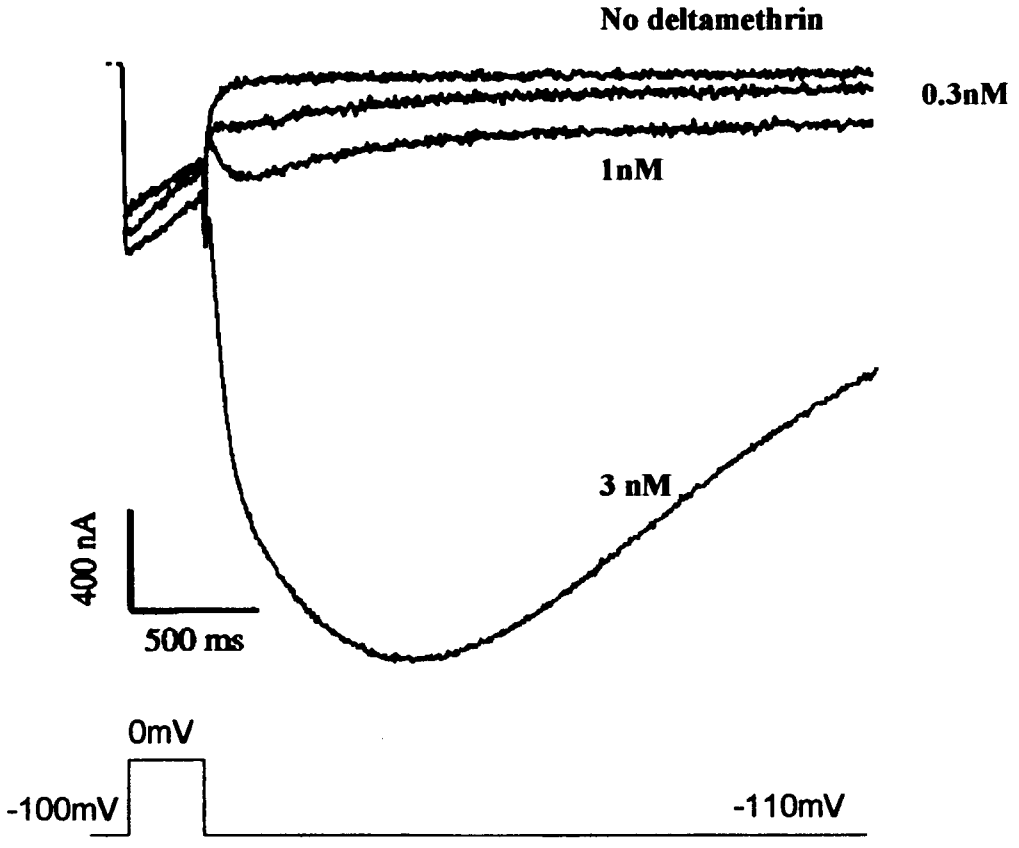

Figure 3.9. *Para* wild type tail currents following a single 320ms depolarising pulse to 0mV from –100mV in the presence of 500nM ATX-II and different concentrations of deltamethrin. The concentration of deltamethrin used is shown to the right of each tail current (Vais *et al.*, 2000).

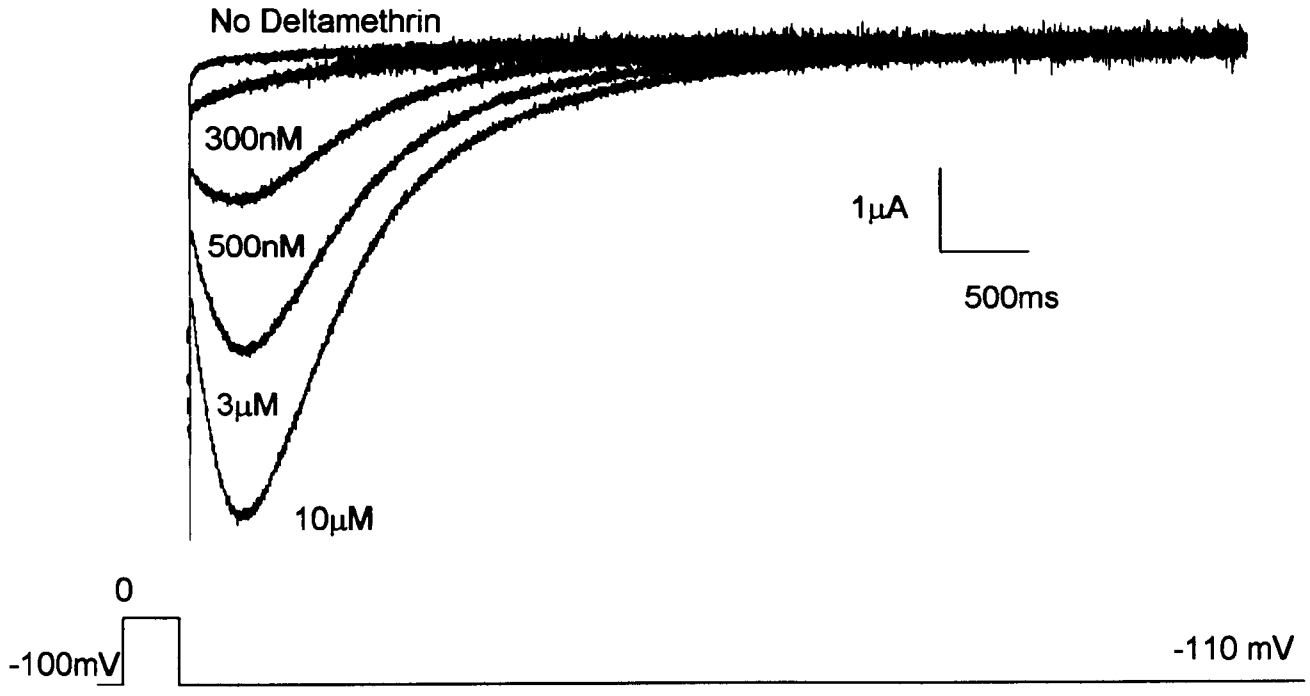

Figure 3.10 M918V tail currents following a single 320ms depolarizing pulse to 0mV from a holding potential of −100mV, in the presence of 500nM ATX-II and different concentrations of deltamethrin. The peak amplitude of each tail current increased with deltamethrin concentration and the rate of tail current decay slowed with increases in deltamethrin concentrations. The concentration of deltamethrin is indicated under each tail current.

$$\%\ \text{channels modified by deltamethrin} = \frac{G_{\text{Na Delt}}}{G_{\text{Na Max}}} \times 100$$

(Equation 3.4)

where

$$G_{\text{Na Delt}} = \frac{\text{Peak tail current}}{(V_{tail} - V_{rev})}$$

(Equation 3.5)

V_{tail} is the voltage at which the tail current is measured and V_{rev} is the reversal potential. The peak tail current was estimated by fitting either one or two exponential functions to the tail current decay profile and recording the extrapolated predicted current at the end of the test pulse (Methods 2.3.8). However, the presence of a brief inward or 'hook' current immediately following repolarisation complicated the estimation of peak tail current. Although the hook was excluded from the fit of the tail current decay, the time delay and concurrent shift to the right of tail current decay resulted in more negative peak current values being recorded than if the decay had started immediately after the end of the test pulse (figure 3.11). This may have resulted in an over-estimation of the peak sodium current at the end of the test pulse. Total conductance was probably underestimated, as even in the presence of ATX-II, it is unlikely that the entire channel population will open during a depolarisation. As a consequence, at deltamethrin concentrations greater than 300nM the maximal amount of modification exceeded 100%.

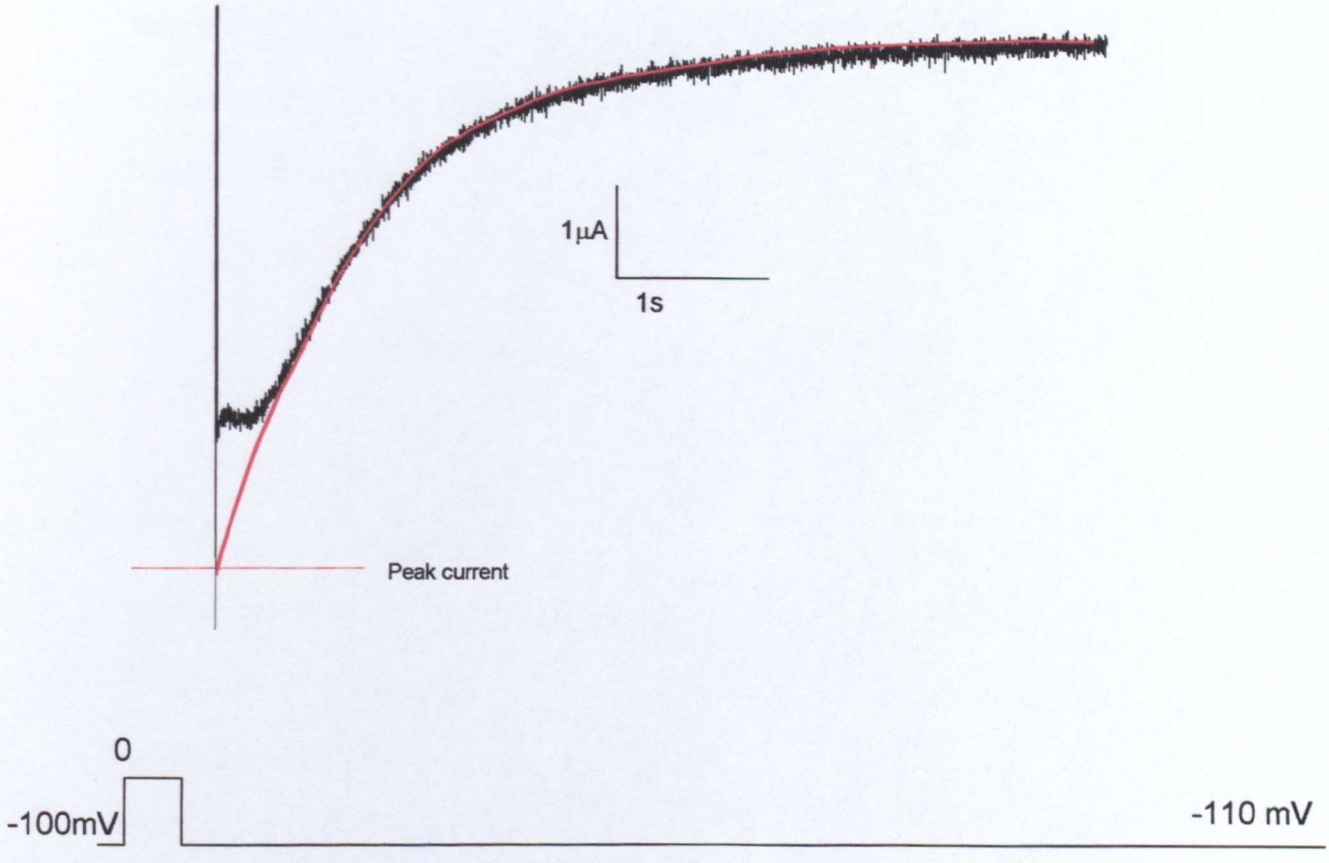

Figure 3.11. M918V tail current in the presence of 1μM deltamethrin. The tail current includes a reactivation hook immediately after repolarisation. This hook was not included when fitting the tail current decay with exponential functions. The extrapolated current (red line) at the end of the test pulse was recorded as the estimate of peak tail current.

Therefore points were fitted with a delimited sigmoidal concentration-response relationship (Equation 3.6) where the maximum value of percentage modification is not limited to 100%. From this concentration-response equation, the Hill coefficient and the Kd values were determined. (figure 3.12).

$$\%\ \text{channels modified} = \frac{Max}{1 + \left(Kd / [Deltamethrin]\right)^{n}}$$

(Equation 3.6)

Where Max is the maximum percentage modification, [Deltamethrin] is the concentration of deltamethrin, Kd is the concentration of deltamethrin at which 50% of the channels are modified and n is the Hill coefficient at 50% channel modification.

The Hill coefficient estimated from the slope of the concentration-response relationship for the wild type channel was greater than two (Hill coefficient =2.05) but for the M918V channel is was less than two (Hill coefficient =1.6). The concentrations at which 50% of the channels were modified (Kds) were also significantly different (wild type = 4.4±0.16nM; M918V = 67±10nM). Therefore, M918V confers an approximately 16-fold reduction in channel sensitivity to deltamethrin. The reduction in sensitivity conferred by the single M918T is >100–fold (Vais *et al.*, 2001) which is clearly far greater than that recorded here. However, the M918T mutation results in the replacement of the hydrophobic side chain of methionine with the aliphatic, hydrophilic hydroxyl side chain of threonine. The difference in the nature of the residue replacement in M918V channels is not as dramatic, as valine has a hydrophobic side chain in

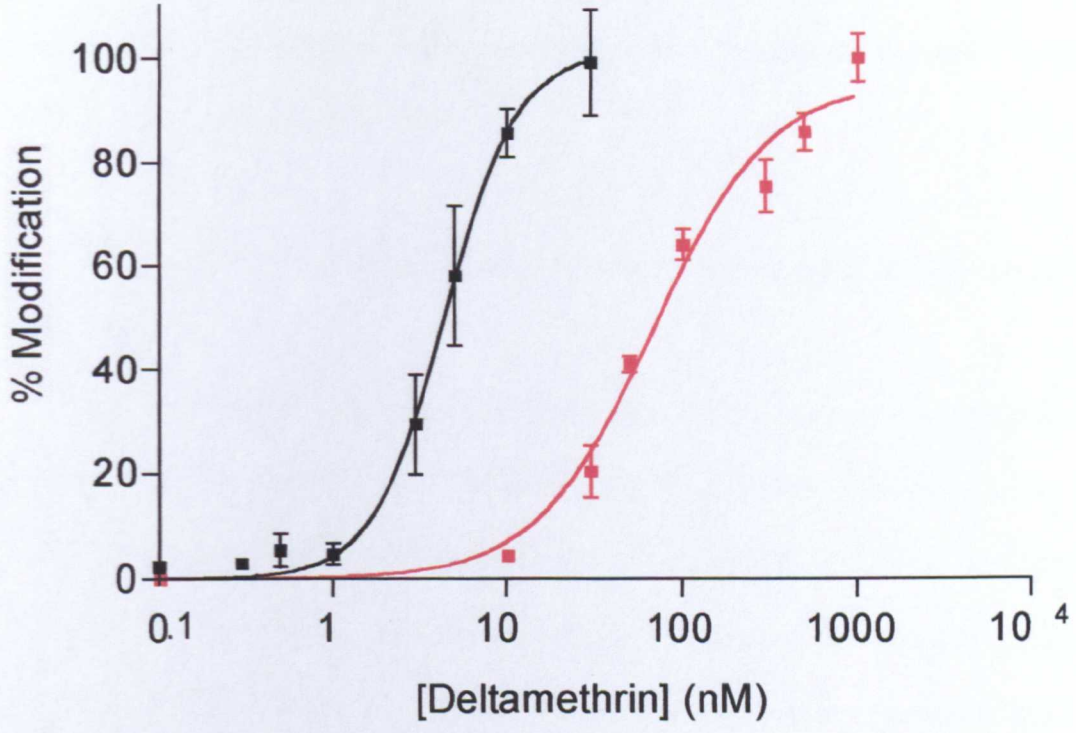

Figure 3.12 Concentration-response relationships for deltamethrin action on the M918V *para* sodium channels and the *drosophila para* wild type sodium channel. The percentage of modified channels was calculated using Equations 3.4 and 3.5 and plotted as a function of deltamethrin concentration. The data was fitted with a concentration-response equation (Equation 3.6).

▪ Concentration-response relationship for deltamethrin action on M918V channels (Kd= 67nM ±10; Hill coefficient = 1.6). ▪ Concentration-response relationship for deltamethrin action on the drosophila para wild type sodium channel (Kd= 4.4nM±0.16; Hill coefficient = 2). (Points show the mean ± SEM, n = 3).

common with methionine. It might therefore be expected that the difference in sensitivity to deltamethrin conferred by the M918V mutation is smaller than that conferred by the M918T mutation.

3.2.5 Tail currents of the M918V mutant channels and wild type channels treated with deltamethrin

Following perfusion of an oocyte with deltamethrin, oocytes treated with 500nM ATX-II and clamped to –100mV were subjected to a single 320ms depolarization to 0mV resulting in tail currents on repolarisation. The M918V tail current decay, at concentrations below 3 μM deltamethrin, could be described by a single exponential function (Methods 2.3.8). The tail currents of M918V mutant channels treated with concentrations of 3μM deltamethrin or greater were best fitted with two exponentials. The fitting of the decay profile was complicated by the occurrence of secondary channel activation appearing as a hook current immediately after repolarisation (Figure 3.11). This hook current was not included when measuring the rate of tail current decay. The fitting of two exponentials to the M918V tail currents is analogous to the results for the *para* wild type current tail current which were also described by a multi -exponential function (Vais *et al.*, 2000).

At high concentrations of deltamethrin, M918V tail currents take significantly less time to return to zero current than those of wild type channels. At 5nM deltamethrin, wild type τ_1= 710ms and τ_2=17.7s, while at 10 μM deltamethrin M918V τ_1= 575ms and τ_2= 9s. However, both time courses fitted to M918V mutant channel decay profiles

slowed as the concentration of deltamethrin increased which was also the case with wild type channels. The hooked tail current and the biphasic decay characteristic of tail currents of deltamethrin-treated M918V channels appeared unaffected by ATX-II. This suggests that the presence of tail currents and their decay profile is the consequence of deltamethrin action on channel deactivation rather than fast inactivation that is inhibited by ATX-II.

3.3 Interaction of M918V channels with Permethrin

The M918V mutation confers a 16-fold reduction in the sensitivity of the *para* mutant channel to deltamethrin, a Type II pyrethroid. The effect of the single super-kdr mutation M918V was also tested against permethrin, a Type I pyrethroid.

M918V tail currents recorded in the presence of permethrin decayed more rapidly than those of the wild type channel, suggesting that the affinity and, therefore, the potency of the insecticide is reduced by the M918V mutation.

3.3.1 Tail currents of the M918V mutant channels and wild type channels treated with permethrin

Following perfusion of an oocyte with permethrin, oocytes treated with 500nM ATX-II and clamped to −100mV were subjected to a single 320ms depolarization to 0mV resulting in tail currents on repolarisation. Exponential relationships were fitted to the resulting tail currents. The tail current decay of M918V channels treated with permethrin could be described by a single exponential at all concentrations of the pyrethroid. The average time constant for M918V tail current decay at all permethrin concentrations was 98±2.8ms. The permethrin induced M918V channel tail currents also lacked the presence of a significant hook on repolarisation (figure 3.13).

3.3.2 Permethrin and channel binding

At 1μM permethrin and in the absence of ATX-II, oocytes expressing M918V mutant channels were subjected to trains of 5ms depolarisations from a holding potential of-100mV to 0 mV at 66Hz. The frequency of the pulses was increased from 10 to 200 and

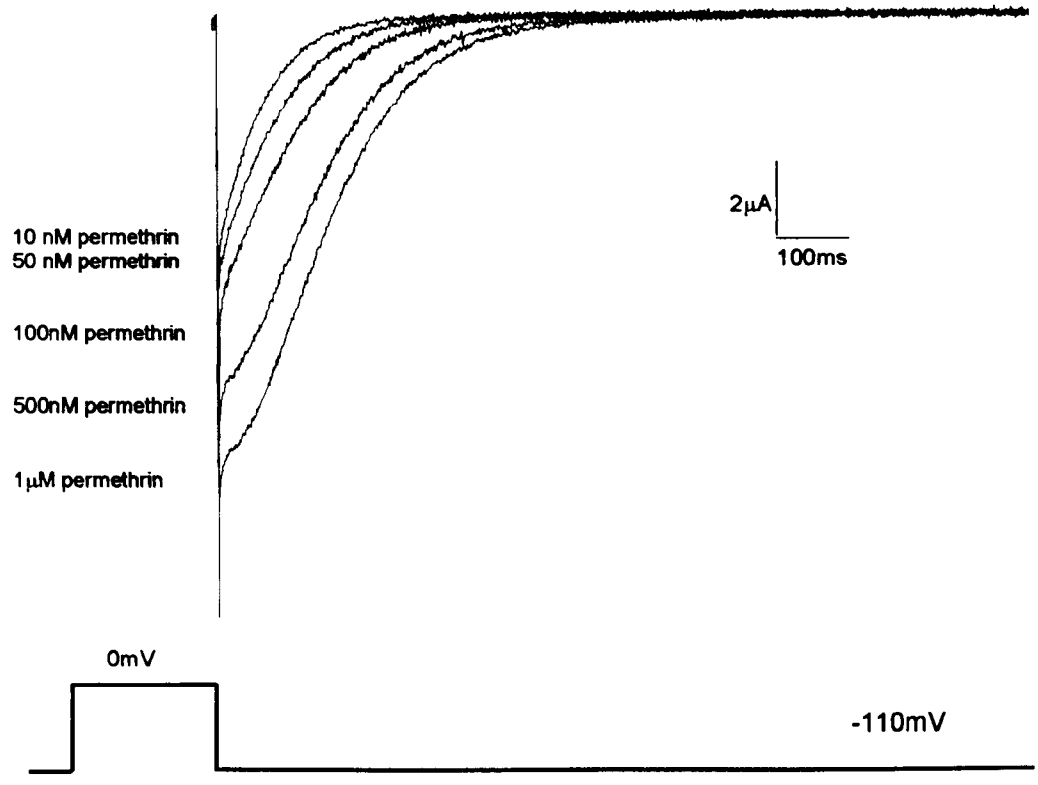

Figure 3.13. M918V tail currents following a single 320ms depolarizing pulse to 0mV from a holding potential of −100mV, in the presence of 500nM ATX-II and different concentrations of permethrin. The peak amplitude of each tail current increased with permethrin concentration, while the rate of tail current decay remained constant at different concentrations of permethrin (τ = 98 $\pm$2.8 ms). The concentration of permethrin is indicated to the left of each tail current.

the resulting peak tail currents were recorded. The amplitudes of the tail currents were then used to calculate the fraction of channels modified as a function of pulse number (Equation 3.4 and 3.5). As the pulse frequency was raised, the percentage of channels modified by permethrin increased in an exponential fashion. Sodium channels remained open for a longer period as the number of pulses and concurrently the duration of the pulse train increased. Permethrin, therefore, also preferentially binds to the M918V mutant channel open state. At 30 pulses, the number of channels modified saturated at 9.5%. This is in contrast to deltamethrin where modification only began to saturate at 200 pulses (Figure 3.14). This may be because the affinity of the sodium channel for deltamethrin is greater than the affinity of the channel for permethrin. This is supported by the Kd values for the action of each pyrethroid on M918V channels. During a train of 200 pulses, channels that bound deltamethrin at the beginning of the train remain occupied, while other channels continue to bind the insecticide in an additive manner. The percentage of modified channels therefore increased. However, channels bound by permethrin at the beginning of a train may not remain occupied during the entire train duration. Hence, the percentage of modified channels saturates at a shorter pulse train duration.

3.3.3 The effect of the M918V mutation on the percentage of channels modified by permethrin.

The percentage of channels modified by permethrin was estimated as for deltamethrin. The Hill coefficient for both the wild type and M918V was <1 (*Para* wild type Hill coefficient =0.9, M918V Hill coefficient = 0.6).

Figure 3.14. (A) Percentage of M918V deltamethrin-modified channels, as a function of the number of depolarising pulses in a train. Maximum channel modification for 1μM deltamethrin is 8.5%. (B) Percentage of M918V permethrin-modified channels, as a function of the number of depolarising pulses in a train. Maximum channel modification for 1μM permethrin is 9.5%. (Points show the mean + SEM, n = 4).

(A)

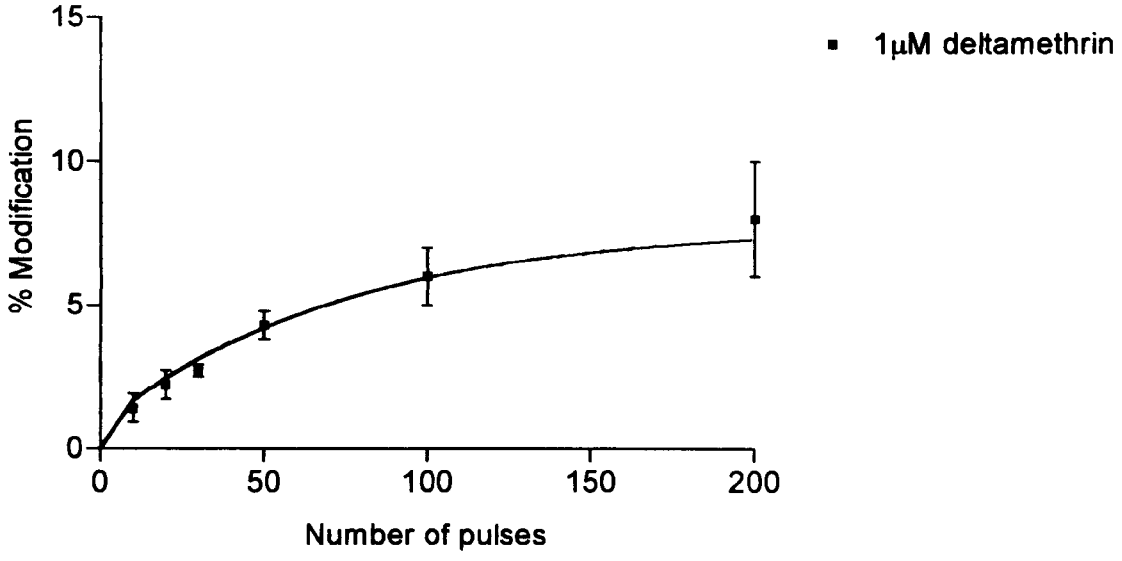
15
10
5
0
% Modification
0
50
100
150
200
Number of pulses
1μM deltamethrin

(B)

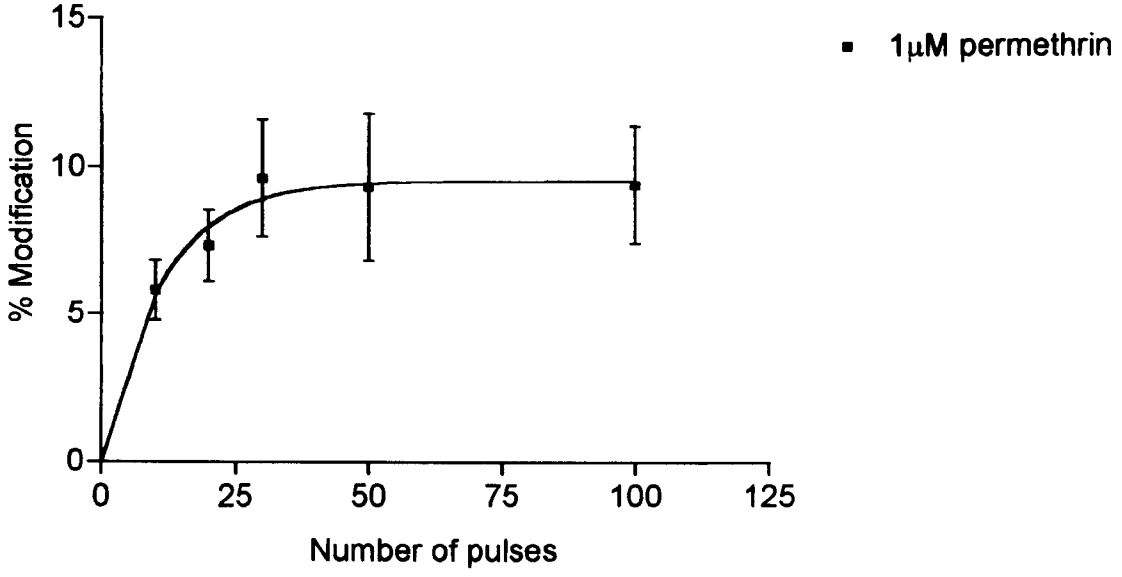
15
10
5
0
% Modification
0
25
50
75
100
125
Number of pulses
1μM permethrin

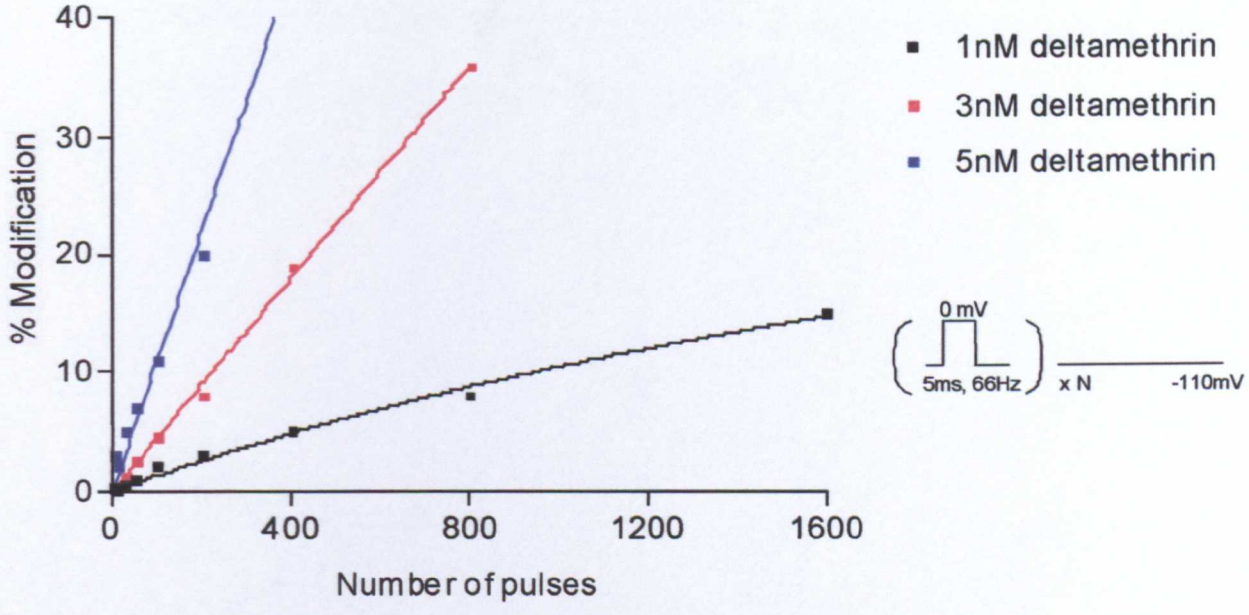

Figure 3.15. Percentages of modified para wild type channels as a function of the number of pulses in a train, at different concentrations of deltamethrin. Data was fitted to an exponential relationship. Maximum channel modification for 1nM deltamethrin is 48%. For 3nM and 5nM deltamethrin 100% of para wild type channels were assumed to be modified (from *Vais et al.*, 2000).

However the mutation conferred a very large 800-fold resistance factor (*Para* wild type Kd =10.3±1.0nM, M918V Kd=8.4±2.4μM) (Figure 3.16).

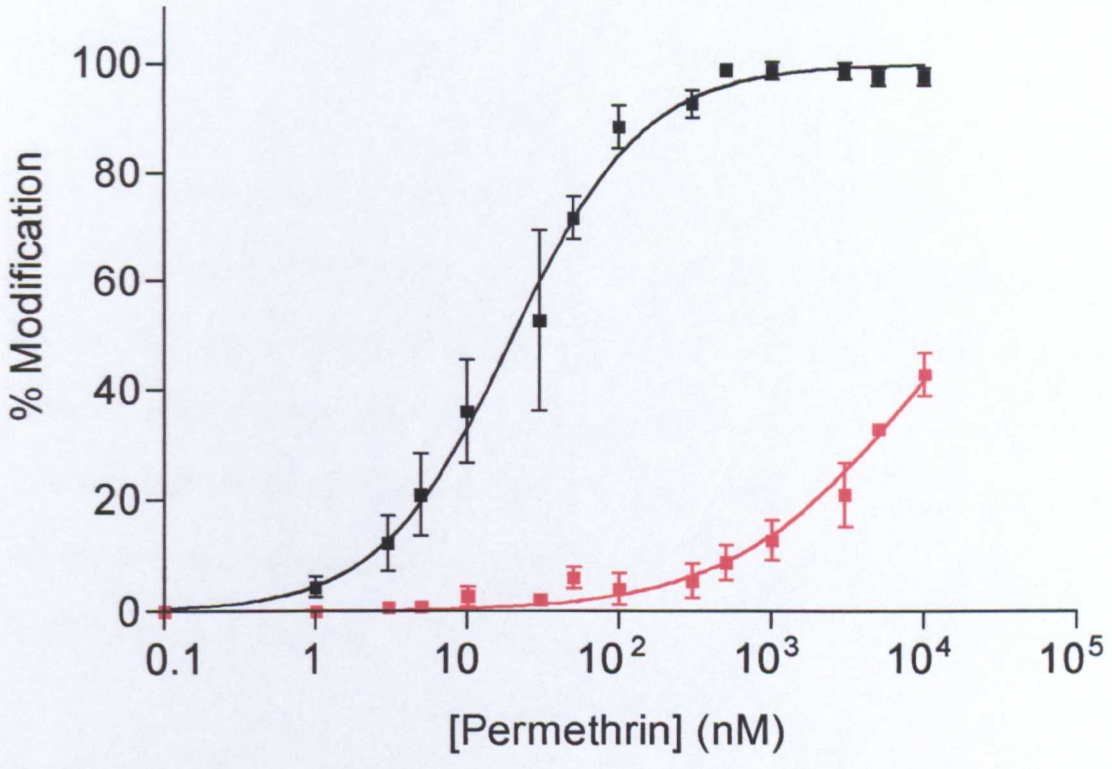

Figure 3.16 Concentration-response relationships for permethrin action on the *para* M918V sodium channel and *drosophila para* wild type sodium channel. The percentage of modified channel was calculated using Equation 3.4 and 3.5 and plotted as a function of permethrin concentration. The data was fitted with a concentration-response equation (Equation 3.6). ▪ Concentration-response relationship for permethrin action on M918V channels (Kd = 8.4μM±2.4; Hill coefficient = 0.6). ▪ Concentration-response relationship for permethrin action on *para* wild type channels (Kd = 10.3±1.0nM; Hill coefficient = 0.9). (Points show the mean + SEM, n=3).

3.4 Discussion of the basis of resistance of M918V channels to deltamethrin and permethrin

3.4.1 M918V is a resistance mutation

M918V is a resistance mutation *in vitro*. It confers resistance levels intermediate between the kdr (L1014F) mutation and the super-kdr (L1014F+M918T) double mutation against deltamethrin and very high levels of resistance against permethrin. Although M918V appears to confer the same type of mechanisms of resistance as the kdr and super-kdr, it remains rare in insect populations, suggesting that the fitness costs that the insect incurs are high.

3.4.2 Effect of kinetics parameters on the fitness costs of M918V channels

Changes in the gating kinetics of the sodium channel can affect the responsiveness of the phenotype. $V_{1/2}$ for inactivation of M918V channels is significantly more negative than that for the wild type channel. M918V channels inactivate more at negative potentials than wild type channels. Therefore, at any given test potential, less M918V channels are available for opening and this could also result in a reduced response to a stimulus.

Mutations that shift the voltage dependence of activation in a depolarising direction require a larger voltage step to be made before channels will open. The probability of an action potential being generated in response to a stimulus is therefore reduced and this might account for "sluggish" responses seen in the phenotype (Lee et al., 1999a).

However, there was no significant difference between the voltage dependence of activation between M918V and *para* wild type channels.

Caution should be employed when extrapolating the effects seen in the oocyte expression system to effects *in vivo*. Changes in the voltage dependence of activation in neurons expressing a resistance mutation V421M found in *Helicoverpa amigera* were far greater than those found when the same mutated channel was expressed in oocytes (Zhao *et al.*, 2000). This may also be the case with M918V where an apparently insignificant shift to more positive potentials in oocytes may be much greater *in vivo* and result in a major fitness cost to the insect. Equally, the significant shift to more negative potentials of the voltage dependence of inactivation in M918V channels, clearly seen in oocyte studies, could translate to a substantial effect *in vivo*. Although it can be hypothesized that shifts in the potential at which a particular type of channel inactivate result in substantially fewer channels opening following a depolarisation, the overall consequence on the behavior of a complex neuronal network, cannot be predicted. Therefore, the survival costs of changes in the gating behavior of the channel cannot accurately be predicted based on oocyte expression alone.

The M918V mutation significantly increases the number of channels that inactivate rather than open from the closed state. This could occur for a number of reasons. First, the mutation may disrupt the open conformation, making it unstable and more difficult to adopt, hence the more positive activation potential, and the rapid transition to an inactive state. Second the S4-S5 linkers of Domains III and IV are described as the docking gate for the fast inactivation particle (Smith et al., 1997; McPhee et al 1998).

Given the proposed symmetrical arrangement of the four domains around a central pore, it is possible that mutations within the S4-S5 linkers of domains I and II, such as M918V, might also exert an influence on the speed and ability of the inactivation particle to dock.

M918V is found in the S4-S5 linker of domain II, an area that is commonly associated with Periodic Paralysis and epilepsy. A point mutation, eight residues downstream from M918V has been associated with Generalised epilepsy with febrile seizures-plus in the human skeletal muscle α subunit. It similarly showed an enhancement of both fast and slow inactivation. This is a possible explanation for the occurrence of epileptic seizures through a decrease in the excitability of inhibitory neurons. (Alekov *et al.*, 2001) Fitness costs may be exerted on M918V insects by a similar mechanism.

Other point mutations found within the S4-S5 linker have significantly reduced the rate of inactivation and the potentials at which it occurs (Lehmann-Horn *et al.*, 1999, Bendahhou et al., 2002). It would appear that both the nature and the position of the mutation within this region dictate the effect on the gating kinetics of the channel.

The application of ATX-II induced a six-fold increase in the maximal sodium conductance. Under normal conditions only 16% of the total M918V available channel population opened in response to a single depolarization compared with 50% of *para* wild type channels. This has the benefit of reducing the number of open channels to which pyrethroids bind preferentially, but it may also compromise the ability of a neuron

to generate and transmit action potentials. Studies of axonal conductance have found a large number of surplus sodium channels which act as standby ion pathways to allow fast conduction of current (Hodgkin, 1975). These safety channels may be lost through the enhanced closed-state inactivation that the M918V mutation confers and consequently hinder the ability of the neuron to transmit an action potential.

The hypothesis that the changes in gating kinetics bestow a detrimental effect on the phenotype has not been tested by behavioral studies of M918V. However investigations of other kdr insects where gating behavior has been altered do suggest a fitness cost. Kdr-like mutations found in the *Heliothis viriscens* voltage gated sodium channel, showed a marked shift in voltage dependence of activation to more positive potentials (Zhao *et al.*, 2000). This was thought to coincide with the decreased neuronal excitability and languid behaviour in the phenotype (Lee *et al.*, 1999a). It has been suggested that this may also lead to a reduction in the fecundity and mating success of the species (Campanhola *et al.*, 1991). Once the selective pressure of the pyrethroid insecticide has been removed, both mutations are rapidly lost from the population, further supporting the view that they have high fitness costs (Elzen *et al.*, 1994).

Investigations of insects carrying the classic L1014F kdr mutation have also shown clear maladaptive behavior. Aphids expressing kdr singly show an inability to react to temperature gradients, which may affect their longevity, fecundity and rate of ovarian development. They are also much less responsive to alarm pheromone, increasing the risk of predation and parasitism (Foster *et al.*, 2000)

However, mutations need not necessarily carry a fitness cost. Some organisms carrying resistance mutations are more successful than their susceptible counterparts, even in the absence of insecticides (Mason, 1998, Haubruge *et al.*, 2001).

3.4.3 Mechanisms of Resistance

The mutation M918V found in a strain of *Bemisia tabaci* is a resistance mutation *in vitro*. It influences the amount of sodium channel modification by both deltamethrin and permethrin suggesting that this residue affects a binding site common to both insecticides either directly or through kinetic or steric alteration. The mechanisms by which it confers this resistance are similar to those of the super-kdr and the kdr.

The study with ATX-II suggests that the M918V mutation increases the fraction of channel undergoing closed state-inactivation. Fewer M918V channels are therefore available for modification by either pyrethroid, both of which preferentially bind to the open state.

Of the channels that do open and bind, the affinity between the protein and the insecticide is significantly reduced. This is reflected in the faster rates of decay of the M918V tail currents, which may act as a measure of how quickly the channel and insecticide molecule dissociate, and the increased Kd values for deltamethrin and permethrin action on the M918V channel.

3.4.4 Deltamethrin Binding

The classic super-kdr, M918T+ L1014F, results in monophasic decay and a reduction in the Hill coefficient from 2 to 1 (Vais *et al.*, 2000). This has been interpreted as the loss of one of the two deltamethrin binding sites. In contrast, the single M918V and single kdr merely reduce the affinity of the channel for deltamethrin. One interpretation is that the kdr and super kdr together form a single binding site and therefore both must be mutated for the site to be lost. This is supported by the close proximity of the two mutations within the predicted 3D structure of the protein (Williamson, personal communication), which might not exceed the length of the pyrethroid molecule in space.

Studies using a range of neurotoxins have identified at least eight distinct neurotoxin binding sites on the sodium channel. These sites can affect ion transport directly or indirectly by modifying the gating process. Allosteric interactions between sites also affect channel functioning and relate to the state dependence of binding. This is shown in the enhanced effect of deltamethrin in the presence of ATX-II. Three of these sites have been highlighted for molecules with similar actions to pyrethroids. Batrachotoxin and veratridine are alkaloids that bind at sites 2 and 5. Pyrethroids are thought to interact with binding site 6. Resistance mutations in various regions of the channels including IIIS6, IVS6 and IS6 confer resistance to both pyrethroids and batrachotoxin suggesting an overlap of these binding regions (Pittendrigh et al 1997; Linford *et al.*, 1998 Wang et al 1999). An area of binding site 2 or 5 could therefore act as a second deltamethrin docking zone as well as influencing pyrethroid binding in other areas of the channel (Vais *et al.*, 2000).

An alternative explanation is that binding is dependent on the nature of the site 918 replacement. A weak interaction with deltamethrin is still formed with valine at the 918 residue, but is completely absent with threonine. M918V +L1014F would therefore still show weak multiple binding. Determining the Hill coefficient of deltamethrin concentration-response curves for M918V +L1014F channels could test this hypothesis.

Kdr and super-kdr may not form a binding site at all, but act together to kinetically or sterically prevent access to another independent binding site. As single mutations they may only partially impede access. Certainly M918V data compared with the double super-kdr mutant hints that M918T and L1014F are not acting independently with respect to deltamethrin binding.

3.4.5 Permethrin Binding

The potency of permethrin is less than that of deltamethrin, with tail currents decaying more rapidly and the proportion of channels modified reduced. The permethrin concentration-response relationship for the wild type channel is characteristic of 1:1 binding (Vais, personal communication). The presence of M918V does not change this ratio. However, affinity of permethrin for the 918 site is greatly reduced. This may be the result of steric hindrance rather than a direct alteration of the permethrin binding site.

Percentage modification by 1μM permethrin saturated at 30 pulses. Higher test pulse frequencies did not increase the number of channels modified by the insecticide. The exponential fit of deltamethrin modification only began to plateau at a pulse frequency

of 200. The enhancement of pyrethroid binding by channel opening is not as great for permethrin as it is for deltamethrin. This may be because the single permethrin binding site is located around the M918V residue area outside the pore and so accessibility is less dependent on channel state. Deltamethrin modification is far more dependent on channel state because a second putative deltamethrin binding site may only be accessible when the channel is open.

3.4.6 Reasons for the rarity of the M918V mutation in field populations.

A number of hypotheses have been put forward as to why the super-kdr mutation has not been found without the kdr. It has been suggested that the evolution of knockdown resistance is a sequential process. The kdr mutation must be present before any change can be made at the super-kdr site on the same allele (Jamroz *et al.*, 1998). An alternative explanation is that the kdr counters the fitness costs incurred by the single super-kdr. This would stabilise the presence of the super-kdr even in the absence of pyrethroid pressure (Jamroz *et al.*, 1998)

Support for this idea comes from studies done on resistance mutations found in German cockroach sodium channels. Alterations of sodium current magnitudes from channels containing single super-kdr like mutations located in the linker between domains I and II of the German cockroach sodium channels are restored to the wild type level and channel sensitivity to deltamethrin markedly reduced when co-expressed with the kdr L993F mutation found in German cockroach (Tan *et al.*, 2002). These studies have also found that when expressed alone, the super-kdr like mutation of the D1-D2 linker does

not confer resistance. This is in marked contrast to M918V mutant channels, which alone reduces sodium channel sensitivity to deltamethrin and permethrin.

Other studies have found that the M918T mutant expresses poorly in *Xenopus* oocytes leading to the conclusion that for functional expression of the channels containing the super-kdr mutation, the stabilizing presence of the kdr is required (Lee *et al.*, 1999). However, the M918V mutation alone causes a significant percentage of channels to undergo closed-state inactivation, which may explain reduced current magnitudes.

The data presented here suggests that fitness costs incurred by changes in the channel kinetics might outweigh the benefits of pyrethroid resistance in the absence of selection. Larger numbers of M918V channels undergo closed state inactivation at more hyperpolarising potentials than either the wild type, kdr or super-kdr mutants. The M918V mutation may force sodium channel kinetic thresholds to be crossed, after which functioning of the entire neuron is severely compromised.

However, the resistance factors of the target site are large, over 800-fold for permethrin, a widespread and frequently used Type I pyrethroid. Sufficient selection pressure therefore exists for the mutation to appear more commonly. M918V appears to use the same resistance mechanisms as the kdr and super-kdr; a reduction in channel opening and a decreased affinity between the insecticide and the channel, neither of which do not seems to bestow any severe phenotypic handicap.

Small gating changes and high levels of closed-state inactivation detected in the oocyte expression system may inflict large changes when M918V channels are expressed *in vivo*.

CHAPTER 4

SENSITIVITY OF THE PARA T929V AND T929M VOLTAGE-GATED SODIUM CHANNEL MUTANT TO DELTAMETHRIN

4.0 Introduction

In addition to the kdr and super-kdr mutations of insect *para* sodium channels, mutations of the threonine residue at site 929, which is located very close to the intracellular end of the S5 segment of domain II, can also confer resistance to pyrethroid insecticides. A pyrethroid-resistance mutation (T929I) at this site was first detected in conjunction with the kdr L1014F mutation in a pyrethroid resistant strain of the diamondback moth *Plutella xylostella* (Schuler *et al*, 1998). It confers similar levels of resistance to that found in houseflies carrying both the kdr L1014F mutation and the super-kdr mutation M918T. A T929I mutation has since been found in conjunction with an L932F mutation in headlice, *Pediculus capititus* (Lee *et al*, 2000). In a deltamethrin-resistant strain of the tobacco whitefly *Bemisia tabaci,* T929 is mutated to T929V. Bioassay data from this Lnfu-1 strain showed high levels of resistance to both DDT and Type II pyrethroids (Goodson, personal communication).

Hyperkalemic periodic paralysis (HYPP) is an inheritable myotonic disease, which results in episodes of electrical inexcitability and paralysis of skeletal muscles. The condition results from genetic mutations in the human skeletal muscle Na channel. To date, six mutations thought to cause HYPP have been described, all of which are localised at the intracellular membrane interface (Bendahhou *et al.,* 2002; Yang *et al.,* 1994; Wagner *et al.,* 1997; Hayward *et al.,* 1997; Rojas *et al.,* 1991). Interestingly, the most common HYPP mutation, T704M (Plácek *et al*, 1991) in the human skeletal muscle Na channel, maps to the corresponding T929 residue mutated in the pyrethroid resistant insect Na channel. Studies of the T698M residue in rat skeletal muscle Na channels expressed in human embryonic kidney 293 cells, showed a significant

hyperpolarizing shift in the voltage-dependence of activation of the mutant channel (Cannon and Strittmatter, 1993; Cummins *et al.*, 1993; Yang *et al.*, 1994) and a dramatic impairment of its "slow" inactivation (Cummins and Sigworth., 1996) These changes in channel kinetics are thought to underlie the persistent current which result in the periods of muscle paralysis seen in HYPP sufferers. Are the same kinetic changes seen when the HYPP mutation is introduced into the *para* Na channel of *Drosophila,* i.e. the mutation T929M and does this mutation confer resistance to deltamethrin?

The aim of the work described here was to compare the kinetics and deltamethrin sensitivity of the novel T929V mutated channel reported in *Bemisia tabaci* and the T929M sodium channel mutation responsible for the HYPP condition. Although mutations of threonine at the 929 position have been recorded in other pyrethroid resistant insect species, the mechanism by which these mutations confer resistance has not been investigated. However, the proximity of the 929 residue to the 1014 and 918 residues associated with kdr and super-kdr residues, suggests that mutations of the 929 residue may similarly alter channel kinetics (Section 3.4.3) and change a putative pyrethroid binding site which the 918, 929 and 1014 residues form within the *para* channel protein.

4.1 Comparison of *para* wild type sodium channels and channels with the T929V and T929M mutation.

4.1.1 The voltage dependence of activation and inactivation of T929V and T929M channels

The same pulse protocol used to measure M918V steady state activation was used for investigating the T929V mutant and the T929M mutant. Both T929V and T929M channels activate at more negative potentials than *para* wild-type channels. This is seen when the conductance-voltage relationships for these channels are compared (Figures 4.1 and 4.2). The mid-point potentials of activation of the T929V mutant and the T929M mutant were significantly (P=0.011 and P=0.0066 respectively; two-tailed t-test) more negative than that of the wild type Na channel. With T929V, there was a hyperpolarizing 5mV shift in activation and with T929M there was a hyperpolarizing 6mV shift.

The voltage dependence of inactivation of the T929V mutant and the T929M mutant was determined using the same pulse protocols as those employed for studying the M918V mutant. The midpoint potentials for inactivation for T929V channels and T929M channels were not significantly different (P>0.01, two-tailed t-test) from the midpoint potential of the *para* wild type channel.

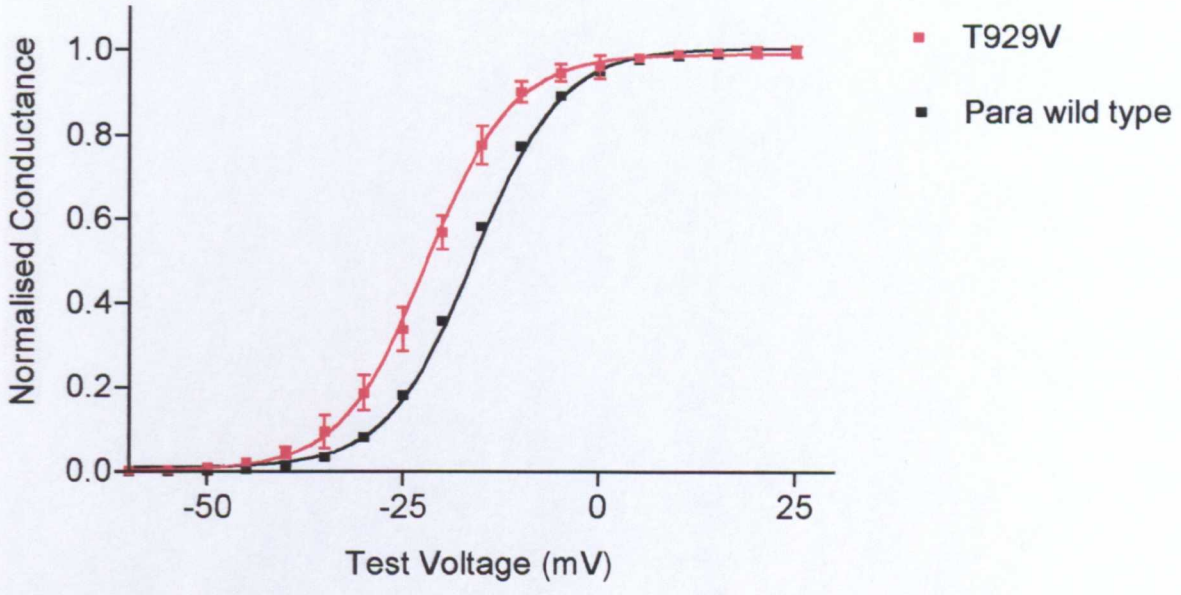

Figure 4.1. Voltage dependence of activation of T929V and *para* wild type channels. Channels were pulsed from a holding potential of –70mV to the test voltage. From the resulting peak current, conductance was calculated using Equation 3.5. Data was normalised to maximum peak conductance and fitted with a Boltzmann relationship. T929V channels activate at significantly (P=0.011; two-tailed t-test) more negative potentials than *para* wild type channels (T929V, $V_{1/2}$ = -22.1±1.2; *para* wild type, $V_{1/2}$ = -16.9±1.4). (Points show mean ± SEM, n=10).

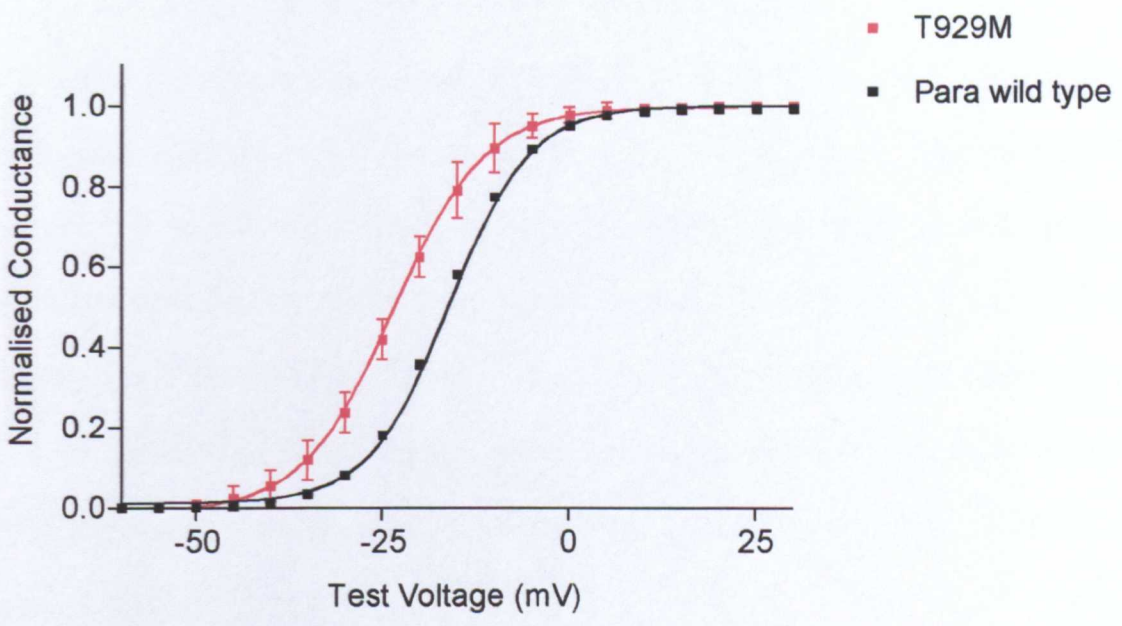

Figure 4.2. Voltage dependence of activation of T929M and *para* wild type channels. Channels were pulsed from a holding potential of –70mV to the test voltage. From the resulting peak current, conductance was calculated using Equation 3.5. Data was normalised to maximum peak conductance and fitted with a Boltzmann relationship. T929M channels activate at significantly (P=0.0066; two-tailed t-test) more negative potentials than *para* wild type channels (T929M, $V_{1/2}$ = -23.5±1.3, n=6; *para* wild type, $V_{1/2}$ = -16.9±1.4, n=10). (Points show mean ± SEM).

4.1.2 The kinetics of inactivation of T929V and T929M channels

The onset of, and recovery from, fast inactivation of the mutant channels was determined using the multi-pulse protocol detailed in Section 3.1.3. Like the M918V mutant, the T929V mutant inactivates significantly more quickly at all pre-pulse potentials than the wild type channel (pre-pulse, –40mV; T929V, τ = 5.08 $\pm$ 0.6ms; wild-type, τ = 13.9 $\pm$ 1.6ms; two-tailed t-test, P = 0.0067). Using a conditioning pre-pulse of –50mV, the T929V channel was found to recover significantly more quickly from inactivation than the wild-type channel (pre-pulse –50mV; T929V, τ = 6.83 $\pm$ 0.7ms; wild type, τ = 11.4 $\pm$ 1.1ms; P = 0.025).

T929M channels also showed accelerated kinetics of inactivation. The onset of inactivation in T929M channels was significantly faster than in wild type channels (pre-pulse –40mV; T929M, τ = 4.8 $\pm$ 2.57ms; wild-type, τ = 13.9 $\pm$ 1.6ms; two-tailed t-test, P = 0.039). The mutant recovered from inactivation more quickly than the wild-type at all pre-pulse potentials (pre-pulse, –50mV; T929M, τ = 7.3 $\pm$ 1.78ms; wild-type, τ = 11.4 $\pm$ 0.4ms; two-tailed t-test, P = 0.09).

4.1.3. Analysis of the effect of deltamethrin insecticide on T929V and T929M channel gating.

The effect of deltamethrin was investigated using the same method employed to study the effect of the insecticide on M918V channels (Section 3.2.1). The amplitude and rate of decay of the tail current seen following repolarisation provided a measure of T929V and T929M channel sensitivity to the deltamethrin.

4.1.4. Binding of deltamethrin to the T929V and T929M channels

T929V sodium channel tail current amplitudes in the presence of deltamethrin were larger following a train of a hundred 5ms pulses to 0mV at 66Hz from a holding potential of −100mV, than following a single pulse to 0mV of equal duration (Vais *et al.* 2000). The interval between pulses was 10ms, which was sufficient to allow channels to recover from open state inactivation. Tail current amplitudes increased with the train duration (Figure 4.3), suggesting that deltamethrin binds preferentially to the T929V channel open state. A similar result was seen with the T929M channel.

4.1.5. The effect of T929V mutation and the T929M mutation on closed-state inactivation

As shown in Vais *et al.* (2000) and discussed in section 3.2.3 of this study, different proportions of *para* L1014F channels, *para* L1014F + M918T channels, *para* M918V channels and *para* wild type channels undergo closed-state inactivation. Treatment of oocytes expressing *Drosophila para* Na channels with ATX-II toxin slowed inactivation from the closed channel state such that it was effectively eradicated (Warmke *et al.*, 1997). Comparisons of the total maximal conductance in the presence of the toxin with the total maximal conductance in the absence of the toxin, can give a measure of the proportion of channel populations undergoing closed-state inactivation (Figure 4.4).

In the presence of ATX-II, the maximum conductance for the *para* wild type sodium channel population increased >2-fold, the maximum conductance of T929V channel population increased ~4-fold, and the maximum conductance of the T929M channel

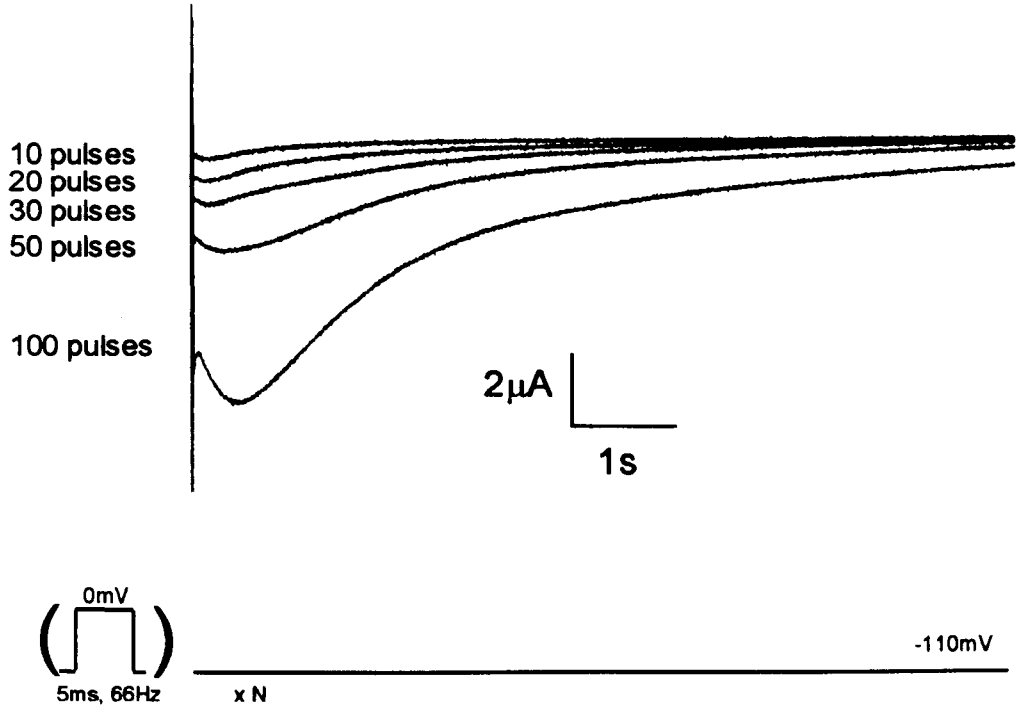

Figure 4.3. Changes in the T929V tail current amplitude are induced by varying the number of depolarizing pulses in a train in the presence of 10μM deltamethrin. Tail currents were measured following 5ms depolarization to 0mV at 66Hz from a holding potential of –100mV. N represents the number of pulses in a train and is shown to the left of each tail current.

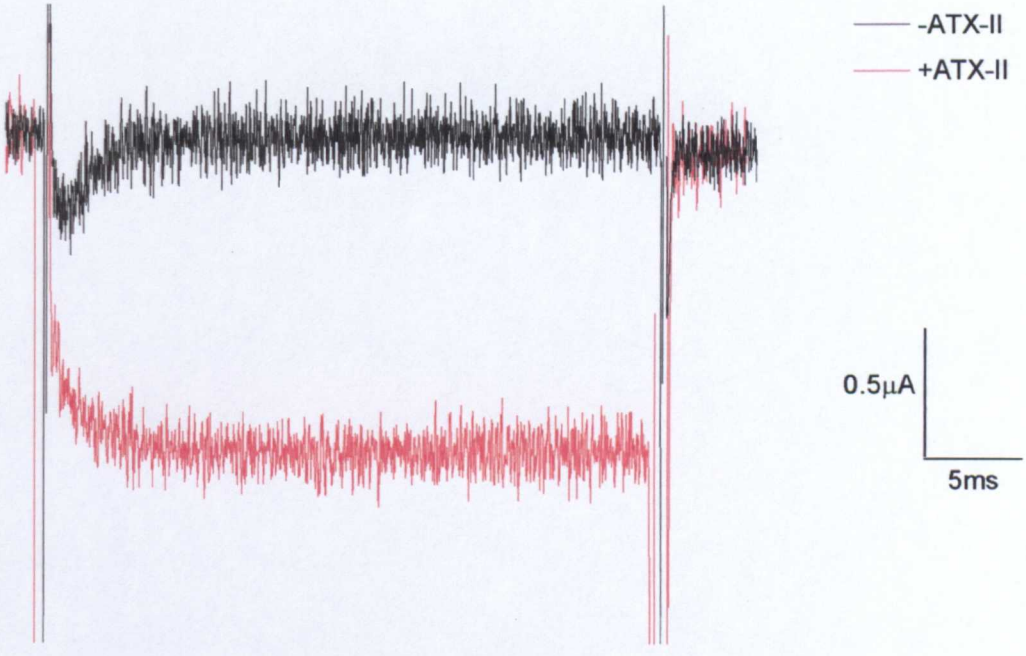

Figure 4.4. Sodium currents recorded during a 32ms depolarising pulse to –10mV with (-) and without (-) the toxin ATX-II, from an oocyte expressing T929Vchannels. Peak current in the absence of ATX-II is 310nA. In the presence of ATX-II the peak current is 1.3μA, and remains at this current for the duration of the depolarising pulse.

population increased ~5-fold (*para* wild type: $G_{Na\ Max} = 2.2 \pm 0.4$; T929V $G_{Na\ Max} = 3.7 \pm 0.3$; T929M $G_{Na\ Max} = 4.8 \pm 0.3$) (Figure 4.5). Therefore, in the absence of the toxin, approximately 25% of available T929V channels and 21% of available T929M channels open following a strong depolarising pulse compared with 45% of available wild-type channels. It follows that the T929V and T929M mutations confer significant increases in the number of channels entering the inactivated state rather than the open state to which deltamethrin preferentially binds.

4.1.6. Sensitivity of the T929V and the T929M mutant to deltamethrin

To estimate and compare the proportions of mutant and wild type channels that bind the insecticide, differences in the fraction of channels that enter the open state in response to a test pulse must be removed. Therefore, oocytes expressing the T929V mutant or the T929M mutant were treated with 500nM ATX-II to inhibit closed-state inactivation and then exposed to deltamethrin at concentrations ranging from 10nM to 10μM. The peak tail current and the rate of decay of the tail current, obtained from single 320ms depolarising pulses from –100mV to 0mV, was recorded for each concentration of deltamethrin.

Tail currents for both T929V channels and T929M channels decayed completely following exposure to 10μM deltamethrin. This was a preliminary indication that both mutations confer resistance to the pyrethroid. Tail currents of the wild-type channel did not recover to zero current when deltamethrin was applied at a concentration of 30nM or more.

Figure 4.5. Single experiments showing the relative conductance as a function of test voltage of (A) T929M channels and (B) T929V channels, in the presence (▪) and absence (▪) of ATX-II. Conductance of channels in the presence and absence of the toxin at each test potential was calculated using Equation 3.5 and the resulting curve fitted with a Boltzmann relationship. ATX-II increased T929M maximum conductance, $G_{Na\ Max}$, 4.8±0.3 – fold and T929V maximum conductance 3.7±0.3 – fold.

(A)

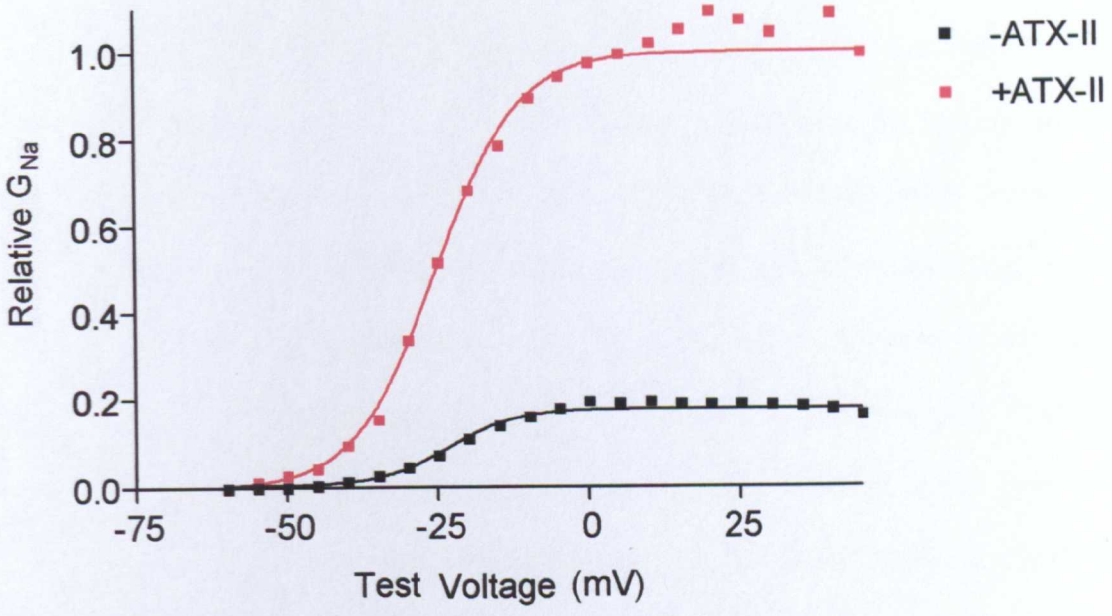
Relative G_{Na}
1.0
0.8
0.6
0.4
0.2
0.0
-75
-50
-25
0
25
Test Voltage (mV)
-ATX-II
+ATX-II

(B)

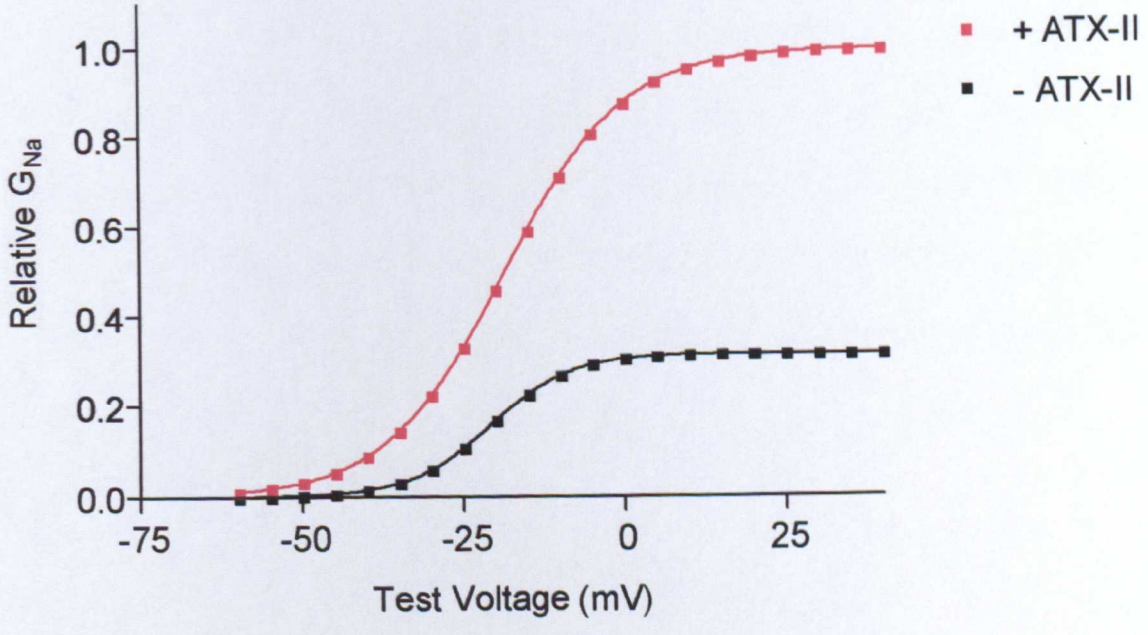
Relative G_{Na}
1.0
0.8
0.6
0.4
0.2
0.0
-75
-50
-25
0
25
Test Voltage (mV)
+ ATX-II
- ATX-II

Concentration-response relationships for each channel type were constructed using the methods described in section 3.2.4. A reactivation hook seen in *para* wild type and M918V channel tail current traces was also seen in T929V channel tail currents and T929M channel tail currents but the hook was not included in the determination of peak tail current. The percentage of channels modified by the pyrethroid was estimated using Equation 3.4 and 3.5 and plotted as a function of deltamethrin concentration. These data were then fitted with a variable sigmoidal equation (Equation 3.6), from which a Kd value and a Hill coefficient were estimated. The T929V mutation caused a ~2600-fold decrease in the sensitivity of the wild-type channel to deltamethrin (T929V, Kd = 11.7 $\pm$ 5μM; wild-type, Kd = 4.4 $\pm$ 0.16nM). The Hill coefficient for the mutant was <1, whereas that of the wild type was 2 (T929V, Hill coefficient = 0.88; wild type, Hill coefficient = 2.05) (Figure 4.6). The T929M mutation caused a similar decrease in the sensitivity of the mutant *para* sodium channel (T929M, Kd = 11.4 $\pm$ 1.7μM; wild-type, Kd = 4.4 $\pm$ 0.16nM). The Hill coefficient for the T929M channel was also <1 (T929M, Hill coefficient = 0.6) (Figure 4.7). Although the Hill coefficient is not a direct measure of the number of deltamethrin binding sites, it does set a lower limit. The concentration-response relationships suggest that *para* wild type channels with 2 or more binding sites are reduced to one binding site when the T929V mutation or the T929M mutation is introduced.

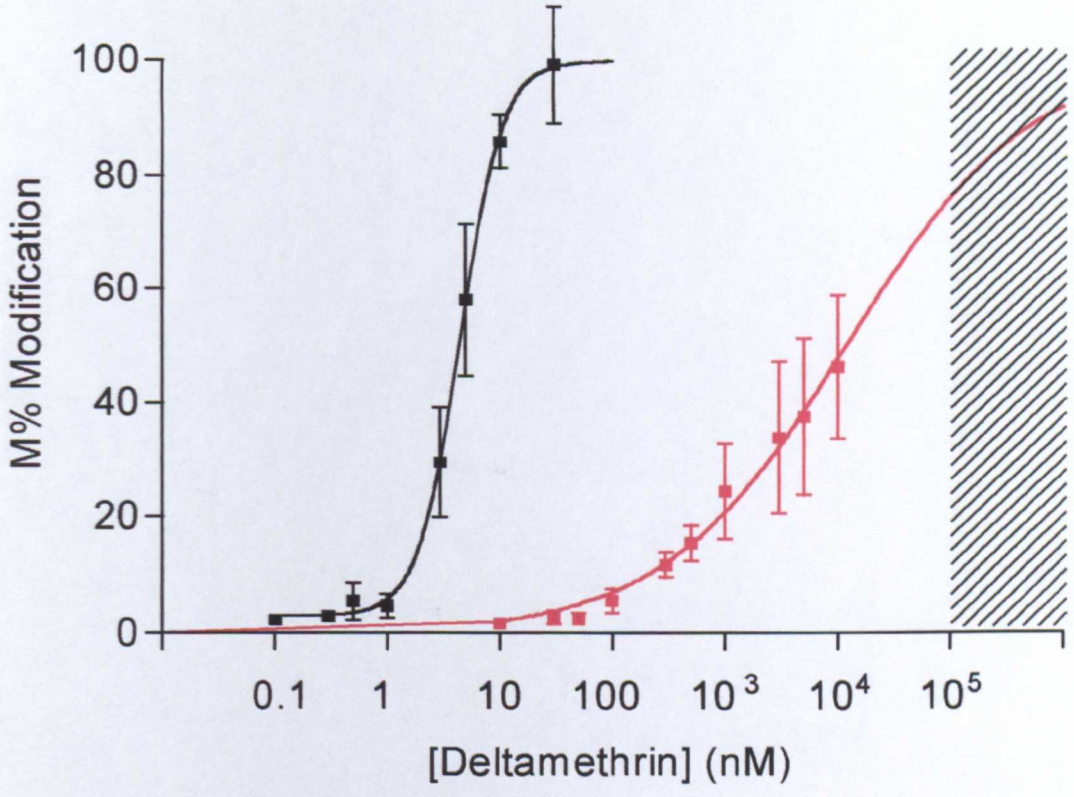

Figure 4.6. Concentration-response relationships for deltamethrin action on the T929V *para* sodium channels and the *drosophila para* wild type sodium channel. The percentage of modified channels was calculated using Equations 3.4 and 3.5 and plotted as a function of deltamethrin concentration. The data was fitted with a concentration-response equation (Equation 3.6)

(▪) Concentration-response relationship for deltamethrin action T929V para channels (Kd= 11.7 ±5μM; Hill coefficient = 0.88). (•) Concentration-response relationship for deltamethrin action on the *Drosophila para* wild type sodium channel (Kd= 4.4±0.16 nM; Hill coefficient = 2). (Points show mean ± SEM, n =3).

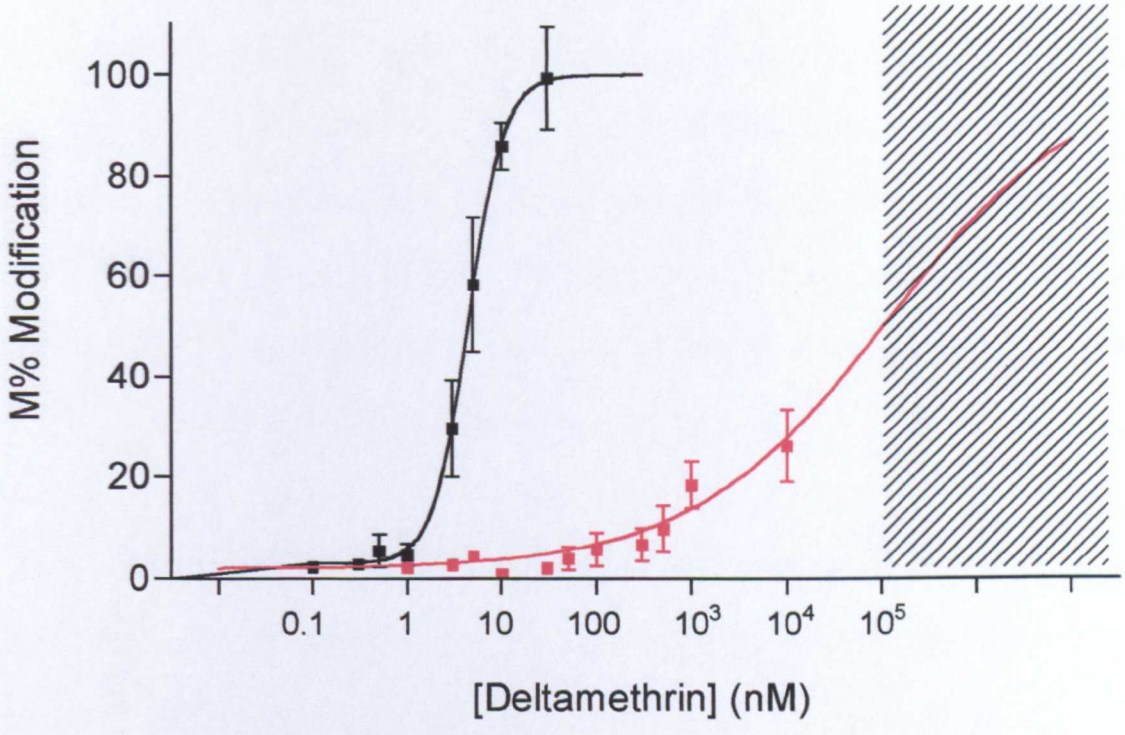

Figure 4.7. Concentration-response relationships for deltamethrin action on the T929M *para* sodium channels and the *Drosophila para* wild type sodium channel. The percentage of modified channels was calculated using Equations 3.4 and 3.5 and plotted as a function of deltamethrin concentration. The data was fitted with a concentration-response equation (equation 3.6).

(▪) Concentration-response relationship for deltamethrin action *para* T929M channels (Kd= 11.4 ±1.7μM; Hill coefficient = 0.6). (▪) Concentration-response relationship for deltamethrin action on the *Drosophila para* wild type sodium channel (Kd= 4.4±0.16nM; Hill coefficient = 2). (Points show mean ± SEM, n = 3).

4.1.7 Tail currents of the T929V mutant channel and the T929M mutant channel

The rate of tail current decay following a single 320ms depolarising pulse to 0mV from a holding potential of −100mV in the presence of ATX-II and deltamethrin was estimated from exponential functions fitted to the tail current profiles of T929V and T929M channels (Methods 2.3.8). The decay of tail currents of both T929V and T929M mutants was preceded by an inward current, the amplitude of which was dependent on the concentration of deltamethrin.

Tails currents from T929V mutants could be fitted with two exponential functions at all concentrations of deltamethrin when the reactivation hook was excluded. The faster of the two time constants was independent of deltamethrin concentration (τ_1 = 1.33 ± 0.17s). The slower of the two time constants was dependent on deltamethrin concentration and increased as the concentration of the pyrethroid increased. For example, at 1μM deltamethrin, τ_2 = 6s, whereas at 10μM deltamethrin τ_2 = 10s (Figure 4.8).

Tail currents from T929M mutants could also be described by two exponential functions. Again, the faster of the two time constants was independent of deltamethrin concentration (τ_1 = 0.96 ± 0.12s) whereas the slower time constant increased as the concentration of deltamethrin was increased (Figure 4.8). The fast component, τ_1, of T929V tail current decay was not significantly different (P =0.15, two-tailed t-test) from the fast component of T929M tail current decay.

Figure 4.8. Tail current traces from (A) T929V channels in the presence of 500nM ATX-II and different concentrations of deltamethrin, which are indicated to the left of each tail current. Both T929V tail currents were best described by two exponential functions (1μM deltamethrin, $\tau 1$=1.13s, $\tau 2$= 6s; 10μM deltamethrin, $\tau 1$=1.13s, $\tau 2$= 10s). Tail current traces from (B) T929M channels in the presence of 0.5mM ATX-II and different concentrations of deltamethrin, which are indicated to the left of each tail current. Both T929M tail currents were also best described by two exponential functions (1μM deltamethrin, $\tau 1$=1.16, $\tau 2$= 18s; 10μM deltamethrin, $\tau 1$=1.17, $\tau 2$=23s).

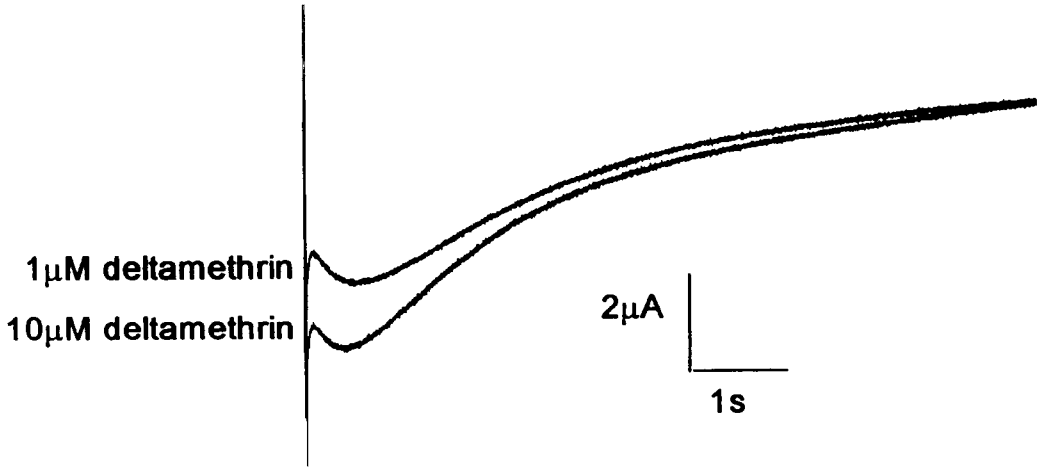

(A) T929V

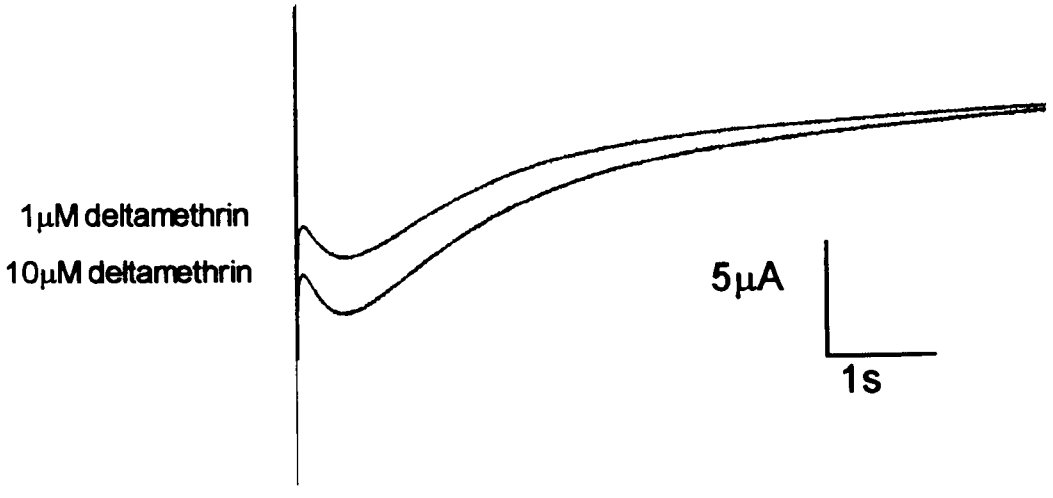

(B) T929M

Both T929M and T929V tail currents decay significantly more quickly than those of the *para* wild type channel in the presence of deltamethrin and ATX-II and this suggests that the mutations counter the slowing of channel deactivation induced by deltamethrin.

4.2 The effect of T929M and T929V sodium channel sensitivity to deltamethrin

T929V channels and T929M channels are significantly less sensitive to deltamethrin than *para* wild type channels. This is perhaps unsurprising, as the 929-residue position has already been highlighted as important in a number of pyrethroid-resistant pest species (Schuler *et al*, 1998, Lee *et al.*, 2000; Goodson *et al.*, RES unpublished).

Both mutations appear to affect the *Drosophila para* Na channel properties in a similar way as the mutations L1014F, M918T (Vais *et al.*, 2000) and M918V (Chapter 3). Analysis of tail currents following single and multiple pulsing regimes suggests that deltamethrin binds preferentially to the open state of both T929M and T929V channel mutants. Comparisons of the maximum conductance in the presence and absence of ATX-II, a toxin that essentially eradicates closed-state fast inactivation (Warmke *et al.*,1997), suggest that both T929V and T929M mutations cause a larger proportion of mutant channel populations to enter the fast-inactivated state, rather than the open state to which deltamethrin preferentially binds. This finding together with a recent model proposing that fast inactivation inhibits the onset of slow inactivation (Hilber *et al.*, 2002), could explain the significant inhibition of slow inactivation observed in T704M mutant human skeletal muscle sodium channels (Bendahhou *et al.*, 1999). Indeed, these studies now suggest that the S5 segment where T704M is located, could act as a coupling site for fast and slow inactivation.

Interestingly, the small, persistent sodium current that is characteristic of the HYPP condition can be reproduced in normal muscle by the *in vitro* application of ATX-II (Cannon *et al.*, 1993). However, this increase in the steady-state open probability of sodium channels common to HYPP mutant channels and wild type channels treated with ATX-II could belie different causes of the same symptom. ATX-II eradicates fast inactivation (Warmke *et al.*, 1997), while the T704M mutation inhibits the onset of slow inactivation (Bendahhou *et al.*, 1999) and both effects would result in more channels being available for activation.

Of the T929M and T929V channels that do activate following a depolarising pulse, the affinity between the open channel and the deltamethrin molecule is reduced compared with the *para* wild type channel. Kd values obtained from concentration-response relationships are consistent with estimate that the T929V mutation and T929M mutation reduce mutant channel sensitivity to deltamethrin approximately 2600-fold. This is reflected in the bioassay data collected from the *B. tabaci* strain carrying the T929V mutation. 100% and 80% survival of the T929V *B. tabaci* strain was recorded at cypermethrin and DDT concentrations which resulted in 100% mortality of the wild type strain (Goodson, personal communication).

Both T929V and T929M tail currents can be described by two time constants, a fast component, which is independent of deltamethrin concentration, and a second, slower time constant, which increases with deltamethrin concentration. The multi-exponential fit to the tail current decay of T929M and T929V channels suggest complex recovery kinetics.

The concentration-response relationships for deltamethrin action on both T929V and T929M channels, based on tail current amplitudes, have a Hill coefficient of 1, which suggests a single binding site. This is in contrast to the *para* wild type channel, which has a Hill coefficient of 2, suggesting at least two binding sites (Vais *et al.*, 2001). Predictions of the interaction between this insecticide and binding sites on the *Drosophila* Na channel are difficult because a detailed 3D model of the protein has not yet been obtained. The T929V and T929M mutations may reduce deltamethrin binding by directly destroying a deltamethrin binding site. An alternative possibility is that mutations at T929 indirectly reduce the affinity of deltamethrin by altering the tertiary structure of the intracellular interface of the S5 segment of domain II, thereby influencing the conformation of a deltamethrin binding site at a location elsewhere on the *Drosophila* Na channel.

Despite the high level of deltamethrin resistance conferred by the T929M mutation, this single mutation has not yet been recorded in the wild. Whilst it may already reside in insect pest populations and simply awaits detection, the T929M mutant may not be a viable channel and therefore would never have been selected. The significant hyperpolarising shift in the voltage dependence of activation and a large proportion of channels undergoing closed-state inactivation may significantly compromise functioning *in vivo*.

Although it is not known how kinetic changes conferred by the T929M mutation affect insect behaviour *in vivo*, similar kinetic changes recorded when the mutation is

introduced into the rat muscle sodium channel (T689M) and studied in human embryonic kidney (HEK) cells are thought to account for the HYPP condition seen in humans and equines. A 10-15mV hyperpolarizing shift in the voltage dependence of activation resulting in a persistent sodium current that activated near –70mV(Cummins *et al*, 1993) are thought to contribute to the myotonia

Despite Western immunoblots detecting similar amounts of rat wild-type and rat T698M channels in HEK cells, T698M channel peak currents elucidated by depolarising pulses were consistently smaller than wild type channel peak currents elucidated by the same depolarising protocol (Cummins *et al.*, 1993). A number of possible explanations have been suggested, including an increase in the proportion of the synthesised channels retained within the cell rather than migrating to the membrane surface (Cummins *et al.*, 1993; Ukomanda *et al.*, 1992). However, as shown in the this study with T929M *para* channels expressed in oocytes, it seems likely that the T689M mutation increases the number of rat channels undergoing closed-state inactivation and therefore reduces the maximum conductance of the channel population.

The equivalent T704M mutation in human skeletal muscle sodium channels also shows severely impaired slow inactivation and a significant hyperpolarising shift in the voltage dependence of activation when expressed in HEK cells (Cummins and Sigworth, 1996). Together with a slowing of channel deactivation, this could account for the sustained currents characteristic of HYPP (Bendahhou *et al.*, 1999). T929V mutants and T929M mutants also showed a significant hyperpolarising shift in the voltage dependence of

activation although slow inactivation of the *para* mutants was not studied in this instance.

Interestingly however, the slowing of channel deactivation, characteristic of deltamethrin modification and also now seen in T704M human skeletal muscle sodium channel mutants (Bendahhou *et al.*, 1999), is significantly reduced in T929M *para* mutants in comparison to *para* wild type channels when exposed to the insecticide in the presence of ATX-II. Although the rate of T929M *para* sodium channel deactivation was not studied in the absence of deltamethrin, it may, like its T704M human skeletal sodium channel counterpart, also slow the rate of channel deactivation. Therefore, despite possibly inducing the same effect as deltamethrin, the rate of deactivation is not further slowed when T929M mutants are exposed to deltamethrin. Indeed the opposite is true as T929M significantly reduces the deltamethrin-induced slowing of deactivation of mutant channels in comparison to the *para* wild type channels. The effect may not be additive because T929M reduces the affinity of deltamethrin for the channel mutant directly and indirectly through elevated levels of closed-state inactivation.

CHAPTER 5

SENSITIVITY OF RAT IIA BRAIN VOLTAGE-GATED SODIUM CHANNEL MUTANTS TO DELTAMETHRIN

5.0 Introduction

Mammalian sodium channels are ~4500 fold less sensitive to pyrethroids than their insect counterparts. Until recently, pyrethroid insensitivity of mammals *in vivo* was thought to be the consequence of the higher metabolic rates and body temperatures of these animals (Narahashi, 1992). However, pyrethroid molecules that do manage to overcome these metabolic obstacles and reach neuronal sodium channels find their target highly insensitive (Song and Narahashi, 1996b). What differences between the insect and mammalian sodium channels could account for such a large difference in their pyrethroid sensitivities? The *Drosophila para* sodium channel shares 50% homology with its counterparts in mammalian excitable tissues (Warmke *et al.*, 1997). When the sequences of these two proteins are aligned it is clear that the kdr residue is conserved in both suggesting that this is not the region responsible for differences in sensitivity. The two channels do, however, differ at the super-kdr site (position 874 in the rat brain IIA sodium channel and site 918 in the *para* sodium channel) with isoleucine found in place of the methionine residue that is always found in wild type insects. Replacement of the isoleucine with methionine could therefore raise the mammalian sodium channel sensitivity to pyrethroids.

To investigate this possibility, methionine was substituted for isoleucine at the super-kdr position in the rat IIA brain sodium channel (I874M) (Figure 5.1). The mutant I874M channel and the rat IIA wild type channel were expressed in *Xenopus laevis* oocytes, exposed to a range of deltamethrin concentrations and their sensitivities tested using voltage clamp. Other amino acids were also substituted at the 874 position in a further attempt to clarify the interaction between deltamethrin and the rat IIA sodium channel.

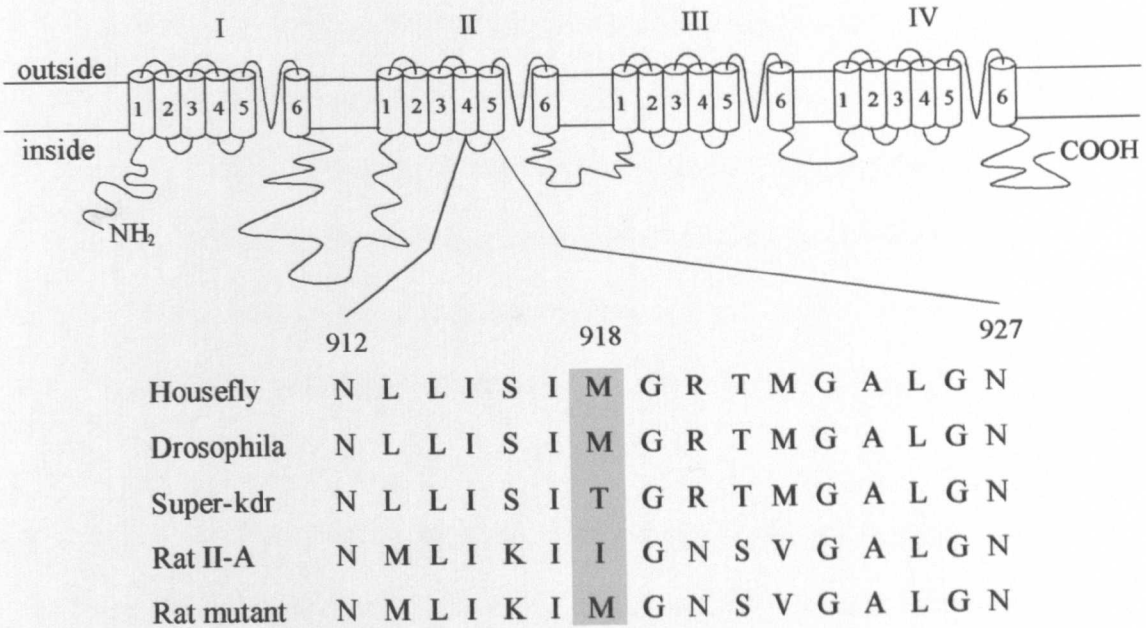

Figure 5.1 A generalised sodium channel α-subunit with the amino acid sequence alignment, from a number of species, of the S4-S5 linker in domain II. The highlighted residues are those found at the super-kdr position (eg M918 in *Drosophila para* sodium channel and I874 in rat IIA sodium channels). The alignment of amino acid sequences in the region of the super-kdr mutation, M918T, suggests that mutation of the isoleucine in the equivalent 874 position in the rat IIA brain sodium channel to methionine, could raise the sensitivity of this mutant channel to pyrethroids.

5.1 The kinetics of I874M

The voltage dependence of activation and inactivation were tested using the same pulse protocols as for the *Drosophila para* sodium channels (Section 3.1.1 and Section 3.1.2). No significant difference was found between mutated and wild type channels.

The speed of onset and recovery from inactivation was determined using the same pulse protocols as those used with the *Drosophila para* sodium channel (Section 3.1.3). No significant difference was found between the two channel types (Table 5.1).

5.2 The effect of I874M on the rat channel sensitivity to deltamethrin.

As with *Drosophila para* sodium channels, tail currents following repolarisation of the oocytes membrane to –110mV were used as a measure of sensitivity to deltamethrin.

5.2.1 Binding of deltamethrin to the I874M channel

The tail current amplitudes for wild type and mutated *Drosophila para* sodium channels, in the presence of deltamethrin, were larger following a train of a hundred 5ms depolarisations to 0mV at 66Hz from a holding potential of –100mV, than following a single pulse to 0mV of equal duration. This is also true for the rat wild type and rat I874M channel. When the pulse frequency was increased at a constant deltamethrin concentration, the peak amplitude of the tail currents also increased. Sodium channels remain open for a longer period as the number of pulses and concurrently the duration of the train of pulses increases. This suggests that that deltamethrin also binds preferentially to the open state of the rat IIA sodium channel (Figure 5.2).

	Wild Type	I874M mutant	I874C mutant
Activation			
$V_{1/2}$ (mV)	-23.8±0.7	-24.7±0.9	-26.4±1.6
k (mV)	5.54±0.23	5.5±0.12	4.10±0.37
Inactivation			
$V_{1/2}$ (mV)	-54.9±0.8	-54.1±0.5	-51.6±0.54
k (mV)	5.1±0.1	5.2±0.1	5.05±0.29
τ_{onset} (ms) (-40mV)	19.0±2.2	17.2±1.6	26.0±1.89
τ_{recov} (ms) (-50mV)	36.7±0.89	34.4±1.9	24.5±4.84
Deltamethrin			
K_d (μM)	95	0.65±0.001	1.2±0.13
τ_{tail} (-100mV)	86±2ms	505±7ms	230±25ms

Table 5.1. Kinetics of activation and inactivation and the onset of, and recovery from, inactivation of I874M, I874C and rat wild type channels. Kd is the dissociation constant of the I874M, I874C and rat wild type channels. τ is the time constant of onset and recovery from inactivation for the I874M, I874C and wild type channels.

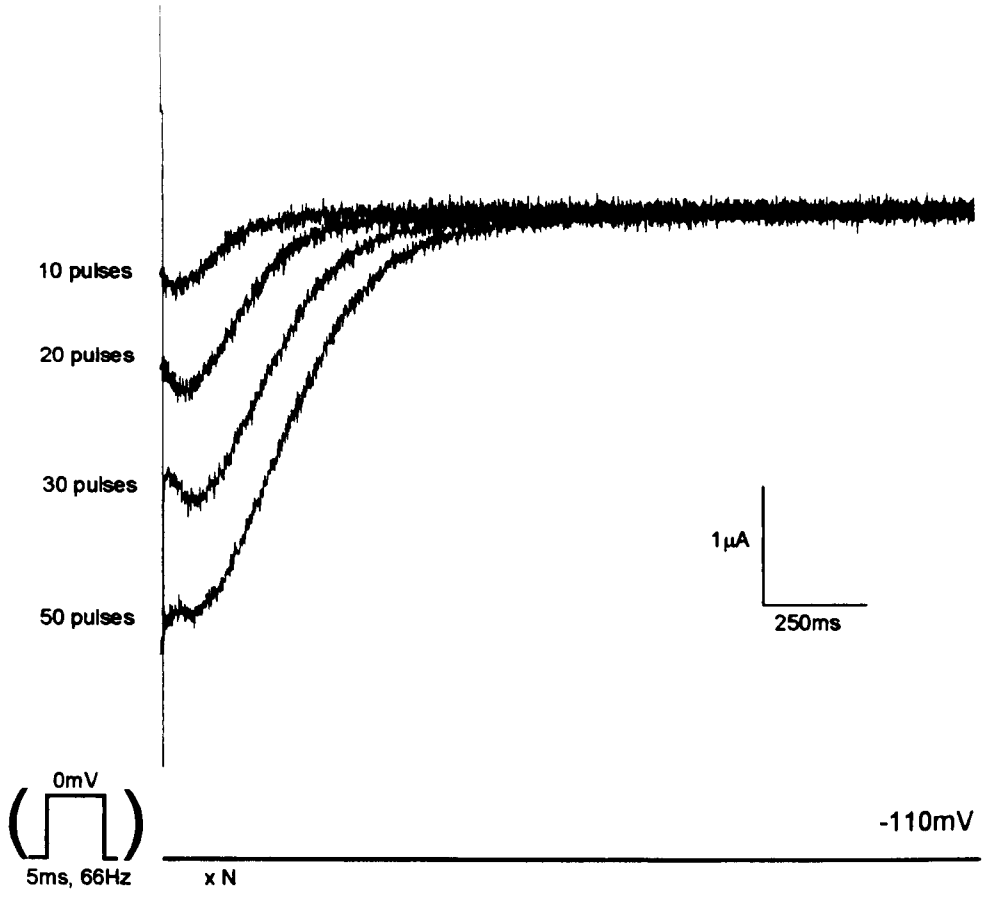

Figure 5.2. Changes in the I874M tail current amplitude are induced by varying the number of depolarizing pulses in a train in the presence of 1μM deltamethrin. Tail currents were measured following 5ms depolarisations to 0mV at 66Hz from a holding potential of −100mV. N represents the number of pulses in a train and is shown to the left of each tail current.

5.2.2 The effect of the mutation I874M on channel opening

Resistance mutations including L1014F and M918V introduced into the *para* sodium channel increased the proportion of channels that inactivate from the closed channel state (Vais *et al.*, 2000; Section 3.2.3). To reduce closed-state inactivation, oocytes were treated with the anemone toxin ATX-II. This toxin greatly slows the rate of fast inactivation and at concentrations >100nM ATX-II *para* sodium channel fast inactivation is nearly eliminated (Warmke *et al.*, 1997). Maximal conductance is doubled because ATX-II causes channels that would normally inactivate following a depolarising step, to activate instead (Warmke *et al.*, 1997; Vais *et al.*, 2000). As a consequence, the discrepancy caused by different levels of closed state inactivation of *para* wild type channels and mutant *para* channels should be removed and equal proportions of each channel type should open following a depolarisation.

Unfortunately, the toxin does not elicit such a potent effect on mammalian channels, as fast inactivation cannot be completely eradicated (Warmke *et al.*, 1997; Cannon *et al*, 1993). Studies done on the effects of ATX-II on rat brain IIA wild type channels show only a slight slow down in the speed of fast inactivation and little change in the maximal sodium conductance (Warmke *et al.*, 1997). As a result, no experiments were done on the mammalian channels in the presence of ATX-II as closed state inactivation could not be removed. It remains possible, therefore, that the I874M mutation decreases closed state inactivation and, thereby increases the probability of deltamethrin binding.

5.2.3 The effect of the mutation I874M on the number of channels modified by deltamethrin

Following perfusion of deltamethrin, oocytes expressing the I874M mutant channel and clamped at –100mV, were subjected to a series of one hundred 5ms pulses to 0mV at 66Hz. The resulting tail current decay was fitted with a single exponential and the peak tail current recorded by extrapolating the exponential fit to the end of the test pulse. A reactivation hook, which characterises *para* tail current decay, was also seen in the I874M mutant channel tail currents but was not included in the exponential fit. The peak current of each tail current was recorded at a range of deltamethrin concentrations to estimate the percentage of channels modified by the pyrethroid (Equation 3.4 and 3.5). The percentage of channels modified was plotted as a function of deltamethrin concentration and fitted by a variable slope sigmoidal concentration-response relationship (Equation 3.6) (Figure 5.3)

Only small tail currents could be elucidated from rat wild type channels even with 10μM deltamethrin, the highest concentration at which this pyrethroid is fully soluble in saline. The Kd value of the rat wild type channel was, therefore, estimated by extrapolating the sigmoidal concentration-response fit to the concentration-response relationship and assuming a Hill coefficient of 1 (Horia Vais, personal communiation). The Kd value for the I874M mutant channel was significantly smaller than for the wild type channel (I874M, Kd = 650 ± 1.0nM; rat wild type, Kd = 95μM) and the Hill coefficient remained 1. The I874M mutation, therefore, causes a >100-fold increase in the sensitivity of the rat sodium channel to deltamethrin.

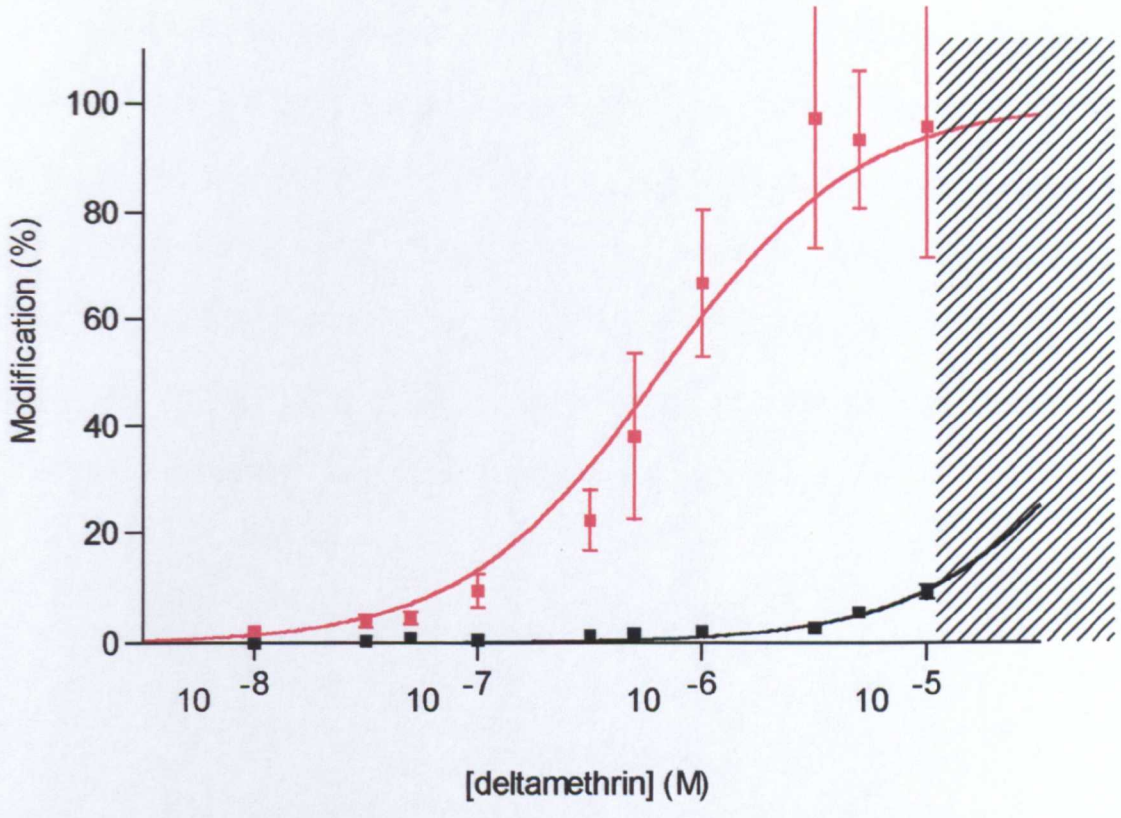

Figure 5.3. Concentration-response relationships for deltamethrin action on the rat I874M sodium channel and the rat wild type sodium channel. The percentage of modified channels was calculated using Equations 3.4 and 3.5, and plotted as a function of deltamethrin concentration. The data was fitted with a concentration-response equation (Equation 3.6).

▪ Concentration-response relationship for deltamethrin action on I874M channels (Kd = 650±1nM; Hill coefficient =1). ▪ Concentration-response relationship for deltamethrin action on rat wild type channels (Kd = 95μM; Hill coefficient =1). The dashed box drawn beyond 10^{-5} M deltamethrin indicated the solubility limit of deltamethrin in ND96. (Points show the mean ± SEM, I874M n = 4).

5.2.4 Tail current decays of the I871M mutant channel and the rat wild type channel

The rate of tail current decay was determined from exponential fits to tail currents. I874M mutant channel tail currents could be fitted with a single exponential if the reactivation hook was excluded from the fit. The rate of tail current decay was slower for I874M channels than for wild type channels (I874M, τ= 505ms $\pm$ 7; wild type, τ= 86ms$\pm$ 2). Also, the time constant for tail current decay did not change with deltamethrin concentration for either channel type.

5.3 The effect of the mutation I874C on the sensitivity of the rat brain IIA sodium channel to deltamethrin.

Following the discovery of the large increase in sensitivity of the rat brain IIA channel to deltamethrin resulting from the introduction of the I874M mutation, the isoleucine found at this position was replaced by other amino acids to further investigate the interaction between the channel and the insecticide. Cysteine was chosen because, like methionine, it contains a single sulphur atom in its side chain, which may be crucial in the association of the two molecules.

5.3.1 Voltage-dependence of activation and inactivation

The voltage-dependence of activation and inactivation were investigated using the same pulse protocols as those detailed in sections 3.1.1 and 3.1.2. No significant difference ($p>0.01$, two-tailed t-test) was found in the voltage dependence of activation or inactivation between I874C mutant channels and I874M mutant channels and rat wild type channels.

5.3.2 Speed of onset and recovery from inactivation

The speed of onset and recovery from inactivation was determined using the same pulse protocols as in sections 3.1.3. The rate of inactivation induced by a –40mV inactivating pre-pulse was slower ($p=0.0423$, two-tailed t-test) for I874C channels than for wild type channels (I874C τ = 26.0±1.89ms; I874M τ =17.2±1.6ms; rat wild type τ = 19.0±2.2ms). The speed of recovery from inactivation was not significantly ($p=0.1067$,

two-tailed t-test) faster than wild type channels (I874C, τ = 24.5±4.84ms; I874M, τ =34.4±1.9ms; rat wild type τ = 36.7±0.89ms).

5.3.3 Binding of I874C to deltamethrin

Deltamethrin-induced tails currents of I874C mutant channels were larger following a train of 100 5ms pulses to 0mV from a holding current of −100mV than following a single pulse of equal total duration. Deltamethrin, therefore, also binds preferentially to open I874C channels.

As was seen with the I874M mutant and the *Drosophila* wild type sodium channel, the peak amplitude of I874C tail currents increased concurrently with the number of pulses in a depolarising train. The percentage of modified channels was calculated (Equation 3.4) at different deltamethrin concentrations and plotted as a function of pulse number. The data could be fitted with a single exponential (Figure 5.4). 100% of I874C channels were modified following 100 5ms pulses in the presence of 10μM deltamethrin, while only 77% of I874C channels were modified following 50 5ms pulses. 70% of channels were modified following 100 5ms pulses in the presence of 1μM deltamethrin.

5.3.4 The effect of the I874C mutation on the number of channels modified by deltamethrin.

I874C channel tail currents following a train of 100 5ms pulses from −100mV to -0mV in the presence of deltamethrin, have significantly larger peak amplitudes and slower rates of decay than wild type channels (Figure 5.5). As for I874M channel tail currents, I874C channel tail currents could be fitted with a single exponential. The rate of I874C

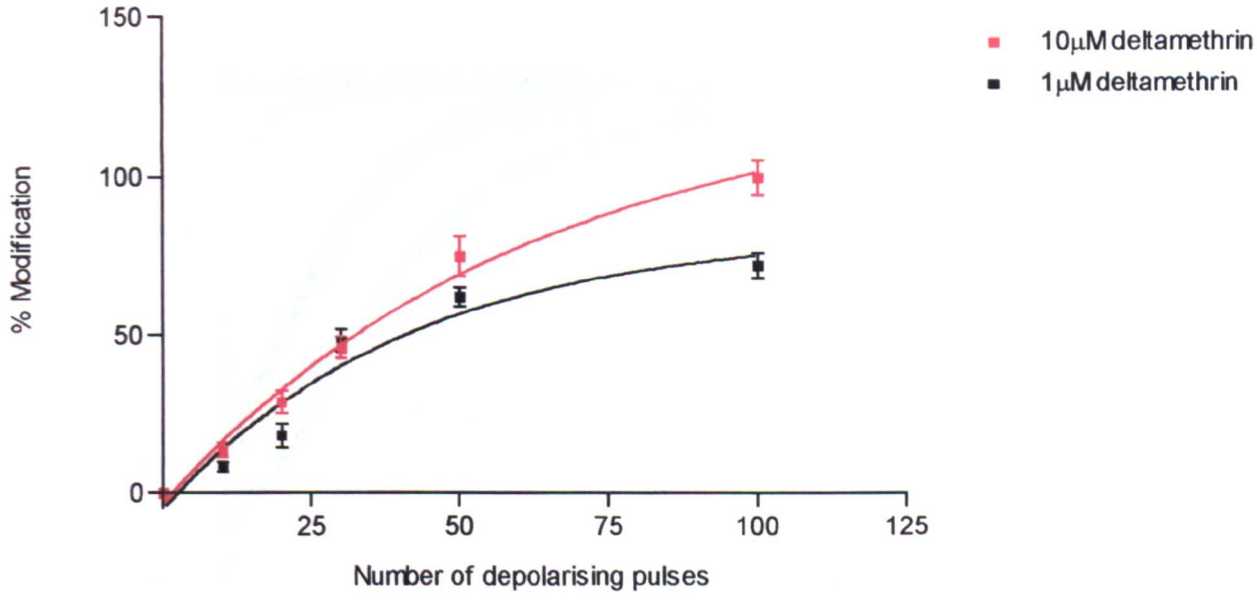

Figure 5.4 The percentage of I874C channels modified by deltamethrin is plotted against the number of 5ms depolarising pulses in a train, using equation 3.4. and 3.5. 100% of I874C channels were modified following 100 5ms pulses in the presence of 10μM deltamethrin and 77% of I874C channels were modified following 50 5ms pulses in the presence of 10μM deltamethrin. 70% of I874C channel were modified following 100 5ms pulses in the presence of 1μM deltamethrin. (Points show the mean ± SEM, n = 4).

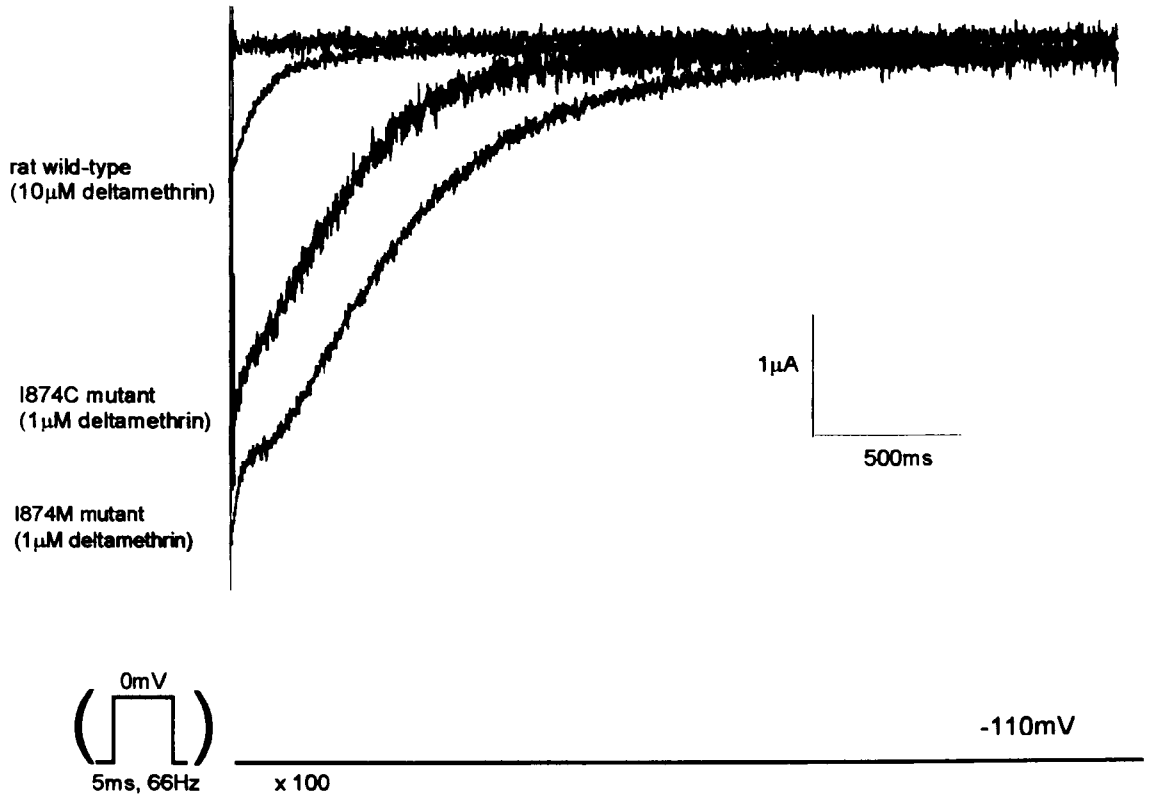

Figure 5.5. Comparison of I874C, I874M and rat wild type tail currents, at different concentrations of deltamethrin, induced following a train of 100 pulses of 5ms duration to 0mV from a holding current of −100mV. The peak amplitude of the I874C tail current is larger (3.2μA) than the peak amplitude of the rat wild type tail current (0.8μA) but smaller than the I874C tail current (4μA). The I874C tail current also decayed more slowly (τ=360ms) than the wild type tail current (τ=95ms) but faster than the I874M tail current (τ=565ms). The maximal sodium conductances (G_{max}) were 64.1μS for I874 and 61.1μS for I874M and 68.0μS for I874C.

tail current decay was also slower than that of the wild type and remained constant throughout the deltamethrin concentration range. (I874C τ = 230+25ms, rat wild type τ = 86±2ms). The I874C mutation does not increase deltamethrin sensitivity of the rat sodium channel to the same extent as the I874M mutation. Dissociation of deltamethrin was faster from I874C than I874M mutated channels (I874C τ = 230±25ms, I874M τ = 505±7ms).

The percentage of I874C channels modified by different concentrations of deltamethrin was calculated using the same method as for I874M mutant channels (Section 5.2.3).

The percentage of modified I874C channels was plotted as a function of deltamethrin concentration and fitted with a concentration-response relationship from which the Kd value and the Hill coefficient were estimated. I874C channels are >80-fold more sensitive to deltamethrin than the wild type channels (I874C Kd = 1.2±0.13μM, rat wild type Kd = 95μM) but less sensitive to deltamethrin than I874M channels (I874M, Kd = 650+1.0nM). The Hill coefficient remained at 1. The concentration-response relationships of I874M channels, I874C channels, rat brain IIA wild type channels and *Drosophila para* wild type (Horia Vais, personal communication) are shown in Figure 5.6.

5.4 The effect of other I874 residue substitutions.

Other amino acids were introduced at position 874 in the rat brain IIA sodium channel to determine the interaction between deltamethrin and the sodium channel. The same technique of differently charged amino acid substitution was used to clarify the effects of residue charges within the S6 segment during inactivation (O'Reilly, Wang and

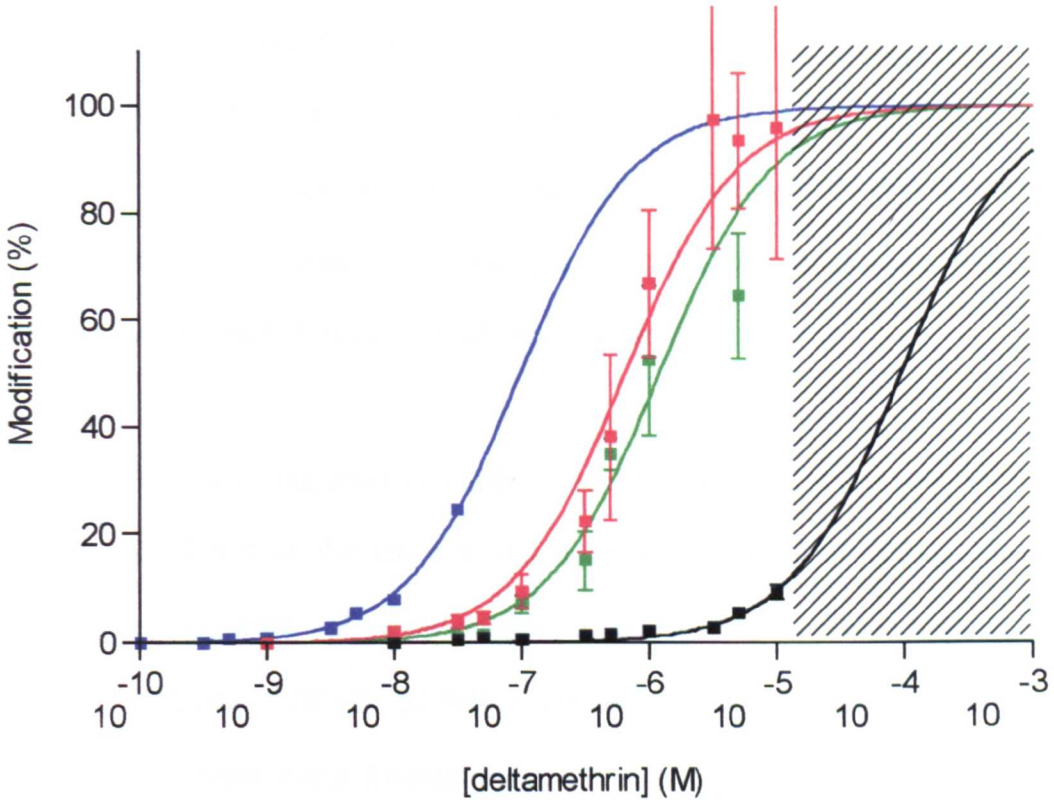

Figure 5.6 Concentration-response relationships for deltamethrin action on the rat I874C sodium channel, the rat I874M sodium channel, the rat wild type channel and the *drosophila para* sodium channel. The percentage of modified channels was calculated using Equations 3.4 and 3.5 and plotted as a function of deltamethrin concentration. The data was fitted with a concentration-response equation (Equation 3.6).

- Concentration-response relationship for deltamethrin action on rat wild type channels (Kd=95μM; Hill coefficient=1).
- Concentration-response relationship for deltamethrin action on *para* wild type channels (Kd= 92nM; Hill coefficient=1).
- Concentration-response relationship for deltamethrin action on I874M channels (Kd=650nM±1nM; Hill coefficient=1). (Points show the mean ± SEM, n= 4).
- Concentration-response relationship for deltamethrin action on I874C channels (Kd=1.2±0.13μM; Hill coefficient=1). (Points show the mean ± SEM, n= 3).

Wang, 2000). Histidine has a neutral side chain, while aspartate has a negative carboxylic acid at the terminal end of its side chain. If a direct interaction between channel and insecticide is based upon the electrical properties of the region surrounding the 874 locus then differences in deltamethrin sensitivity may occur when these residues replace the isoleucine 874 found in wild type channels.

Although changes to the kinetics of these mutated channels were seen both in the voltage -dependence of the channel and the speed of channel gating, these were statistically insignificant. More importantly, no differences were seen between the tail currents of the mutated I874H and I874D channels and the tail currents of rat wild type channels in the presence of deltamethrin.

5.5 The sensitivity of I874M compared with the Drosophila *para* wild type channel.

To estimate and compare the proportions of I874M and *para* wild type channels that are modified by deltamethrin, concentration-response curves were constructed for both channel types (Figure 5.6). As discussed in previous chapters, deltamethrin binds preferentially to the sodium channel open state and therefore equal proportions of channel populations must open following a depolarisation to allow comparisons of the fractions of different channel populations modified by the insecticide. This can be achieved in *Drosophila para* sodium channels type using the toxin ATX-II, which removes the discrepancy of different levels of closed state inactivation by inhibiting and slowing fast inactivation to such an extent that it is almost removed (Warmke *et al.*, 1997). However, ATX-II does not remove rat channel fast inactivation (Cannon *et al.*, 1993; Warmke *et al.*, 1997) and therefore the deltamethrin concentration-response

curves for both I874M and *para* wild type were estimated in the absence of the toxin. Maximum channel opening can be achieved by repetitive pulsing (section 5.2.2) and, therefore, the percentage of I874M channels and *para* wild type channels modified by deltamethrin was calculated by estimating the peak tail current following a train of 100 depolarising pulses (Section 5.2.3).

The *para* wild type sodium channel is highly sensitive to deltamethrin. *Para* wild type channel tail currents did not recover following exposure to 30nM deltamethrin (Vais *et al.*, 2000) and oocyte leakage could not be controlled. The *para* wild type concentration-response curve could, therefore, only be predicted on a few points. The *para* wild type Hill coefficient was assumed to be one and the extrapolated Kd value estimated to be 92nM. The I874M mutated rat IIA channel remains approximately 7-fold less sensitive to deltamethrin than the *Drosophila para* wild type channel (*para* wild type, Kd= 92nM (Horia Vais, personal communication); I874M, Kd = 650nM).

5.6 The I874M mutation increases the sensitivity of the rat brain IIA sodium channel to deltamethrin

Rat brain IIA sodium channels and the insect *para* sodium channels share 50% sequence homology, with many known functional areas such as the fast inactivation particle and its docking site being almost identical. The affinities of these channels for pyrethroids are, however, very different, the mammalian channel being ~4500 times less sensitive to deltamethrin than its insect counterpart.

Studies described herein have shown that a single isoleucine to methionine replacement, position 874 in the rat IIA channel, increases sensitivity to deltamethrin over one hundred fold. What are the mechanisms that underlie this dramatic increase in deltamethrin potency?

An important consequence of the knockdown resistance mutations in insects is an increase in the proportion of sodium channels that inactivate from the closed channel state, thereby reducing the number of sodium channels in the open state to which deltamethrin and permethrin preferentially bind. Pulse protocols applied to both mutant rat channels and wild type rat channels also showed preferential binding to the channel open state. Unfortunately, ATX-II, the anemone toxin used to abolish increased amounts of closed state inactivation typical of pyrethroid resistant insect channels, does not completely eradicate this state pathway in rat IIA channels. An increase in the proportion of channels opening and therefore available for deltamethrin binding, as a consequence of the I874M mutation may contribute to the increased sensitivity of mutated channels populations to the insecticide. However, no significant difference

between the kinetics and voltage dependence of inactivation of I874M and wild type channels was seen, suggesting that a reduction in the number of channels undergoing closed-state inactivation, which might account for the increase in rat mutant channel sensitivity, was probably not occurring.

The I874M and I874C mutations may alter the three-dimensional structure of the 874 region and thereby indirectly cause a structural change elsewhere within the channel, which could allow easier access to a deltamethrin binding site. However, such a significant change in the structure of the channel usually causes changes in the kinetics of channel gating (Vais *et al.*, 1997). Indeed, the incorporation of the domain II from the *para* channel into the rat brain channel results in the mutant rat channel acquiring the inherent activation parameters of the wild type *para* sodium channel as well as a substantial increase in sensitivity to the anti-insect-selective scorpion toxin AahIT (Shichor *et al.*, 2002). No significant differences in gating kinetics were seen between the I874M mutant and the rat wild type channel, suggesting that the increase in pyrethroid sensitivity of the rat mutant channel is due to a direct increase in the channel's affinity for deltamethrin.

The Hill coefficient determined from concentration-response relationships of deltamethrin action on I874M and I874C channels, does not define the number of deltamethrin binding sites, however it does set a lower limit (Vais *et al.*, 2000). The concentration-response relationship for deltamethrin action on I874M channels and I874C channels gives an estimate for the Hill coefficient of 1, which is consistent with a

1:1 drug-receptor reaction (Zong *et al.*, 1992) and with data obtained from other studies on mammalian sodium channels (Song and Narahashi, 1996).

A direct increase in the affinity of deltamethrin binding to the channel has been suggested in a model that proposes nucleophilic attraction between the lone pair of electrons on the sulphur atom of the methionine side chain and the electropositive α-carbon of the pyrethroid alcohol (Williamson *et al*, 1996) (Figure 5.7). The increased activity of the Type II pyrethroids is the result of the cyano group on the α-carbon of the 3-phenoxybenzyl alcohol that stabilises the preferred conformation around the C- αO bond (Mullaley and Taylor, 1994). The electropositive charge of the α-carbon is the result of the strong electron withdrawing capacity of the triple bond in the cyano group, one of the chemical moieties that defines the Type II pyrethroids. The super-kdr mutation reduces the sensitivity of the *para* sodium channel to both Type I and Type II pyrethroids but it is with Type II insecticides that the effect is most dramatic, with the kdr and super-kdr double mutation conferring a resistance factor of over 500-fold *in vivo* (Farnham *et al.*, 1997). The effect of the super-kdr mutation in insects may be greater for Type II pyrethroids because of the loss of a strong interaction created between the methionine at the 918 site of the *para* sodium channel and the α-carbon of deltamethrin made electropositive by the cyano group.

The importance of the sulphur atom at position 874 in conferring the large increase in the sensitivity of the rat channel to deltamethrin is supported by the increased sensitivity of rat channels containing the I874C mutation. Cysteine, like methionine, has a sulphur

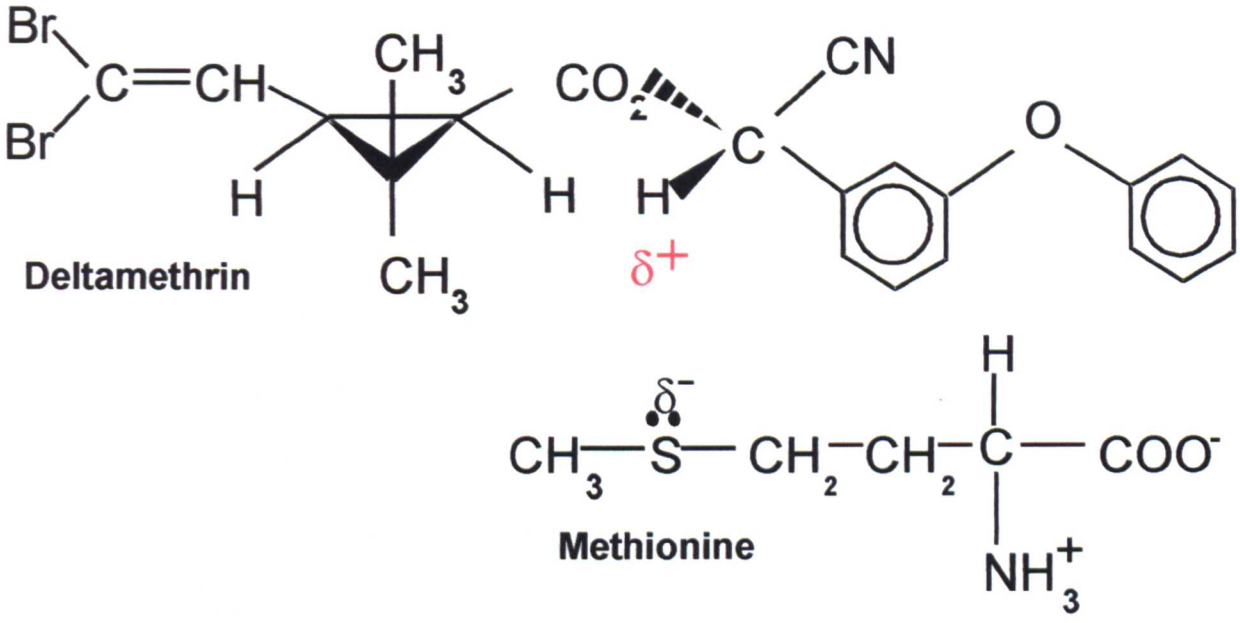

Figure 5.7. A model of the proposed nucleophilic attraction between the lone pair electrons on the sulphur atom of the methionine side chain and the electropositive α-carbon of the pyrethroid alcohol. This electropositive charge is thought to be a result of the strong electron withdrawing capacity of the triple bond in the cyano group.

atom in its side chain. The concentration-response relationship of I874C channel estimates > 80-fold increase in the sensitivity of I874C channels to deltamethrin. The rate of I874C channel tail current decay is also significantly slower than the wild type channel tail current decay.

The role of the electronegativity conferred by the lone pair of electrons on the sulphur atom in both cysteine and methionine was further investigated with the introduction of other amino acid residues at position 874. The carboxylate group forming part of the aspartate side chain confers an electronegative charge. This was predicted to attract the proton of the deltamethrin α-carbon, thereby strengthening the bonding between the two molecules and rendering the channel more sensitive to the insecticide. Histidine has an imidazole moiety in its side chain, which is electrically neutral in the physiological environment and was to act as a control to aspartate. This would crudely confirm if direct nucleophilic attraction was occurring between the 874 residue and the delta-positive carbon of the Type II pyrethroid. However in both cases, sensitivity of the mutated rat channels to deltamethrin showed no difference to the sensitivity of the rat wild type channels to the insecticide. In hindsight, this is unsurprising. The substitution of one amino acid for another is a blunt method of elucidating a bonding model. Both histidine and aspartate are chemically very different from cysteine and methionine. Furthermore, such stark residue changes alter the hydration motif of the surrounding region and may even change the entire tertiary structure of the domain.

A number of factors are thought to account for the selective toxicity of deltamethrin in mammals and insects. Pyrethroids are more effective at inducing repetitive after-discharges at lower rather than higher temperatures (Song and Narahashi, 1996). The effect of the insecticide would, therefore, be more potent in insects, which are poikilothermic organisms with an average body temperature approximately 10°C lower than that of mammals. A lower body temperature also reduces the rate of enzymatic detoxification of pyrethroids. Degradation of the insecticides is estimated to be three times faster in mammals than in insects. Another important element is the larger mammalian body size, which increases the probability of pyrethroid detoxification before the insecticide can reach it target. However, it is the insensitivity of the voltage gated sodium channel that is considered the primary reason for mammal insensitivity to pyrethroid insecticides (Song and Narahashi, 1996).

Interestingly, the introduction of a DIIIS6 mutation found in two pyrethroid resistant strains of the cattle tick *Boophilus micropuls* (He *et al.*, 1999) at the equivalent residue site in the mutant I847M rat channel reversed the deltamethrin sensitivity conferred by the I874M mutation (Wang, Barile and Wang, 2001). This may highlight a pyrethroid binding site within the channel pore in addition to that generated by the I874M mutation within the domain II S4-S5 linker.

Although I874M and I874C channels are highly sensitive to deltamethrin they still remain ~10 fold less sensitive to the insecticide than the *Drosophila melanogaster* wild type channels. This suggests a secondary association may be occurring between deltamethrin and the *Drosophila para* sodium channels, which increases the affinity

between the protein and the insecticide. It is possible that other amino acid changes in the rat brain IIA channel co-expressed with the I874M mutation could confer deltamethrin sensitivity equal to that of the *para* wild type channel. The mammalian SNS/PNS (TTX-resistant) channel, which is preferentially expressed in the peripheral nervous system, is highly sensitive to both Type I and Type II pyrethroids, in contrast to the rat IIA sodium channel (Smith and Soderlund, 1999). Indeed, the cismethrin concentration producing half-maximal *para* wild type channel modification exceeds that of the PN3/SNS channel, suggesting the insect channel is less sensitive to this pyrethroid than the rat PN3/SNS channel (Smith *et al.*, 1998).

A true measure of the importance of the sensitivity of the sodium channel in conferring pyrethroid resistance would be to express the mutated I874M form *in vivo* and determine the potency of the insecticide under these conditions. This may also have implications for the possible use of pyrethroids in mammalian pest control.

CHAPTER 6

SENSITIVITY OF THE RAT I874C VOLTAGE-GATED SODIUM CHANNEL MUTANT TO PERMETHRIN AND OTHER PYRETHROID ANALOGUES

6.0 Introduction

Establishing the nature and location of deltamethrin binding on the voltage-gated sodium channel will be fundamental in the design of any future synthetic pyrethroids effective against pest insects. The dramatic increase in sensitivity of the I874M and I874C mutated rat IIA sodium channels to deltamethrin, shown in chapter 5, supports the model of a nucleophilic attraction between the benzylic or α-carbon of deltamethrin and the lone pair of electrons of the sulphur found in the side chain of the methionine 918 residue of the insect *para* wild type channels (Williamson et al, 1996) (Figure 5.8). This idea relies on the presence of the cyano group, which chemically defines the Type II pyrethroids (Section 1.2). The electron-withdrawing cyano group makes the α-carbon of the pyrethroid δ-positive. This δ-positive α-carbon could interact with the negative lone-pair of electrons of sulphur of the methionine 918 residue in the *para* wild type channel or the sulphur of the methionine 874 residue or cysteine 874 residue in the mutant rat channels. In the absence of the cyano group, the polarising effect is reduced at the α-carbon and this form of nucleophilic attraction may not be established.

The purpose of this study was to investigate the sensitivity of the I874C rat mutant to permethrin, a pyrethroid that is very similar to deltamethrin but one that lacks the cyano group and has a dichlorovinyl rather than a dibromovinyl terminal group. Pyrethroid interaction with the sodium channel was further investigated by testing the sensitivity of *para* and rat channels to pyrethroids in which constituent chemical moieties common to both deltamethrin and permethrin are absent.

6.1. The effect of permethrin on the I847C rat IIA sodium channel.

The kinetics of I874C channel gating have been described in Chapter 5. No significant difference was found in the voltage dependence of activation or inactivation between the rat I874C mutant and the rat wild type channel. No significant difference was found in the onset of inactivation or recovery from inactivation between I874C channels than in rat wild type channels.

I874C channels were exposed to a series of permethrin concentrations ranging from 10nM to 10μM. Small tail currents were seen following a train of a hundred 5ms pulses to 0mV from a holding potential of –100mV in the presence of 50nM permethrin. No rat IIA wild type tail currents were seen at the same concentration. This is a preliminary indication that the I874C mutation confers sensitivity to permethrin. The I874C tail currents increased in peak amplitude with permethrin concentrations greater than 50nM (Figure 6.1).

A measure of I874C sensitivity to permethrin was estimated from the Kd value of the concentration-response relationship for the insecticide, where the percentage of permethrin-modified I874C channels was plotted as a function of permethrin concentration and fitted with a variable gradient, sigmoidal concentration-response equation (Equation 3.6) (Figure 6.2). A quantitive measure of rat IIA wild type sensitivity to permethrin could not be obtained in this manner because at 10μM permethrin, the limit of permethrin solubility in saline, only an average of 2% of channels were modified. Therefore, a full concentration-response relationship could not be obtained. However, from an extrapolation of the incomplete relationship, it is reasonable to conclude that the Kd for rat IIA wild type channels is greater than 100μM.

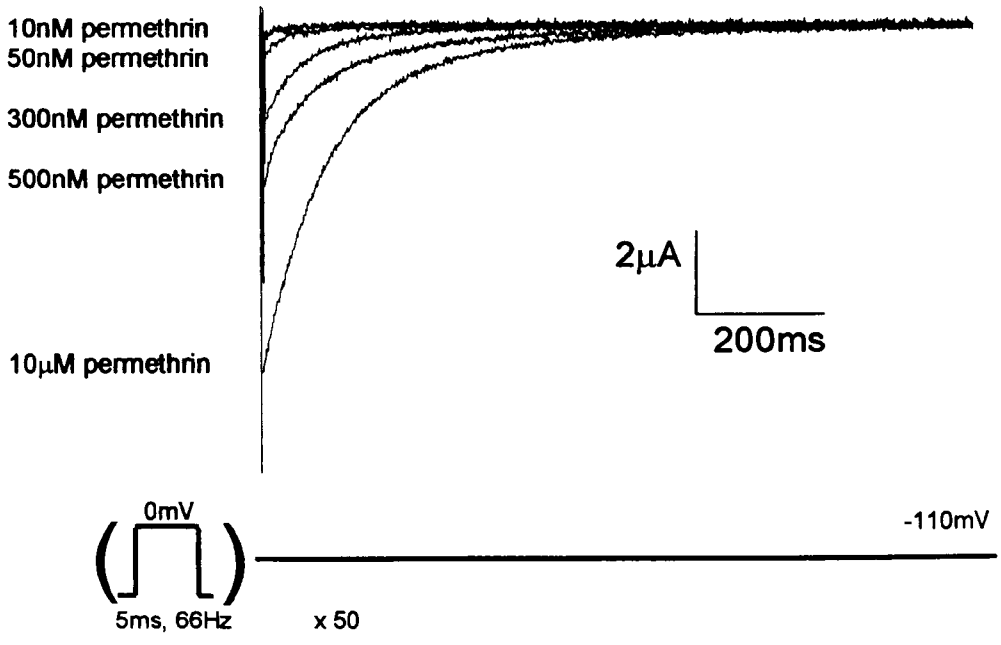

Figure 6.1. Comparisons of I874C tail currents at different concentrations of permethrin, induced following a train of 50 pulses of 5ms duration to 0mV from a holding current of −100mV. The peak tail current amplitude increased as the concentration of permethrin increased. Tail current decay could be described by single exponential functions at all permethrin concentrations.

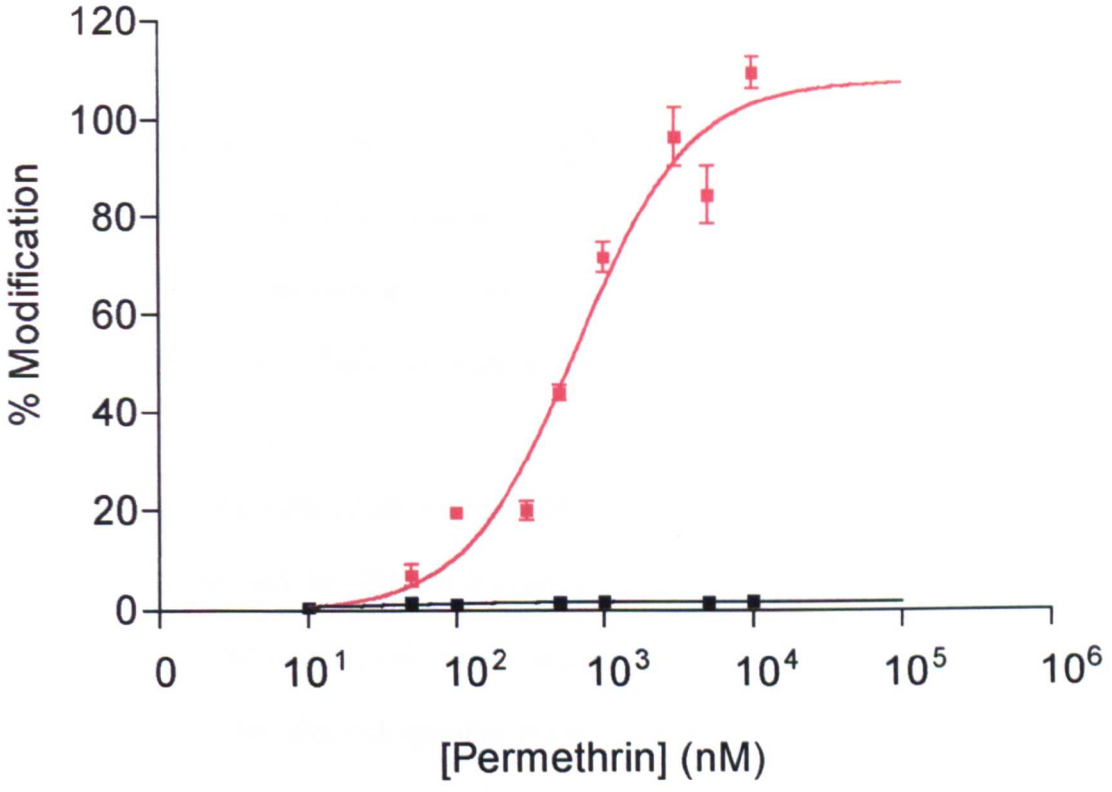

Figure 6.2. Dose-response relationship for permethrin action on the rat I874C sodium channel and the rat wild type sodium channel. The percentage of modified channels was calculated using Equation 3.4 and 3.5 and plotted as a function of permethrin concentration. The data was fitted with a dose-response relationship (Equation 3.6)

- Dose-response relationship for permethrin action on I874C channels (Kd = 0.67±0.16nM; Hill coefficient =1). (Points show the mean ± SEM, n= 4).
- Dose-response relationship for permethrin action on rat wild type channels (Kd >100μM). (Points show the mean ± SEM, n= 3).

In contrast, the concentration-response relationship for permethrin action on I874C channels gave a Kd of 0.67 $\pm$ 0.16μM, which shows that that the mutation significantly increases the sensitivity of the rat IIA channel to permethrin.

The rate of decay of I874C tail currents was very fast and remained constant at 100ms, at all permethrin concentrations, following a hundred 5ms pulses to 0mV from a holding potential of -100mV. Each tail current could be fitted with a single exponential function.

I874C tail currents were larger on repolarisation following a train of a hundred 5ms depolarisations to 0mV at 66Hz from a holding potential of –100mV than following a single pulse to 0mV of equal total duration (500ms). A 500ms train of pulses continually promotes channel opening because channels recovered from inactivation during the intervals between the pulses. In contrast, during a single depolarisation, channels have a low probability of recovery from inactivation. The discovery that permethrin action is enhanced with trains of brief depolarizations compared with a single long-duration pulse suggests that permethrin binds preferentially to the I874C open state. When the pulse frequency was increased from ten to fifty depolarizations, the peak amplitude of the tail current increased. However, the peak amplitude following a hundred 5ms pulses to 0mV was smaller than that following ten, thirty and fifty 5ms depolarising pulses, respectively. Also, the tail current decay following 100 pulses was visibly slower than that following 50 pulses (Figure 6.3).

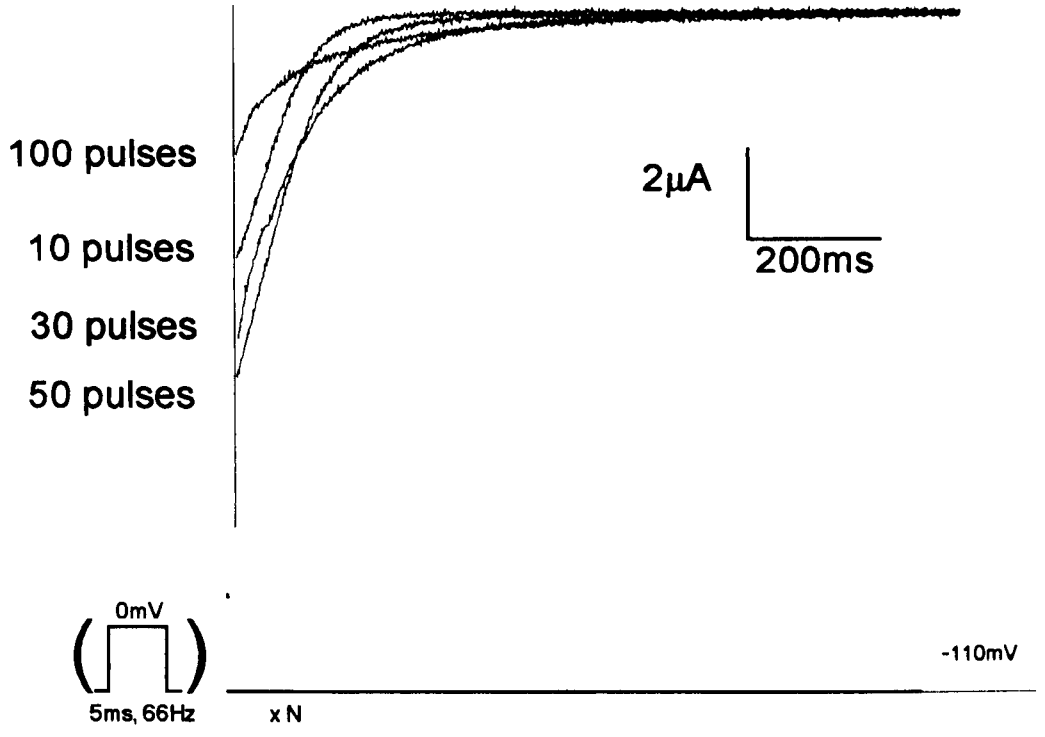

Figure 6.3. Changes in the tail current amplitude are induced by varying the number of depolarizing pulses in a train in the presence of 10μM permethrin. Tail currents were measured following 5ms depolarisations to 0mV at 66Hz from a holding potential of –100mV. N represents the number of pulses in a train and is shown to the left of each tail current.

6.2. The sensitivity of rat IIA mutant I874C channel and *para* wild type channel to the pyrethroids etofenprox and 10042.

A nucleophilic attraction model was proposed in the previous chapter as a possible interaction between deltamethrin and the I874M rat channel. This model depends on the presence of the cyano group, which typifies the Type II pyrethroids. The previous section (6.1) shows that the open I874C channel is more sensitive to permethrin, a Type I pyrethroid that lacks the cyano group, than the open wild type channel. This result does not mean that the cyano group exerts no influence on the binding of Type II pyrethroids to the I874C mutant; however, the moiety is not central to the interaction between pyrethroids and a putative binding site at the 874 position. Indeed, a comparison of the Kd values determined from permethrin and deltamethrin action on I874C channels suggests that the mutant channel is more sensitive to permethrin than deltamethrin (permethin, I874C mutant Kd = 0.67 $\pm$ 0.16μM; deltamethrin, I874C mutant Kd = 1.2$\pm$ 0.13μM). Other chemical groups common to both deltamethrin and permethrin must, therefore, play a greater role in the interaction of the 874 cysteine residue with the pyrethroid molecule.

To identify which chemical moieties may be responsible for a possible direct interaction with the 874 mutated residue, novel pyrethroids were synthesised but with certain moieties common to both the permethrin and the deltamethrin molecule absent. The sensitivity of I874C channels to these pyrethroids was tested to clarify which part of the pyrethroid molecule may be interacting with the rat 874 cysteine residue, if a direct interaction is occurring. As explained in the introduction, both natural pyrethrins and synthetic pyrethroids are formed by an acid moiety connected to an alcohol moiety by an

ester linkage. In addition, synthetic non-ester pyrethroids, in which the central ester functionality has been replaced by an alternative linker e.g. alkane, alkene or ether linkage, also have insect *in vivo* activity comparable to deltamethrin and permethrin. Two pyrethroid insecticides were tested on the mutant I874C channel. The first was MTI500, commonly known as etofenprox (Figure 6.4), which is widely used in the control of paddy rice insect pests as well as on livestock pests (Pesticide Manual, 12th Edition). It retains the *m*-phenoxybenzyl alcohol substructure, in common with permethrin and deltamethrin, but the ester linkage has been replaced with an ether linkage. The second was 10042, a variant of the soil insecticide Tefluthrin (Pesticide Manual, 12th Edition), which has the ester linkage and dibromovinyl group also common to deltamethrin and permethrin, but it loses the *m*-phenoxybenzyl alcohol substituent, which is replaced with a tetrafluorobenzyl alcohol (Figure 6.4).

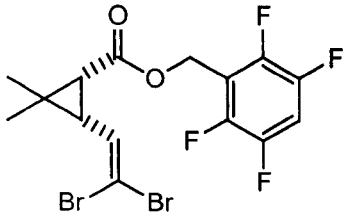

10042

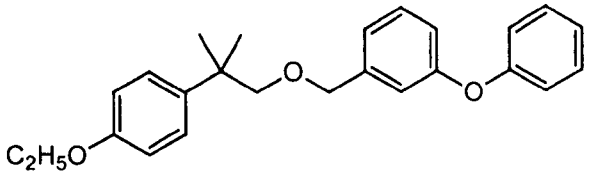

etofenprox

Figure 6.4. Molecular structure of the pyrethroids 10042 and etofenprox.

Bioassay studies have found both theses chemicals to be active against the wild type house fly, *Musca domestica* (Beddie et al., 1996). As I874C rat mutant channels are

comparable to *para* wild type channels in terms of their sensitivity to pyrethroids, it is hoped that this modular approach will define which part of the pyrethroid is binding to the Cys874 residue site within the channel, through differences in I874C sensitivity to etofenprox and 10042. Again, this assumes a direct interaction between pyrethroids and the 874 residue is occurring.

6.2.1 The sensitivity of the I874C mutated channel to etofenprox and 10042.

The sensitivity of the I874C rat IIA channel to etofenprox and 10042 was studied using the same methods that were employed to study deltamethrin and permethrin. Concentration ranges of both etofenprox and 10042 were made by dissolving the insecticide in ethanol before diluting it to the desired concentration in saline. The I874C mutant tail currents were recorded after oocytes had been subjected to a variety of pulse protocols both in the presence and absence of the two pyrethroid variants.

Oocytes expressing the mutant I874C channel were subjected to a train of thirty, fifty or one hundred 5ms pulses to 0mV from a holding potential of −100mV. In previous experiments this elicited the greatest effect in terms of peak amplitude and rate of decay of the tail currents obtained on repolarisation following the pulse train. Unfortunately, no tail currents could be detected following any of these pulse protocols at 10μM, the highest concentration of both etofenprox and 10042 that could be employed.

The absence of tail currents following rat wild type channel exposure to etofenprox and 10042 also suggests that rat wild type channels were insensitive to both pyrethroid variants.

6.2.2. The sensitivity of the *para* wild type channel to etofenprox and 10042.

In bioassays, etofenprox and 10042 have been shown to be active against the housefly, *Musca domestica* (Beddie et al., 1996). To ascertain that these pyrethroid compounds were also acting upon the voltage gated sodium channel, oocytes expressing the *para* wild type sodium channel were exposed to etofenprox and 10042. As with all previous experiments described, tail currents following repolarisation after one or more depolarising pulses were used as measure of channel sensitivity to each insecticide.

Both etofenprox and 10042, at concentrations greater than 10nM, elicited *para* wild type tail currents following a hundred 5ms pulses to 0mV from a holding potential of -100mV. Concentration-response relationships for both compounds were constructed using the same method as described in Section 3.2.4. However, due to time constraints, only two experiments on *para* wild type channels with each compound were performed, none of which was in the presence of ATX-II.

$$\%\ \text{of channels modified} = \left(\frac{\text{Peak tail current}}{V_{tail} - V_{rev}}\right) \Big/ \left(G_{NaMax} \bullet \text{ATX - II fold - increase}\right)$$

(Equation 6.1).

Therefore, to obtain an estimate of the percentage of modified channels at different concentrations of each pyrethroid, the ATX II fold-increase (Table 3.1) in maximum conductance for the *para* wild type channel was used (Vais et al, 2000). This assumes that both etofenprox and 10042 bind preferentially to the open state of the sodium channel. Unfortunately, again due to time constraints, it was not possible to determine whether this is the case. Kd values were estimated from the concentration-response

relationship fitted to the plot of the percentage of channel modified against the concentration of each pyrethroid (Figure 6.5). The Kd value of 10042 was found to be higher than that of etofenprox (10042, Kd = 5.5 ± 0.62μM; etofenprox, Kd = 1.4 ± 0.13μM). The Kd values of both compounds are clearly much greater than those for deltamethrin or permethrin action on *para* wild type channels (deltamethrin action on *para* wild type channel, Kd = 4.4+0.16nM permethrin action on *para* wild type channel, Kd = 10.3+1.0nM).

Tail currents from *para* wild type channels treated with etofenprox were best-fitted with single exponential (Section 2.3.8). The time course of tail current decay was independent of etofenprox concentration (τ = 133 + 17.7ms) (Figure 6.6). Tail currents from *para* wild type channels treated with 10042 were also best-fitted with a single exponential and the rate of tail current decay was independent of 10042 concentration (τ = 231 ± 17.2ms) (Figure 6.7).

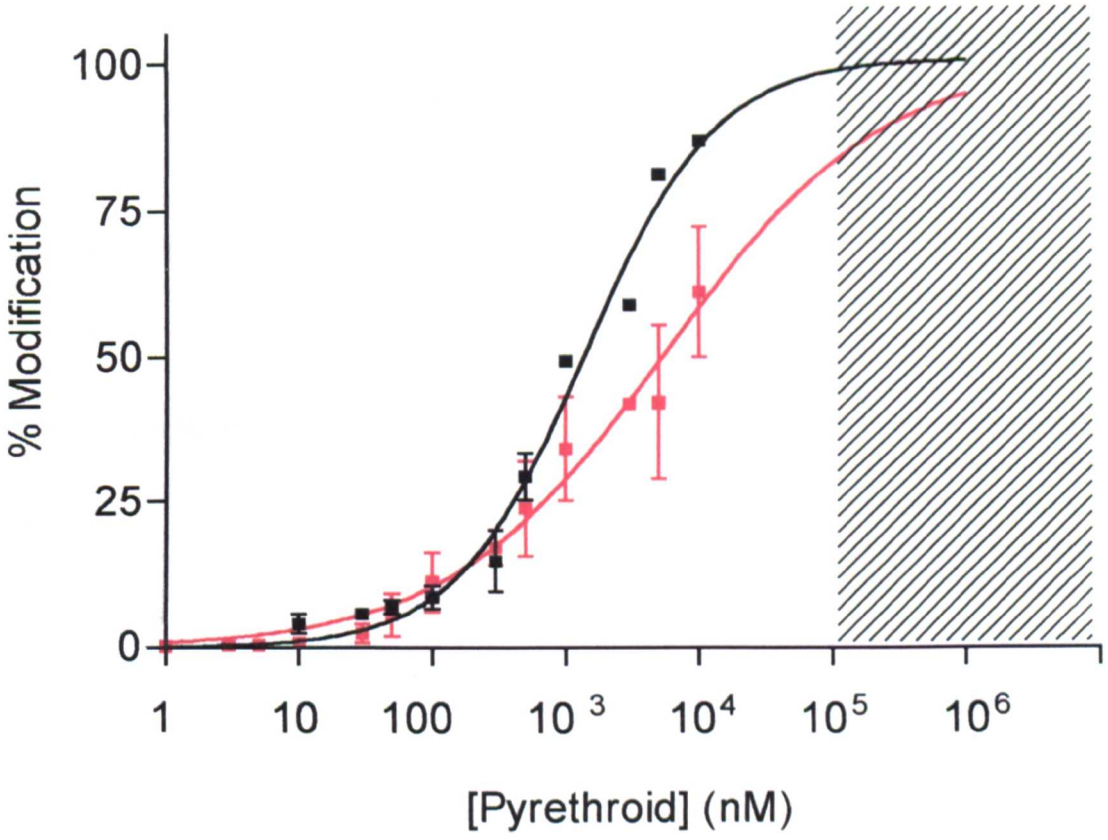

Figure 6.5. Concentration-response relationship for etofenprox and 10042 action on para wild type sodium channels. The percentage of modified channels was calculated using Equation 6.1 and 3.5 and plotted as a function of pyrethroid concentration. The data was fitted with a concentration-response equation (Equation 3.6).

▪ Concentration-response relationship for 10042 action on para wild type channels (Kd = 5.5±0.62 μM; Hill coefficient =0.5). ▪ Concentration-response relationship for etofenprox action on para wild type channels (Kd =1.4 +0.13μM; Hill coefficient =1). (Points show the mean ± SEM, n= 2).

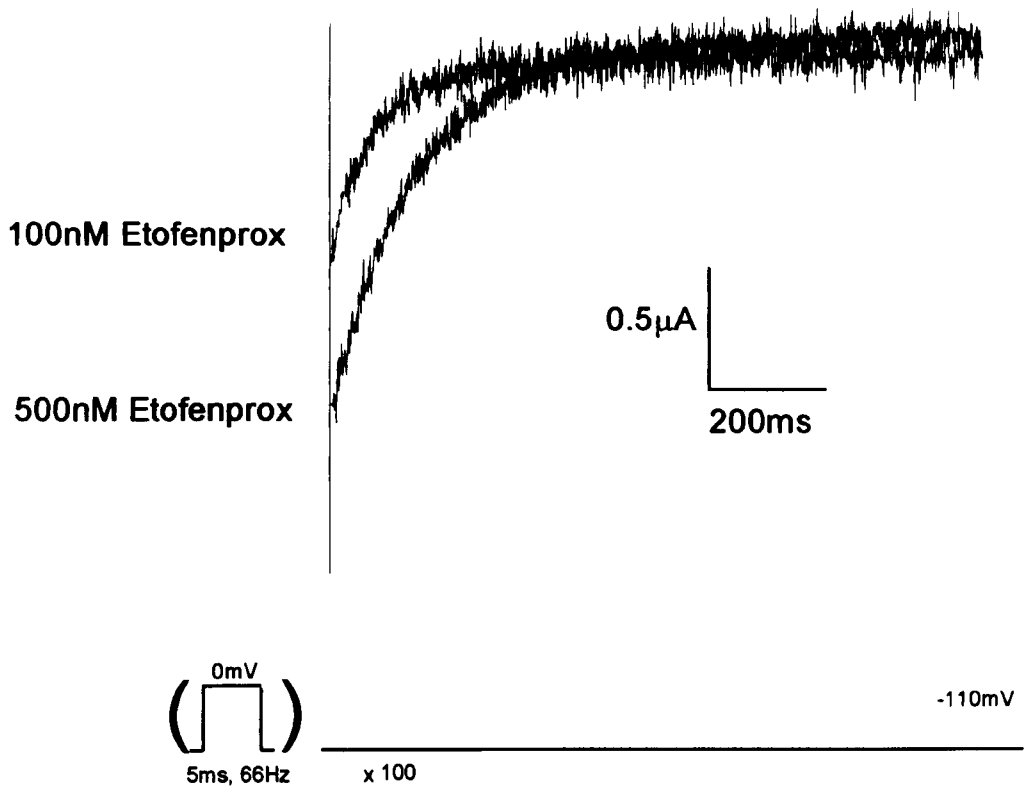

Figure 6.6. Comparisons of para wild type tail currents at different concentrations of Etofenprox, induced following a train of 100pulses of 5ms duration to 0mV from a holding current of −100mV. Tail current decay could be described by a single exponential function at all Etofenprox concentrations. The rate of tail current decay was independent of Etofenprox concentration (τ= 133±17.7ms).

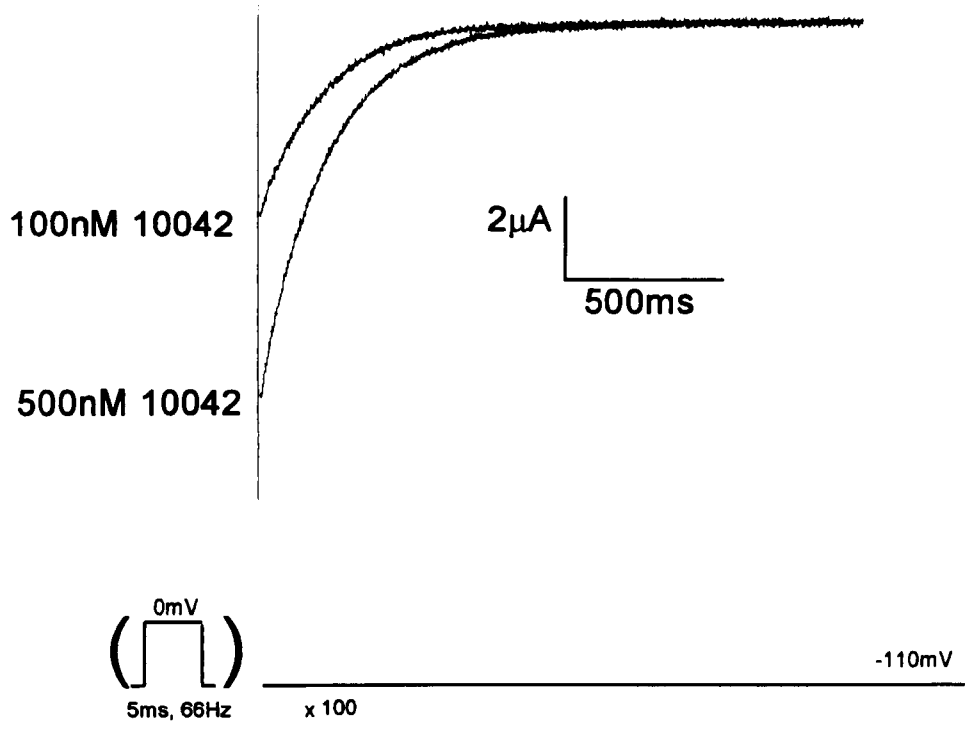

Figure 6.7. Comparisons of para wild type tail currents at different concentrations of 10042, induced following a train of 100pulses of 5ms duration to 0mV from a holding current of −100mV. Tail current decay could be described by a single exponential function at all 10042 concentrations. The rate of tail current decay was independent of 10042 concentration (τ= 231+17.2ms).

6.3. The mutant I874C rat IIA channel is sensitive to permethrin.

The I874C mutant rat channel was ~150-fold more sensitive to permethrin than the wild type rat IIA sodium channel, indeed, the clear change in the Hill coefficient suggest that I874C forms a permethrin binding site. As explained in section 6.1, the sensitivity of the I874C mutant to permethrin contradicts the model described in Chapter 5, which proposed an nucleophilic attraction between the negatively lone pair of electrons surrounding the sulphur atom in the side chain of cysteine 874 residue and the δ-positive α-carbon resulting from the electron withdrawing capacity of the cyano group of deltamethrin. Permethrin lacks the cyano group, however the mutant I874C channel still displays significantly higher levels of sensitivity to the Type I pyrethroid than the rat IIA wild type. The sensitivity of the mutant I874C channel to deltamethrin does not, therefore, rely on the presence of the cyano group. Indeed, the I874C channel showed greater sensitivity to permethrin than deltamethrin.

The mutant I874C channel tail currents seen following a hundred 5ms depolarising pulses had larger amplitudes and slower rates of decay than tail currents elucidated by a single depolarising pulse of equal duration. Again, because channels recover from inactivation in the pulse experiments, an interpretation of this result is that permethrin preferentially binds to the I874C mutant channel open state.

However, the mutant I874C tail current following a train of a hundred pulses was noticeably smaller than tail currents following thirty or fifty 5ms depolarising pulses. This is in contrast to the results seen with deltamethrin and mutated rat and insect

channels, where tail current amplitude, and, in some cases, the duration of decay, increased as the pulse number rose from 1 to 200. This could be a consequence of the different affinities of permethrin and deltamethrin for the mutated I874C channel. Although permethrin appears to bind preferentially to the mutant I874C open state, following pulse train durations greater than 250ms, channels and permethrin molecules that bonded at the beginning of the train may begin to dissociate which would manifest itself in smaller tail currents. Deltamethrin affinity for the mutant I874C channel could be greater than that of permethrin. Hence, the channel-deltamethrin association lasts for longer. Channels bound to the Type II pyrethroid at the beginning of the train remain bound for a longer duration before they begin to dissociate. Hence, deltamethrin induced tail currents only begin to decrease in amplitude after pulse train durations greater than one second (Chapter 5). This explanation, however, contradicts the affinities estimated by the Kd values of deltamethrin and permethrin action on I874C channels.

6.4. The sensitivity of the mutant I874C rat channel and *para* wild type channel to pyrethroid analogues.

Results from Section 6.1 suggest that the cyano moiety of deltamethrin does not bind to the side chain of the cysteine 874 residue of the rat channel as this channel mutant was also sensitive to permethrin, a pyrethroid that lacks the cyano moiety. Other chemical groups common to both deltamethrin and permethrin must, therefore, be responsible for the interaction with the side chain of the 874 cysteine. To identify which constituent chemical groups of the deltamethrin and permethrin molecules may be directly interacting with the channel Cys874 side chain, chemical moieties common to both

insecticides were absent from synthesised pyrethroid analogues, which were then tested on oocytes expressing the mutant I874C channel. Etofenprox contains the *m*-phenoxy benzyl alcohol moiety common to deltamethrin and permethrin but lacks the dihalovinyl cyclopropane carboxylate ester, also common to both deltamethrin and permethrin. In the pyrethroid 10042, the situation is reversed. It contains the dihalovinyl cyclopropane carboxylate ester but lacks the *m*-phenoxy benzyl alcohol moiety (Figure 6.8). Any difference in the sensitivity of the mutated rat channel to either compound would implicate one of the two entities as likely sites of channel-insecticide binding.

A similar, but far more detailed structural investigation of pyrethrin I was undertaken by Elliott *et al.* (1978) to identify the chemical constituents of the pyrethrin that were essential for insecticidal activity. The natural pyrethrin I was used as the 'parent' molecule and divided into specific structural or chemical components each comprising of individual bonds or single chemical entities (Figure 1.1). Each component was then removed and replaced by a unit of analogous structure and the insecticidal activity of the altered compound measured (Elliott et al, 1978).

It may be as a consequence of the absence of so many chemical units from both etofenprox and 10042, when compared with deltamethrin and permethrin, that neither rat IIA wild type channel nor the mutant I874C rat channel showed any sensitivity to either of the these novel pyrethroids. High insecticidal activity is thought to be primarily dependent on the overall shape of the molecule (Elliott, 1977), and in this respect etofenprox and 10042 through the absence of substantial components of the 'parent' molecule, differ greatly from more active pyrethroids (Figure 6.8).

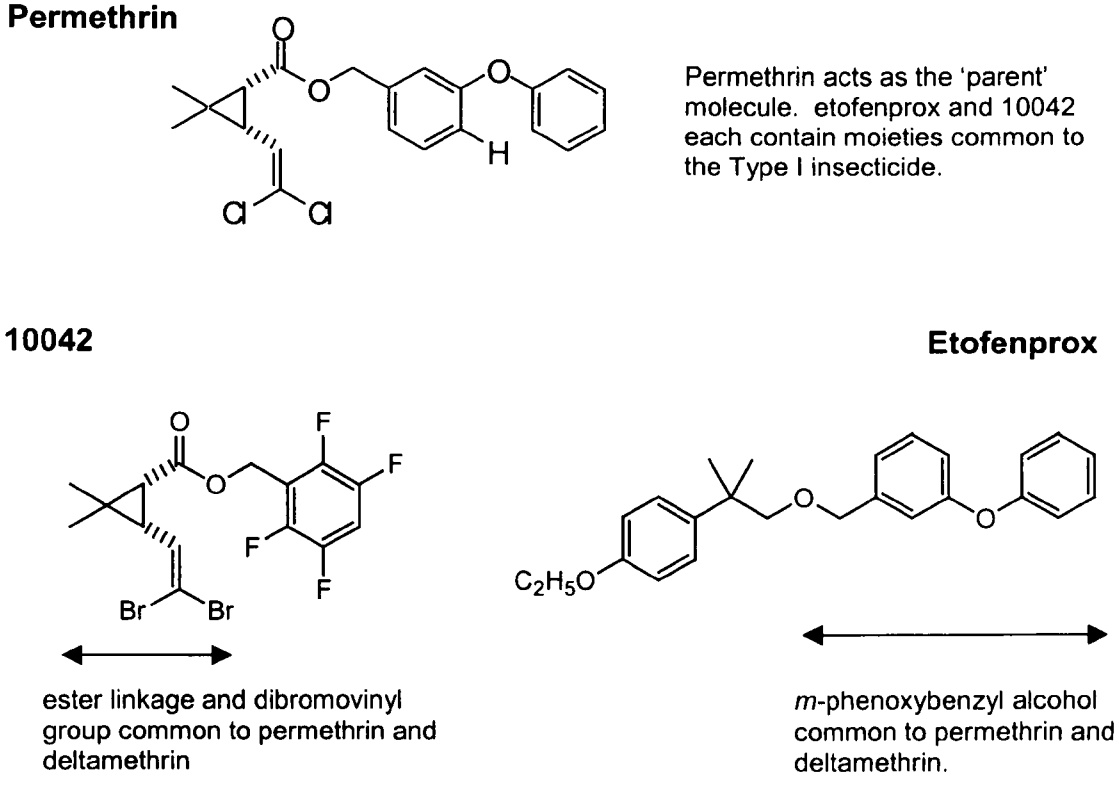

Figure 6.8. Structure of Permethrin, 10042 and etofenprox. The arrows indicate the chemical groups that 10042 and etofenprox have in common with permethrin

Equally, pyrethroid-channel binding may not rely solely on the interaction of one moiety of the insecticide with one active site; rather a number of key structural or chemical features may be needed for an effective interaction to occur. Indeed, the absence of one component of the pyrethroid may prevent the subsequent binding of another to the channel. This 'zipper' or cooperative binding model has been suggested in previous studies of pyrethroid-channel interactions where a conformational adjustment of both the insecticide and the channel may occur in a number of discrete, successive steps

(Vijverberg et al, 1983). Etofenprox and 10042 may require both the *m*-phenoxy benzyl alcohol moiety and dibromovinyl cyclopropane carboxylate ester linkage common to both permethrin and deltamethrin before any further interaction with the sulphur-containing side chains of methionine or cysteine can occur.

The *para* wild type channel did show clear sensitivity to both etofenprox and 10042, thereby not discounting the possibility of some direct form of interaction with the Met918 residue. However, the sensitivity of the wild type channel to both pyrethroid analogues was significantly less than the sensitivity of the same channel to either permethrin or deltamethrin. This is firstly reflected in the ability of the channels to recover quickly following exposure to 10μM of both etofenprox and 10042. *Para* wild type channels exposed to the same concentration of deltamethrin or permethrin do not recover. Secondly, although the etofenprox and 10042 Kd values should not be viewed as an accurate quantitative measure of *para* wild type sensitivity to these compounds, as only two experiment were performed in each case and none in the presence of ATX-II, they are clearly larger than the Kd values calculated for both deltamethrin (Vais et al, 2000). and permethrin. This suggests a lower affinity between the *para* wild type channel and these novel pyrethroid variants. This low affinity, even with the highly permethrin and deltamethrin-sensitive *para* wild type channel, may, in part, explain the lack of response displayed by the less permethrin and deltamethrin-sensitive mutant I874C rat channel to etofenprox and 10042 (*para* wild type; Kd deltamethrin = 4.4nM; Kd permethrin = 10.3nM: I874C; Kd deltamethrin = 1.2μM, Kd permethrin = 0.67μM).

CHAPTER 7

TECHNIQUES FOR THE DETECTION OF KDR AND SUPER-KDR MUTATIONS IN FIELD POPULATIONS OF *MUSCA DOMESTICA*

7.0. Introduction

Resistant pest management is defined as preventing or reversing the development of resistance in pests and this is a vital part of integrated pest management schemes (Denholm and Rowland, 1992; Denholm and Jespersen, 1998).

An important component of resistance management in field populations is the ability to detect resistance mutations rapidly in individual insects so that the potential for wide-spread resistance may be detected early. Certain screening methods could also offer the potential to highlight other target site mutations conferring resistance to pyrethroids and other current insecticides.

A number of techniques for detecting point mutations have been used in a wide variety of fields including human genetics and microbial pathogenesis. These include PASA (PCR Amplification of Specific Alleles) (Hensel *et al.*, 1991; Sommer, Groszbach and Bottema, 1992), SSCP (Single Stranded Conformational Polymorphism) (Lessa and Applebaum, 1993; Coustau and ffrench-Constant, 1995) and microsequencing (Zhang *et al.*, 1999).

An SSCP technique has been used to detect sodium channel mutations in the Colorado Potato Beetle, *Leptinotarsa decemlineata* (Clark *et al.*, 2001) and cyclodiene resistance-associated mutations in the whitefly *Bemisia tabaci* (Anthony *et al.*, 1995). PASA has similarly been used to detect pyrethroid resistance mutations in housefly (Williamson *et al.*, 1996), and cyclodiene-resistance mutations in *Bemisia tabaci* and *Drosophila*

melanogaster (Anthony *et al.*, 1995; Aronstein, Ode and ffrench-Constant, 1995; Steichen and ffrench-Constant, 1994).

PASA involves the generation of allelle-specific PCR primers with either the resistance-associated base or the wild type base at their 3′ end. When the PCR conditions are correct, each primer will only amplify its matching allele and this is detected by the presence or absence of bands of a specific size when the PCR products are examined by agarose gel electrophoresis. A drawback of this technique is that the PCR reaction is extremely sensitive to slight changes in parameters such as the annealing temperature and $MgCl_2$ concentration and even slight variations in these between batches can produce false results.

SSCP is a faster and more robust procedure and can be used on genomic DNA (Zhang *et al.*, 1999). The technique detects single base differences in the sequence of short single-stranded DNA fragments of equal size and charge when they are electrophoresed on a high percentage polyacrylamide or agarose gel. Base differences alter the secondary conformation that the single-stranded DNA adopts and this in turn affects the speed at which the fragments migrate through a non denaturing gel (General overview figure 2.2).

The aim of the present study was to see if a SSCP assay could be developed as a reliable diagnostic of kdr and super-kdr mutations in the housefly sodium channel gene. Initial experiments were done on standard strains of housefly where the kdr and super-kdr status had been determined by bioassay (M Hedges, personal communication)

7.1. Developmental Diagnostics

7.1.1. Rapid screening of the super-kdr mutation in housefly samples.

The housefly sodium channel gene has been fully sequenced (Williamson *et al.*, 1996a) and the kdr and super-kdr mutations identified in two highly conserved coding regions. Primers were designed to span the super-kdr mutation (see figure 7.1) and nested PCRs performed. Secondary reactions with primers MW104 and MW97 produced a fragment of 144bp and this was confirmed on agarose gel electrophoresis (see figure 7.2). Since the super-kdr fragment contains a single base difference from the wild type channel, when the fragments were denatured and run on a 10% polyacrylamide gel this was shown as a mobility difference (see figure 7.3) with the super-kdr fragment running more slowly (lanes 2, 3, 6 and 7), than the wild type (lanes 1, 9-12). The PCR products amplified from strains heterozygous for the super-kdr mutation strain (lanes 4-5, 8, 13) showed both bands. Thus, the SSCP diagnostic successfully identified the three genotypes in standard strains of known susceptible and super-kdr phenotypes.

7.1.2. Rapid screening of the kdr mutation in samples of housefly.

For kdr analysis, primers MW97 and MW104 spanning the kdr site were used (see figure 7.1). The nested PCR produced a 390bp fragment when analysed on an agarose gel (see figure 7.4). This contains the 125bp intron immediately downstream of the kdr mutation, in addition to 265bp of exon sequence. The fragments were denatured and run on a 15% polyacrylamide gel (see figure 7.5). No clear banding pattern could be identified in the region of the single-stranded fragments, probably due to variation

Figure 7.1. Partial sequence of the domain IIS4-IIS6 region of the housefly sodium channel gene showing the coding (cDNA) sequence (black, uppercase), the position of two unsequenced introns (marked by 'I') and the full sequence of the short, 120bp intron downstream of the kdr mutation site(red, lowercase). The kdr /super-kdr codons are boxed, and nucleotide sequences between susceptible (upper liner), kdr (middle line) and super-kdr (bottom line) with the intron sequence are shown. Tsp 509 I restriction sites are highlighted in green; primers used in this analysis are denoted by blue arrows.

Intron sequences are not published and were kindly provided by Martin Williamson at Rothamsted.

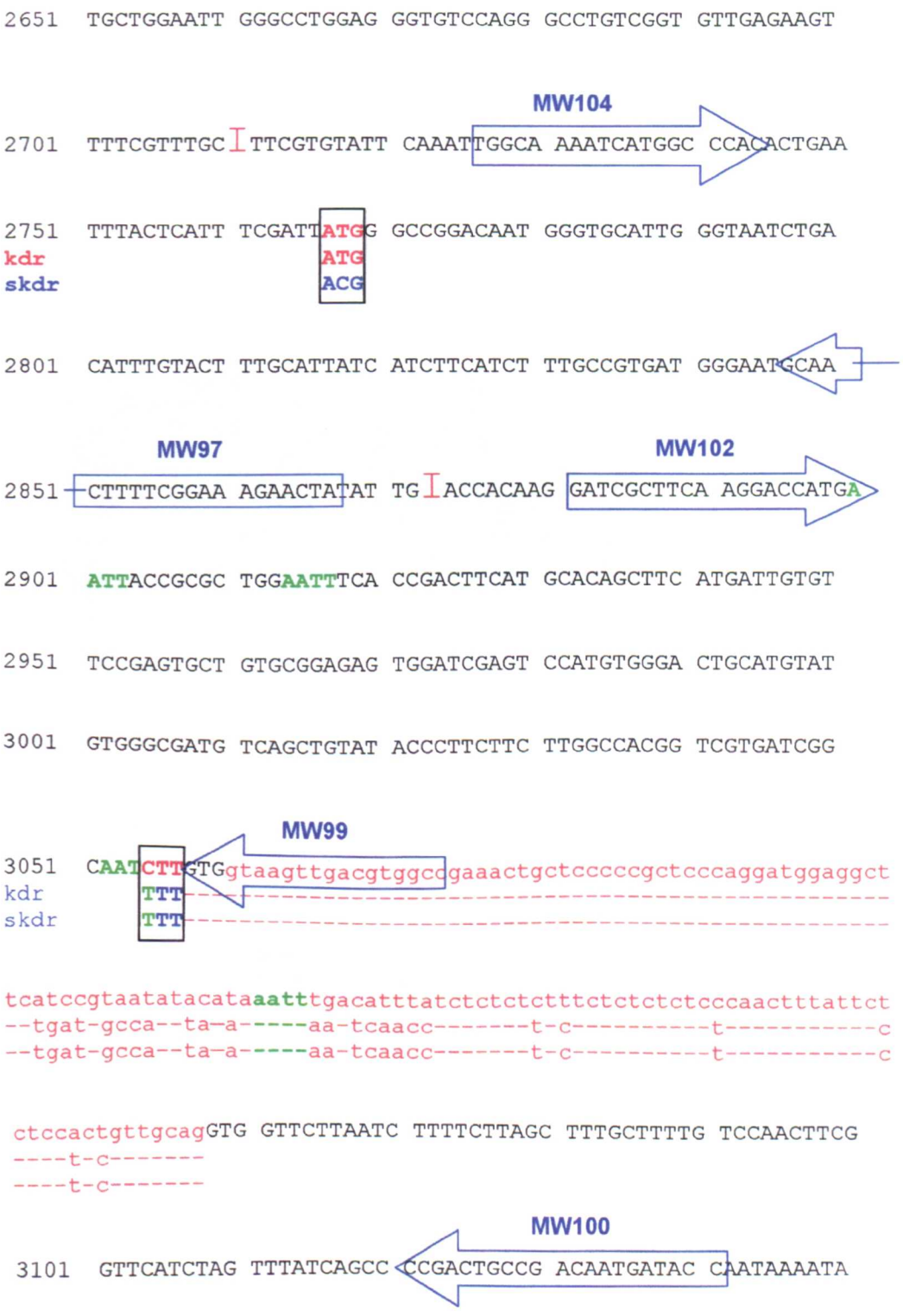
2651 TGCTGGAATT GGGCCTGGAG GGTGTCCAGG GCCTGTCGGT GTTGAGAAGT
MW104
2701 TTTCGTTTGC TTCGTGTATT CAAATTGGCA AAATCATGGC CCACACTGAA
2751 TTTACTCATT TCGATTATGG GCCGGACAAT GGGTGCATTG GGTAATCTGA
kdr ATG
skdr ACG
2801 CATTTGTACT TTGCATTATC ATCTTCATCT TTGCCGTGAT GGGAATGCAA
MW97
MW102
2851 CTTTTCGGAA AGAACTATAT TG ACCACAAG GATCGCTTCA AGGACCATGA
2901 ATTACCGCGC TGGAATTTCA CCGACTTCAT GCACAGCTTC ATGATTGTGT
2951 TCCGAGTGCT GTGCGGAGAG TGGATCGAGT CCATGTGGGA CTGCATGTAT
3001 GTGGGCGATG TCAGCTGTAT ACCCTTCTTC TTGGCCACGG TCGTGATCGG
MW99
3051 CAATCTTGTGgtaagttgacgtggccgaaactgctccccgctcccaggatggaggct
kdr TTT----------
skdr TTT----------
tcatccgtaatatacataaatttgacatttatctctctctttctctctctcccaactttattct
--tgat-gcca--ta-a-----aa-tcaacc-------t-c----------t----------c
--tgat-gcca--ta-a-----aa-tcaacc-------t-c----------t----------c
ctccactgttgcagGTG GTTCTTAATC TTTTCTTAGC TTTGCTTTTG TCCAACTTCG
----t-c-------
----t-c-------
MW100
3101 GTTCATCTAG TTTATCAGCC CCGACTGCCG ACAATGATAC CAATAAAATA

Figure 7.2. PCR products amplified from the gDNA of 13 standard Rothamsted laboratory *Musca domestica* strains using primers MW 104 and MW 97 and run on a 1.5% agarose gel with a 100bp ladder. The diagram below shows the relative positions of the primers, surrounding introns and the super-kdr mutation.

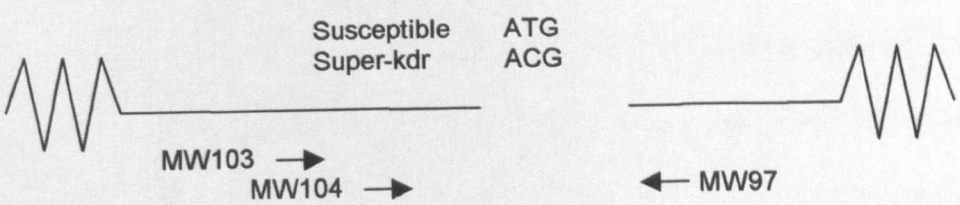

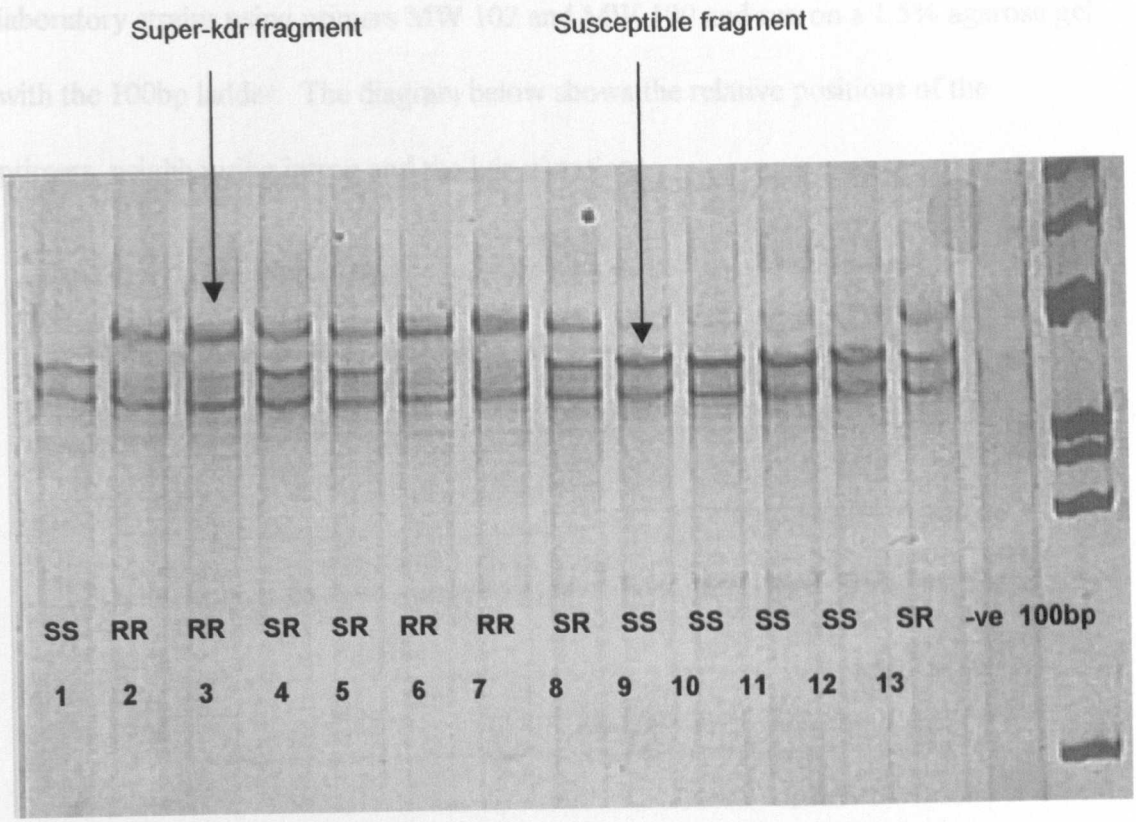

Figure 7.3. Denatured PCR products amplified from the gDNA of 13 individual flies from standard Rothamsted laboratory *Musca domestica* strains of known super-kdr genotype using primers MW 104 and MW 97 and run on a 10% polyacrylamide gel with a 100bp ladder. A different banding pattern appeared depending on whether the individual fly carried the super-kdr mutation or not. The super-kdr fragment migrated more slowly through the gel than the susceptible fragment while the fastest migrating band at the bottom of the gel was common to all samples. The genotype of each fly sample is shown at the bottom of the gel.

Figure 7.4. PCR products amplified from the gDNA of 13 standard Rothamsted laboratory strains using primers MW 102 and MW 100 and run on a 1.5% agarose gel with the 100bp ladder. The diagram below shows the relative positions of the primers, neighbouring intron and the kdr mutation.

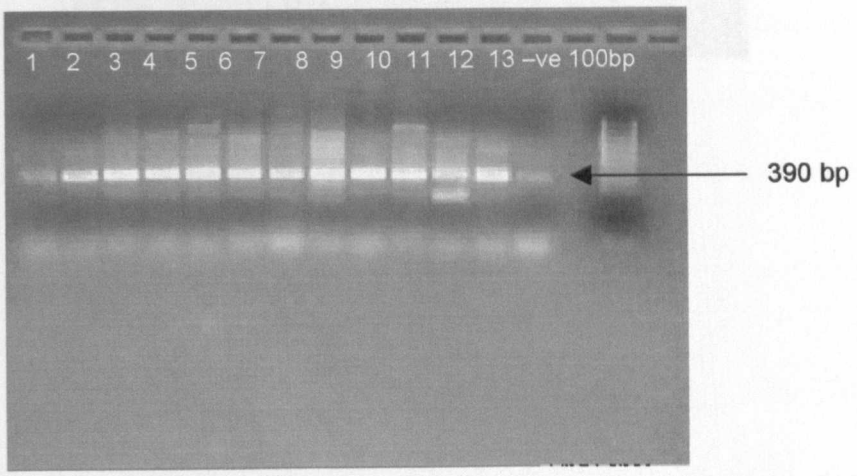

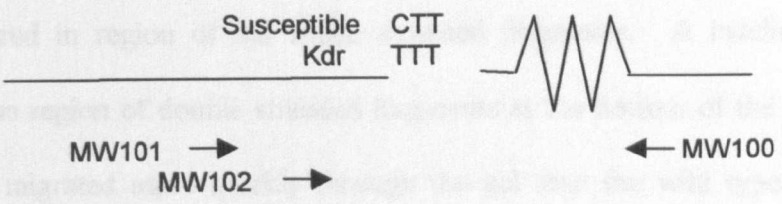

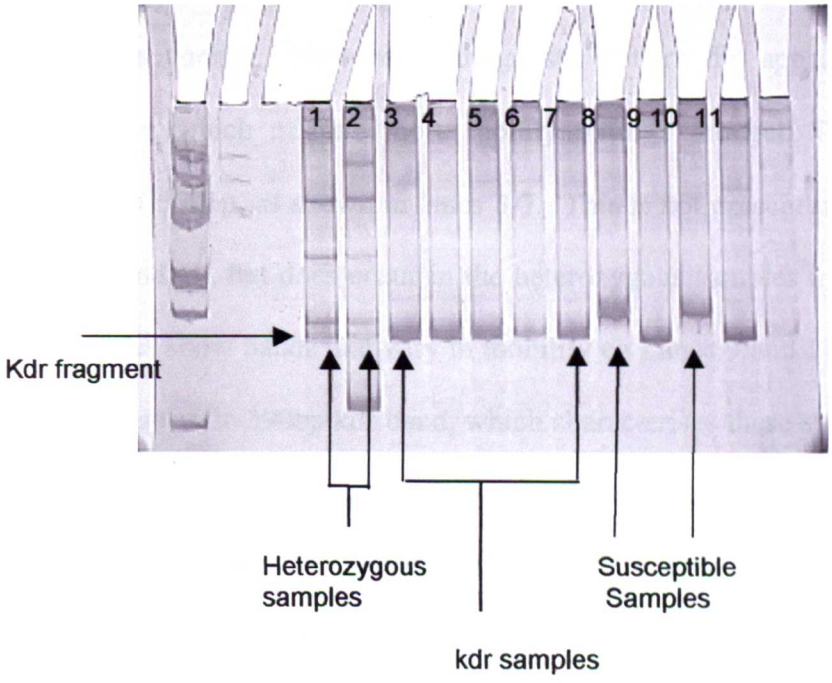

Figure 7.5 Denatured PCR products amplified from the gDNA of 11 flies from standard Rothamsted laboratory *Musca domestica* strains using primers MW 104 and MW 97 and run on a 15% polyacrylamide gel with a 100bp ladder. No banding pattern appeared in region of the single stranded fragments. A banding pattern appeared in the region of double stranded fragments at the bottom of the gel. The kdr fragment migrated more quickly through the gel than the wild type fragment. Both fragments can be seen in the heterozygous samples.

within the intron sequence. However, a diagnostic pattern did appear in the double stranded fragments, which migrate more rapidly through the gel. The kdr samples produced a band of 390bp, as shown in lanes 3-7. This is not present in the susceptible samples, lanes 8 and 10, but does occur in the heterozygous samples in Lanes 1 and 2. Susceptible samples show bands that vary in mobility eg Lanes 9 and 11. It is therefore the absence of the specific 390bp kdr band, which characterises these strains, rather than the presence of a specific non-kdr band. This is sufficiently accurate when the sequence and size of the intron is known, however introns from unknown samples may vary in size and therefore produce a false result.

A second primer, MW99 was designed to anneal to the first few bases within the intron (see figure 7.1). This produced a much shorter 195bp fragment, which did not include the intron. However when samples were run on a gel, no clear scoring pattern could be detected (see figure 7.6) and it was concluded that this SSCP was not suitable as a diagnostic aid.

An alternative method for kdr genotyping was investigated. Closer analysis of the kdr mutation and its surrounding sequence showed that the mutation created an additional restriction site for the endonuclease Tsp 509 I (5'AATT3') (see figure 7.1). PCR amplification of gDNA from laboratory and field populations with MW100 and MW102 produced a fragment 390bp in length which when digested with Tsp 509 I gave five fragments of 21bp, 14bp, 138bp, 75bp and 142bp if the kdr mutation was present, and only four fragments of 21bp, 14bp, 213bp and 142bp if the fragment was amplified from a wild type sample. The digested samples were run on a 10% polyacrylamide gel, from

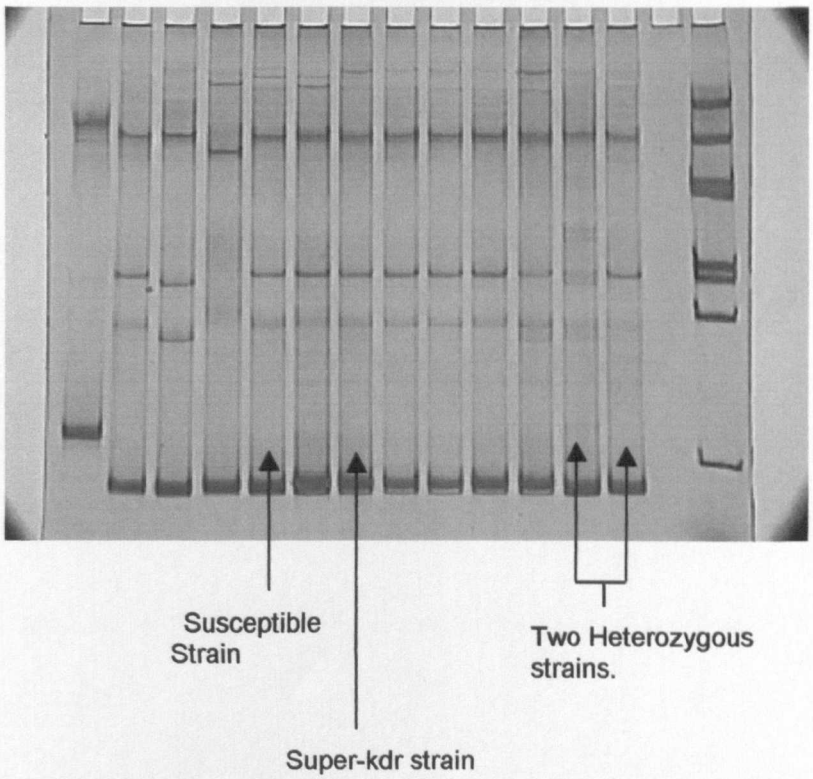

Figure 7.6. Denatured PCR products amplified from the gDNA of 13 individual flies from standard Rothamsted laboratory *Musca domestica* strains of known super-kdr genotype, using primers MW102 and MW99 and run on a 10% polyacrylamide gel with a 100bp ladder. No clear banding pattern could be seen in either the single or the double stranded regions of the gel.

which the homozygous kdr sample gave the 138bp/142bp and 75bp bands as expected. The homozygous wild type gave the expected 213bp band and the heterozygous kdr gave a mixture of 213bp, 138bp/142bp and 75bp bands (Figure 7.7). One of the restriction sites occurs within the intron and this could account for small variability in the size of the predicted 142bp fragment of homozygous wild type samples. However, this diagnostic is based on the presence of either a large ~213bp fragment or a smaller ~75 base pair fragment or a mixture of both. Slight variation in the size of these two fragments should not complicate the diagnostic.

The SSCP technique for super-kdr detection and the restriction fragment diagnostic for kdr detection were therefore used to screen samples of unknown kdr and super-kdr status.

7.2. Detection of the super-kdr mutations in housefly samples exposed to different pyrethroid treatments.

Over sixty houseflies, collected from pig farms, were kindly provided by Dr A. McNichol at MAFF-CSL, York. Four farms, New, Moor, Rail and Pax, were looked at in detail and the insecticide regimes that each farm had employed are given in Table 7.1. New Farm had used the most intensive insecticide treatments, spraying Alfadex, a commercially available natural pyrethrin, every day during the summer in the year prior to collection. Moor, Rail and Pax Farms had used Golden Malrin, a carbamate-based insecticide containing methomyl, in the year prior to collection. This would not be expected to select for sodium channel mutations, but previous to this, Pax and Rail farms

Figure 7.7. PCR products amplified from the *Musca domestica* gDNA of 2 standard Rothamsted laboratory strains and 4 individuals from the New Farm population using primers MW102 and MW100, were digested with Tsp 509 I and run on a 10% polyacrylamide gel. The genotype of each individual is shown at the top of the gel. The kdr mutation introduces a Tsp 509 I restriction site, which results in a ~75bp fragment in kdr samples following digestion of the entire fragment with the enzyme. The diagram below indicates the relative positions of Tsp 509 I restriction sites (⏷) within the amplified fragment, in relation to the kdr mutation and the intron.

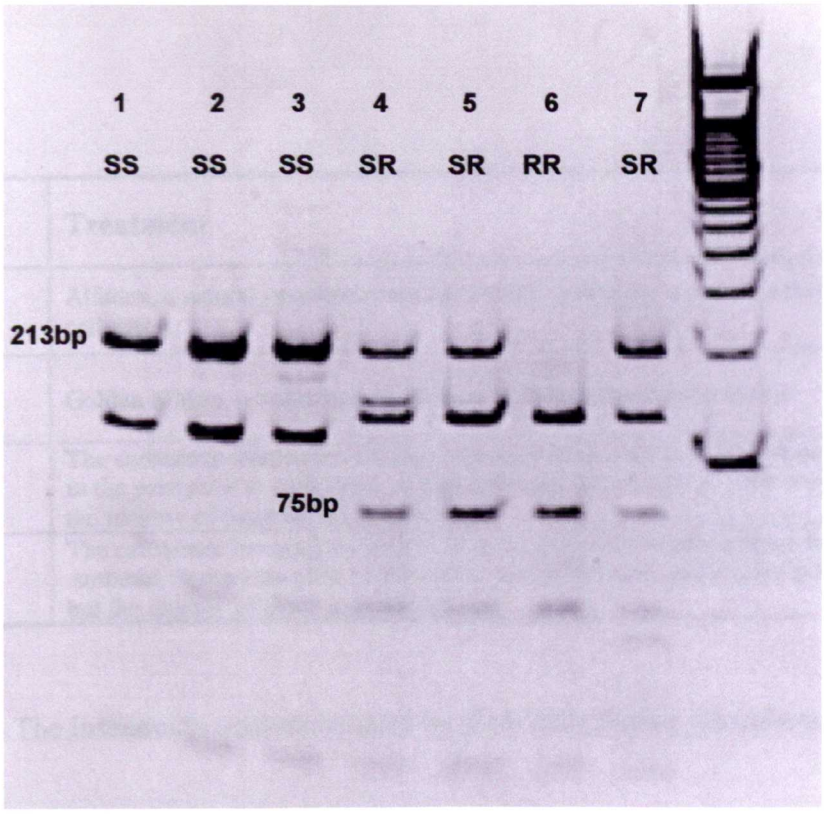
1
2
3
4
5
6
7
SS
SS
SS
SR
SR
RR
SR
213bp
75bp

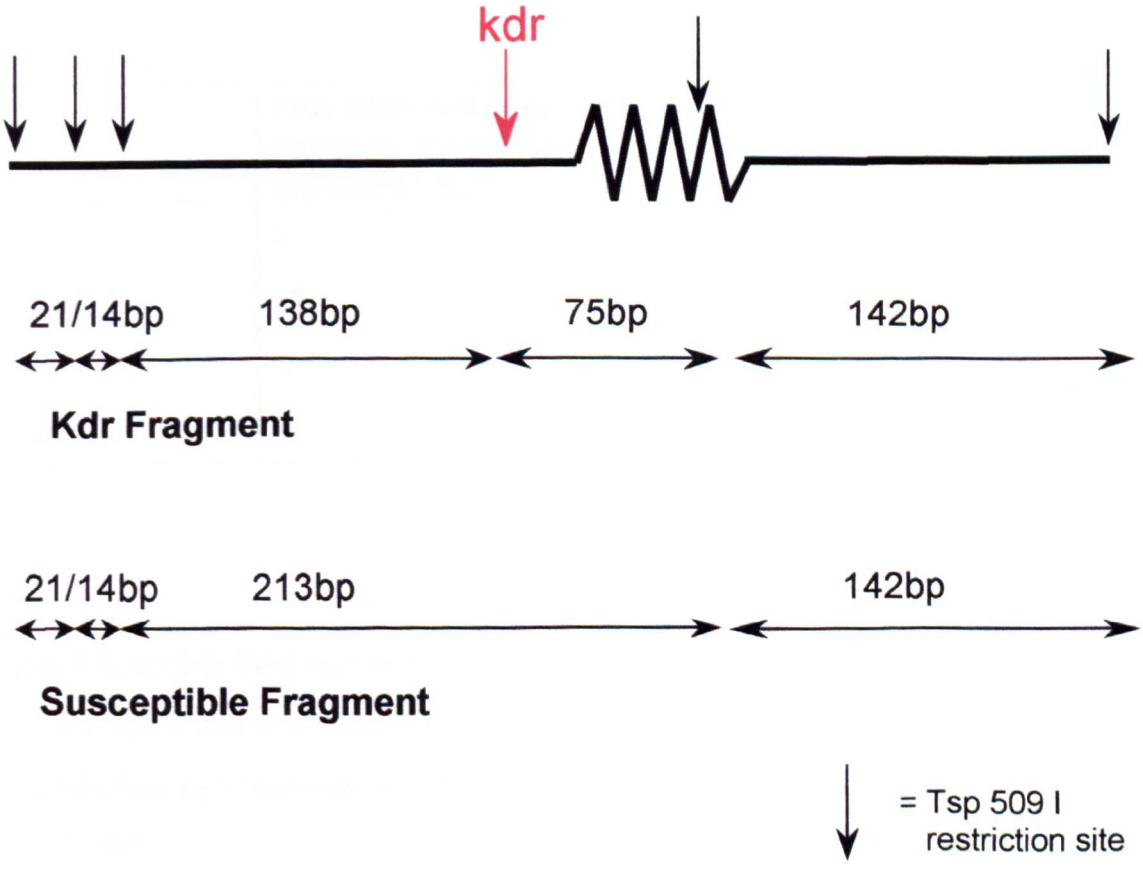
kdr
21/14bp
138bp
75bp
142bp
Kdr Fragment
21/14bp
213bp
142bp
Susceptible Fragment
= Tsp 509 I
restriction site

Farm	Treatment
New	Alfadex, a natural pyrethrum used every day during the summer in the year prior collection
Moor	Golden Malrin, a carbamate-based insecticide containing methomyl
Pax	The carbamate insecticide, Golden Malrin (methomyl), used on bait boards in the year prior to collection. Knockdown pyrethroid sprays were used before the identity of these were not known.
Rail	The carbamate insecticide, Golden Malrin (methomyl) used in heaps throughout the summer, in the year prior to collection. KD pyrethroid sprays used before this, but the identity of these were not known.

Table 7.1. The insecticide treatments used by each farm before the collection of fly samples.

Farm	Flies killed following treatment with 0.016% pyrethrin + 0.16% PB	Survivors following treatment with 0.016% pyrethrin + 0.16% PB
New	0	60
Moor	52	8
Pax	5	55
Rail	14	46

Table 7.2. 60 flies from each farm were tested with 0.016% pyrethrin + 0.16% PB. Each fly was scored as a 'non-survivor' if it was killed by the topically applied pyrethrin dose or a 'survivor' if it remained alive (Work carried out by Dr A. McNichol CSL, York).

had employed pyrethroid sprays, although the exact identity of the insecticides used was unknown.

Bioassays were kindly done by Dr A. McNichol at MAFF, CSL, York. The flies collected from each farm were subjected to a diagnostic dose of pyrethrins (0.016%) plus piperonyl butoxide (0.1%) following which they were scored as either dead or alive (Table 7.2). This showed that 100%, 13%, 92% and 76% survived at New, Moor, Pax and Rail farms respectively. These samples were then frozen and sent to the Rothamsted for genotype analysis. Genomic DNA from each fly was extracted and its super-kdr status determined as described above (Figure 7.8).

The super-kdr resistance mutation was most prevalent in flies from New and Pax Farms, correlating with their high survival rate in the bioassay. At New Farm, over 60% of samples were homozygous for the super kdr mutation and for the Pax flies there were equal numbers of heterozygous and homozygous genotypes. The mutation was much less common in the samples taken from farms Moor and Rail, with just under 80% of flies being homozygous susceptible for the super-kdr mutation (Figure 7.9). This explains the low survival rate in the bioassay for the Moor sample but it is not clear why the Rail samples had such a high survival rate.

Unfortunately, due to time constraints, the kdr status of these flies was not examined. However, the restriction diagnostic described could certainly be used in determining the kdr status of the field samples collected.

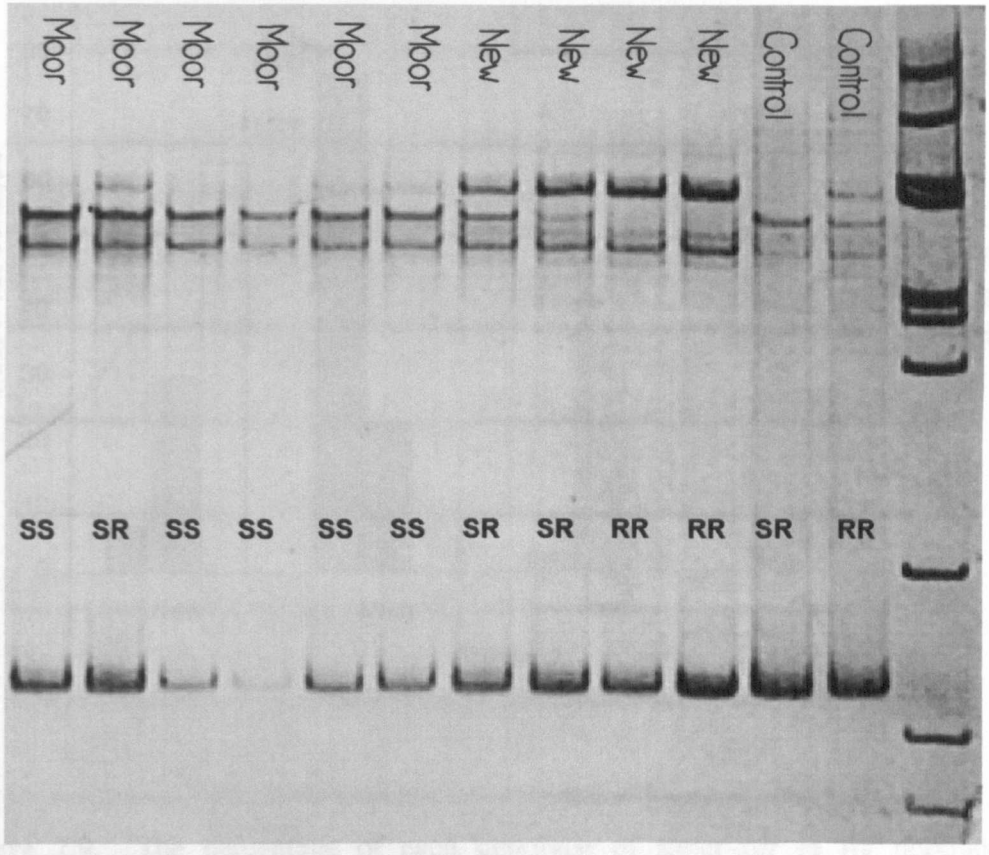

Figure 7.8. 10% polyacrylamide SSCP gel of denatured PCR products amplified from the gDNA of 12 individual flies from the New and Moor farm *Musca domestica* population. The farm origin of each fly is shown at the top of the gel and the genotype is shown at the bottom of the gel.

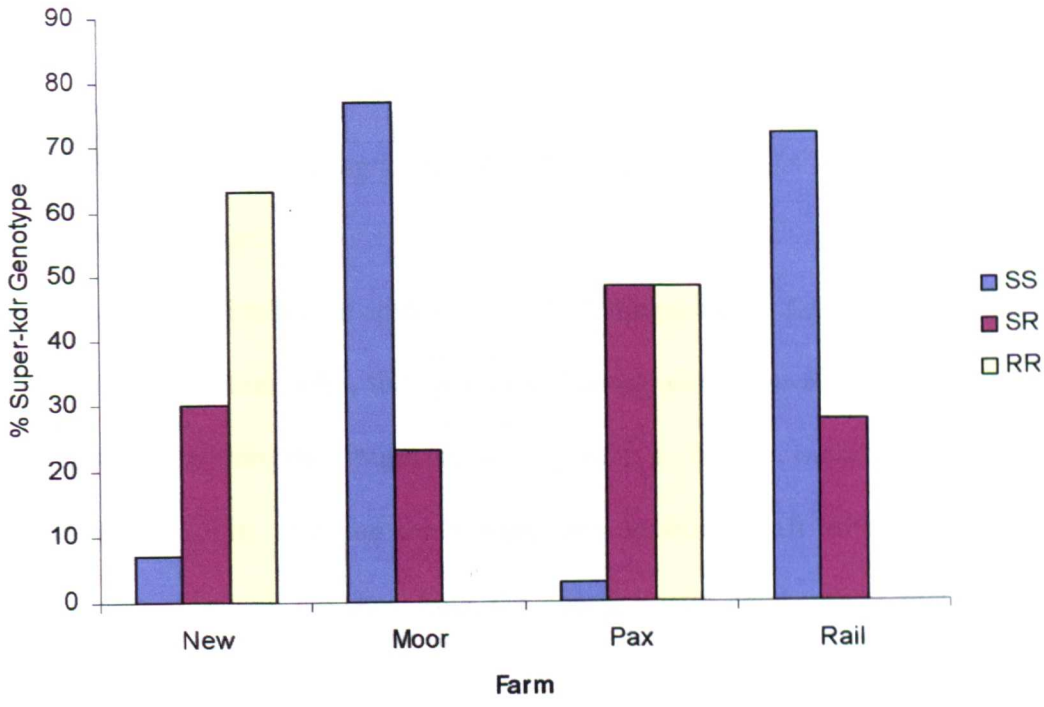

Figure 7.9. The percentage of each genotype of super-kdr in fly populations collected from four different farms.

7.3. Discussion

7.3.1. Assessment of the diagnostics for kdr and super-kdr mutations in Musca domestica field samples.

There are clearly difficulties in applying an SSCP diagnostic to field samples because it depends on the mutation being the only base change within the fragment. In practice, other mutations within the fragment may confer a further mobility shift making diagnosis questionable. On the other hand, any mobility shift within a resistant or susceptible strain, which deviates from the characteristic band, might highlight other mutations.

The fully sequenced housefly sodium channel gene has no other mutations in the central four domain structure of the channel (Williamson *et al.*, 1996a) and hence SSCP would seem to be a good choice of diagnostic. However, the kdr mutation lies just outside a short intron and since intron sequences are not placed under selection pressure, they tend to diverge far more rapidly than coding sequences. It was therefore important that the PCR primer, which has to be within the intron, is as close as possible to its 5' end. Even so, if the region within the intron is too diverse, the primer may not anneal and the amplification will fail. Even for successful amplification, mutations in the intron may cause mobility shifts of the fragments, making the kdr diagnosis unreliable. However, comparison of the intron sequence of different housefly strains found complete sequence homology between the first 22 bases of the intron near the kdr mutation (Martin Williamson, personal communication). From this, the reverse primer MW99 was designed with its 5' end lying three bases away from the kdr mutation and amplification

of the fragment was successful, with the most prominent fragment being the correct 195bp. However, the banding patterns created after denaturing did not give the expected results (see figure 7.6). For example, the two known heterozygous samples did not have the four bands expected from the presence of both alleles. One possible reason for this is the proximity of the kdr mutation to the end of the fragment. A more central base change could have a more drastic effect on the overall conformation of the fragment than one at the termini.

The most successful approach for detecting the kdr mutation was the restriction enzyme diagnostic, or PCR-REN, a technique which has also been used to detect a point mutation conferring GABA receptor insecticide resistance (ffrench-Constant *et al.*, 1993) The PCR based diagnostic relies on the detection of the presence or absence of a Tsp I restriction site introduced by the kdr mutation. The kdr status can therefore be determined by the number of fragments rather than the fragment size, and this removes the complications caused by the variability of the intron.

The SSCP diagnostic for super-kdr was probably successful because the mutation lies centrally within the coding sequence and all primers are located within the highly conserved coding region. All samples screened for the super-kdr mutation showed one of three characteristic banding patterns when run on an SSCP gel. Any deviation from this configuration would have highlighted polymorphisms or other mutations, which may also have conferred pyrethroid resistance

7.3.2. Relevance of the results of this study to the wider field of insecticide resistance

Despite the wide range of insect pests on which chemically diverse insecticides act, the number of mechanisms known to cause insecticide resistance is not large. Adaptations effecting the penetration of the toxicant, the rate at which it is metabolised and the sensitivity of its target are the three major factors which dictate the efficacy of insecticide action. Because many of these mechanisms affect the toxicity of more than one insecticide class, selection for resistance by one compound can confer cross-resistance to another compound. The occurrence of more than one of these mechanisms within a pest population has the potential to produce very high levels of resistance, indeed a *Musca domestica* strain showing approximately 6000-fold resistance to the pyrethroid permethrin contains factors for reduced cuticular penetration, enhanced oxidative metabolism and reduced neuronal sensitivity (Scott and Georghiou, 1986).

Although many farms report using integrated pest management schemes, which involve the used of a variety of measures as means of pest control, there is still a widespread heavy reliance on chemical methods of control (Kaufman, Scott and Rutz, 2001). Populations of *Musca domestica* in pig farms are currently controlled using pyrethrum and Type I pyrethroids such as bioresmethin synergised with piperonyl butoxide, organophosphates such as Azamethiphos and carbamates such as methomyl (Kristensen, Spencer and Jespersen, 2001). However control is becoming evermore difficult as widespread and increasing resistance to the three insecticide classes occurs. This has

been shown by a number of surveys (Pap and Farkas, 1994; Scott, Roush and Rutz, 1989).

In general, there is a strong correlation between the insecticide used and the occurrence of resistance. For example, in the UK resistance to methomyl and azamethophos appeared within a few years of their introduction, whilst pyrethroid resistance decreased after permethrin was withdrawn from use (Chapman and Morgan, 1992; Chapman *et al.*, 1993). Studies undertaken in Denmark showed that even after the cessation of heavy pyrethroid use in livestock farms, high levels of pyrethroid-resistance in *Musca domestica* persisted. In contrast, farms where non-residual pyrethroids sprays were infrequently used showed only low to moderate levels of resistance (Kristensen, Spencer and Jespersen, 2001). A similar pyrethroid resistance pattern was seen in caged-layer poultry facilities in the US, where there was good correlation between the insecticide use histories of the facilities and the levels of resistance in *Musca domestica* populations (Scott *et al.*, 2000)

In this study over 60 flies from field populations were screened for the presence of the super-kdr mutation. In general, the frequency of the resistance mutation correlated well with bioassay results, which in turn reflected the selection pressure imposed on the population by the insecticide regimes each farm had adopted.

New farm had the most intense spraying programme, with the natural pyrethrin Alfadex being used every day during the summer in the year prior to sample collection. This intense selection pressure is reflected in both the phenotype (none of the flies were killed

by the diagnostic pyrethrin dose used in the bioassay) and the genotype, where over 60% were homozygous for super-kdr. However, this large population of super-kdr homozygous flies is somewhat surprising as the mutation is thought to only significantly increase resistance against Type II pyrethroids.

In contrast, Moor farm used a carbamate insecticide, rather than pyrethroids to control pest numbers. This insecticide acts on the central nervous protein acetylcholinesterase AchE (Eto, 1974, Kuhr and Dorough, 1976), the enzyme responsible for hydrolysis of the neurotransmitter acetylcholine and insensitivity is conferred by mutations of the enzyme (Fournier *et al.*, 1992). Carbamates do not act upon the voltage gated sodium channel and therefore the super-kdr mutation would not be selected. This is consistent with only 13% of the population surviving the diagnostic dose, and with the low frequency of super-kdr genotypes. There is no statistical difference in the frequencies of the super-kdr mutation in flies killed by the diagnostic dose used in the bioassay, and those that survived (P=0.23, two-tail paired t-test). This would be expected if no previous selection pressure had been applied, as the super-kdr mutation would appear randomly throughout the population.

Rail and Pax reported using a combination of the carbamate methomyl and Type I pyrethroid insecticides. This is reflected phenotypically by 92% of the Pax fly population surviving the diagnostic dose and genotypically by very high levels of super-kdr homozyogotes and heterozygotes. Unusually, the situation is reversed in Rail farm, where despite 75% of the population surviving the diagnostic dose, the majority of flies scored as homozygous susceptible for the super-kdr mutation. As carbamates and

pyrethroids act upon different targets, insensitivity to the diagnostic pyrethrin dose would not have arisen from AchE resistance selected for by carbamate use in the field. Although no screening of the kdr status of field houseflies was undertaken in this study, it is reasonable to predict that the high level of Rail farm flies surviving the diagnostic dose was due to the presence of the kdr. As the super-kdr M918T mutation is, to date, always found in conjunction with the kdr (Williamson *et al.*, 1996; Guerrero *et al.*, 1997), approximately 25% of the Rail fly population tested, must be either heterozygous or homozygous for the kdr genotype. Other resistance mechanisms, which may explain high levels of survival in the Rail fly population, include enhanced Cytochrome P450-dependent monooxygenase (dimethylnitrosamine demethylase) activity. Enhanced oxidative metabolism by this enzyme has been implicated as a resistance mechanism against all insecticide classes except the chlorinated cyclodienes (Scott, 1990). This resistance mechanism has been extensively studies in *Musca domestica* pyrethroid resistant and susceptible strains. Enhanced oxidative activity that accounts in part for high pyrethroid resistance, is the result of constitutive over expression of cytochrome P450 isozymes that are normally expressed at low levels in susceptible insects (Soderlund and Bloomquist, 1990)

This study agrees with the findings of Chapman and others that a correlation is seen between the insecticide used and the occurrence of insecticide resistance; high levels of pyrethroid resistance have been detected in *Musca domestica* populations that have been exposed to pyrethrum and Type I pyrethroid while low levels of resistance have been detected to populations controlled with a carbamate insecticide. In general, levels of pyrethroid resistance were reflected in the frequency of the super-kdr mutation.

CHAPTER 8

FINAL DISCUSSION

8.0. Final discussion

Sodium channels are the targets of a variety of neurotoxins including the widely used pyrethroids. Pharmacological approaches have had only limited success in revealing pyrethroid binding sites because of the highly lipophillic nature of these compounds. However, the identification of numerous resistance-associated mutations, including the M918V, T929M and T929V mutations studied here that confer reduced *para* sodium channel sensitivity, has provided valuable insights into the location of pyrethroid binding sites and the nature of pyrethroid action.

8.1 Pyrethroid binding sites

Pyrethroids slow voltage-gated sodium channel activation (Tabarean and Narahashi, 2001) inactivation (Narahashi, 1996; Soderlund et al, 1999) and deactivation (Tatebayashi and Narahashi, 1994). These effects are countered in insect *para* sodium channels by mutations located in a variety of regions within domain II of the voltage-gated protein including the kdr L1014F mutation in the S6 transmembrane segment (Smith *et al.*, 1997; Vais *et al.*, 2000; Tan *et al.*, 2001), the super-kdr mutation M918T (Vais *et al.*, 2000) and M918V mutation (this study) in the S4-S5 linker, and mutations T929I (Schuler *et al.*, 1998), T929V and T929M mutations (this study) found at the start of the S5 segment.

Other resistance mutations have been found in the S6 segments within domains I (Park *et al.*, 1997) and III (He *et al.*, 1999) at locations similar to the kdr mutation in domain II. Similarly, mutations in the S4-S5 linkers of domains I and III are also thought to reduce target site sensitivity (Park, Taylor and Feyersen, 1997). Detailed analysis of

deltamethrin action on *para* wild type, kdr and super-kdr channels suggests the existence of two binding sites for pyrethroids (Vais *et al.*, 2000). Together, these mutations may indicate the possible location of these proposed sites.

The S6 segments of all four domains line the channel pore (Doyle *et al.*, 1998; Lipkind and Fozzard, 2000). Therefore, the existence of a cluster of resistance mutations within these S6 helices, including the L1014F found near the middle of the segment in domain II (Williamson *et al.*, 1996), V410M in domain I (Park, Taylor and Feyersen, 1997) and F1541I in domain III (He *et al.*, 1999), suggests that a deltamethrin binding site might be located within the channel pore. This has also been suggested by Liu *et al.* (2002) and Lee and Soderlund (2001) and is supported by the findings presented here and in other studies (Leibowitz *et al.*, 1987; Salgado and Narahashi, 1993; Vais *et al.*, 2000) that pyrethroids preferentially bind to the open state of the sodium channel. The inverted tepee arrangement of the S6 segments (Doyle *et al.*, 1998) widens and unfolds during activation (Perozo *et al.*, 1998) and this may realign the S6 segments so as to form a pyrethroid binding site (Wang *et al.*, 2001) or to allow access to a binding site already located within the pore. Pyrethroid molecules bound within the pore may trap the channel in its open conformation and this could account for the significant increase in tail current decay thought to be a consequence of slow deactivation of channels by deltamethrin and permethrin of M918V, T929V and T929M mutants in the presence of ATX-II shown in the studies presented here.

The collection of resistance mutations located at the beginning of the S5 transmembrane segment and the S4-S5 linker of domains I, II and III (Schuler *et al.*, 1998; Williamson

et al., 1996; Pittendrigh *et al.*, 1997, Lee *et al.*, 2000) may reveal regions where a secondary pyrethroid binding site could reside. The existence of a pyrethroid binding site around the S4-S5 linker is supported by the increase in channel sensitivity to deltamethrin and permethrin of the rat IIA sodium channel mutants studied here. The wild type rat sodium channel exhibits very high pyrethroid insensitivity compared with the *para* insect channel (Narahashi, 1992; Ertel, Bale and Cohen, 1994). However, the introduction of either methionine or cysteine at the equivalent super-kdr position within the rat channel (residue 874) confers >80-fold increase in the sensitivity of the mutant channel to deltamethrin and >150-fold increase in sensitivity to permethrin. The absence of any substantial changes in the gating behaviour of either rat mutant suggests that an increase in pyrethroid sensitivity is due to a direct increase in affinity between the pyrethroid molecule and the channel. Furthermore, the presence of a sulphur atom in the side chain of both methionine and cysteine would suggest that this constituent element is important in channel -insecticide interactions. Interestingly the super-kdr mutation together with the kdr mutation in insects (M918T) confers a very large increase in resistance to Type II pyrethroids (> 500-fold) (Farnham and Khambay, 1995) and only a moderate increase in resistance to Type I pyrethroids (50-fold). This contrasts with the *in vitro* sensitivities of the mutant I874C channel studied here, which show the mutation to confer high levels of sensitivity to deltamethrin and permethrin, suggesting that both pyrethroid types interact with the 874 locus in the rat mutant.

An alternative is that the kdr and super-kdr mutations together form a single binding site. Predictions of their proximity within the 3D structure have come from the crystal structure of the potassium channel (Doyle *et al.*, 1998), and suggest that the distance

between the two mutations might not exceed the length of the molecule in space (Martin Williamson, personal communication). The kdr mutation in cockroach (L993F) together with the mutation E434K or C764R found at either end of the D1-D2 linker reduces sensitivity to deltamethrin >100-fold (Tan *et al.*, 2001) while the same D1-D2 linker mutations in combination with the V409M mutation, found in resistant strains of *Heliothis virescens* (Park, Taylor and Feyersen, 1997) also reduces deltamethrin sensitivity 100-fold. (Liu *et al.*, 2002). However, in the absence of a crystal structure of the sodium channel protein, predictions as to the possible location of pyrethroid binding sites remain speculative.

8.2 Closed-state inactivation in channel populations expressing pyrethroid resistance mutations.

The binding of the inactivation gate with its docking site is the consequence of a hydrophobic interaction between the IFM motif within the III-IV linker and hydrophobic residues within IVS6 (McPhee *et al.*, 1998) and amino acids in the S4-S5 linker of domain III and IV (Smith *et al.*, 1997; McPhee *et al.*, 1998). M918V is located within the S4-S5 linker of domain II, a region analogous with areas within domains III and IV that are thought to act as the docking site for the fast-inactivation particle. The confirmed symmetrical arrangement of the channel (Sato *et al.*, 2001) could allow areas of the S4-S5 linker of domain II to also act as a constituent part of the docking site and, therefore, mutations of the region may affect the fast-inactivated state. The M918V mutation studied is hydrophobic in nature and could, therefore, stabilize the hydrophobic interaction of the inactivation particle. This may explain the large increase in the fraction of M918V channels undergoing closed state inactivation, a gating pathway in

which the channel bypasses the open state and inactivates immediately from the closed state (Patlak, 1991), and the significant shift in the voltage dependence of M918V channel inactivation.

A similar enhancement of closed-state inactivation is seen in channels expressing the T929V mutation found in a pyrethroid resistant strain of *Bemisia tabaci* (Morin *et al.*, 2002) and channels expressing the T929M mutation, which at the equivalent site in the human skeletal muscle sodium channel is thought to cause the muscle disorder Hyperkalemic Periodic Paralysis (Ptacek *et al.*, 1991). The 929 residue in *para* channels is found at the start of the S5 segment in domain II, which is an area of the channel that has not been identified as part of the fast inactivation particle docking site. However, the same mutation in the human skeletal muscle sodium channel causes a significant impairment of slow inactivation (Bendahhou *et al.*, 1999). As fast inactivation and slow inactivation are thought to be coupled, with the onset of fast inactivation inhibiting slow inactivation (Featherstone, Richmond and Ruben, 1996; Hayward, Brown and Cannon, 1997; Richmond *et al.*, 1998; Hilber *et al.*, 2002) the impairment of slow inactivation in T704M skeletal muscle sodium channels might explain the enhancement of closed-state fast-inactivation seen in this study when the same mutation is expressed in *para* channels (T929M).

Recently, another mutation of the human skeletal muscle sodium channel located four residues upstream from the super-kdr site (L689I), has been identified to cause HYPP through a hyperpolarizing shift in half maximal activation coupled with a significant impairment of slow inactivation (Bendahhou *et al.*, 2002). Its proximity to the super-kdr

site suggests that in insects, the M918V and M918T may similarly incur fitness costs through the inhibition of slow inactivation, although no significant shift in the half maximal activation of M918V channels was recorded.

8.3 Enhanced closed-state inactivation as a mechanism of resistance

An increase in the fraction of mutant populations undergoing closed-state inactivation seen in M918V, T929M and T929V mutant *para* channels, would reduce accessibility to the location of a pyrethroid binding site residing within the pore while the more frequent interaction of the inactivation particle with the S4-S5 linker of domain II as a putative part of the docking site could equally impede access to a second pyrethroid binding site, possibly lying just outside the mouth of the pore. Establishing the state dependency of access to the resistance mutations M918V in domain II S4-S5 linker or T929M or T929V at the cytoplasmic end of the S5 segment of domain II, perhaps using cysteine accessibility scanning (Yang and Horn, 1995), would help clarify whether pyrethroids could bind to these areas while the channel occupies conformations other than the open state. Competition between the pyrethroid molecule and the inactivation particle for the domain II S4-S5 linker as a putative part of the inactivation particle dock could account for the slowing of channel inactivation characteristic of pyrethroid channel modification.

8.4 Reduced pyrethroid-channel affinity as a mechanism of resistance

Whilst these mutations reduce access to binding sites through increased closed-state inactivation, they also may form part of a pyrethroid binding site and could, therefore, directly reduce the affinity between channel and insecticide. This idea is supported by the work done with ATX-II, where despite the inhibition of fast inactivation from open

and closed states by the anemone toxin (Warmke *et al.*, 1997), concentration-response relationships of deltamethrin and permethrin action on all *para* mutants suggest that the affinity between the channel binding site and the pyrethroid is reduced. The increased sensitivity of the rat I874M and I874C mutant channel to both deltamethrin and permethrin also suggest that the domain II S4-S5 linker probably forms part of a pyrethroid binding site.

Channel activation involves the substantial outward screw-helical movement of the rigid S4 transmembrane segments (Catterall, 1986) with the outmost arginine residues of these voltage sensors protruding 1.45nm into the aqueous phase during depolarisation (Yang and Horn, 1995; Yang *et al.*, 1997; Larsson *et al.*, 1996). It is likely that this will have an effect on the S4-S5 linker to which the S4 segment is attached. Although no significant change in the voltage dependence of activation of the M918V channel was recorded in this study, mutation of the equivalent domain II S4-S5 linker of the human skeletal muscle sodium channel, I698T, does result in a significant hyperpolarizing shift in the voltage dependence of activation of the channel (Plassart-Schiess *et al.*, 1998) adding support to the idea that the S4-S5 linker of the domain is involved in the voltage dependence of channel activation. If this site also acts as a pyrethroid binding site, as the study of pyrethroid sensitivity of rat I874M channels suggests, the interaction of the insecticide with the linker may hamper the outward movement of the S4 voltage sensor and this in turn may slow the onset of activation, another characteristic of pyrethroid modification of sodium channels (Tabarean and Narahashi, 2001).

8.5 A model to account for tail currents characteristic of pyrethroid modification.

Previous studies have proposed that mutation of the V409 residue in domain I and the L993 residue in domain II confer insensitivity to pyrethroids in pyrethroid resistant strains of German cockroach and tobacco budworm. These residues may form a high-affinity pyrethroid binding site, while residues mutated in the D1-D2 linker may form a low-affinity binding site (Lee and Soderlund, 2001; Liu *et al.*, 2002). Should the high affinity pyrethroid binding site reside within the channel pore, as the location of the V409 and L993 residues suggest, then this could explain why the action of pyrethroids manifests primarily as a slowing in channel deactivation seen in recent tail current studies (e.g. Tan *et al.*, 2002, Vais *et al.*, in press).

Whilst mutations within S6 segments may highlight a high-affinity binding site, resistance mutations found in the S5 segment and the S4-S5 linker of domain II could together form a second binding site. This is supported by the reduction in the Hill coefficient from >2 to <1 of the concentration response relationship of deltamethrin action on T929M and T929V channels. As discussed in chapter 6, pyrethroids may bind in accordance with the 'zipper' theory of pyrethroid binding, which suggests that binding of one part of the insecticide to the substrate is dependent on the previous binding of another part of the insecticide to the substrate (Vijverberg *et al*, 1983). Removal of the threonine residue at position 929 may prevent the complete binding of the deltamethrin molecule, hence the apparent destruction of a pyrethroid binding site as suggested by the Hill coefficients and the large reduction in affinity indicated by Kd values of the T929M and T929V channels when compared with the *para* wild type channel. The effect on the Hill coefficient and Kd value of M918V channels in *para*

channels is not as drastic as that of the 929 mutations. However, this may be because the mutation is a conservative one, with both methionine and valine containing hydrophobic side chains. Therefore, a weak interaction may still occur between M918V and deltamethrin

A model that could perhaps explain the current profiles seen during a depolarising pulse and following repolarisation in the presence and absence of pyrethroids is shown in figure 8.1. In the absence of pyrethroids, *para* wild type channels activate and inactivate normally during a short depolarisation and immediately deactivate following repolarisation. In the presence of pyrethroids, one pyrethroid molecule binds to a site, possibly around the S4-S5 linker, which slows both activation and inactivation, while a second pyrethroid molecule binds to a putative high affinity site located within the pore. On repolarisation the inactivated channels deinactivate (i.e. recover from the inactive state) before channel deactivation (channel closure) has occurred because pyrethroid bound to the high affinity site within the pore forces the channel to remain open. Therefore, channels reopen from the inactive state and conduct current and this manifests as large hooked tail currents on repolarisation.

8.5 Future work

Pyrethroids are used in a variety of settings both domestic and agricultural. Recent surveys of humans exposed to high levels of the insecticide suggest that pyrethroids could be responsible for a large number of occupational pesticide illnesses (Das *et al.*, 2001). The work reported here suggests that at least part of the mammalian sodium channel insensitivity to pyrethroids may result from the absence of a methionine or

Figure 8.1. Model to account of the tail current profile of voltage-gated sodium channels treated with pyrethroid during a depolarisation and a subsequent repolarisation. The voltage protocol is shown above the current profile in the presence (—) and absence (—)of pyrethroid. A schematic diagram of channel conformations in response to these changes in voltage in the presence and absence of the insecticide, is shown at the top.
In the absence of pyrethroids, *para* wild type channels activate and inactivate normally during a short depolarisation and immediately deactivate following repolarisation. In the presence of pyrethroids, one pyrethroid molecule binds to a site, possibly around the S4-S5 linker, which slows both activation and inactivation, while a second pyrethroid molecule binds to a putative high affinity site located within the pore. On repolarisation the inactivated channels deinactivate (i.e. recover from the inactive state) before channel deactivation (channel closure) has occurred because pyrethroid bound to the high affinity site within the pore forces the channel to remain open. Therefore, channels reopen from the inactive state and conduct current and this manifests as large hooked tail currents on repolarisation.

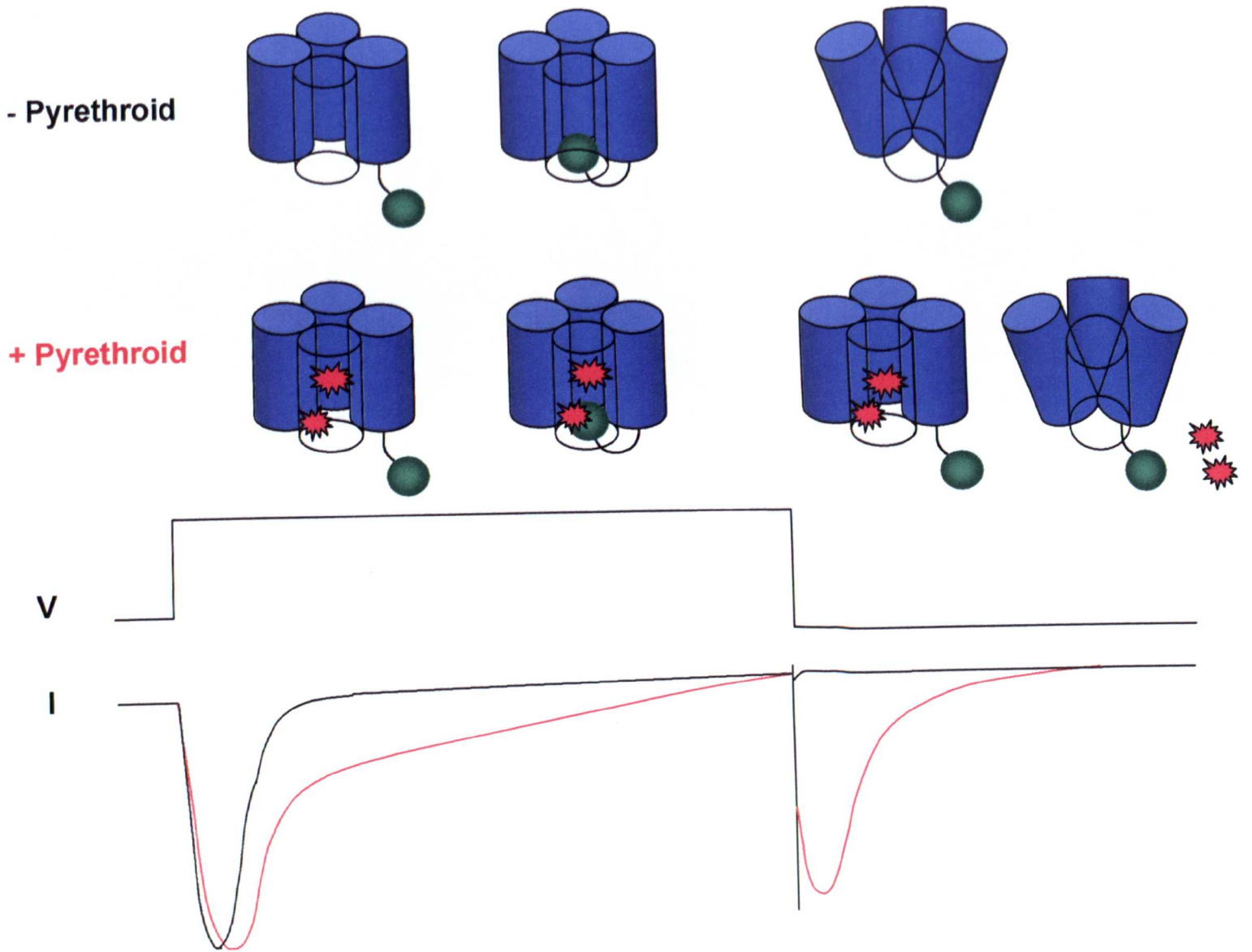
- Pyrethroid
+ Pyrethroid
V
I

cysteine at position 874. It would therefore be interesting to see if human sensitivity to pyrethroids involves mutations at this site, perhaps by using the same SSCP screening technique used to detect super-kdr in *Musca domestica* samples, described in Chapter 7. While the oocyte expression system together with resistance-associated mutations remains a useful tool for pyrethroid binding studies, the exact nature and location of pyrethroid binding will be greatly advanced with ligand binding studies and these will aid the precise design of new compounds effective against already resistant pest species.

APPENDICIES AND REFERENCES

Appendix One. Primers used in Site Directed Mutagenesis

M918V *para* mutant channel

M918Vf 5'TTACTCATTTCGATTGTGGGACGCACCATGGGCGCT3'

M918Vr 5'CCATGGTGCGTCCCATAATCGAAATGAGTAAATTAAGTG3'

T929M *para* mutant channel

T929Mf 5'GCTTTGGGTAATCTGATGTTTGTACTTTGCATTATCATCTTC3'

T929Mr 5'GATGATAATGCAAAGTACAAACATCAGATTACCCAAAGCGCCCA3'

T929V *para* mutant channel

T929Vf 5' GCTTTGGGTAATCTGGTATTTGTACTTTGCATTATCATCTTC3'

T929Vr 5'GATGATAATGCAAAGTACAAATACCAGATTACCCAAAGCGCCCA3'

I874M rat IIA mutant channel

I874Mf 5'ATGCTCATTAAGATCATGGGCAACTCGGTGGGTG3'

I874Mr 5'ACCGAGTTGCCCATGATCTTAATGAGCATGTTCA3'

I874C rat IIA mutant channel

I874Cf 5'ATGCTCATTAAGATCTGC GGCAACTCGGTGGGTG3'

I874Cr 5'ACCGAGTTGCCGCAGATCTTAATGAGCATGTTCA3'

I874H rat IIA mutant channel

I874Hf 5'ATGCTCATTAAGATCCACGGCAACTCGGTGGGTG3'

I874Hr 5'ACCGAGTTGCCGTGGATCTTAATGAGCATGTTCA3'

I874D rat IIA mutant channel

I874Df 5'ATGCTCATTAAGATCGACGGCAACTCGGTGGGTG3'

I874Dr 5'ACCGAGTTGCCGTCGATCTTAATGAGCATGTTCA3'

Appendix Two. Restriction endonucleases for linearisation of plasmid DNA.

Construct	Restriction Endonuclease
Para wild type channel	NotI
M918V para mutant channel	NotI
T929M para mutant channel	NotI
T929V para mutant channel	NotI
Rat wild type channel	ClaI
I874M rat IIA mutant channel	ClaI
I874C rat IIA mutant channel	ClaI
I874H rat IIA mutant channel	ClaI
I874D rat IIA mutant channel	ClaI
Tip E	NotI
β1	XbaI

Appendix Three. Primers for PCR amplification of *Musca domestica* gDNA

MW97	5'ATAGTTCTTTCCGAAAAGTTGC3'
MW99	5'CGGCCACGTCAACTTACCAC3'
MW100	5'GGTATCATTGTCGGCAGTCGG3'
MW101	5'ACCACAAGGATCGCTTCAAGG3'
MW102	5'GATCGCTTCAAGGACCATGA3'
MW103	5'GCTTCGTGTATTCAAA(CT)TGGC3'
MW104	5'TGGCAAAATCATGGCCCAC3'

References

ABBASSY, M.A., ELDERFRAWI, M.E. and ELCERFRAWI, A.T. (1982). Allethrin interactions with the nicotinic acetylcholine receptor channel. *Life Sci.* 31:1547-1552.

AGNEW, W.S., MOORE, A.C., LEVINSON, S.R. and RAFTERY, M.A. (1980). Identification of a large molecular weight peptide associated with a tetrodotoxin binding protein from the electroplax of *Electrophorus electricus*. *Biochem. Biophys. Res. Commun.* 92:860-866.

AKOPIAN, A.N., SIVILOTTI, L. and WOOD, J.N. (1996). A tetrodotoxin-resistant voltage-gated sodium channel expressed by sensory neurons. *Nature* 379:257-62.

ALEKOV, A.K., PETER, W.G., MITROVIC, N., LEHMANN-HORN, F. and LERCHE, H. (2001). Two mutations in the IV/S4-S5 segment of the human skeletal muscle Na+ channel disrupt fast and enhance slow inactivation. *Neurosci. Lett.* 306:173-176.

ANTHONY, N.M., BROWN, J.K., MARKHAM, P.G. and FFRENCH-CONSTANT, R.H. (1995). Molecular Analysis of Cyclodiene Resistance-Associated Mutations among Populations of the Sweet-Potato Whitefly *Bemisia-Tabaci*. *Pest. Biochem. Physiol.* 51:220-228.

ARMSTRONG, C.M. (1971). Interaction of tetraethylammonium ion derivatives with the potassium channels of giant axons. *J. Gen. Physiol.* 58(4):413-37.

ARMSTRONG, C.M. Sodium channels and gating currents. (1981). *Physiol. Rev.* 61:644-83.

ARMSTRONG, C.M. and BEZANILLA, F. (1977). Inactivation of the sodium channel. II. Gating current experiments. *J. Gen. Physiol.* 70:567-90.

ARONSTEIN, K., ODE, P. and FFRENCH-CONSTANT, R.H. (1995). PCR Based Monitoring of Specific *Drosophila* (Diptera, Drosophilidae) Cyclodiene Resistance Alleles in the Presence and Absence of Selection. *Bull. Entomol. Res.* 85:5-9.

BARNARD, E.A., MILEDI, R. and SUMIKAWA, K. (1982). Translocation of exogenous messenger RNA coding for nicotinic acetylcholine receptors produces functional receptors in *Xenopus* oocytes. *Proc. R. Soc. Lond. B Biol. Sci.* 215:241-246.

BEDDIE, D.G., FARNHAM, A.W. and KHAMBAY, B.P.S. (1996). The pyrethrins and related compounds .41. Structure-activity relationships in non-ester pyrethroids against resistant strains of housefly (*Musca domestica* L). *Pestic. Sci.* 48:175-178.

BENDAHHOU, S., CUMMINS, T.R., KULA, R.W., FU, Y.H. and PTACEK, L.J. (2002). Impairment of slow inactivation as a common mechanism for periodic paralysis in DIIS4-S5. *Neurology* 58:1266-1272.

BENDAHHOU, S., CUMMINS, T.R., TAWIL, R., WAXMAN, S.G. and PTACEK, L.J. (1999). Activation and inactivation of the voltage-gated sodium channel: Role of segment S5 revealed by a novel hyperkalaemic periodic paralysis mutation. *J. Neurosci.* 19:4762-4771.

BENESKI, D.A. and CATTERALL, W.A. (1980). Covalent labelling of protein components of the sodium channel with a photoactive derivative of scorpion toxin. *Proc. Natl. Acad. Sci. U S A* 77(1):639-43.

BENITAH, J.P., CHEN, Z., BALSER, J.R., TOMASELLI, G.F. and MARBAN, E. (1999). Molecular dynamics of the sodium channel pore vary with gating: interactions between P-segment motions and inactivation. *J. Neurosci.* 19(5):1577-85.

BLOOMQUIST, J.R. and SODERLUND, D.M. (1988). Pyrethroid and DDT insecticides modify alkaloid-dependent sodium channel activation and its enhancement by sea anemone toxin. *Mol. Pharmacol.* 33:543-50.

BORLAUG, N.E. (2000). Ending world hunger. The promise of biotechnology and the threat of antiscience zealotry. *Plant Physiol.* 124:487-490.

BRADBURY, S.P. and COATS, J.R. (1989). Comparative toxicology of the pyrethroid insecticides. *Rev. Environ. Contam. Toxicol.* 108:133-77.

BUSVINE, J.R. (1951). Mechanisms of resistance to insecticides in houseflies. *Nature* 168:193-195.

CAMPANHOLA, C., MCCUTCHEN, B.F., BAEHRECKE, E.H. and PLAPP, F.W. (1991). Biological constraints associated with resistance to pyrethroids in the tobacco budworm (Lepidoptera, noctuidae). *J. Ecol. Entomol.* 84:1404-1411.

CANNON, S.C. and STRITTMATTER, S.M. (1993). Functional Expression of Sodium-Channel Mutations Identified in Families with Periodic Paralysis. *Neuron* 10:317-326.

CASIDA, J.E. and QUISTAD, G.B. (1998). Golden age of insecticide research: past, present, or future? *Annu. Rev. Entomol.* 43:1-16.

CATTERALL, W.A. (1986). Molecular-Properties of Voltage-Sensitive Sodium-Channels. *Annu. Rev. Biochem.* 55:953-985.

CATTERALL, W.A. (2000). From ionic currents to molecular mechanisms: The structure and function of voltage-gated sodium channels. *Neuron* 26:13-25.

CATTERALL, W.A. (2001). A 3D view of sodium channels. *Nature* 409:988-9.

CHA, A., RUBEN, P.C., GEORGE, A.L., JR., FUJIMOTO, E. and BEZANILLA, F. (1999). Voltage sensors in domains III and IV, but not I and II, are immobilized by Na^+ channel fast inactivation. *Neuron* 22(1):73-87.

CHAPMAN, P.A. and MORGAN, C.P. (1992). Insecticide Resistance in *Musca-Domestica* L from Eastern England. *Pestic. Sci.* 36:35-45.

CHAPMAN, P.A., LEARMOUNT, J., MORRIS, A.W. and MCGREEVY, P.B. (1993). The current status of insecticide resistance in *Musca domestica* in England and Wales and the implications for housefly control in intensive animal units. *Pestic. Sci.* 39(3): 225-235.

CHIAMVIMONVAT, N., PEREZ-GARCIA, M.T., RANJAN, R., MARBAN, E. and TOMASELLI, G.F. (1996a). Depth asymmetries of the pore-lining segments of the Na+ channel revealed by cysteine mutagenesis. *Neuron* (5):1037-47.

CHIAMVIMONVAT, N., PEREZ-GARCIA, M.T., TOMASELLI, G.F. and MARBAN, E. (1996b). Control of ion flux and selectivity by negatively charged residues in the outer mouth of rat sodium channels. *J. Physiol.* 491 (Pt 1):51-9.

CHINN, K. and NARAHASHI, T. (1986). Stabilization of sodium channel states by deltamethrin in mouse neuroblastoma cells. *J. Physiol.* 380:191-207.

CLARK, J.M., LEE, S.H., KIM, H.J., YOON, K.S. and ZHANG, A.G. (2001). DNA-based genotyping techniques for the detection of point mutations associated with insecticide resistance in Colorado potato beetle *Leptinotarsa decemlineata. Pest. Manag. Sci.* 57:968-974.

COLE, K. S. and J. W. MOORE. (1960). Ionic current measurements in the squid giant axon membrane. *J. Gen. Physiol.* 44:123-167.

CORREA, A.M. and BEZANILLA, F. (1994). Gating of the squid sodium channel at positive potentials: II. Single channels reveal two open states. *Biophys. J.* 66:1864-78.

COUSTAU, C. and FFRENCH-CONSTANT, R. (1995). Detection of Cyclodiene Insecticide Resistance-Associated Mutations by Single-Stranded Conformational Polymorphism Analysis. *Pestic. Sci.* 43:267-271.

CUMMINS, T.R. and SIGWORTH, F.J. (1996). Impaired slow inactivation in mutant sodium channels. *Biophys. J.* 71:227-236.

CUMMINS, T.R., ZHOU, J.Y., SIGWORTH, F.J., UKOMADU, C., STEPHAN, M., PTACEK, L.J. and AGNEW, W.S. (1993). Functional Consequences of a Na+ Channel Mutation Causing Hyperkalemic Periodic Paralysis. *Neuron* 10:667-678.

DAS, R., STEEG, A., BARON, S., BECKMAN, J. and HARRISON, R. (2001). Pesticide-related illnesses among migrant farm workers in the United States. *Int. J. Occup. Environ. Health* 7:303-312.

DENHOLM, I. and JESPERSEN, J.B. (1998). Insecticide resistance management in Europe: recent developments and prospects. *Pestic. Sci.* 52:193-195.

DENHOLM, I. and ROWLAND, M.W. (1992). Tactics for Managing Pesticide Resistance in Arthropods - Theory and Practice. *Annu. Rev. Entomol.* 37:91-112.

DEVAUD, L.L. and MURRAY, T.F. (1988). Involvement of peripheral-type benzodiazepine receptors in the proconvulsant actions of pyrethroid insecticides. *J. Pharmacol. Exp. Ther.* 247:14-22.

DOHERTY, J.D., LAUTER, C.J. and SALEM, N., JR. (1986). Synaptic effects of the synthetic pyrethroid resmethrin in rat brain in vitro. *Comp. Biochem. Physiol. C* 84:373-379.

DONG, K. (1997). A single amino acid change in the para sodium channel protein is associated with knockdown-resistance (kdr) to pyrethroid insecticides in German cockroach. *Insect Biochem. Mol. Biol.* 27:93-100.

DOYLE, D.A., MORAIS CABRAL, J., PFUETZNER, R.A., KUO, A., GULBIS, J.M., COHEN, S.L., CHAIT, B.T. and MACKINNON, R. (1998). The structure of the potassium channel: molecular basis of K+ conduction and selectivity. *Science* 280:69-77.

DYSON, T. (1999). World food trends and prospects to 2025. *Proc. Natl. Acad. Sci. U S A* 96:5929-36.

DUCE, I.R., KHAN, T.R., GREEN, A.C., THOMPSON, A.J., WARBURTON, S.P.M. and WONG, J. (1999). Calcium channels in insects. *Progress in Neuropharmacology and Neurotoxicology of Pesticides and Drugs*. pp 56-66 (Ed D.J. Beadle) Royal Society of Chemistry , Oxford, UK.

DURELL, S.R. and GUY, H.R. (1992). Atomic scale structure and functional models of voltage-gated potassium channels. *Biophys. J.* 62:238-47.

EAHOLTZ, G., SCHEUER, T. and CATTERALL, W.A. (1994). Restoration of inactivation and block of open sodium channels by an inactivation gate peptide. *Neuron* 12(5):1041-8.

ELLIOTT, M., FARNHAM, A.W., JANES, N.F., NEEDHAM, P.H., PULMAN, D.A. and STEVENSON, J.H. (1973). A photostable pyrethroid. *Nature* 246:169-70.

ELLIOTT, M., FARNHAM, A.W., JANES, N.F., NEEDHAM, P.H. and PULMAN, D.A. (1974). Synthetic insecticide with a new order of activity. *Nature* 248:710-111.

ELZEN, G.W., MARTIN, S.H., LEONARD, B.R. and GRAVES, J.B. (1994). Inheritance, Stability, and Reversion of Insecticide Resistance in Tobacco Budworm (Lepidoptera, Noctuidae) Field Populations. *J. Econ. Entomol.* 87:551-558.

ERTEL, E.A., BALE, T.A. and COHEN, C.J. (1994). Modification of insect neuronal Na and Ca channels by deltamethrin. *Soc. Neurosci. Abstr.* 20:717.

ETO, M. (1974). Organophosphorus Pesticides: Organic and Biological Chemistry. CRC Press, Cleveland, OH.

FARNHAM, A.W. (1977). Genetics of resistance of houseflies (*Musca domestica*) to pyrethroids. I. Knockdown resistance. *Pesticide. Sci.* 8:631-636.

FARNHAM, A.W., MURRAY, A.W.A., SAWICKI, R.M., DENHOLM, I. and WHITE, J.C. (1987). Characterization of the Structure Activity Relationship of Kdr and 2 Variants of Super-Kdr to Pyrethroids in the Housefly (*Musca-Domestica* L). *Pestic. Sci.* 19:209-220.

FARNHAM, A.W. and KHAMBAY, B.P.S. (1995). The Pyrethrins and Related-Compounds .39. Structure-Activity- Relationships of Pyrethroidal Esters with Cyclic Side-Chains in the Alcohol Component against Resistant Strains of Housefly (*Musca-Domestica*). *Pestic. Sci.* 44:269-275.

FEATHERSTONE, D.E., RICHMOND, J.E. and RUBEN, P.C. (1996). Interaction between fast and slow inactivation in Skml sodium channels. *Biophys. J.* 71:3098-3109.

FENG, G., DEAK, P., CHOPRA, M. and HALL, L.M. (1995). Cloning and functional analysis of TipE, a novel membrane protein that enhances *Drosophila para* sodium channel function. *Cell* 82(6):1001-11.

FFRENCH-CONSTANT, R.H., ROCHELEAU, T.A., STEICHEN, J.C., and CHALMERS, A.E. (1993). A Point Mutation in a *Drosophila* GABA Receptor Confers Insecticide Resistance. *Nature* 363:449-451.

FOSTER, S.P., WOODCOCK, C.M., WILLIAMSON, M.S., DEVONSHIRE, A.L., DENHOLM, I. and THOMPSON, R. (1999). Reduced alarm response by peach-potato aphids, *Myzus persicae* (Hemiptera : Aphididae), with knock-down resistance to insecticides (kdr) may impose a fitness cost through increased vulnerability to natural enemies. *Bull. Entomol. Res.* 89:133-138.

GEORGHIOU, G.P. (1990). Overview of Insecticide Resistance. Acs Symposium Series 421:18-41.

GINSBURG, K.S. and NARAHASHI, T. (1993). Differential sensitivity of tetrodotoxin-sensitive and tetrodotoxin-resistant sodium channels to the insecticide allethrin in rat dorsal root ganglion neurons. *Brain. Res.* 627(2):239-48.

GOLDIN, A.L. (1991). Expression of ion channels by injection of mRNA in to Xenopus oocytes. *Methods Cell Biol.* 36:487-509.

GOLDIN, A.L. (1999). Diversity of mammalian voltage-gated sodium channels. *Ann. N Y Acad. Sci.* 868:38-50.

GOLDIN, A.L., SNUTCH, T., LUBBERT, H., DOWSETT, A., MARSHALL, J., AULD, V., DOWNEY, W., FRITZ, L.C., LESTER, H.A., DUNN, R. and ET AL. (1986). Messenger RNA coding for only the alpha subunit of the rat brain Na channel is sufficient for expression of functional channels in *Xenopus* oocytes. *Proc. Natl. Acad. Sci. U S A* 83(19):7503-7.

GRAY, A.J. (1985). Pyrethroid structure-toxicity relationships in mammals. *Neurotoxicology* 6(2):127-37.

GROOME, J., FUJIMOTO, E., WALTER, L. and RUBEN, P. (2002). Outer and central charged residues in DIVS4 of skeletal muscle sodium channels have differing roles in deactivation. *Biophys. J.* 82(3):1293-307.

GUERRERO, F.D., JAMROZ, R.C., KAMMLAH, D. and KUNZ, S.E. (1997). Toxicological and molecular characterization of pyrethroid-resistant horn flies, Haematobia irritans: identification of kdr and super-kdr point mutations. *Insect Biochem. Mol. Biol.* 27(8-9):745-55.

GUSTAFSON, T.A., CLEVINGER, E.C., O'NEILL, T.J., YAROWSKY, P.J. and KRUEGER, B.K. (1993). Mutually exclusive exon splicing of type III brain sodium channel alpha subunit RNA generates developmentally regulated isoforms in rat brain. *J. Biol. Chem.* 268(25):18648-53.

GUY, H.R. and SEETHARAMULU, P. (1986). Molecular-Model of the Action-Potential Sodium-Channel. *Proc. Natl. Acad. Sci. U. S. A.* 83:508-512.

HAUBRUGE, E. and ARNAUD, L. (2001). Fitness consequences of malathion-specific resistance in red flour beetle (Coleoptera : Tenebrionidae) and selection for resistance in the absence of malathion. *J. Econ. Entomol.* 94:552-557.

HAYWARD, L.J., BROWN, R.H. and CANNON, S.C. (1997). Slow inactivation differs among mutant Na channels associated with myotonia and periodic paralysis. *Biophys. J.* 72:1204-1219.

HE, H., CHEN, A.C., DAVEY, R.B., IVIE, G.W., WAGNER, G.G. and GEORGE, J.E. (1999). Sequence analysis of the knockdown resistance-homologous region of the para-type sodium channel gene from pyrethroid-resistant *Boophilus microplus* (Acari: Ixodidae). *J. Med. Entomol.* 36(5):539-43.

HEAD, D.J., MCCAFFERY, A.R. and CALLAGHAN, A. (1998). Novel mutations in the para-homologous sodium channel gene associated with phenotypic expression of nerve insensitivity resistance to pyrethroids in *Heliothine lepidoptera. Insect Mol. Biol.* 7:191-196.

HEINEMANN, S.H., TERLAU, H., STUHMER, W., IMOTO, K. and NUMA, S. (1992). Calcium channel characteristics conferred on the sodium channel by single mutations. *Nature* 356(6368):441-3.

HENSEL, C.H., XIANG, R.H., SAKAGUCHI, A.Y. and NAYLOR, S.L. (1991). Use of the single strand conformation polymorphism technique and PCR to detect p53 gene mutations in small cell lung cancer. *Oncogene* 6:1067-1071.

HILBER, K., SANDTNER, W., KUDLACEK, O., GLAASER, I.W., WEISZ, E., KYLE, J.W., FRENCH, R.J., FOZZARD, H.A., DUDLEY, S.C. and TODT, H. (2001). The selectivity filter of the voltage-gated sodium channel is involved in channel activation. *J. Biol. Chem.* 276(30):27831-9.

HILBER, K., SANDTNER, W., KUDLACEK, O., SCHREINER, B., GLAASER, I., SCHUETZ, W., FOZZARD, H.A., DUDLEY, S.C. and TODT, H. (2002). Interaction between fast and ultra-slow inactivation in the voltage-gated sodium channel: Does the inactivation gate stabilize the channel structure? *J. Biol. Chem.* 277(40):37105-37115.

HILLE, B. (1984). Ionic Channels of Excitable Membranes, First Edition. Sinauer Associates, Inc. Sunderland MA.

HIRSCHBERG, B., ROVNER, A., LIEBERMAN, M. and PATLAK, J. (1995). Transfer of twelve charges is needed to open skeletal muscle Na+ channels. *J. Gen. Physiol.* 106(6):1053-68.

HODGES, D.D., LEE, D., PRESTON, C.F., BOSWELL, K., HALL, L.M. and O'DOWD, D.K. (2002). tipE regulates Na+-dependent repetitive firing in *Drosophila* neurons. *Mol. Cell Neurosci.* 9(3):402-16.

HODGKIN, A.L. (1975). The optimum density of sodium channels in an unmyelinated nerve. *Phil. Trans. Roy. Soc. Lond.* 270:297-300.

HODGKIN, A.L. and HUXLEY A.F., (1952). A quantitative description of membrane current and its application to conduction and excitation in nerve. *J. Physiol.* 117:500-544.

HOLLOWAY, S.F., SALGADO, V.L., WU, C.H. and NARAHASHI, T. (1989). Kinetic properties of single sodium channels modified by fenvalerate in mouse neuroblastoma cells. *Pflugers Arch.* 414(6):613-21.

HONG, C.S. and GANETZKY, B. (1994). Spatial and temporal expression patterns of two sodium channel genes in *Drosophila*. *J. Neurosci.* 14(9):5160-5169.

HORN, R. (2002). Molecular basis for function in sodium channels. In Sodium Channels and Neuronal Hyperexcitability. *Novartis. Found. Symp.* 241:21-6; discussion 26-33.

HORN, R., DING, S. and GRUBER, H.J. (2000). Immobilizing the moving parts of voltage-gated ion channels. *J. Gen Physiol.* 116(3):461-76.

ISOM, L.L., DEJONGH, K.S., PATTON, D.E., REBER, B.F.X., OFFORD, J., CHARBONNEAU, H., WALSH, K., GOLDIN, A.L. and CATTERALL, W.A. (1992). Primary Structure and Functional Expression of the Beta-1- Subunit of the Rat-Brain Sodium-Channel. *Science* 256:839-842.

ISOM, L.L., SCHEUER, T., BROWNSTEIN, A.B., RAGSDALE, D.S., MURPHY, B.J. and CATTERALL, W.A. (1995). Functional co-expression of the beta-1 and type IIA alpha-subunits of sodium-channels in a mammalian-cell line. *J. Bio. Chem.* 270:3306-3312.

JAMROZ, R.C., GUERRERO, F.D., KAMMLAH, D.M. and KUNZ, S.E. (1998). Role of the kdr and super-kdr sodium channel mutations in pyrethroid resistance: correlation of allelic frequency to resistance level in wild and laboratory populations of horn flies (Haematobia irritans). *Insect Biochem. Mol. Biol.* 28(12):1031-7.

KAUFMAN, P.E., SCOTT, J.G. and RUTZ, D.A. (2001). Monitoring insecticide resistance in houseflies (Diptera : Muscidae) from New York dairies. *Pest Manag. Sci.* 57:514-521.

KELLENBERGER, S., SCHEUER, T. and CATTERALL, W.A. (1996). Movement of the sodium channel inactivation gate during inactivation. *J. Biol. Chem.* 271:30971-30979.

KELLENBERGER, S., WEST, J.W., SCHEUER, T. and CATTERALL, W.A. (1997a) Molecular analysis of the putative inactivation particle in the inactivation gate of brain type IIA Na+ channels. *J. Gen. Physiol.* 109(5):589-605.

KELLENBERGER, S., WEST, J.W., CATTERALL, W.A. and SCHEUER, T. (1997b) Molecular analysis of potential hinge residues in the inactivation gate of brain type IIA Na+ channels. *J. Gen. Physiol.* 109(5):607-17.

KEYNES, R.D. (1994). The kinetics of the voltage-gated sodium channel. *Q. Rev. Biophys.* 27:339-434.

KEYNES, R.D. (2002). Studies of multimodal gating of the sodium channel. In Sodium Channels and Neuronal Hyperexcitability. *Novartis. Found. Symp.* pp. 5-20.

KEYNES, R. D. and ELINDER, F. (1999). The screw-helical voltage gating of ion channels. *Proc. R. Soc. Lond. Ser. B-Biol. Sci.* 266:843-852.

KONTIS, K.J., ROUNAGHI, A. and GOLDIN, A.L. (1997). Sodium channel activation gating is affected by substitutions of voltage sensor positive charges in all four domains. *J. Gen. Physiol.* 110(4):391-401.

KRISTENSEN, M., SPENCER, A.G. and JESPERSEN, J.B. (2001). The status and development of insecticide resistance in Danish populations of the housefly *Musca domestica L. Pest Manag. Sci.* 57:82-89.

KUHN, F.J. and GREEFF, N.G. (1999). Movement of voltage sensor S4 in domain 4 is tightly coupled to sodium channel fast inactivation and gating charge immobilization. *J. Gen Physiol.* 114(2):167-83.

KUHR, R.J. and DOROUGH, H.W. (1976). Carbamate Insecticides: Chemistry, Biochemistry and Toxicology. CRC Press, Cleveland, OH.

KUO, C.C. and BEAN, B.P. (1994). Na+ channels must deactivate to recover from inactivation. *Neuron* 12(4):819-29.

LARSSON, H.P., BAKER, O.S., DHILLON, D.S. and ISACOFF, E.Y. (1996). Transmembrane movement of the Shaker K+ channel S4. *Neuron* 16:387-397.

LAWRENCE, L.J. and CASIDA, J.E. (1993). Stereospecific action of pyrethroid insecticides on the gamma-aminobutyric acid receptor ionophore complex. *Science* 221:1399-1401.

LEE, D., PARK, Y., BROWN, T.M. and ADAMS, M.E. (1999a). Altered properties of neuronal sodium channels associated with genetic resistance to pyrethroids. *Mol. Pharmacol.* 55:584-593.

LEE, S.H., SMITH, T.J., INGLES, P.J. and SODERLUND, D.M. (2000). Cloning and functional characterization of a putative sodium channel auxiliary subunit gene from the housefly (*Musca domestica). Insect Biochem. Mol. Biol.* 30(6):479-87.

LEE, S.H., SMITH, T.J., KNIPPLE, D.C. and SODERLUND, D.M. (1999b). Mutations in the house fly Vssc1 sodium channel gene associated with super-kdr resistance abolish the pyrethroid sensitivity of Vssc1/tipE sodium channels expressed in *Xenopus* oocytes. *Insect Biochem. Mol. Biol.* 29:185-194.

LEE, S.H. and SODERLUND, D.M. (2001). The V410M mutation associated with pyrethroid resistance in *Heliothis virescens* reduces the pyrethroid sensitivity of house fly sodium channels expressed in *Xenopus* oocytes. *Insect Biochem. Mol. Biol.* 31:19-29.

LEE, S.H., YOON, K.S., WILLIAMSON, M.S., GOODSON, S.J., TAKANO-LEE, M., EDMAN, J.D., DEVONSHIRE, A.L. and CLARK, J.M. (2000). Molecular analysis of kdr-like resistance in permethrin- resistant strains of head lice, *Pediculus capitis. Pest. Biochem. Physiol.* 66:130-143.

LEHMANN-HORN, F. and JURKAT-ROTT, K. (1999). Voltage-gated ion channels and hereditary disease. *Physiol. Rev.* 79:1317-1372.

LESSA, E.P. and APPLEBAUM, G. (1993). Screening Techniques for Detecting Allelic Variation in DNA- Sequences. *Mol. Ecol.* 2:119-129.

LINFORD, N.J., CANTRELL, A.R., QU, Y.S., SCHEUER, T. and CATTERALL, W.A. (1998). Interaction of batrachotoxin with the local anesthetic receptor site in transmembrane segment IVS6 of the voltage-gated sodium channel. *Proc. Natl. Acad. Sci. U. S. A.* 95:13947-13952.

LIPKIND, G.M. and FOZZARD, H.A. (2000). KcsA crystal structure as framework for a molecular model of the Na+ channel pore. *Biochemistry* 39:8161-8170.

LIU, Y., HOLMGREN, M., JURMAN, M.E. and YELLEN, G. (1997) Gated access to the pore of a voltage-dependent K+ channel. *Neuron* 19(1):175-84.

LIU, Z., TAN, J., VALLES, S.M. and DONG, K. (2002). Synergistic interaction between two cockroach sodium channel mutations and a tobacco budworm sodium channel mutation in reducing channel sensitivity to a pyrethroid insecticide. *Insect Biochem. Mol. Biol.* 32(4):397-404.

LLINAS, R.R. (1982). Calcium in synaptic transmission. *Sci. Am.* 247(4):56-65.

LOMBET, A., MOURRE, C. and LAZDUNSKI, M. (1988). Interaction of insecticides of the pyrethroid family with specific binding sites on the voltage-dependent sodium channel from mammalian brain. *Brain Res.* 459(1):44-53.

LOUGHNEY, K. and GANETZKY, B. (1989). The para locus encodes a protein homologous to the vertebrate sodium-channel. *J. Neurogenet.* 5:262-262.

LUND, A.E. and NARAHASHI, T. (1981). Modification of sodium channel kinetics by the insecticide tetramethrin in crayfish giant axons. *Neurotoxicology* 2(2):213-29.

LUND, A.E. and NARAHASHI, T. (1983). Kinetics of Sodium-Channel Modification as the Basis for the Variation in the Nerve Membrane Effects of Pyrethroids and DDT Analogs. *Pest. Biochem. Physiol.* 20:203-216.

MARTINEZ-TORRES, D., CHANDRE, F., WILLIAMSON, M.S., DARRIET, F., BERGE, J.B., DEVONSHIRE, A.L., GUILLET, P., PASTEUR, N. and PAURON, D. (1998). Molecular characterization of pyrethroid knockdown resistance (kdr) in the major malaria vector *Anopheles gambiae s.s. Insect Mol. Biol.* 7(2):179-84.

MARTINEZ-TORRES, D., FOSTER, S.P., FIELD, L.M., DEVONSHIRE, A.L. and WILLIAMSON, M.S. (1999). A sodium channel point mutation is associated with resistance to DDT and pyrethroid insecticides in the peach-potato aphid, *Myzus persicae* (Sulzer) (Hemiptera: Aphididae). *Insect Mol. Biol.* 8(3):339-46.

MASON, P.L. (1998). Selection for and against resistance to insecticides in the absence of insecticide: a case study of malathion resistance in the saw-toothed grain beetle, *Oryzaephilus surinamensis* (Coleoptera : Silvanidae). *Bull. Entomol. Res.* 88:177-188.

MCCLATCHEY, A.I., MCKENNAYASEK, D., CROS, D., WORTHEN, H.G., KUNCL, R.W., DESILVA, S.M., CORNBLATH, D.R., GUSELLA, J.F. and BROWN,

R.H. (1992). Novel Mutations in Families with Unusual and Variable Disorders of the Skeletal-Muscle Sodium-Channel. *Nature Genet.* 2:148-152.

MCEWEN, F.L. (1978). Food production – the challenge for pesticides. *Bioscience* 28:773-777.

MCLAUGHLIN, G.A. (1973). History of pyrethrum. *Pyrethrum, the Natural Insecticide.* pp.3-16 (Ed. J.E. Casida) Academic Press, New York.

MCPHEE, J.C., RAGSDALE, D.S., SCHEUER, T. and CATTERALL, W.A. (1998). A critical role for the S4-S5 intracellular loop in domain IV of the sodium channel alpha-subunit in fast inactivation. *J. Biol. Chem.* 273(2):1121-9.

MCPHEE, J.C., RAGSDALE, D.S., SCHEUER, T. and CATTERALL, W.A. (1994). A mutation in segment IVS6 disrupts fast inactivation of sodium channels. *Proc. Natl. Acad. Sci. U S A.* 91(25):12346-50.

MESSNER, D.J. and CATTERALL, W.A. (1985). The sodium channel from rat brain. Separation and characterization of subunits. *J. Biol. Chem.* 260(19):10597-604.

MITROVIC, N., GEORGE, A.L., JR. and HORN, R. (2000). Role of domain 4 in sodium channel slow inactivation. *J. Gen. Physiol.* 115(6):707-18.

MIYAZAKI, M., OHYAMA, K., DUNLAP, D.Y. and MATSUMURA, F. (1996). Cloning and sequencing of the para-type sodium channel gene from susceptible and kdr-resistant German cockroaches (*Blattella germanica*) and housefly (*Musca domestica*). *Mol. Gen. Genet.* 252(1-2):61-8.

MOORE, R.A., ERICSSON, C., KOSHLUKOVA, S.E. and HALL, L.M. (2001). The effect of the Tip E protein on *Para* sodium channel trafficking. *Biophys. J.* 80:937.

MORIN, S., WILLIAMSON, M.S., GOODSON, S.J., TABASHNIK, B.E. and DENNEHY, T.J. (2002). Mutations in the *Bemisia tabaci* sodium channel gene associated with resistance to a pyrethroid plus organophosphate mixture. *Insect Biochem. Mol. Biol. (In press).*

MOTOMURA, H. and NARAHASHI, T. (2001). Interaction of tetramethrin and deltamethrin at the single sodium channel in rat hippocampal neurons. *Neurotoxicology* 22(3):329-39.

MULLALEY, A. and TAYLOR, R. (1994). Conformational Properties of Pyrethroids. *J. Comput.-Aided Mol. Des.* 8:135-152.

MURAYAMA, K., ABBOTT, N.J., NARAHASHI, T. and SHAPIRO, B.I. (1972). Effects of Allethrin and Condylactis toxin on the kinetics of sodium conductance of crayfish axon membranes. *Comp. Gen. Pharmacol.* 3(12):391-400.

MUTERO, A., PRALAVORIO, M., BRIDE, J.M. and FOURNIER, D. (1994). Resistance-associated point mutations in insecticide-insensitive acetylcholinesterase. *Proc. Natl. Acad. Sci. U S A.* 91:5922-6.

NARAHASHI, T. (1962a). Effect of the insecticides allethrin on membrane potentials of cockroach giant axons. *J. Cell. Comp. Physiol.* 59:61-66.

NARAHASHI, T. (1962b). Nature of the negative after-potential increase by the insecticide allethrin in cockroach giant axons. *J. Cell. Comp. Physiol.* 59:67-76.

NARAHASHI, T. (1992). Nerve Membrane Na+ Channels as Targets of Insecticides. *Trends. Pharmacol. Sci.* 13:236-241.

NARAHASHI, T. (1996). Neuronal ion channels as the target sites of insecticides. *Pharmacol. Toxicol.* 79:1-14.

NARAHASHI, T. and ANDERSON, N.C. (1967). Mechanism of excitation block by the insecticide allethrin applied externally and internally to squid giant axons. *Toxicol. Appl. Pharmacol.* 10(3):529-47.

NODA, M., SHIMIZU, S., TANABE, T., TAKAI, T., KAYANO, T., IKEDA, T., TAKAHASHI, H., NAKAYAMA, H., KANAOKA, Y., MINAMINO, N. and ET AL. (1984). Primary structure of *Electrophorus electricus* sodium channel deduced from cDNA sequence. *Nature* 312:121-7.

NODA, M., SUZUKI, H., NUMA, S. and STUHMER, W. (1989). A single point mutation confers tetrodotoxin and saxitoxin insensitivity on the sodium channel II. *FEBS Lett* 259(1):213-6.

O'REILLY, J.P., WANG, S.Y. and WANG, G.K. (2000). Residue-specific effects on slow inactivation at V787 in D2-S6 of Na(v)1.4 sodium channels. *Biophys. J.* 81:2100-11.

PAP, L. and FARKAS, R. (1994). Monitoring of resistance of insecticide in-house fly (*Musca-domestica*) populations in Hungary. *Pestic. Sci.* 40(4):245-258.

PARK, Y. and TAYLOR, M.F. (1997) A novel mutation L1029H in sodium channel gene hscp associated with pyrethroid resistance for *Heliothis virescens* (Lepidoptera:Noctuidae). *Insect Biochem. Mol. Biol.* 27(1):9-13.

PARK, Y., TAYLOR, M.F.J. and FEYEREISEN, R. (1997). A valine421 to methionine mutation in IS6 of the hscp voltage-gated sodium channel associated with pyrethroid resistance in *Heliothis virescens F. Biochem. Biophys. Res. Commun.* 239:688-691.

PARK, Y.S., LEE, D.W., TAYLOR, M.F.J., HOLLOWAY, J.W., OTTEA, J.A., ADAMS, M.E. and FEYEREISEN, R. (2000). A mutation Leu1029 to His in *Heliothis virescens* F-hscp sodium channel gene associated with a nerve-insensitivity mechanism of resistance to pyrethroid insecticides. *Pest. Biochem. Physiol.* 66:1-8.

PATLAK, J. (1991). Molecular Kinetics of Voltage-Dependent Na+ Channels. *Physiol. Rev.* 71:1047-1080.

PELHATE, M., HUE, B. and SATTELLE, D.B., (1980). Actions of natural and synthetic toxins on the axonal sodium channels of the cockroach. *Insect Neurobiology and Pesticides Action. Neurotox.* 79, pp 65-73, Society of Chemical Industry, London.

PEREZ-GARCIA, M.T., CHIAMVIMONVAT, N., MARBAN, E. and TOMASELLI, G.F. (1996). Structure of the sodium channel pore revealed by serial cysteine mutagenesis. *Proc. Natl. Acad. Sci. U S A.* 93(1):300-4.

PEROZO, E., CORTES, D.M. and CUELLO, L.G. (1998). Three-dimensional architecture and gating mechanism of a K+ channel studied by EPR spectroscopy. *Nat. Struct. Biol.* 5(6):459-69.

PITTENDRIGH, B., REENAN, R., FFRENCHCONSTANT, R.H. and GANETZKY, B. (1997). Point mutations in the *Drosophila* sodium channel gene para associated with resistance to DDT and pyrethroid insecticides. *Mol. Gen. Genet.* 256:602-610.

PLASSART-SCHIESS, E., LHUILLIER, L., GEORGE, A.L., FONTAINE, B. and TABTI, N. (1998). Functional expression of the Ile693Thr Na+ channel mutation associated with paramyotonia congenita in a human cell line. *J. Physiol.-London* 507:721-727.

POSTMA, S.W. and CATTERALL, W.A. (1984). Inhibition of binding of [3H]batrachotoxinin A 20-alpha-benzoate to sodium channels by local anesthetics. *Mol. Pharmacol.* 25(2):219-27.

PTACEK, L.J., GEORGE, A.L, GRIGGS, R.C., TAWIL, R., KALLEN, R.G., BARCHI, R.L., ROBERTSON, M. and LEPPERT, M.F. (1991). Identification of a Mutation in the Gene Causing Hyperkalemic Periodic Paralysis. *Cell* 67:1021-1027.

RAY, D.E., LISTER, T. and FORSHAW, P.J. (1999). A new basis for therapy against Type-II pyrethroid poisoning. *Progress in Neuropharmacology and Neurotoxicology of Pesticides and Drugs.* pp 204-214 (Ed D.J. Beadle) Royal Society of Chemistry, Cambridge, UK.

RICHMOND, J.E., FEATHERSTONE, D.E., HARTMANN, H.A. and RUBEN, P.C. (1998). Slow inactivation in human cardiac sodium channels. *Biophys. J.* 74:2945-2952.

ROHL, C.A., BOECKMAN, F.A., BAKER, C., SCHEUER, T., CATTERALL, W.A. and KLEVIT, R.E. (1999). Solution structure of the sodium channel inactivation gate. *Biochemistry* 38(3):855-61.

ROJAS, C.V., WANG, J.Z., SCHWARTZ, L.S., HOFFMAN, E.P., POWELL, B.R. and BROWN, R.H. (1991). A Met-to-Val Mutation in the Skeletal-Muscle Na+ Channel Alpha- Subunit in Hyperkalemic Periodic Paralysis. *Nature* 354:387-389.

RUFF, R.L. (1997). Sodium channel regulation of skeletal muscle membrane excitability. *Ann. N Y Acad. Sci.* 835:64-76.

RUIGT, G.S.F. (1985). Pyrethroids. Comprehensive Insect Physiology and Biochemistry and Pharmacology. *Insect Control.* 12:184-262.

SALGADO, V.L., HERMAN, M.D. and NARAHASHI, T. (1989). Interactions of the pyrethroid fenvalerate with nerve membrane sodium channels: temperature dependence and mechanism of depolarization. *Neurotoxicology* 10(1):1-14.

SALGADO, V.L. and NARAHASHI, T. (1993). Immobilization of Sodium-Channel Gating Charge in Crayfish Giant-Axons by the Insecticide Fenvalerate. *Mol. Pharmacol.* 43:626-634.

SALKOFF, L., BUTLER, A., WEI, A., SCABARDO, N., GIFFEN, K., IFUNE, C., GOODMANN, R. and MANDEL, G. (1987). Genomic organisation and deduced amino acid sequence of a putative sodium channel gene in *Drosophila*. *Science* 237:744-749.

SANGAMESWARAN, L., FISH, L.M., KOCH, B.D., RABERT, D.K., DELGADO, S.G., ILNICKA, M., JAKEMAN, L.B., NOVAKOVIC, S., WONG, K., SZE, P., TZOUMAKA, E., STEWART, G.R., HERMAN, R.C., CHAN, H., EGLEN, R.M. and HUNTER, J.C. (1997). A novel tetrodotoxin-sensitive, voltage-gated sodium channel expressed in rat and human dorsal root ganglia. *J. Biol. Chem.* 272(23):14805-9.

SATO, C., UENO, Y., ASAI, K., TAKAHASHI, K., SATO, M., ENGEL, A. and FUJIYOSHI, Y. (2001). The voltage-sensitive sodium channel is a bell-shaped molecule with several cavities. *Nature* 409(6823):1047-51.

SAWICKI, R.M. (1978). Unusual response of DDT-resistant houseflies to carbinol analogues of DDT. *Nature* 275(5679):443-4.

SCHULER, T.H., MARTINEZ-TORRES, D., THOMPSON, A.J., DENHOLM, I., DEVONSHIRE, A.L., DUCE, I.R. and WILLIAMSON, M.S. (1998). Toxicological, electrophysiological, and molecular characterisation of knockdown resistance to pyrethroid insecticides in the diamondback moth, *Plutella xylostella* (L.). *Pest. Biochem. Physiol.* 59:169-182.

SCOTT, J.G. (1990). Pesticide resistance in arthropods (Editors R.T. Roush and B.E. Tabashnik). Chapman and Hall, New York, NY.

SCOTT, J.G., ALEFANTIS, T.G., KAUFMAN, P.E. and RUTZ, D.A. (2000). Insecticide resistance in house flies from caged-layer poultry facilities. *Pest. Manag. Sci.* 56:147-153.

SCOTT, J.G. and GEORGHIOU, G.P. (1986). Mechanisms Responsible for High-Levels of Permethrin Resistance in the Housefly. *Pestic. Sci.* 17:195-206.

SCOTT, J.G., ROUSH, R.T. and RUTZ, D.A. (1989). Resistance of houseflies to five insecticides at dairies across New York. *J. Agric. Entomol.* 6:53-64.

SHAPIRO, B.I. (1977). Effects of strychnine on the sodium conductance of the frog node of Ranvier. *J. Gen. Physiol.* 69(6):915-26.

SHEETS, M.F., KYLE, J.W., KALLEN, R.G. and HANCK, D.A. (1999). The Na channel voltage sensor associated with inactivation is localized to the external charged residues of domain IV, S4. *Biophys. J.* 77(2):747-57.

SHICHOR, I., ZLOTKIN, E., NITZA, I., CHIKASHVILI, D., STUHMER, W., GORDAN, D. and LOTAN, I. (2002). Domain 2 of the *Drosophila* para Voltage gated sodium channel confers insect properties to a rat brain channel. *J. Neurosci.* 22(11):4364-4371.

SMITH, M.R. and GOLDIN, A.L. (1997). Interaction between the sodium channel inactivation linker and domain III S4-S5. *Biophys. J.* 73(4):1885-95.

SMITH, T.J., INGLES, P.J. and SODERLUND, D.M. (1998). Actions of the pyrethroid insecticides cismethrin and cypermethrin on house fly Vssc1 sodium channels expressed in *Xenopus* oocytes. *Arch. Insect Biochem. Physiol.* 38:126-136.

SMITH, T.J., LEE, S.H., INGLES, P.J., KNIPPLE, D.C. and SODERLUND, D.M. (1997). The L1014F point mutation in the house fly Vssc1 sodium channel confers knockdown resistance to pyrethroids. *Insect Biochem. Mol. Biol.* 27(10):807-12.

SMITH, T.J. and SODERLUND, D.M. (1998). Action of the pyrethroid insecticide cypermethrin on rat brain IIA sodium channels expressed in *Xenopus* oocytes. *Neurotoxicology* 19:823-832.

SMITH, T.J. and SODERLUND, D.M. (2001). Potent actions of the pyrethroid insecticides cismethrin and cypermethrin on rat tetrodotoxin-resistant peripheral nerve (SNS/PN3) sodium channels expressed in *Xenopus* oocytes. *Pest. Biochem. Physiol.* 70:52-61.

SODERLUND, D.M. and BLOOMQUIST, J.M. (1990). Molecular mechanisms of insecticide resistance. Pesticide resistance in arthropods (Editors RT Roush, BE Tabashnikin) Chapman and Hall, New York, NY, pp 58-96.

SODERLUND, D.M., SMITH, T.J., LEE, S.H., INGLES, P.J. and KNIPPLE, D.C. (1999). Expression of cloned housefly sodium channels in *Xenopus* oocytes; action of pyrethroid and analysis of resistance-associated mutations. In progress in Neuropharmamcology and Neurotoxicology of Pesticides and Drugs, (Ed. J Beadle) Roy. Soc. Chem., Cambridge, 46-55.

SODERLUND, D.M., CLARK, J.M., SHEETS, L.P., MULLIN, L.S., PICCIRILLO, V.J., SARGENT, D., STEVENS, J.T. and WEINER, M.L. (2002). Mechanisms of pyrethroid neurotoxicity: implications for cumulative risk assessment. *Toxicology* 171:3-59.

SODERLUND, D.M., SMITH, T.J. and LEE, S.H. (2000). Differential sensitivity of sodium channel isoforms and sequence variants to pyrethroid insecticides. *Neurotoxicology* 21(1-2):127-37.

SOMMER, S.S., GROSZBACH, A.R. and BOTTEMA, C.D.K. (1992). PCR Amplification of Specific Alleles (PASA) Is a General- Method for Rapidly Detecting Known Single-Base Changes. *Biotechniques* 12:82-87.

SONG, J.H., NAGATA, K., TATEBAYASHI, H. and NARAHASHI, T. (1996). Interactions of tetramethrin, fenvalerate and DDT at the sodium channel in rat dorsal root ganglion neurons. *Brain Res.* 708:29-37.

SONG, J.H. and NARAHASHI, T. (1996a). Differential effects of the pyrethroid tetramethrin on tetrodotoxin-sensitive and tetrodotoxin-resistant single sodium channels. *Brain Res.* 712(2):258-64.

SONG, J.H. and NARAHASHI, T. (1996b). Modulation of sodium channels of rat cerebellar Purkinje neurons by the pyrethroid tetramethrin. *J. Pharmacol. Exp. Ther.* 277:445-453.

STAATZ, C.G., BLOOM, A.S. and LECH, J.J. (1982). A Pharmacological Study of Pyrethroid Neurotoxicity in Mice. *Pest. Biochem. Physiol.* 17:287-292.

STAKUS, J.H. and NARAHASHI, T. (1978). Temperature dependence of allentrhin-induced repetitive discharges in nerves. *Pest. Biochem. Physiol.* 9:225-230.

STEICHEN, J.C. and FFRENCH-CONSTANT, R.H. (1994). Amplification of Specific Cyclodiene Insecticide Resistance Alleles by the Polymerase Chain-Reaction. *Pest. Biochem. Physiol.* 48:1-7.

STUHMER, W., CONTI, F., SUZUKI, H., WANG, X.D., NODA, M., YAHAGI, N., KUBO, H. and NUMA, S. (1989). Structural parts involved in activation and inactivation of the sodium channel. *Nature* 339(6226):597-603.

SUMIKAWA, K., HOUGHTON, M., EMTAGE, J.S., RICHARDS, B.M. and BARNARD, E.A. (1981) Active multi-subunit Ach receptor assembled by translation of heterologous messenger-RNA in *Xenopus* oocytes. *Nature* 292:862-864.

SUN, Y.M., FAVRE, I., SCHILD, L. and MOCZYDLOWSKI, E. (1997). On the structural basis for size-selective permeation of organic cations through the voltage-gated sodium channel. Effect of alanine mutations at the DEKA locus on selectivity, inhibition by Ca2+ and H+, and molecular sieving. *J. Gen. Physiol.* 110(6):693-715.

TABAREAN, I.V. and NARAHASHI, T. (1998). Potent modulation of tetrodotoxin-sensitive and tetrodotoxin-resistant sodium channels by the type II pyrethroid deltamethrin. *J. Pharmacol. Exp. Ther.* 284(3):958-65.

TABAREAN, I.V. and NARAHASHI, T. (2001). Kinetics of modulation of tetrodotoxin-sensitive and tetrodotoxin-resistant sodium channels by tetramethrin and deltamethrin. *J. Pharmacol. Exp. Ther.* 299:988-997.

TADDESE, A. and BEAN, B.P. (2002). Subthreshold sodium current from rapidly inactivating sodium channels drives spontaneous firing of tuberomammillary neurons. *Neuron* 33(4):587-600.

TAKAHASHI, M.P. and CANNON, S.C. (1999). Enhanced slow inactivation by V445M: a sodium channel mutation associated with myotonia. *Biophys. J.* 76(2):861-8.

TAN, J., LIU, Z., NOMURA, Y., GOLDIN, A.L. and DONG, K. (2002). Alternative splicing of an insect sodium channel gene generates pharmacologically distinct sodium channels. *J. Neurosci.* 22:5300-9.

TAN, J., LIU, Z., TSAI, T.-D., VALLES, S.M., GOLDIN, A.L. and DONG, K. (2001). Novel para mutations abolish sodium channel sensitivity to pyrethroids. *Insect Biochem. Molec. Bio.* 32:445-454.

TAN, J., LIU, Z., TSAI, T.D., VALLES, S.M., GOLDIN, A.L. and DONG, K. (2002). Novel sodium channel gene mutations in *Blattella germanica* reduce the sensitivity of expressed channels to deltamethrin. *Insect Biochem. Mol. Biol.* 32(4):445-54.

TATEBAYASHI, H. and NARAHASHI, T. (1994). Differential mechanism of action of the pyrethroid tetramethrin on tetrodotoxin-sensitive and tetrodotoxin-resistant sodium channels. *J. Pharmacol. Exp. Ther.* 270(2):595-603.

TERLAU, H., HEINEMANN, S.H., STUHMER, W., PUSCH, M., CONTI, F., IMOTO, K. and NUMA, S. (1991). Mapping the site of block by tetrodotoxin and saxitoxin of sodium channel II. *FEBS Lett.* 293(1-2):93-6.

THE PESTICIDE MANUAL (12TH EDITION) (2000). (Editor C.D.S. Tomlin) British Crop Protection Council, Farnham, Surrey, UK.

TRAINER, V.L., BROWN, G.B. and CATTERALL W.A. (1996). Site of covalent labeling by a photoreactive batrachotoxin derivative near transmembrane segment IS6 of the sodium channel alpha subunit. *J. Biol. Chem.* 271:11261-7.

TRAINER, V.L., MCPHEE, J.C., BOUTELET-BOCHAN, H., BAKER, C., SCHEUER, T., BABIN, D., DEMOUTE, J.P., GUEDIN, D. and CATTERALL, W.A. (1997). High affinity binding of pyrethroids to the alpha subunit of brain sodium channels. *Mol. Pharmacol.* 51(4):651-7.

TSUSHIMA, R.G., LI, R.A. and BACKX, P.H. (1997a). Altered ionic selectivity of the sodium channel revealed by cysteine mutations within the pore. *J. Gen. Physiol.* 109(4):463-75.

TSUSHIMA, R.G., LI, R.A. and BACKX, P.H. (1997b). P-loop flexibility in Na+ channel pores revealed by single- and double-cysteine replacements. *J. Gen. Physiol.* 110(1):59-72.

VAIS, H., WILLIAMSON, M.S., DEVONSHIRE, A.L., WARMKE, J.W., USHERWOOD, P.N.R. and COHEN, C.J. (1998). Knock-down resistance mutations confer insensitivity to deltamethrin on *Drosophila para* sodium channels. *Biophys. J.* 74:A149.

VAIS, H., ATKINSON, S., ELDURSI, N., DEVONSHIRE, A.L., WILLIAMSON, M.S. and USHERWOOD, P.N.R. (2000). A single amino acid change makes a rat neuronal sodium channel highly sensitive to pyrethroid insecticides. *FEBS Lett* 470(2):135-8.

VAIS, H., WILLIAMSON, M.S., DEVONSHIRE, A.L. and USHERWOOD, P.N.R (2001). The molecular interactions of pyrethroid insecticides with insect and mammalian sodium channels. *Pest Manag. Sci.* 57(10):877-88.

VAIS, H., WILLIAMSON, M.S., GOODSON, S.J., DEVONSHIRE, A.L., WARMKE, J.W., USHERWOOD, P.N.R. and COHEN, C.J. (2000). Activation of *Drosophila*

sodium channels promotes modification by deltamethrin. Reductions in affinity caused by knock-down resistance mutations. *J. Gen. Physiol.* 115(3):305-18.

VAIS, H., WILLIAMSON, M.S., HICK, C.A., ELDURSI, N., DEVONSHIRE, A.L. and USHERWOOD, P.N.R. (1997). Functional analysis of a rat sodium channel carrying a mutation for insect knock-down resistance (kdr) to pyrethroids. *FEBS Lett* 413(2):327-32.

VASSILEV, P., SCHEUER, T. and CATTERALL, W.A. (1989). Inhibition of inactivation of single sodium channels by a site-directed antibody. *Proc. Natl. Acad. Sci. U S A* 86(20):8147-51.

VAUGHN, D.E. and BJORKMAN, P.J. (1996). The (Greek) key to structures of neural adhesion molecules. *Neuron* 16:261-273.

VERSCHOYLE, R.D. and ALDRIDGE, W.N. (1980). Structure-activity relationships of some pyrethroids in rats. *Arch. Toxicol.* 45(4):325-9.

VIJVERBERG, H.P. and VAN DEN BERCKEN, J. (1982). Annotation. Action of pyrethroid insecticides on the vertebrate nervous system. *Neuropathol. Appl. Neurobiol.* 8(6):421-40.

VIJVERBERG, H.P.M., VANDERZALM, J.M., VANKLEEF, R. and VANDENBERCKEN, J. (1983). Temperature-Dependent and Structure-Dependent

Interaction of Pyrethroids with the Sodium-Channels in Frog Node of Ranvier. *Biochimica Et Biophysica Acta* 728:73-82.

WAGNER, S., LERCHE, H., MITROVIC, N., HEINE, R., GEORGE, A.L. and LEHMANNHORN, F. (1997). A novel sodium channel mutation causing a hyperkalemic paralytic and paramyotonic syndrome with variable clinical expressivity. *Neurology* 49:1018-1025.

WANG, C.M., NARAHASHI, T. and SCUKA, M. (1972). Mechanism of negative temperature coefficient of nerve blocking action of allethrin. *J. Pharmacol. Exp. Ther.* 82(3):442-53.

WANG, S.Y., BARILE, M. and WANG, G.K. (2001). A phenylalanine residue at segment D3-S6 in Nav1.4 voltage- gated Na+ channels is critical for pyrethroid action. *Mol. Pharmacol.* 60:620-628.

WANG, S.Y., and WANG, G.K. (1997). A mutation in segment I-S6 alters slow inactivation of sodium channels. *Biophys. J.* 72(4):1633-40.

WANG, S.Y. and WANG, G.K. (1999). Batrachotoxin-resistant Na+ channels derived from point mutations in transmembrane segment D4-S6. *Biophys. J.* 76:3141-3149.

WARMKE, J.W., REENAN, R.A.G., WANG, P.Y., QIAN, S., ARENA, J.P., WANG, J.X., WUNDERLER, D., LIU, K., KACZOROWSKI, G.J., VANDERPLOEG, L.H.T.,

GANETZKY, B. and COHEN, C.J. (1997). Functional expression *of Drosophila para* sodium channels - Modulation by the membrane protein TipE and toxin pharmacology. *J. Gen. Physiol.* 110:119-133.

WEST, J.W., PATTON, D.E., SCHEUER, T., WANG, Y., GOLDIN, A.L. and CATTERALL, W.A. (1992). A cluster of hydrophobic amino acid residues required for fast Na(+)-channel inactivation. *Proc. Natl. Acad. Sci. U S A* 89(22):10910-4.

WILLIAMSON, M.S., DENHOLM, I., BELL, C.A. and DEVONSHIRE, A.L. (1993). Knockdown resistance (kdr) to DDT and pyrethroid insecticides maps to a sodium channel gene locus in the housefly (*Musca domestica*). *Mol. Gen.Genet.* 240(1):17-22.

WILLIAMSON, M.S., MARTINEZ-TORRES, D., HICK, C.A. and DEVONSHIRE, A.L. (1996). Identification of mutations in the housefly para-type sodium channel gene associated with knockdown resistance (kdr) to pyrethroid insecticides. *Mol. Gen. Genet.* 252(1-2):51-60.

WU, C.F. and GANETZKY, B. (1980). Genetic alteration of nerve membrane excitability in temperature-sensitive paralytic mutants of *Drosophila melanogaster*. *Nature* 286:814-816

XIAO, Z.C., RAGSDALE, D.S., MALHOTRA, J.D., MATTEI, L.N., BRAUN, P.E., SCHACHNER, M. and ISOM, L.L. (1999). Tenascin-R is a functional modulator of sodium channel beta subunits. *J. Biol. Chem.* 274:26511-26517.

YAMAMOTO, D., QUANDT, F.N. and NARAHASHI, T. (1983). Modification of single sodium channels by the insecticide tetramethrin. *Brain Res.* 274(2):344-9.

YANG, N.B. and HORN, R. (1995). Evidence for Voltage-Dependent S4 Movement in Sodium-Channels. *Neuron* 15:213-218.

YANG, N.B., GEORGE, A.L. and HORN, R. (1996). Molecular basis of charge movement in voltage-gated sodium channels. *Neuron* 16:113-122.

YANG, N.B., GEORGE, A.L. and HORN, R. (1997). Probing the outer vestibule of a sodium channel voltage sensor. *Biophys. J.* 73:2260-2268.

YANG, N.B., JI, S., ZHOU, M., PTACEK, L.J., BARCHI, R.L., HORN, R. and GEORGE, A.L. (1994). Sodium-Channel Mutations in Paramyotonia-Congenita Exhibit Similar Biophysical Phenotypes *in-Vitro*. *Proc. Natl. Acad. Sci. USA* 91:12785-12789.

YAMAMOTO, D., QUANDT, F.N. and NARAHASHI, T. (1983). Modification of single sodium channels by the insecticide tetramethrin. *Brain Res.* 274(2):344-9.

YEH, J.Z. and ARMSTRONG, C.M. (1978). Immobilisation of gating charge by a substance that simulates inactivation. *Nature* 273:387-9.

YEH, J.Z. and NARAHASHI, T. (1977). Kinetic analysis of pancuronium interaction with sodium channels in squid axon membranes. *J. Gen. Physiol.* 69:293-323.

YELLEN, G. (1998). The moving parts of voltage-gated ion channels. *Q. Rev. Biophys.* 31:239-95.

YOSHII, M., TSUNOO, A. and NARAHASHI, T. (1985). Effects of pyrethroids and veratridine on two types calcium channels in neuroblastoma cells. *Soc. Neurosci. Abst.* 11:158.9.

ZHANG, A.G., DUNN, J.B. and CLARK, J.M. (1999). An efficient strategy for validation of a point mutation associated with acetylcholinesterase sensitivity to azinphosmethyl in Colorado potato beetle. *Pest Biochem. Physiol.* 65:25-35.

ZHAO, Y., PARK, Y. and ADAMS, M.E. (2000). Functional and evolutionary consequences of pyrethroid resistance mutations in S6 transmembrane segments of a voltage-gated sodium channel. *Biochem. Biophys. Res. Commun.* 278:516-21.

ZONG, X.G., DUGAS, M. and HONERJAGER, P. (1992). Relation between Veratridine Reaction Dynamics and Macroscopic Na Current in Single Cardiac-Cells. *J. Gen. Physiol.* 99:683-697.